

**STRUCTURAL, COMPUTATIONAL AND BIOLOGICAL
STUDIES OF FERULIC ACID AND ITS AMIDE
DERIVATIVES**

Ph.D. THESIS

by

NARESH KUMAR



**DEPARTMENT OF BIOTECHNOLOGY
INDIAN INSTITUTE OF TECHNOLOGY ROORKEE
ROORKEE - 247667 (INDIA)
MAY, 2015**

**STRUCTURAL, COMPUTATIONAL AND BIOLOGICAL
STUDIES OF FERULIC ACID AND ITS AMIDE
DERIVATIVES**

A THESIS

*Submitted in partial fulfilment of the
requirements for the award of the degree of*

**DOCTOR OF PHILOSOPHY
In
BIOTECHNOLOGY**

by

NARESH KUMAR



**DEPARTMENT OF BIOTECHNOLOGY
INDIAN INSTITUTE OF TECHNOLOGY ROORKEE
ROORKEE - 247667 (INDIA)
MAY, 2015**

**©INDIAN INSTITUTE OF TECHNOLOGY ROORKEE, ROORKEE-2015
ALL RIGHTS RESERVED**



INDIAN INSTITUTE OF TECHNOLOGY ROORKEE ROORKEE

CANDIDATE'S DECLARATION

I hereby certify that the work which is being presented in the thesis entitled **“STRUCTURAL, COMPUTATIONAL AND BIOLOGICAL STUDIES OF FERULIC ACID AND ITS AMIDE DERIVATIVES”** in partial fulfillment of the requirements for the award of the **Degree of Doctor of Philosophy** and submitted in the **Department of Biotechnology** of the **Indian Institute of Technology Roorkee, Roorkee** is an authentic record of my own work carried out during a period from July, 2010 to May, 2015 under the supervision of Prof. Vikas Pruthi, Department of Biotechnology, Indian Institute of Technology Roorkee, Roorkee.

The matter presented in this thesis has not been submitted by me for the award of any other degree of this or any other Institute.

(Naresh Kumar)

This is to certify that the above statement made by the candidate is correct to the best of my knowledge.

Dated: May 14, 2015

(Vikas Pruthi)
Supervisor

DEDICATION

To my beloved parents

CONTENTS

	Page No.
<i>Candidate's Declaration</i>	
<i>Acknowledgement</i>	i
<i>Abstract</i>	v
<i>List of Publications</i>	ix
<i>Abbreviations</i>	xi
<i>List of Tables</i>	xiii
<i>List of Figures</i>	xv
CHAPTER-1: Introduction and literature review	1-16
1.1. Introduction.....	1
1.2. Ferulic acid: natural sources and isolation.....	4
1.3. Metabolism of ferulic acid.....	5
1.4. Industrial and biological usages of ferulic acid.....	9
1.4.1. Ferulic acid as an antioxidant.....	9
1.4.2. Ferulic acid as an anti-diabetic and anti-ageing agent.....	10
1.4.3. Ferulic acid as preclusion of food discoloration and growth enhancing agent.....	10
1.4.4. Ferulic acid as precursor of vanillin.....	11
1.4.5. Uses of ferulic acid in cosmetics.....	12
1.4.6. Ferulic acid as an anticancer agent.....	12
1.4.7. Pulmonary protection and cardiovascular effect of ferulic acid....	13
1.4.8. Ferulic acid as food preservative.....	14
1.5. Additional applications of ferulic acid	14
1.6. Concluding remarks.....	16
CHAPTER-2: Isolation, structural, thermal and quantum chemical studies of <i>p</i>-coumaric, caffeic and ferulic acids from <i>Parthenium hysterophorus</i> L.	17-46
2.1. Introduction.....	17
2.2. Experimental section	18
2.2.1. Materials.....	18
2.2.2. Extraction and purification.....	18

2.2.2.1.	<i>p</i> -Coumaric acid (PCA).....	19
2.2.2.2.	Caffeic acid (CA).....	19
2.2.2.3.	Ferulic acid (FA).....	20
2.2.3.	Instrumentation.....	20
2.2.4.	Quantum chemical calculations and statistical analysis.....	21
2.3.	Results and discussion	21
2.3.1.	Extraction and purification.....	21
2.3.2.	Spectroscopic analysis.....	22
2.3.3.	Crystal structure description.....	32
2.3.4.	Thermal analysis.....	35
2.3.5.	Geometry optimization and Statistical analysis.....	37
2.3.6.	Frontier molecular orbital (FMOs) analysis.....	42
2.4.	Concluding remarks.....	45
 CHAPTER-3: Synthesis, structural and thermal characterization of mono and bis-amide derivatives of ferulic acid		47-108
3.1.	Introduction.....	47
3.2.	Experimental section.....	48
3.2.1.	Materials.....	48
3.2.2.	Instrumentation	48
3.2.3.	Syntheses of amide derivatives ferulic acid	49-68
3.3.	Results and discussion	68
3.3.1.	Chemistry.....	68
3.3.2.	Thermal analysis.....	104
3.4.	Concluding remarks.....	107
 CHAPTER-4: Biological applications of ferulic acid amide derivatives		109-118
4.1.	Introduction.....	109
4.2.	Experimental section.....	110
4.2.1.	Materials.....	110
4.2.2.	<i>In vitro</i> cytotoxicity assay.....	111
4.2.3.	<i>In vitro</i> antioxidant activity assay.....	111
4.3.	Results and discussion.....	112
4.3.1.	<i>In vitro</i> anticancer activity.....	112

4.3.2.	<i>In vitro</i> antioxidant activity.....	115
4.4.	Concluding remarks.....	117
CHAPTER-5: Quantum chemical calculations and 3D-quantitative structure activity relationship (QSAR) modeling of ferulic acid amide derivatives		119-152
5a.1.	Quantum chemical calculations.....	119
5a.2.	Theoretical methods.....	120
5a.3.	Results and discussion	122
5a.3.1.	Geometry optimization.....	122
5a.3.2.	Frontier Molecular Orbital (FMOs) Analysis.....	122
5a.4.	Concluding remarks.....	135
5b.1.	3D-Quantitative Structure Activity Relationships (3D-QSAR).....	136
5b.2.	Theoretical methods.....	136
5b.2.1.	3D-QSAR modeling.....	136
5b.2.2.	Statistical analysis.....	139
5b.3.	Results and discussion.....	140
5b.3.1.	Analysis of 3D-QSAR results.....	140
5b.3.2.	Analysis of statistical results.....	144
5b.4.	Concluding remarks.....	151
CHAPTER-6: Summary and Future scope.....		153-156
Bibliography.....		157-179

AKNOWLEDGEMENT

Time flies when I look back and recollect memories, the moments flash instantly across the memory lane, and it feels as only few days have passed. I still remember the first day at Department of Biotechnology, Indian Institute of Technology Roorkee, when I entered with a nostalgic feeling. I was happy when I was given the opportunity to finish my Doctoral degree with a project from here, a sweet realization dawned upon me that this exactly is the place to gain higher levels of consciousness on both academic and personal frontiers. It has been a memorable stint of five years marked with a number of valued experiences. Today when I am leaving this place, I wish to thank everyone who touched my life in this precious and valuable time.

I am indebted to my supervisor, Professor Vikas Pruthi for his enlightening guidance and inspiring instruction in the development and completion of this study. He is an idol of limitless patience and perseverance. His calm and balanced nature, organized approach and vigilant interpretation of experimental results combined with his motivating attitude always gave me a moral boost up to move ahead with the project. I am also grateful to Dr. Parul Aggarwal Pruthi for her keen cooperation and guidance.

I owe a deep sense of gratitude to Prof. S. M. Sondhi, Prof. P.V. Bharatam, and Prof. Partha Roy who provided me an opportunity to work in their laboratories.

I would like to extend my heartfelt thanks to all teaching and non-teaching staff at Department of Biotechnology, IIT Roorkee for their support during my thesis tenure.

At this time words fail to express my feelings, yet I take this opportunity to express my heartfelt gratitude and regards for my parents, family members and relatives. Without their

blessings I would have never reached this stage. They have always shown me the way and helped me choose between right and wrong. I especially thank to my brothers Kishan Chand, Rakesh, Ghanshyam, Yogesh, and Sonu for their constant love and support at every stage of my life. I am in dearth of proper words to express my abounding feelings to my sisters, Hame Lata, Jyoti, Archana and niece Shalu for their encouragement and the love they showed on me at every stage. They have been all the strength, inspiration and guiding force for all my life, and I have tried to meet their expectations.

I will always cherish my friendship with Prof. T.C. Bhalla, Dr. Rekha, Dr. Uday Singh, Dr. Pavan Kumar, Dr. Arif, Dr. Sandeep Kumar, Dr. Heero Hito, Dr. M.S. Baghel, Dr. Ashok Kumar, Dr. Arjun Kumar, Dr. C.N. Ramachandran, Mr. Mukhtar Khan, Mr. BabuRam, Mr. TilakRam, Mr. Madanpal, Mr. Ram Naresh Indoria, Mr. Anil Kumar Saini, Mr. Vishwajeet Vishwakarma, Mr. Anil, Dr. Lalit Kumar, Dr. Pramod Kumar, Dr. Kranti, Dr. Umashanker, Dr. Devdutt, Dr. Jitendra Kumar, Dr. Ramkeval, Arvind Kumar, Harish Kumar, Shakher, Siddhu, Rohit, Brajesh Kumar, Raghu, Nikhil, Pankaj Pratap Singh, Chinmoy, Kamlesh Kumar, Shalini, Gangaram, Arvind, Jaibhagwan, Hempal, Archit, Gaurav, Akash, Vijay, Ashish, Amit, Pramod, Umesh, Shashank, Amol, Yogesh, and Somesh who contributed directly or indirectly towards the successful completion of my thesis in their own special way. Their help and co-operation are unforgettable.

I would like to express deep and sincere words to my talented and emerging students (Sachin Kumar, Mahendra Pratap, Amit Kumar, Jitendra Kumar, Manjeet Kumar, Arun Kumar Azad, Manindra Kumar) for their memorable support and efforts.

I am also thankful to my lab mates (Vivekanand, Harmeet, Alok, Navdeep, Priya, Sonal, Suma, Richa, Sonam, and Neha) through these years for their help and memories.

I would like to acknowledge Council of Scientific and Industrial Research, New Delhi (CSIR-9885-35-44/61) for financial support.

I am also grateful to Prof. Surendra Kumar (Department of Chemical Engineering, IIT Roorkee) for his precious support in my startup of research work and other essential help.

I express my deepest sense of gratitude to Dr. Nidhi Goel for her immense care, guidance, encouragement and invaluable support. I cannot forget her kind help and cooperation in bringing me to this position. Her advices were indispensable for useful discussions in the understanding of my research work.

I want to express my deepest love and thanks to my beloved for her understanding support and love during the past few years. Her motivation and encouragement was in the end what made this study possible.

At the end, I am extremely grateful to those people, whose names have been unknowingly left, thank you very much for your prayers. It had really helped a lot. I apologize and believe that they will be always with me as they were during the times of need.

Most of people do not stop to read the acknowledgement, since you did, Thanks to you.

Naresh Kumar

ABSTRACT

Hydroxycinnamic acids are natural source of antioxidants; arise from the metabolism of L-phenylalanine and L-tyrosine through shikimate pathway in plants. The hydroxycinnamic acids are the largest class of phenolic compounds, represented by *p*-coumaric, caffeic and ferulic acids. They have been consistently associated with the reduced risk of cardiovascular disease, cancer and other chronic diseases. The *p*-coumaric acid is a ubiquitous plant metabolite known to exhibit useful biological activities viz., antioxidant, anti-inflammatory, antiplatelet, anti-melanogenic; inhibits melanin synthesis in B16F10 cells without affecting CREB phosphorylation or tyrosinase protein production. The caffeic acid is a polar compound with a strong chelating capacity towards metals, and coffee is the primary source of it in the human diet. However, it can also be found in other food sources. Like other phenolics, caffeic acid also exhibits strong antioxidant activity. Ferulic acid is an abundant phenolic phytochemical, known to enhance the stability of cytochrome c, inhibits the apoptosis induced by cytochrome c, increases the IgE binding to peanut allergens and many more. During its formation, phenylalanine and tyrosine are converted into cinnamic and *p*-coumaric acid with the help of phenylalanine ammonia lyase and tyrosine ammonia lyase, respectively. The *p*-coumaric gets converted into ferulic by hydroxylation and methylation reaction. Oxidation and methylation of ferulic acid and other aromatic compounds give di- and tri-hydroxy derivatives of cinnamic acid, which takes part in the lignin formation together with ferulic acid. In 1925, it was chemically synthesized and its structure was confirmed by spectroscopic techniques, depicted the presence of an unsaturated side chain and existence of two isomeric forms (*cis* and *trans*). The resonance stabilized phenoxy radical accounts for the effective antioxidant activity of ferulic acid. It catalyzes the stable phenoxy radical formation upon

absorption of ultra-violet light, which gives the strength to ferulic acid for terminating free radical chain reactions.

Isolation of the hydroxycinnamic acids from *Parthenium hysterophorus* L. followed by their structural characterization using elemental analysis, FT-IR, NMR, ESI-MS and single X-ray crystallography had been carried out. Molecular structures of these acids were confirmed by single crystal X-ray diffractometer, which showed that the *p*-coumaric acid crystallized in the monoclinic crystal system with space group *P 21/c*, while caffeic and ferulic acids were crystallized in the monoclinic crystal system with space group *P 21/n*. The thermograms of the acids clearly indicate that all three acids are stable up to 100°C but at higher temperatures, curves shows irregular pattern with one stage thermal decomposition during thermal analysis. The molecular geometry, harmonic vibrational frequencies and structural parameters were computed at DFT/B3LYP/6-311G** basis set by Gaussian 09. The comparisons between experimental and simulated data of spectroscopic analysis and geometrical parameters were accomplished for their statistical validation by curve fitting analysis and found statistically close to each other with the values of correlation coefficient for bond lengths and bond angles 0.985, 0.992, 0.984, 0.975, and 0.913, 0.933 in *p*-coumaric, caffeic and ferulic acids, respectively. The HOMO and LUMO analysis were also carried out to find out the charge transfer within the molecule.

Motivated by the broad spectrum of biological activities shown by ferulic acid, its derivatives and the compounds possessing amide moiety, we have developed a strategy towards the synthesis of a number of novel derivatives by the structural modifications of ferulic acid. The design, synthesis and characterization of four series of mono and bis- amide derivatives (**IIIa-IIIo**, **Va-Vg**, **VIIa-VIIg** and **IXa-IXe**) of ferulic acid had been carried out by microwave irradiation under solvent free reaction conditions. The previously extracted ferulic acid together with the

different categories of primary amines were taken in equimolar concentration in a petri dish, mixed carefully and subjected to microwave irradiation at 300-450W power for 3-10 min. The structural studies of all the newly synthesized compounds had been performed by FT-IR, NMR, mass spectroscopy and elemental analysis for C, H, and N. The $^1\text{H-NMR}$ was taken after keeping all of those for ten days and six months at room temperature did not show any change, confirmed that the compounds are stable in solid as well in liquid phase. These results were also supported by their thermal studies.

Further, all the synthesized compounds have been screened for their *in vitro* cytotoxicity and free radical scavenging activity by MTT against five different human cancer cell lines, i.e. breast (MDA-MB-231 and MCF-7), cervical (HeLa), lung (A549), and liver (HepG2) as well as one normal stem cell line at $10\mu\text{M}$ concentration and DPPH assay, respectively. The results of MTT assay showed that 21 compounds exhibited good activity against all types of cancer cell lines and very less or negligible activity alongside normal stem cells. These 21 compounds were further studied for their IC_{50} value and found that the compounds **Va-Vg** (containing acridine moiety) exhibited the best IC_{50} (07.11-11.08 μM). The compound **Vb** was found to be the most promising against breast (MCF-7; $\text{IC}_{50} = 07.49 \mu\text{M}$ and MDA-MB-231; $\text{IC}_{50} = 07.28 \mu\text{M}$), **Vd** against lung (A549; $\text{IC}_{50} = 07.11\mu\text{M}$) and liver (HepG2; $\text{IC}_{50} = 08.32 \mu\text{M}$) and **Ve** against cervical (HeLa; $\text{IC}_{50} = 07.14 \mu\text{M}$) cancer cell line. Data obtained free radical scavenging activity revealed that nine compounds (**III f, III, III o, VII e and IX a-IX e**) showed good antioxidant activity (EC_{50} ; 18.37 to 25.44 μM) as compared to L-ascorbic acid (EC_{50} ; 20.14 μM), thirteen compounds showed poor activity (EC_{50} values more than 35 μM), and twelve compounds exhibited moderate activity (EC_{50} ; 26.89-34.81 μM).

The theoretical calculations were also performed in two manners; **Firstly**, the quantum chemical calculations of all the compounds for their geometry optimization and computation of structural parameters based on DFT with a hybrid function B3LYP at 6-311G** basis set. To evaluate the behavior in terms of energy of synthesized compounds, calculations were done both in solvent and gaseous phase. The values of energies (HOMO and LUMO), electro-negativity (χ), chemical hardness (η), chemical softness (S), electronic chemical potential and electrophilic index (ω) were also calculated using Koopman's theorem for closed shell molecule. The optimized geometry showed the positive harmonic vibrational frequencies, indicates that optimized geometries attained the global minimum state on the potential energy surface. **Secondly**, the 3D-QSAR (quantitative structure activity relationship) studies for anticancer and antioxidant activities were also carried out by using CoMFA (comparative molecular field analysis). In the work, six (6) different models were generated (5 for anticancer and 1 for antioxidant) and analyzed. The statistical, contour map, steric and electrostatic effects analysis were carried out to understand the structure–activity relationship of ferulic acid derivatives. Commenting on the statistical results, we inferred that 3D-QSAR values lie statistically closed to the values obtained from experimental results for *in vitro* anticancer and antioxidant activity, and outcome for all the cases to be worthy in respect to their statistical significance for correlation.

LIST OF PUBLICATIONS

1. **Naresh Kumar**, Sandeep Kumar, Sheenu Abbat, Kumar Nikhil, Sham M. Sondhi, P.V. Bharatam, Partha Roy and Vikas Pruthi (2015) 3D-QSAR modeling of ferulic acid and its amide derivatives: Synthesis, structural characterization, anticancer and antioxidant activities (Under review: European Journal of Medicinal Chemistry).
2. **Naresh Kumar** and Vikas Pruthi (2015) Theoretical studies on Electronic Structure and Properties of Some Ferulic Acid Amide Derivatives (to be communicated).
3. **Naresh Kumar**, Vikas Pruthi and Nidhi Goel (2015) Structural, Thermal and Quantum Chemical Studies of *p*-coumaric and caffeic acids. Journal of Molecular Structure 1085:242-248.
4. **Naresh Kumar** and Vikas Pruthi (2014) Potential applications of ferulic acid from natural sources. Biotechnology Reports 4:86-93.
5. **Naresh Kumar** and Vikas Pruthi (2014) Structural elucidation and molecular docking of ferulic acid from Parthenium hysterophorus possessing COX-2 inhibition activity. 3 Biotech (DOI 10.1007/s13205-014-0253-6).
6. **Naresh Kumar** and Vikas Pruthi (2012) DFT studies of ferulic acid derivative, FA15 using computational approach. J Biotechnol Biomater., 2(6):236.
7. **Naresh Kumar**, Richa Panwar and Vikas Pruthi (2012) Structural conformation of ferulic acid isolated from Parthenium. 15th International Biotechnology Symposium & Exhibition, Daegu, South Korea (In Proceeding).

Participation in Workshops and Symposia:

1. CEP Short Term Course on “**Introduction to Systems and Synthetic Biology for Scientists and Engineers**” from April 22-25, 2013, Indian Institute of Technology Bombay, India.
2. Two day workshop on “**Recent Advances in Computational Biology and Structural Based Drug Designing**” Conducted at Biotechnology-2012 Conference from September 13-15, 2012 at Hyderabad International Convention Centre, India.
3. Workshop on “**Data analysis for research & decision-making using SPSS**” from July 27-28, 2012 at Amrapali Institute, Shiksha Nagar, Lamachaur, Haldwani, India.
4. QIP workshop on “**Interaction of Academia-Industry on Mathematical Modeling**” on March 31, 2012, organized by Department of Mathematics, Indian Institute of Technology Roorkee, Roorkee, India.
5. Workshop on “**Introduction to Gaussian: Theory and Practice**” from December 17-21, 2012, New Delhi, India conducted by SCUBE Scientific Software Solutions (P) Ltd, New Delhi, India.
6. Two days short term course on Patenting in IPR cell Indian Institute of Technology Roorkee, Roorkee, India.

ABBREVIATIONS

Abbreviation	Full name
PCA	<i>p</i> -coumaric acid
CA	Caffeic acid
FA	Ferulic acid
TLC	Thin layer chromatography
HPLC	High Performance Liquid Chromatography
m.p.	Melting Point
FT-IR	Fourier Transform Infrared Spectroscopy
NMR	Nuclear Magnetic Resonance
ppm	Parts Per Million
TMS	Tetramethylsilane
GC-MS	Gas Chromatography-Mass Spectrometry
APCI-MS	Atmospheric Pressure Chemical Ionization-Mass Spectrometry
Å	Angstrom
°	Degree
TG	Thermogravimetry
DTA	Differential Thermal Analysis
DTG	Derivative Thermogravimetry
Endo	Endothermic
DFT	Density Functional Theory
HOMO	Highest Occupied Molecular Orbital
LUMO	Lowest Unoccupied Molecular Orbital
a.u	Hartree (a unit of energy)
eV	Electronvolt
nm	Nanometer
AIDS	Acquired Immune Deficiency Syndrome
MTT	3-(4,5-dimethyl-2-thiazolyl)-2,5diphenyl-2H tetrazolium bromide
DMSO	Dimethyl Sulfoxide
OD	Optical Density

μL	Microleter
μM	Micromolar
DPPH	1,1-diphenyl-2-picrylhydrazyl radical
NCCS	National Center for Cell Science
RH	Relative Humidity
QSAR	Quantitative Structure Activity Relationship
CoMFA	Comparative Molecular Field Analysis

LIST OF TABLES

Table No.	Caption	Page No.
Table 2.1	Crystallographic data collection and refinement parameters for <i>p</i> -coumaric, caffeic and ferulic acids	32
Table 2.2:	Non-covalent interactions for ferulic acid [Distances (Å) Angles (°)]	34
Table 2.3	TG-DTA-DTG data of <i>p</i> -coumaric, caffeic and ferulic acids	37
Table 2.4	Comparison of X-ray structure and calculated bond angles for PCA, CA and FA extracted from <i>Parthenium hysterophorus</i> L	39
Table 2.5	Comparison of X-ray structure and calculated bond angles for PCA, CA and FA extracted from <i>Parthenium hysterophorus</i> L	40-41
Table 2.6	Calculated values of total energy, dipole moment, energy for HOMO-LUMO, electronegativity, electrophilic index, chemical potential, chemical hardness and chemical softness for PCA, CA and FA in gas phase at DFT/B3LYP/6-311G** basis set	43
Table 3.1	TG-DTA-DTG data of compounds IIIa-IIIo, Va-g, VIIa-g and IXa-e	106-107
Table 4.1	<i>In vitro</i> anticancer activity (% growth inhibition) of ferulic acid amide derivatives at 10 µM concentration	113-114
Table 4.2	IC ₅₀ (µM) values of <i>in vitro</i> anti-proliferative activity of active ferulic acid amide derivatives	115
Table 4.3	EC ₅₀ (µg/ml) values of <i>in vitro</i> free radical scavenging activity of active ferulic acid derivatives	116
Table 5.1	Calculated values of total energy, dipole moment, frontier molecular orbitals, electronegativity, Chemical potential, chemical hardness, chemical softness, and electrophilic index for ferulic acid amides derivatives at DFT/B3LYP/6-311G** basis set	133-134
Table 5.2	Results of the CoMFA analysis for anticancer and antioxidant activities of ferulic acid derivatives at 2.0 Å grid spacing	140
Table 5.3	pIC ₅₀ (experimental and predictive) for all six cases (<i>In vitro</i> anticancer and antioxidant activity evaluation)	145-148

LIST OF FIGURES

Figure No.	Caption	Page No.
Figure 1.1	Chemical structure of hydroxycinnamic acids	1
Figure 1.2	Schematic representation of two different isomeric forms (a) <i>cis</i> and (b) <i>trans</i> conformation of ferulic acid	3
Figure 1.3	Schematic depiction of synthesis of ferulic acid and other aromatic compounds via shikimate pathway {PAL: Phenylalanine ammonia lyase; TAL: Tyrosine ammonia lyase; SAM: S-adenosyl methionine (acts as a methyl donor)}	7
Figure 1.4	Pathway for ferulic acid catabolism in <i>S. paucimobilis</i> SYK-6 {HMPHP-CoA: 4-Hydroxy-3-Methoxyphenyl- β -Hydroxyprpionyl CoA}	8
Figure 1.5	Bioconversion of ferulic acid into vanillin	11
Figure 1.6	Schematic representation of different activities shown by ferulic acid	15
Figure 2.1	¹ H-NMR spectrum of <i>p</i> -coumaric acid isolated from <i>Parthenium hysterophorus</i> L	23
Figure 2.2	¹³ C-NMR spectrum of <i>p</i> -coumaric acid isolated from <i>Parthenium hysterophorus</i> L	24
Figure 2.3	GC-Mass spectrum of <i>p</i> -coumaric acid isolated from <i>Parthenium hysterophorus</i> L	25
Figure 2.4	¹ H-NMR spectrum of caffeic acid isolated from <i>Parthenium hysterophorus</i> L	26
Figure 2.5	¹³ C-NMR spectrum of caffeic acid isolated from <i>Parthenium hysterophorus</i> L	27
Figure 2.6	GC-Mass spectrum of caffeic acid isolated from <i>Parthenium hysterophorus</i> L	28
Figure 2.7	¹ H-NMR spectrum of ferulic acid isolated from <i>Parthenium hysterophorus</i> L	29
Figure 2.8	¹³ C-NMR spectrum of ferulic acid isolated from <i>Parthenium hysterophorus</i> L	30
Figure 2.9	GC-Mass spectrum of ferulic acid isolated from <i>Parthenium</i>	31

hysterophorus L

Figure 2.10	Ball & stick models of the solid state single crystal structure of PCA, CA and FA. Color code: C, grey; H, orange; O, red	33
Figure 2.11	Various O-H•••O non-covalent interactions in ferulic acid	34
Figure 2.12	Three dimensional zig-zag views representing the arrangement of atom present in ferulic acid	35
Figure 2.13	Simultaneous TG-DTG analysis curves of <i>p</i> -coumaric, caffeic and ferulic acids	36
Figure 2.14	Optimized geometries of PCA, CA and FA at DFT/B3LYP/6-311G** basis set.	38
Figure 2.15	Pictorial presentation of linear correlation plots between experimental and simulated values of bond lengths for PCA, CA and FA	41
Figure 2.16	Pictorial presentation of linear correlation plots between experimental and simulated values of bond angles for PCA, CA and FA	42
Figure 2.17	Molecular orbital surfaces and energy (eV) of PCA, CA and FA for HOMO and LUMO in gas phase	44
Figure 3.1	¹ H, ¹³ C-NMR and GC-MS spectra of IIIa	70
Figure 3.2	¹ H, ¹³ C-NMR and GC-MS spectra of IIIb	71
Figure 3.3	¹ H, ¹³ C-NMR and GC-MS spectra of IIIc	72
Figure 3.4	¹ H, ¹³ C-NMR and GC-MS spectra of IIId	73
Figure 3.5	¹ H, ¹³ C-NMR and GC-MS spectra of IIIe	74
Figure 3.6	¹ H, ¹³ C-NMR and GC-MS spectra of IIIf	75
Figure 3.7	¹ H, ¹³ C-NMR and GC-MS spectra of IIIg	76
Figure 3.8	¹ H, ¹³ C-NMR and GC-MS spectra of IIIh	77
Figure 3.9	¹ H, ¹³ C-NMR and GC-MS spectra of IIIi	78
Figure 3.10	¹ H, ¹³ C-NMR and GC-MS spectra of IIIj	79
Figure 3.11	¹ H, ¹³ C-NMR and GC-MS spectra of IIIk	80
Figure 3.12	¹ H, ¹³ C-NMR and GC-MS spectra of IIIl	81
Figure 3.13	¹ H, ¹³ C-NMR and GC-MS spectra of IIIm	82
Figure 3.14	¹ H, ¹³ C-NMR and GC-MS spectra of IIIn	83
Figure 3.15	¹ H, ¹³ C-NMR and GC-MS spectra of IIIo	84

Figure 3.16	^1H , ^{13}C -NMR and APCI-MS spectra of Va	85
Figure 3.17	^1H , ^{13}C -NMR and APCI-MS spectra of Vb	86
Figure 3.18	^1H , ^{13}C -NMR and APCI-MS spectra of Vc	87
Figure 3.19	^1H , ^{13}C -NMR and APCI-MS spectra of Vd	88
Figure 3.20	^1H , ^{13}C -NMR and APCI-MS spectra of Ve	89
Figure 3.21	^1H , ^{13}C -NMR and APCI-MS spectra of Vf	90
Figure 3.22	^1H , ^{13}C -NMR and APCI-MS spectra of Vg	91
Figure 3.23	^1H , ^{13}C -NMR and GC-MS spectra of VIIa	92
Figure 3.24	^1H , ^{13}C -NMR and GC-MS spectra of VIIb	93
Figure 3.25	^1H , ^{13}C -NMR and GC-MS spectra of VIIc	94
Figure 3.26	^1H , ^{13}C -NMR and GC-MS spectra of VIId	95
Figure 3.27	^1H , ^{13}C -NMR and GC-MS spectra of VIIe	96
Figure 3.28	^1H , ^{13}C -NMR and GC-MS spectra of VIIf	97
Figure 3.29	^1H , ^{13}C -NMR and GC-MS spectra of VIIg	98
Figure 3.30	^1H , ^{13}C -NMR and APCI-MS spectra of IXa	99
Figure 3.31	^1H , ^{13}C -NMR and APCI-MS spectra of IXb	100
Figure 3.32	^1H , ^{13}C -NMR and APCI-MS spectra of IXc	101
Figure 3.33	^1H , ^{13}C -NMR and APCI-MS spectra of IXd	102
Figure 3.34	^1H , ^{13}C -NMR and APCI-MS spectra of IXe	103
Figure 3.35	Simultaneous TG-DTG analysis curves of IIIa, Va, VIIa, and IXa under nitrogen	105
Figure 5.1	Optimized structure of (a) IIIa-IIIo (b) Va-Vg (c) VIIa-VIIg and (d) IXa-IXe at DFT/B3LYP/6-311G** basis set.	123-126
Figure 5.2	Frontier molecular orbitals for optimized geometries of (a) IIIa-IIIe (b) IIIf-IIIk and (c) IIIk-IIIo at DFT/B3LYP/6-311G** basis set.	127-129
Figure 5.3	Frontier molecular orbitals for optimized geometries of Va-Vg at DFT/B3LYP/6-311G** basis set	130
Figure 5.4	Frontier molecular orbitals for optimized geometries of VIIa-VIIg at DFT/B3LYP/6-311G** basis set.	131
Figure 5.5	Frontier molecular orbitals for optimized geometries of IXa-IXe at DFT/B3LYP/6-311G** basis set.	132

Figure 5.4	Alignment of molecules used for the making of CoMFA model (a) anticancer and (b) antioxidant activities of ferulic acid derivatives	137-138
Figure 5.5	STDDEV*COEFF plots of the CoMFA steric and electrostatic contour maps for (a) MCF-7 (b) MDA-MB-231 (c) A549 (d) HepG2 and (e) HeLa (f) antioxidant models (The most active molecule is displayed in the background. Green region: sterically favoured; yellow region: sterically disfavoured; red region: negatively charged favoured; blue region: positively charged favoured)	142
Figure 5.6	Plots of linear correlation between experimental and simulated values of training sets for in vitro anticancer and free radical scavenging activity	149
Figure 5.7	Plots of linear correlation between experimental and simulated values of test sets for in vitro anticancer and free radical scavenging activity	150

CHAPTER-1

Introduction and literature review

Naresh Kumar and Vikas Pruthi (2014) Potential applications of ferulic acid from natural sources. *Biotechnology Reports* 4 (2014) 86-93.

1.1. Introduction

Hydroxycinnamic acids are the natural source of antioxidants; arise through shikimate pathway from the metabolism of phenylalanine and tyrosine in plants [Kumar et al. 2014]. They have been consistently related with the reduced risk of cardiovascular, cancer and many other chronic diseases [Spencer et al. 2008; Rocha et al. 2012]. The hydroxycinnamic acids shown in Figure 1.1 are the largest class of phenolic compounds, represented by *p*-coumaric, caffeic and ferulic acid [Huang et al.1986; Herrmann 1989; Lafay et al. 2008; Karakaya 2004; Crozier et al. 2009].

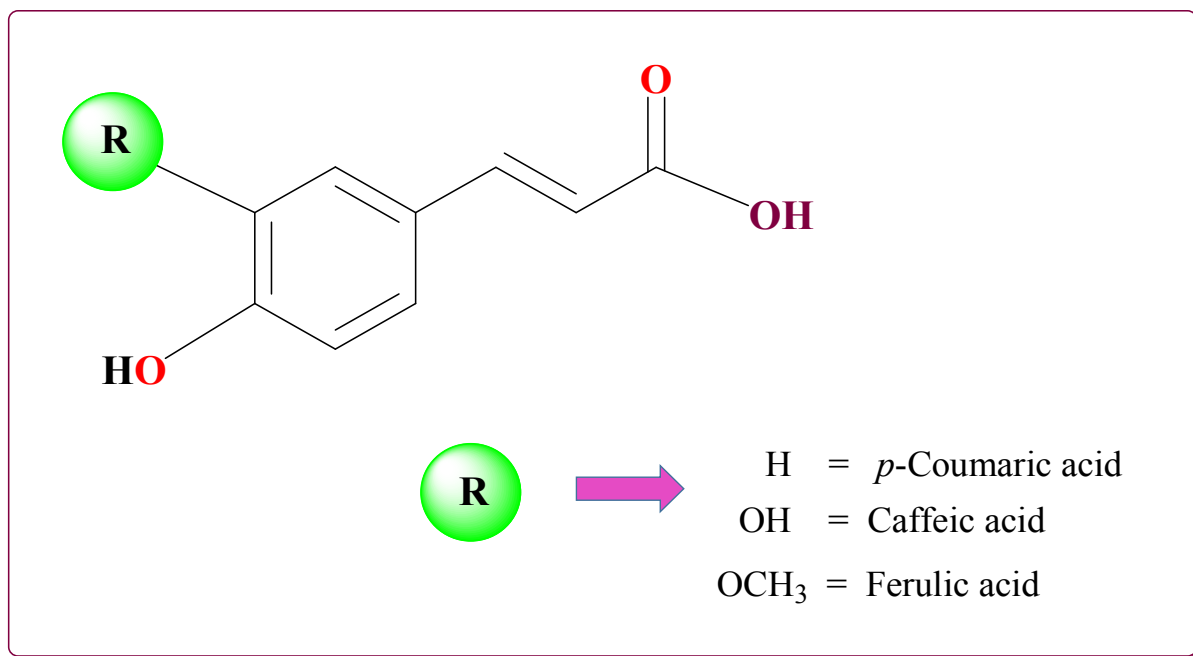


Figure 1.1: Chemical structure of hydroxycinnamic acids.

The *p*-coumaric acid is a ubiquitous plant metabolite known to exhibit useful activities viz., antioxidant, anti-inflammatory, antiplatelet, anti-melanogenic; inhibits the synthesis of melanin in B16F10 cells without affecting the phosphorylation of CREB or production of tyrosinase protein [Luceri et al. 2007; An et al. 2008; Park et al. 2008]. There is a recent report in which shows the successful inhibitory effects of *p*-coumaric acid during quorum sensing in 5999, NTL4 and *P. chlororaphis* [Bodini et al. 2009]. Caffeic acid is a polar compound with a strong chelating capacity towards metals [Medina et al. 2007], and coffee is the primary source of it in the human diet. However, it can also be found in other food sources [Clifford 1999; Llorach et al. 2002]. Like other phenolics, caffeic acid also exhibits strong anti-oxidative activities [Marinova et al. 2006; Nardini et al. 1995; Taubert et al. 2003; Wei-Min et al. 2007; Bors et al. 1995; Pietta 2000]. Ferulic acid (4-hydroxy-3-methoxycinnamic acid, FA) is also an abundant phenolic phytochemical, reported to enhance the stability of cytochrome c, inhibits the apoptosis induced by cytochrome c, and increases the IgE binding to peanut allergens [Yang et al. 2007; Chung et al. 2011]. FA has been recently reported as a β -secretase modulator with therapeutic potential against Alzheimer's disease in hypertensive rats [Mori et al. 2013; Alam et al. 2013], and has been globally approved as a food additive to inhibit the lipid peroxidation for its effectiveness to scavenge the superoxide anion radical [Srinivasan et al. 2007]. First time, FA was isolated from *Ferula foetida* for its structure determination, and its name was based on the botanical name of the plant [Hlasiwetz and Barth 1866]. In 1925, it was chemically synthesized and structurally confirmed by spectroscopic techniques, depicted the presence of an unsaturated side chain in FA, and also the existence of both *cis* and *trans* isomeric forms [Dutt 1925; Nethaji et al. 1988]. The double bond

present in the side chain is subjected to *cis-trans* isomerization (Figure 1.2), and the resonance stabilized phenoxy radical accounts for its effectual antioxidant activity.

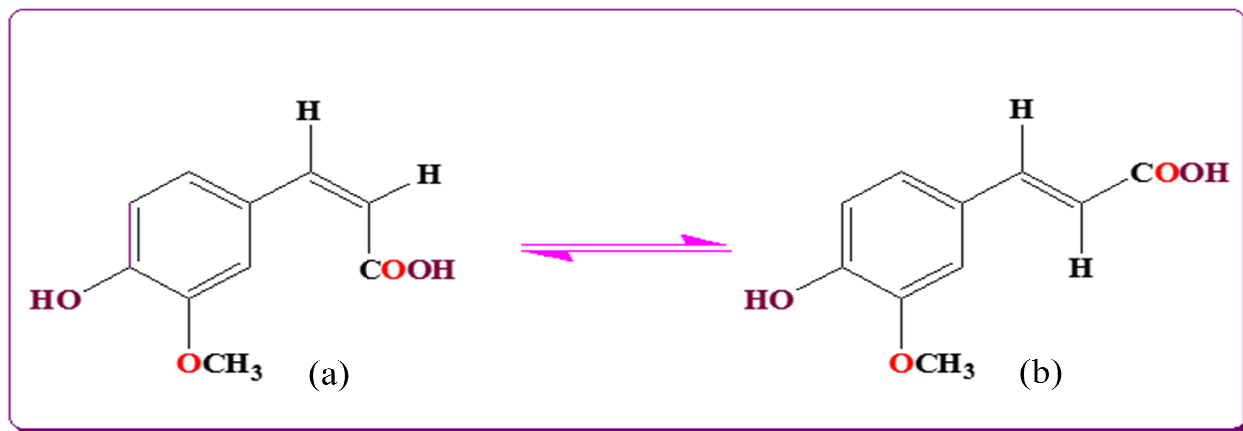


Figure 1.2: Schematic representation of two different isomeric forms (a) *cis* and (b) *trans* conformation of ferulic acid.

FA catalyzes the stable phenoxy radical formation upon absorption of ultra-violet light, which gives the strength to it for terminating free radical chain reactions. FA is an enormously copious and almost ubiquitous phytochemical phenolic derivative of cinnamic acid, present in plant cell wall components as covalent side chains [Rosazza et al. 1995]. Collectively with dihydroferulic acid, it is the component of lignocelluloses, where it confers rigidity to the cell wall by making the crosslink between polysaccharides and lignin. It has been found that FA is linked with a variety of carbohydrates as glycosidic conjugates, different esters and amides with a broad range of natural products [Strack 1990]. It makes esters by binding with a variety of molecules such as polysaccharides, long chain alcohols, various sterols of plant, tetra-hydroisoquinoline-monoterpene glucoside, a cyanogenetic glycoside and an amino-hydroxy-cyclopentenone, flavonoids and different types of hydroxycarboxylic acids including gluconic, tartaric, malic,

hydroxycitric, tartronic, quinic, and hydroxy fatty acids [Graf 1992; Herrmann 1989 and 1990; Boven et al. 1994].

1.2. Ferulic acid: natural sources and isolation

FA is commonly found in commelinid plants (rice, wheat, oats, and pineapple), grasses, grains, vegetables, flowers, fruits, leaves, beans, seeds of coffee, artichoke, peanut and nuts [Bourne and Rice-Evans 1998; Mattila and Hellstrom 2007; Mattila et al. 2006; Mattila et al. 2005; Srinivasan et al. 2007; Wong et al. 2011]. Cell walls (1.4% of dry weight) of cereal grains and a variety of food plants (pineapple, bananas, spinach, and beetroot) contains 0.5-2% extractable amount of FA, mostly in the *trans*-isomeric form, and esterified with the specific polysaccharides [Harris and Hartley 1980; Hartley and Ford 1989; Hartley and Harris 1981; Nicholas, 1996].

Extraction of FA offers accessible business fortuity, and provides supplementary environmental and economic encouragement for industries as it is used in ingredients of many drugs, functional foods and nutraceuticals. Numerous alkaline, acidic and enzymatic methods for the extraction of FA from different sources have been proposed in literature [Kim et al. 2006; Anwar et al. 2009; Soto et al. 2011; Xu et al. 2005; Mathew and Abraham 2005]. However, optimization of critical parameters for isolation of FA such as time of extraction, pH and temperature is essential for its high yield. Study was conducted with the help of response surface methodology, which showed 1.3 fold increases in the production of FA as compared to the unoptimized conventional extraction technique [Tilay et al. 2008]. FA is insoluble in water at room temperature but it is soluble in hot water, ethyl acetate, ethanol and ethyl ether, and it has been found that ethanol (60%) is suitable for the successful extraction of FA [Guo et al. 2003].

Although, the FA is found ubiquitously in cell wall of woods, corn hulls and grasses, but it is not effortlessly available from natural sources as it is found covalently linked with a variety of carbohydrates as a glycosidic conjugate/an ester/amide. Therefore, it can only be released from these natural products by alkaline hydrolysis [Tilay et al. 2008]. Generally, FA obtained from the chemical process cannot be considered as natural, so various attempts have been made for enzymatically release of FA from natural sources. Isolation of FA for commercial production by enzymatic means is a difficult challenge because most of the FA contents in plants are covalently linked with lignin and other biopolymers. Recently Uraji and coworkers successfully enhanced the enzymatic production of FA from defatted rice bran, and suggested that the enzymes (α -L-arabinofuranosidase, multiple xylanases, and an acetyl xylan esterase) from *Streptomyces* can also be used for the extraction of FA from other sources viz., raw rice bran, wheat bran and corncob [Uraji et al. 2013]. The TLC separation of crude extracts and visualization by a range of spraying reagents and UV-light offers a quick way for the regular high-throughput detection of FA. Approximately >45% (>2.0%/g dry weight) of total FA content was released during enzymatic treatment of sweet potato stem that had been achieved through the incubation period of 12 h with 1.0% Ultraflo L [Min et al. 2006]. Biotransformation studies for the production of FA from eugenol have been carried out by using the recombinant strain of *Ralstonia eutropha* H16 [Overhage 2002]. Lambert and coworkers got almost 90% yields in the production of FA from eugenol and coniferyl alcohol by using a recombinant strain of *Saccharomyces cerevisiae* [Lambert et al. 2013].

1.3. Metabolism of ferulic acid

The formation of FA in plants occurs through the metabolic route of shikimate pathway starting with aromatic amino acids, L-phenylalanine and L-tyrosine as key entities. Initially,

phenylalanine and tyrosine are converted into cinnamic and *p*-coumaric acid with the help of phenylalanine ammonia lyase and tyrosine ammonia lyase, respectively [Graf 1992]. The *p*-coumaric acid gets converted into FA by hydroxylation and methylation reaction [Gowri et al. 1991]. Oxidation and methylation of FA and other aromatic compounds give di- and tri-hydroxy derivatives of cinnamic acid, which takes part in the lignin formation together with FA. The conversion reactions occur during the formation of FA and other aromatic compounds, which are schematically represented in Figure 1.3.

In vivo studies on FA metabolism suggests that it gets converted into a variety of metabolites such as ferulic acid-sulfate, ferulic acid-glucuronide, ferulic acid-sulfoglucuronide (major metabolites in the plasma and urine of rats), ferulic acid-diglucuronide, dihydroferulic acid, feruloylglycine, vanillic acid, *m*-hydroxyphenylpropionic acid, and vanilloylglycine [Zhao et al. 2003a, 2003b; Zhao and Moghadasian 2008]. The data obtained from these outcomes recommends that the major pathway of FA metabolism is the conjugation reaction with glucuronic acid or sulfate. The conjugation reactions of FA takes place chiefly in the liver through the activities of sulfotransferases and uridine diphosphate (UDP) glucuronosyl transferases, while small amount of conjugation reaction also takes place in the intestinal mucosa and kidney [Zhao et al. 2004; Zhao et al. 2003b; Chang et al. 1993; Kern et al. 2003b].

A small portion of free FA is probably metabolized through the β -oxidation in liver [Chesson et al. 1999]. A study was carried out by Overhage and coworkers with the help of *Pseudomonas sp.* strain HR199 at the end of twentieth century which revealed that the genes involved in the catabolic mechanism of FA were present on a DNA region, which was covered by two EcoRI fragments, E230 and E94, respectively. These genes were *fcs*, *ech*, and *aat* encoding for feruloyl coenzyme A synthetase, enoyl-CoA hydratase/aldolase, and β -ketothiolase, respectively [Overhage et al. 1999].

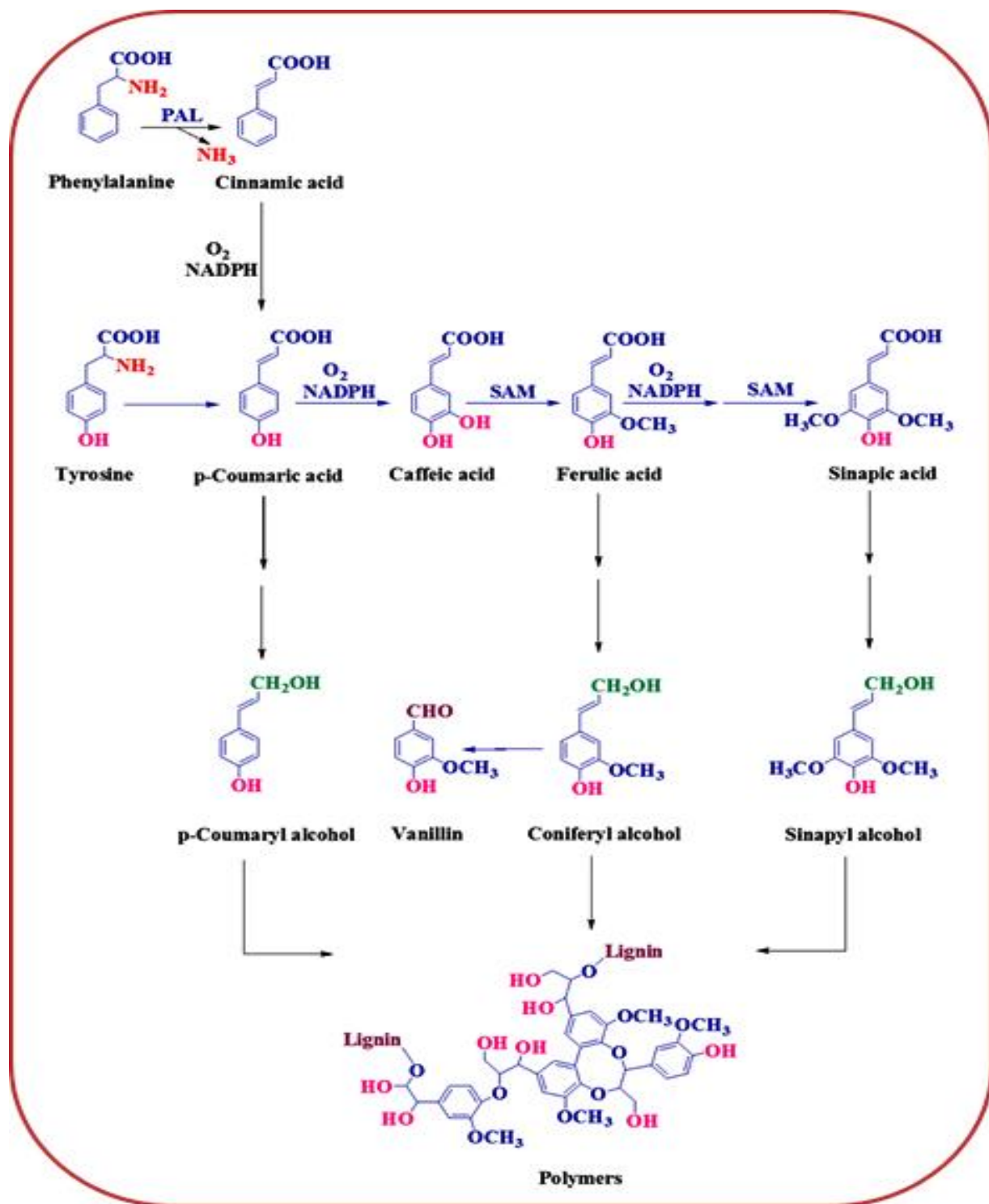


Figure 1.3: Schematic depiction of synthesis of ferulic acid and other aromatic compounds via shikimate pathway {PAL: Phenylalanine ammonia lyase; TAL: Tyrosine ammonia lyase; SAM: S-adenosyl methionine (acts as a methyl donor)}.

Report on the degradation of FA into vanillin and other useful organic compounds through protocatechuate 4,5-cleavage (PCA) pathway in *Sphingomonas paucimobilis* SYK-6 confirmed that FA got converted into feruloyl-CoA by feruloyl-CoA synthetase (FerA), and further into HMPMP-CoA (4-hydroxy-3-methoxyphenyl-β-hydroxypropionyl-coenzyme A) with the help of feruloyl-CoA hydratases/lyases (FerB and FerB2). It subsequently resulted into vanillin with the removal of CH₃COSCoA (acetyl coenzyme A), and finally vanillin transformed into pyruvate and oxaloacetate through the PCA pathway [Masai et al. 2002]. The end products of FA catabolism enter into the TCA (tricarboxylic acid cycle), and produce energy in the biological system as shown in Figure 1.4.

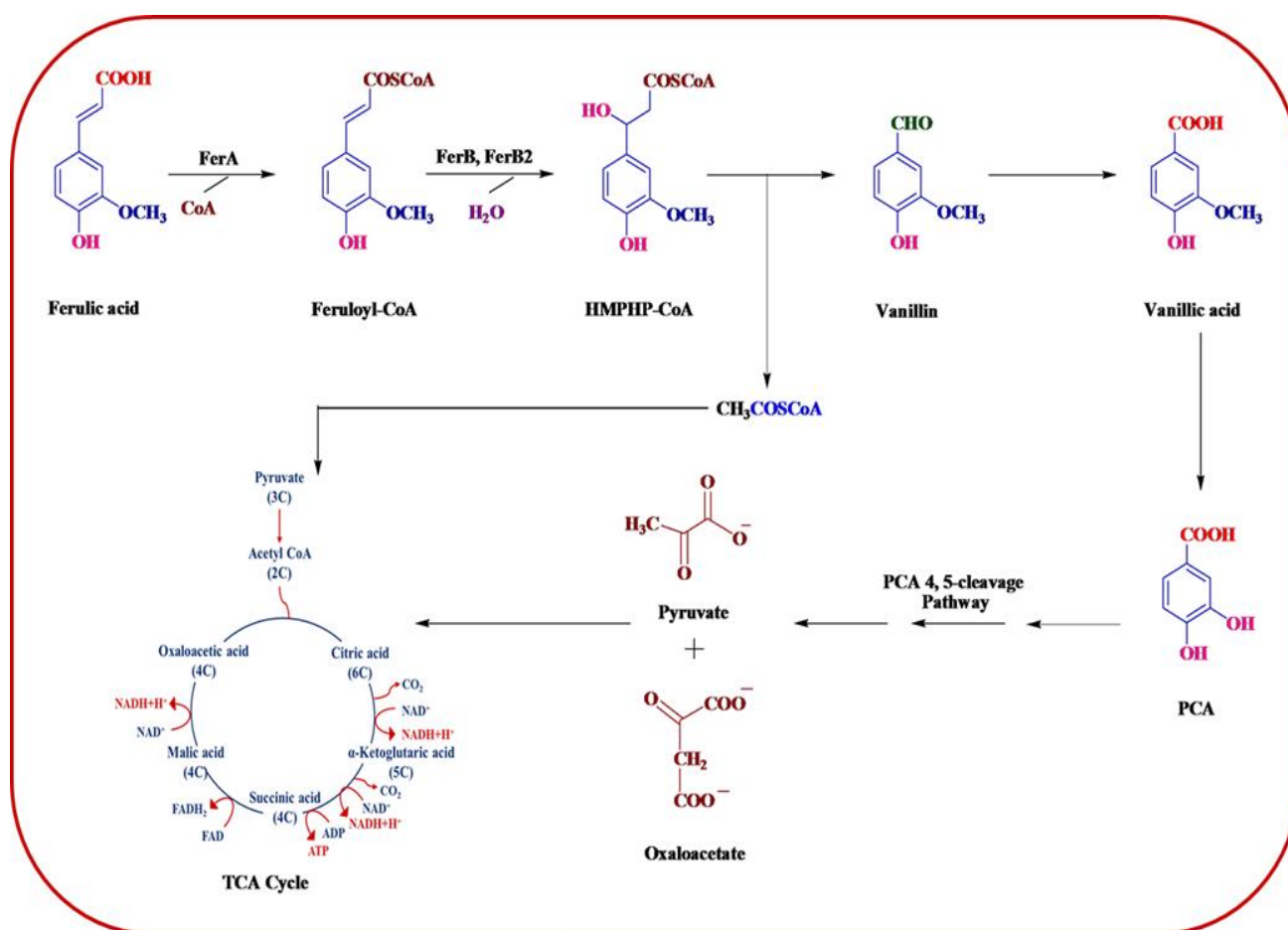


Figure 1.4: Pathway for ferulic acid catabolism in *S. paucimobilis* SYK-6 {HMPMP-CoA: 4-Hydroxy-3-Methoxyphenyl-β-Hydroxypropionyl CoA}.

1.4. Industrial and biological usages of ferulic acid

The biological usages of FA came into notice when a group of Japanese researchers discovered the antioxidant properties of rice oil extracted steryl esters of it [Yagi and Ohishi 1979]. The FA exhibits a wide range of biomedical effects including antioxidant, antiallergic, hepatoprotective, anticarcinogenic, anti-inflammatory, antimicrobial, antiviral, vasodilatory effect, antithrombotic, and helps to increase the viability of sperms [Akihisa et al. 2000; Graf 1992; Ou and Kwok 2004; Rukkumani et al. 2004]. Also it has applications in food preservation as a cross linking agent [Oosterveld et al. 2001], photoprotective constituent in sunscreens and skin lotions [Saija et al. 2000]. An amide derivative of FA, form by the condensation of it with tyramine may be used as an indicator of environmental stress in plants. In baking industry, amides of FA with amino acids or dipeptides are commonly used for the purpose of preservation [Graf 1992]. In many countries, use of FA as food additive has been approved by their government as it affectively scavenges superoxide anion radical, and inhibits the lipid peroxidation [Srinivasan et al. 2007].

1.4.1. Ferulic acid as an antioxidant

Like several other phenols, FA also exhibits antioxidant activity in response to free radicals via donating one hydrogen atom from its phenolic hydroxyl group, as a result it shows strong anti-inflammatory activity in a carrageenan-induced rat paw edema model and other similar systems [Ou and Kwok 2004; Kikuzaki et al. 2002; Natalia et al. 2013]. It has been revealed that the antioxidant capacity of phenolic acid is equivalent to lecithin upon comparison with *Ghee* on inhibition of time dependent peroxide value. The resonance stabilization of FA is the main cause of its antioxidant nature. In addition, the reactive oxygen species of FA show the scavenging effect, which is similar to that of superoxide dismutase [Graf 1992].

1.4.2. Ferulic acid as an anti-diabetic and anti-ageing agent

Diabetes, most widespread endocrine disorder in human beings, is characterized by the over-production of free radicals, hyperglycemia, and oxidative stress [Aragno et al. 2000]. Due to the oxidative stress, an imbalance is started between the levels of pro-oxidants and antioxidants which lead to cellular injury in biological systems [Villa Caballero et al. 2000]. The FA helps in neutralizing the free radicals present in the pancreas, which is produced by the use of streptozotocin, thus it decreases the toxicity of streptozotocin. It has been discussed in literature that the blood glucose level in case of streptozotocin induced diabetic animals is controlled by the administration of FA. The reduction in oxidative stress/toxicity might help the β cells to get proliferate and radiate more insulin in the pancreas. Increased secretion of insulin causes increase in the utilization of glucose from extra hepatic tissues that decreases the blood glucose level [Balasubashini et al. 2004]. Reports are also available on the stimulatory effects of insulin secretion in rat pancreatic RIN-5F cells by FA amide [Nomura et al. 2003].

1.4.3. Ferulic acid as preclusion of food discoloration and growth enhancing agent

FA reduces the bacterial contamination and has been used to maintain the color of green peas, prevent the discoloration of green tea, and oxidation of banana turning black color [Masaji 1999]. FA and γ -oryzanol were found to prevent the photo-oxidation of lutein and astaxanthin in Red Sea Bream [Maoka et al. 2008]. Due to the structural similarity of FA with normetanephrine (first metabolite of norepinephrine), it mimics the stimulatory effect on somatotrophin in pituitary gland and hence enhance the growth [Gorewit 1983].

1.4.4. Ferulic acid as precursor of vanillin

In past years, the occurrence of vanillin as an intermediate in the microbial degradation of FA has been reported by many research groups [Rosazza et al. 1995, Muheim and Lerch 1999; Mathew and Abraham 2006; Hua et al. 2007]. Natural vanillin has a high demand in the flavor market as it is used as a flavoring agent in foods, beverages, pharmaceuticals and other industries [Hagedorn and Kaphammer 1994]. Industries such as chocolate and ice cream together capture about 75% of the total market of vanillin, while the small amount is used in baking. Vanillin is also used in the fragrance industry for the making of good quality of perfumes, in cleaning products, in livestock fodder and pharmaceuticals to cover the unpleasant odors or tastes of medicines. Biosynthesis of vanillin from FA (Figure 1.5) is achieved by the conversion of FA into feruloyl SCoA (reduced feruloyl coenzyme A) using ATP (Adenosine triphosphate) and CoASH (reduced coenzyme A). Removal of water and CH_3COSCoA (reduced acetyl coenzyme A) molecule converts feruloyl SCoA finally into vanillin. In addition of above functions, vanillin can also be used in visualization of components in thin layer chromatography staining plates. These stains give a range of colors for the different components. *Pseudomonas putida* is found to convert the FA to into vanillic acid very efficiently.

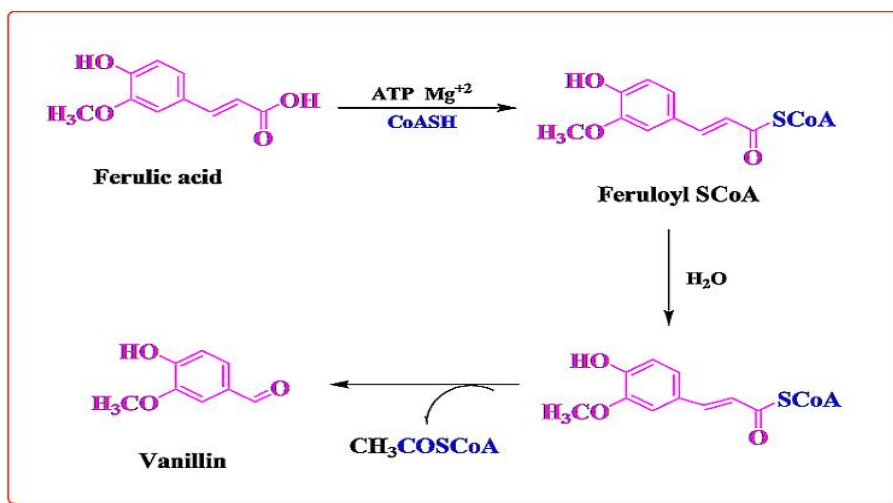


Figure 1.5: Bioconversion of ferulic acid into vanillin.

1.4.5. Uses of ferulic acid in cosmetics

Reactive Oxygen Species (ROS) formation is the main cause of UV-induced skin damage. During the exposure to radiation, a photon interact with *trans*-urocanic acid in skin and generates a singlet oxygen which can activate the entire oxygen free radical cascade with oxidation of proteins, nucleic acid and lipids, that results in the photoaging changes and skin cancer [Barone et al. 2009; Blume 2013]. FA is a strong UV absorber [Graf 1992], and skin absorbs it at the same rate both in acidic or neutral pH conditions [Saija et al. 2000]. FA structure is similar to tyrosine, and it is believed that FA inhibits the melanin formation through competitive inhibition with tyrosine. It gives a considerable protection to the skin in a time dependent manner against the UVB-induced erythema [Saija et al. 2000]. FA by itself or in the aggregation of vitamin C and E provide almost 4-8 times more protection against solar-simulated radiation damage on most likely interacting prooxidative intermediates. Successful photoprotection with solar-simulated ultraviolet induced photodamage was recorded on a pig (*invivo* experiments) by using a mixture of FA (0.5%), vitamin E (1%) and, vitamin C (15%) [Lin et al. 2005].

1.4.6. Ferulic acid as an anticancer agent

In the etiology of cancer, free radical plays a major role; therefore antioxidants present in diet have fastidious consideration as potential inhibitors of abandoned cell growth. FA's anticarcinogenic activity is related to its capability of scavenging ROS and stimulation of cytoprotective enzymes [Barone et al. 2009]. By doing this, FA diminished the lipid peroxidation, rupture of DNA single strand, inactivation of certain proteins, and disruption of biological membranes [Hirose et al. 1999]. Due to the construction of free radicals in leucocytes and other cells, nicotine is supposed to have a key role in the pathogenesis of lung cancer. In 2007 Sudheer and co-researchers worked on rat peripheral blood lymphocytes, and concluded that FA (10-150

μM) counteracted nicotine-induced lipid peroxidation and reduction in GSH (reduced glutathione) level [Sudheer et al. 2007].

Stimulation of detoxification enzyme seems to be another mechanism for the anticarcinogenic action of FA; it enhances the UGTs enzyme (UDP-glucuronosyltransferases) activity, drastically in liver. Due to this reason better detoxification of carcinogenic compounds occurs, and subsequently leads to the prevention of gastrointestinal cancer [Van der Logt et al. 2003]. UGTs catalyzes the conjugation of exogenous and endogenous compounds with glucuronic acid, which results in less biologically active molecules with enhanced water solubility that facilitates the excretion through bile or urine [King et al. 2001]. FA also inhibits the growth of colon cancer cells [Mori et al. 1999]. Further its inhibitory effect on carcinogenesis of colon cancer in rats was confirmed by *in vivo* test [Hudson et al. 2000]. Polyphenols, including FA, comprise tumor-suppression potential in breast cancer cell lines as well [Menendez et al. 2008]. FA has been claimed to decrease the side effects of chemo and radiotherapy of carcinomas by increasing the natural immune defense [Liu 1987].

1.4.7. Pulmonary protection and cardiovascular effect of ferulic acid

Nicotine is one of the major hazardous compounds of cigarette smoke [Warren and Singh 2013]. It causes the oxidative cellular injury by increasing the lipid peroxidation, which is supposed to play a key role in the pathogenesis of several smoking related diseases [Yildiz et al. 1998]. Due to the administration of FA, a reverse reaction occurs in the damage, which was induced by nicotine. FA causes a significant increase in the endogenous antioxidant defense, which protect the cells from oxidative damage. FA protects the membrane by successfully quenching of free radicals from attacking the membrane. It also inhibits the leakage of marker enzymes into circulation, and increase the antioxidant status in circulation [Sudheer et al. 2005]. It has been shown that the blood pressure was decreased in both SHRSP (stroke-prone spontaneously

hypertensive) rats and SHR (spontaneously hypertensive rats) with a maximum effect (-34 mmHg) after 2 hrs of oral intake of FA (1-100 mg/kg body weight) [Ohsaki et al. 2008; Suzuki et al. 2002]. Studies also showed that sodium salt of FA decreases the serum lipids, inhibits platelet aggregation and prevents thrombus formation [Wang et al. 2004].

1.4.8. Ferulic acid as food preservative

Report on the first use of FA as food preservative was done in Japan; to preserve oranges and to inhibit the autoxidation of linseed oil [Tsuchiya and Takasawa 1975]. With the addition of copper (Cu) or iron (Fe), phenolic compounds were also found to stabilize the lard and soybean oil. Mixtures of FA and amino acids or dipeptides (such as glycylglycine or alanylalanine) exert a synergistic inhibitory consequence on the peroxidation of linoleic acid. Complete inhibition of oxidation of biscuits (30°C for 40 days) was done by using the mixture of FA (0.05%) and glycine (0.5%) [Okada et al. 1982].

1.5. Additional applications of ferulic acid

Besides the above discussed functions, it also has key role in numerous other applications. It has been proved by *in situ* experiments that mixture of FA and tetramethylpyrazine showed the synergistic inhibitory effect on spontaneous movement in rat [Ozaki and Ma 1990]. FA utilizes the anthocyanin-type pigments present in tulip flowers having cosmetic properties to stabilize the rouge against oxidative discoloration [Kawai et al. 1990]. FA also increases the stability of cytochrome C, and hence inhibits the apoptosis, which is induced by cytochrome C [Yang et al. 2007]. Recently, *in vitro* and *in vivo* angiogenic activity of FA via stimulation of the VEGF, PDGF and HIF-1 α pathways has been done, and concluded that the angiogenic effects of FA occur via two pathways which are called as PI3K and MAPK pathway. FA is a new potential therapeutic agent for ischemic diseases [Lina et al. 2010]; it also enhances IgE binding to pea nut allergens

[Chung and Champagne 2011]. Different functional role and biomedical applications of FA are schematically represented in Figure 1.6.

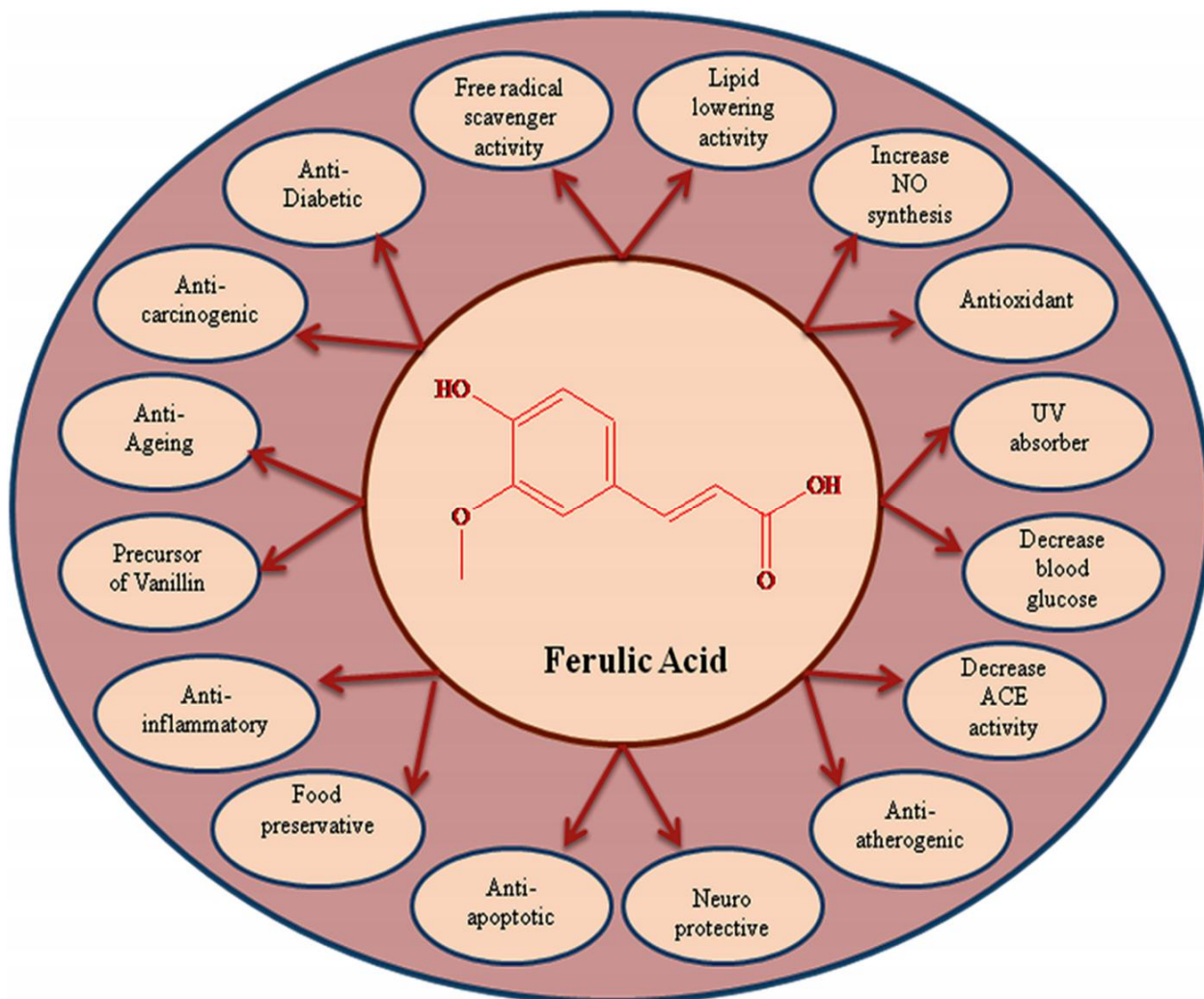


Figure 1.6: Schematic representation of different activities shown by ferulic acid.

It has been proved that FA acts as a β -secretase modulator with therapeutic potential against Alzheimer's disease [Mori et al. 2013], and found to improve the structure and function of the heart, blood vessels, liver, and kidneys in hypertensive rats [Alam et al. 2013]. Uses of FA grafted chitosan as an antioxidant in food, cosmetics, food packaging, biomedical and pharmaceutical is recently discovered [Sarekha and Rangrong 2013]. In plants, environmental

stress can be resolute by the use of FA amides with putrescine, tyramine or tryptamine. FA amides with amino acid or dipeptides are used as preservatives in baking [Graf 1992]. Researchers have also proved that at lower concentration (25-50 μM), FA reduced the cell death in hippocampal neuronal cells induced by peroxy radical, while at higher concentration (250-500 μM), it diminished the hydroxyl radicals induced by protein oxidation and peroxidation of lipid [Kanski et al. 2002]. FA (200 μM) helped in the reduction of lipid peroxidation in peripheral blood mononuclear cells induced by H_2O_2 [Khanduja et al. 2006]. Administration of FA for a very long time inhibits the expression of endothelial and inducible NOS (iNOS) in mouse, hippocampus and rat cortical neurons [Cho et al. 2005; Sultana et al. 2005].

1.6. Concluding remarks

This chapter provides adequate information about the natural sources, synthesis, structure, metabolism, and uses of ferulic acid in biomedical as well as other industries. Industries such as cosmetic, pharmaceutical, baking, ice cream, chocolate, food processing have high demand for FA. Most of the activities as shown by FA can be attributed to its potent antioxidant capacity because of conjugation in its nucleus and side chain. These investigations greatly support the regular ingestion of FA for providing significant protection associated with a range of oxidative stress related disease. Significant efforts have been made for the development of biotechnological processes as the consumption of natural products in food, cosmetics, pharmaceutical and other industries, and are increasing day by day that's why the demand and supply of natural products should be maintained.

CHAPTER-2

Isolation, structural, thermal and quantum chemical studies of p-coumaric, caffeic and ferulic acids from Parthenium hysterophorus L.

1. **Naresh Kumar**, Vikas Pruthi and Nidhi Goel (2015) Structural, Thermal and Quantum Chemical Studies of *p*-coumaric and caffeic acids. Journal of Molecular Structure 1085:242-248.
2. **Naresh Kumar** and Vikas Pruthi (2014) Structural elucidation and molecular docking of ferulic acid from *Parthenium hysterophorus* possessing COX-2 inhibition activity. 3 Biotech (DOI: 10.1007/s13205-014-0253-6).

Isolation, structural, thermal and quantum chemical studies of p-coumaric, caffeic and ferulic acids from Parthenium hysterophorus L.

2.1. Introduction

Structural, thermal and computational studies of three hydroxycinnamic acids viz., *p*-coumaric, caffeic and ferulic acid extracted from *Parthenium hysterophorus* L. have been carried out in this chapter. *Parthenium hysterophorus* L. is an annual herbaceous, exotic weed which belongs to the asteraceae family. It grows abundantly in agricultural lands, orchards, forest lands, overgrazed pastures, flood plains, wasteland, around residential colonies, railway tracks and along roadsides [Patel 2011]. This noxious weed was introduced in India with the contaminated PL-480 wheat, imported from USA in 1950s. Exposure to *P. hysterophorus* L. manifests the symptoms of hay fever, eczema, skin inflammation, allergic rhinitis, black spots, burning, asthma, blisters around eye, diarrhoea, breathlessness, severe papular erythematous eruptions and choking in human [Maishi et al. 1998]. This weed was reported to cause systemic toxicity in livestock like irreparable damage to liver and kidney, inhibit liver dehydrogenases in buffalo and sheep [Gunaseelan, 1987; Rajkumar et al., 1988]. However, some useful compounds like caffeic, *p*-coumaric, ferulic, vanillic and *p*-anisic acids are also present in it which has been exploited for their biomedical applications [Ferguson et al., 2005; Kikugawa et al., 1983]. There is need to do the utilization-oriented research on this weed. Moreover, several authors envision *Parthenium* as a green manure, compost, biopesticide, nanomedicines, scavenging agents for the bio-treatment of toxic metals, dyes and non-renewal energy source (eco-friendly green fuel) etc. None of them attempted to isolate the hydroxycinnamic acids so far. Structural, thermal and computational

studies of hydroxycinnamic acids like *p*-coumaric, caffeic and ferulic extracted from *Parthenium hysterophorus* L. have been carried out in this chapter. This work attains its pristine nature as the statistical study for the comparison of the experimental and the theoretical data.

2.2. Experimental section

2.2.1. Materials

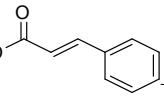
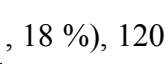
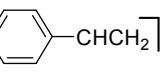
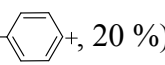
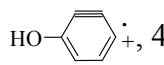
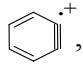
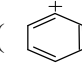
Plant samples have been collected from area nearby Indian Institute of Technology Roorkee and approved by Forest Research Institute (FRI), Dehradun, India as *Parthenium hysterophorus* L. Whole plant samples were thoroughly washed with boiled distilled water and its stem, leaves and flowers were separately collected. Samples were dried under sunlight and kept in oven at 35°C for 24 hrs. The dried samples were ground to powder for experimental analysis. All the chemicals and reagents were analytical quality purchased from Himedia (Mumbai, India) and used without purification.

2.2.2. Extraction and purification

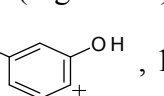
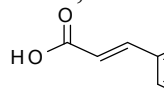
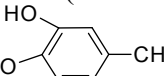
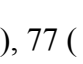
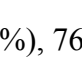
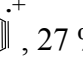
The extraction of above mentioned acids has been carried out by following the literature method with some modifications [Tilay et al. 2008]. Briefly, the plant root, stem, and leaves (2.0 g each) were separately taken in 250 ml round bottom flasks charged with NaHSO₃ (0.001 g) and 60 ml NaOH (2M), and were shaken at 180 rpm at 25°C for 24 hrs. The flasks were then centrifuged at 12,000 rpm for 10 min and supernatant obtained were acidified. Each sample was treated with three volumes of ethyl acetate and subsequently mixed with equal volume of acetonitrile/water for chromatographic analysis. The band of each compound from TLC plate was scraped out and dissolved in 2.0 ml acetonitrile for further purification by HPLC, in which an isocratic procedure was applied, by maintaining a mobile phase of acetonitrile/water (80:20) and 0.1% acetic acid,

20.0 μl injection volume and 1.0 ml/min flow rate [Zupfer et al. 1998]. Purified compounds have been collected, dried and stored for further experimental analysis.

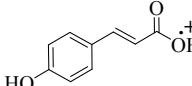
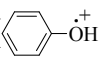
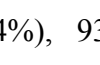
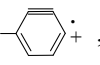
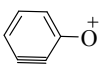
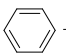
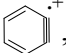
2.2.2.1. *p*-Coumaric acid (PCA)

m.p. 216-218°C, Anal. Calcd. (%) for $\text{C}_9\text{H}_8\text{O}_3$ (164.16): C, 65.85; H, 4.91; Found: C, 63.89; H, 4.79. FT-IR (KBr, cm^{-1}) ν_{max} : 3373.31 (OH strch.), 3074.25 (Ar C-H strch.), 1671.61 (C=O), 1627, 1510, 1449, 1245.66 (C-O), 1171, 900-645 (Ar). $^1\text{H-NMR}$ (500 MHz, $\text{DMSO-}d_6$, ppm, Figure 2.1) δ : 6.268-6.300 (d, 1H, $J = 16\text{Hz}$, Ar), 6.775-6.792 (d, 2H, $J = 8.5\text{Hz}$, Ar), 7.473-7.519 (t, 3H, $J = 8\text{Hz}$, $J = 15\text{Hz}$, Ar), 9.823-9.966 (s, 1H, -OH exch), 12.137 (s, 1H, -COOH exch). $^{13}\text{C-NMR}$ (125 MHz, $\text{DMSO-}d_6$, ppm, Figure 2.2) δ : 115.018, 115.353, 127.211, 127.788, 148.678, 157.207, 170.210. GC-MS (Figure 2.3) m/z : 165 ($\dot{\text{M}}^+_{+1}$, 1.4 %), 164 ($\dot{\text{M}}^+$, 34 %), 163 ($\dot{\text{M}}^{-1}$, 3 %), 147 (, 18 %), 120 (, 15 %), 94 (, 5 %), 93 (, 20 %), 92 (, 4 %), 76 (, 100 %), 75 (, 32 %).

2.2.2.2. Caffeic acid (CA)

m.p. 236-238°C, Anal. Calcd. (%) for $\text{C}_9\text{H}_8\text{O}_4$ (180.16): C, 60.00; H, 4.48; Found: C, 58.98; H, 4.37. FT-IR (KBr, cm^{-1}) ν_{max} : 3433.43 (OH strch.), 3025.21 (Ar C-H strch.), 1644.28 (C=O), 1619, 1526, 1449, 1279 (C-O), 1217, 902-650 (Ar). $^1\text{H-NMR}$ (500 MHz, $\text{DMSO-}d_6$, ppm, Figure 2.4) δ : 6.146-6.178 (d, 1H, Ar- C_2 , $J = 16\text{Hz}$), 6.742-6.758 (d, 1H, $J = 8.0\text{Hz}$, Ar), 6.947-6.967 (dd, 1H, $J = 9\text{Hz}$, $J = 16\text{Hz}$, Ar), 7.014-7.018 (d, 1H, $J = 2\text{Hz}$, Ar), 7.389-7.421 (d, 1H, $J = 16\text{Hz}$, Ar), 9.140 (s, 1H, -OH exch), 9.540 (s, 1H, -OH exch), 12.119 (s, 1H, -COOH exch). $^{13}\text{C-NMR}$ (125 MHz, $\text{DMSO-}d_6$, ppm, Figure 2.5) δ : 113.211, 116.008, 117.455, 120.882, 129.118, 145.145, 147.678, 148.207, 170.110. GC-MS (Figure 2.6) m/z : 181 ($\dot{\text{M}}^+_{+1}$, 1.2 %), 180 ($\dot{\text{M}}^+$, 35 %), 179 ($\dot{\text{M}}^{-1}$, 3 %), 163 (, 11 %), 146 (, 18 %), 137 (, 13 %), 78 (, 38 %), 77 (, 100 %), 76 (, 27 %).

2.2.2.3. Ferulic acid (FA)

m.p. 173-175°C, Anal. Calcd. (%) for C₁₀H₁₀O₄ (194.18): C, 61.85; H, 5.19. Found: C, 61.57; H, 5.09. FT-IR (KBr, cm⁻¹) v_{max}: 3437 (OH strch.), 3080-3030 (Ar C-H strch.), 1689 (C=O), 1278 (C-O), 900-650 (Ar). ¹H-NMR (500 MHz, DMSO-*d*₆, ppm, Figure 2.7) δ: 3.815 (s, 3H, -OCH₃), 6.349-6.381 (d, 1H, *J* = 16Hz, Ar), 6.780-6.797 (d, 1H, *J* = 8.5Hz, Ar), 7.074-7.093 (dd, 1H, *J* = 1.5 Hz, *J* = 8Hz, Ar), 7.280-7.282 (d, 1H, *J* = 1Hz, Ar), 7.472-7.504 (d, 1H, *J* = 16Hz, Ar), 9.568 (s, 1H, -OH exch), 12.140 (s, 1H, -COOH exch). ¹³C-NMR (125 MHz, DMSO-*d*₆, ppm, Figure 2.8) δ: 56.231, 111.684, 116.044, 116.162, 123.363, 126.302, 145.058, 148.447, 149.615, 168.524. GC-MS (Figure 2.9) *m/z*: 195 (\dot{M}^+ , 0.1%), 194 (\dot{M}^+ , 53%), 193 (\dot{M}^+-1 , 0.1%), 164 (, 10%), 94 (, 4%), 93 (, 8%), 92 (, 10%), 91 (, 16%), 77 (, 100%), 76 (, 6%).

2.2.3. Instrumentation

Crystallized *p*-coumaric, caffeic and ferulic acids were carefully dried under vacuum for several hrs prior to elemental analysis by Elementar Vario EL III analyzer. The FT-IR spectra were recorded in KBr pellets on a Perkin-Elmer-1600 series FT-IR Spectrometer. The ¹H-NMR spectra were obtained on Avance 500 Bruker Biospin Intl 500 MHz with Fourier transform technique by using tetramethylsilane as an internal standard. The single crystal X-ray diffraction data for titled compounds was collected on a Bruker Kappa-CCD diffractometer using graphite monochromated MoK α radiation ($\lambda=0.71070$ Å) at 100 K. For data reduction, Lorentz and polarization corrections, empirical absorption corrections were applied [Sheldrick 1996]. Crystal structures were solved by direct methods. Structure solution, refinement, and data output were carried out with the SHELXTL program [Sheldrick 1990, 2000]. Non-hydrogen atoms were refined anisotropically. The hydrogen atoms were placed in geometrically calculated positions by

using a riding model. DIAMOND software was used for image drawing [Brandenburg 1999]. Thermogravimetry (TG), differential thermal analysis (DTA) and derivative thermogravimetry (DTG) were carried out by using a mass of 0.045g at 10°C/min under the nitrogen at 200 ml/min flow rate on a thermogravimetric analyzer (PerkinElmer's, California, USA).

2.2.4. Quantum chemical calculations and statistical analysis

The quantum chemical calculations for PCA, CA and FA have been performed by DFT with a hybrid function B3LYP at 6-311G** basis set using Berny method with the help of Gaussian 09 program [Becke 1993; Stephens et al. 1994; Peng et al. 1996; Frisch et al. 2009]. The Gauss View 5.0 has been used for visualizing the optimized geometries of molecules and for the comparison of structural parameters viz., bond lengths and bond angles obtained from the optimized structure with the crystallographic one. The mathematical relationship between experimental and theoretically computed data for structural parameters has been finding out by the curve fitting analysis using MATLAB R2010a toolbox. The calculations for other parameters like dipole moment, total energy, HOMO-LUMO energy, electronegativity, chemical hardness, chemical softness, electronic chemical potential and electrophilic index have also been carried out by using Koopmans theorem [Koopmans 1934].

2.3. Results and discussion

2.3.1. Extraction and purification

Isolation of titled compounds from *Parthenium hysterophorus* was carried out by alkali treatment method followed by chromatographic (TLC and HPLC) analysis. The TLC chromatogram of samples with commercially procured *p*-coumaric, caffeic and ferulic acids (Sigma Aldrich) indicates the presence of each acid in each sample. The HPLC analysis of TLC spots of titled compounds was done for further purification. The content of titled acids per 100 gm

of whole plant was found to be 115-120 mg (*p*-coumaric acid), 90-110 mg (caffeic acid) and 145-160 mg (ferulic acid), respectively.

2.3.2. Spectroscopic analysis

As compared to the free carboxylic acid (C=O stretch at 1760-1690 cm^{-1} , O-H stretch at 3000-2500 cm^{-1} , C-O stretch from 1320-1210 cm^{-1} , O-H bend from 1440-1395 and 950-910 cm^{-1}), the C=O stretching was appeared at 1671.67, 1644.89 and 1689.49, O-H stretching at 2826.32, 3025.74 and 2930.80 cm^{-1} , C-O stretching at 1283.02, 1352.74 and 1321.74 cm^{-1} , while O-H bending was observed at 1449.77, 1449.92 and 1460.87 cm^{-1} in isolated PCA, CA and FA, respectively. The shifting of stretching in phenolic O-H (3550-3200 cm^{-1}) has been seen at 3373.31, 3433.63 and 3437.17 in PCA, CA and FA, respectively. The observed shifting in the peaks i.e., decrease in wavenumber was due to the H-bonding. So from the spectra, it is clear that ferulic acid and caffeic acids show the intermolecular and intramolecular hydrogen bonding, respectively, while *p*-coumaric acid does not show any H-bonding. In ^1H -NMR spectra, very fewer changes in chemical shift were observed in carboxylic acid of all the hydroxycinnamic acids. The spectroscopic results reported previously are also in line with our results of PCA, CA and FA [Kulik et al. 2009; Swisłocka et al. 2012; Xing et al. 2012; Sajjadi et al. 2012]. The NMR (^1H and ^{13}C -NMR) and GC mass spectra of these acids are given in Figure 2.1 to 2.9.

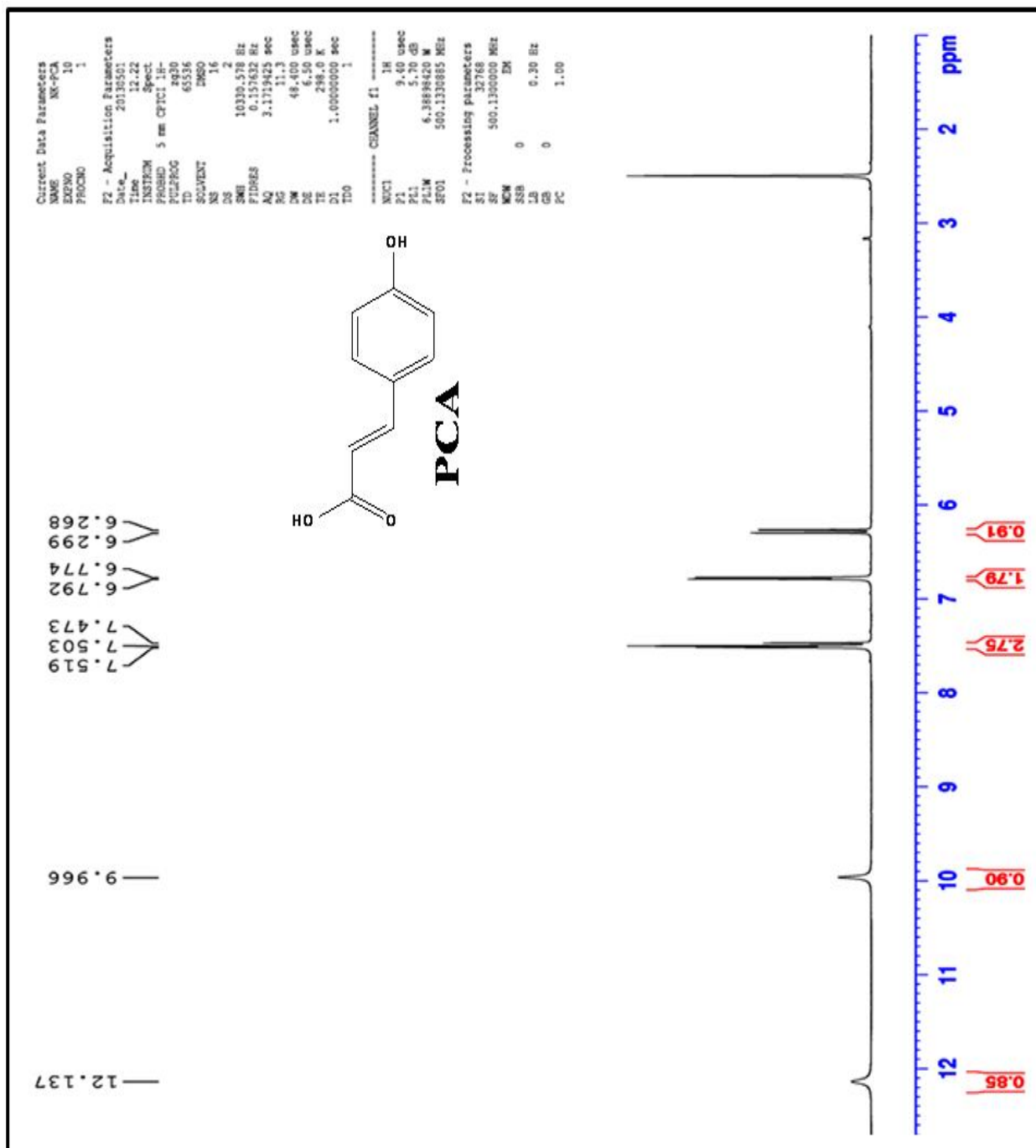


Figure 2.1: ¹H-NMR spectrum of *p*-coumaric acid isolated from *Parthenium hysterophorus* L.

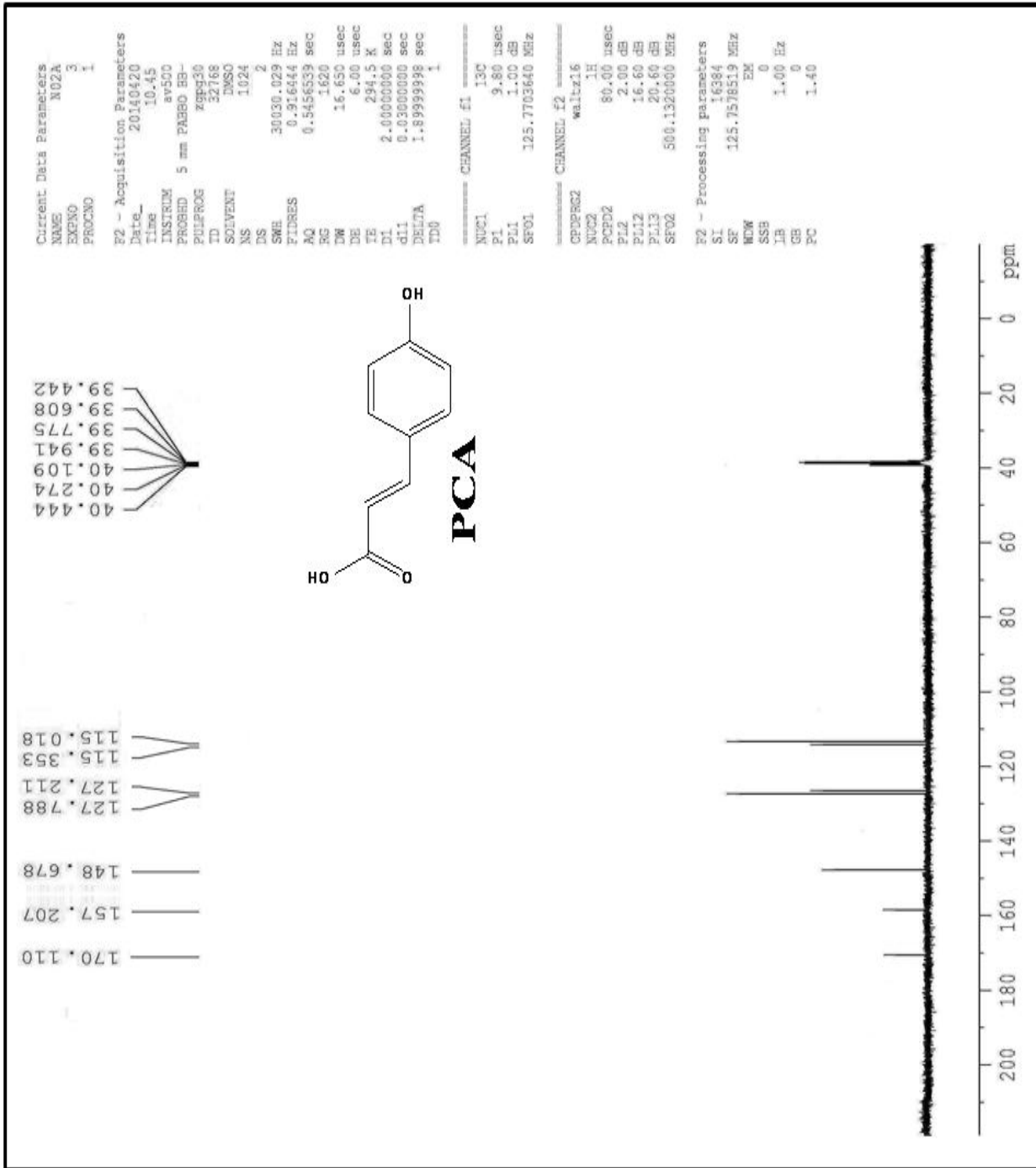


Figure 2.2: ¹³C-NMR spectrum of *p*-coumaric acid isolated from *Parthenium hysterophorus* L.

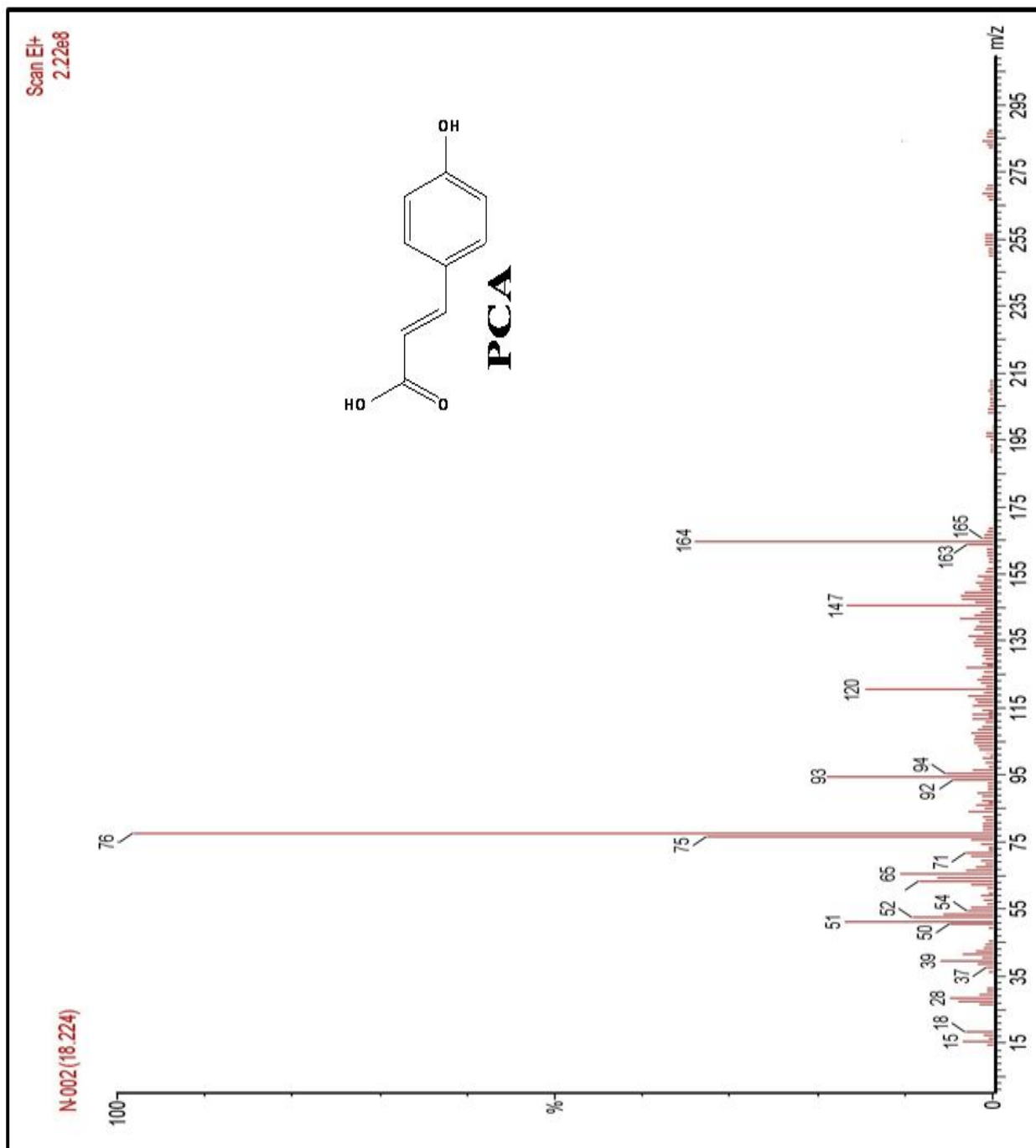


Figure 2.3: GC-Mass spectrum of *p*-coumaric acid isolated from *Parthenium hysterophorus* L.

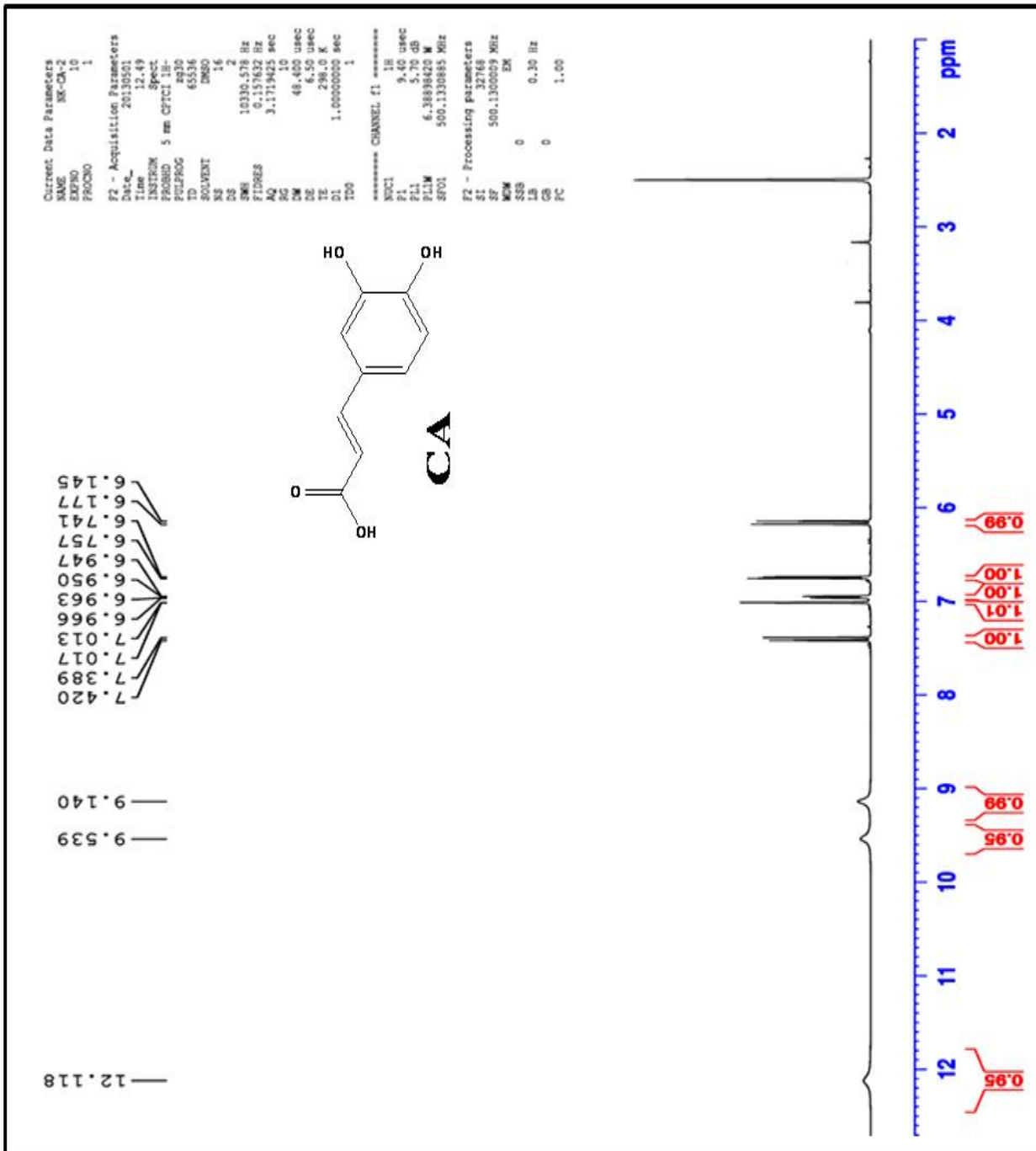


Figure 2.4: ¹H-NMR spectrum of caffeic acid isolated from *Parthenium hysterophorus* L.

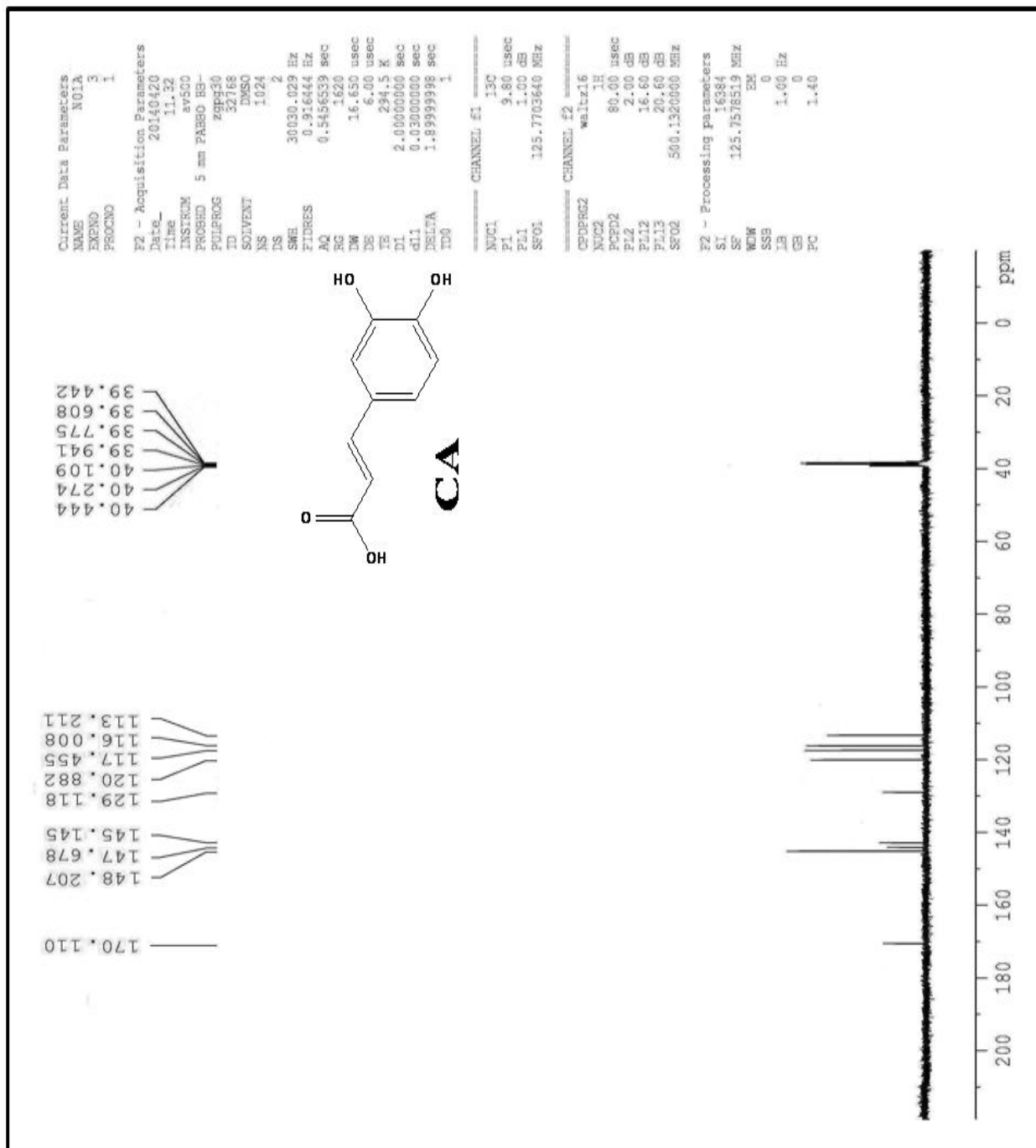


Figure 2.5: ¹³C-NMR spectrum of caffeic acid isolated from *Parthenium hysterophorus* L.

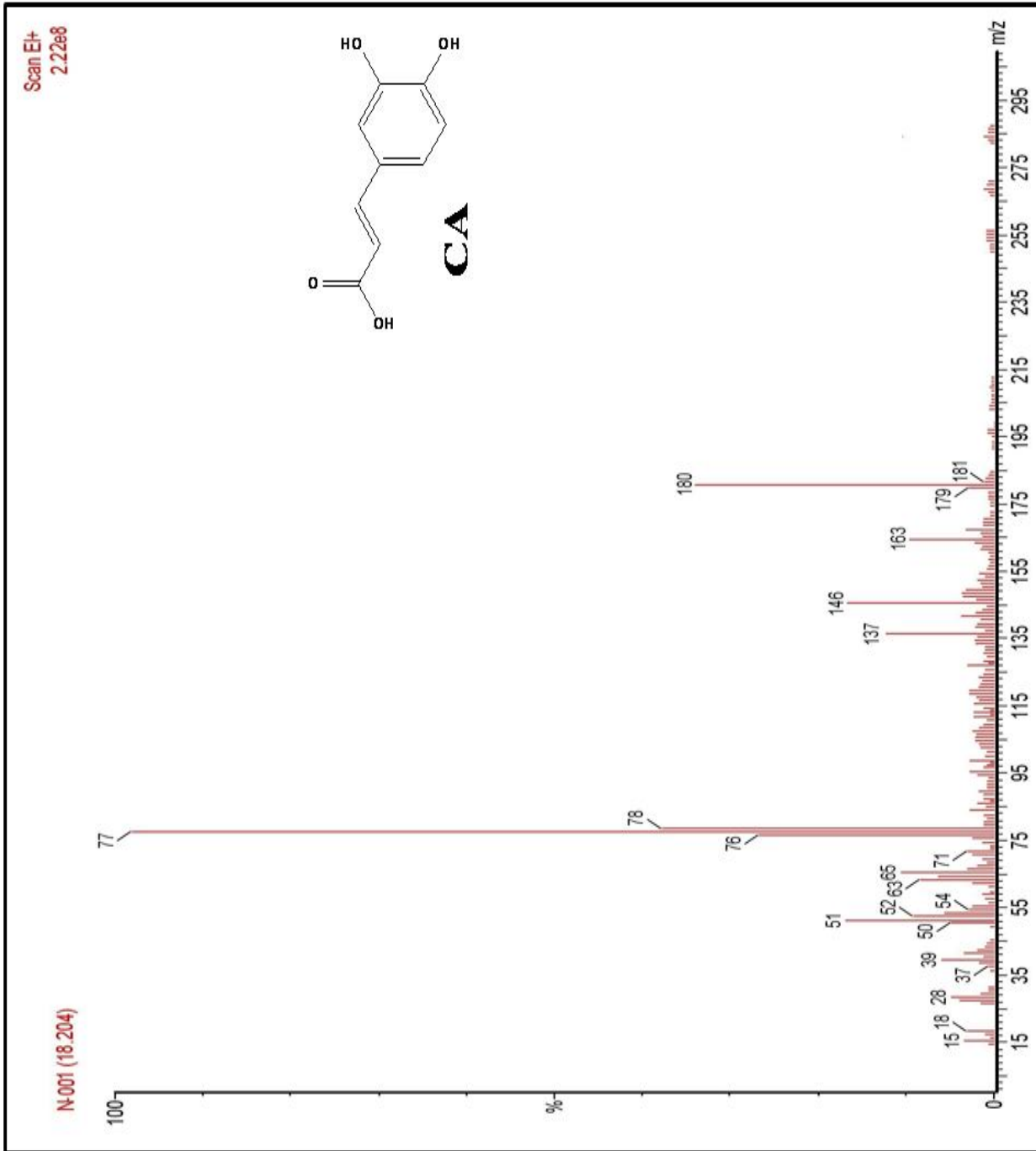


Figure 2.6: GC-Mass spectrum of caffeic acid isolated from *Parthenium hysterophorus* L.

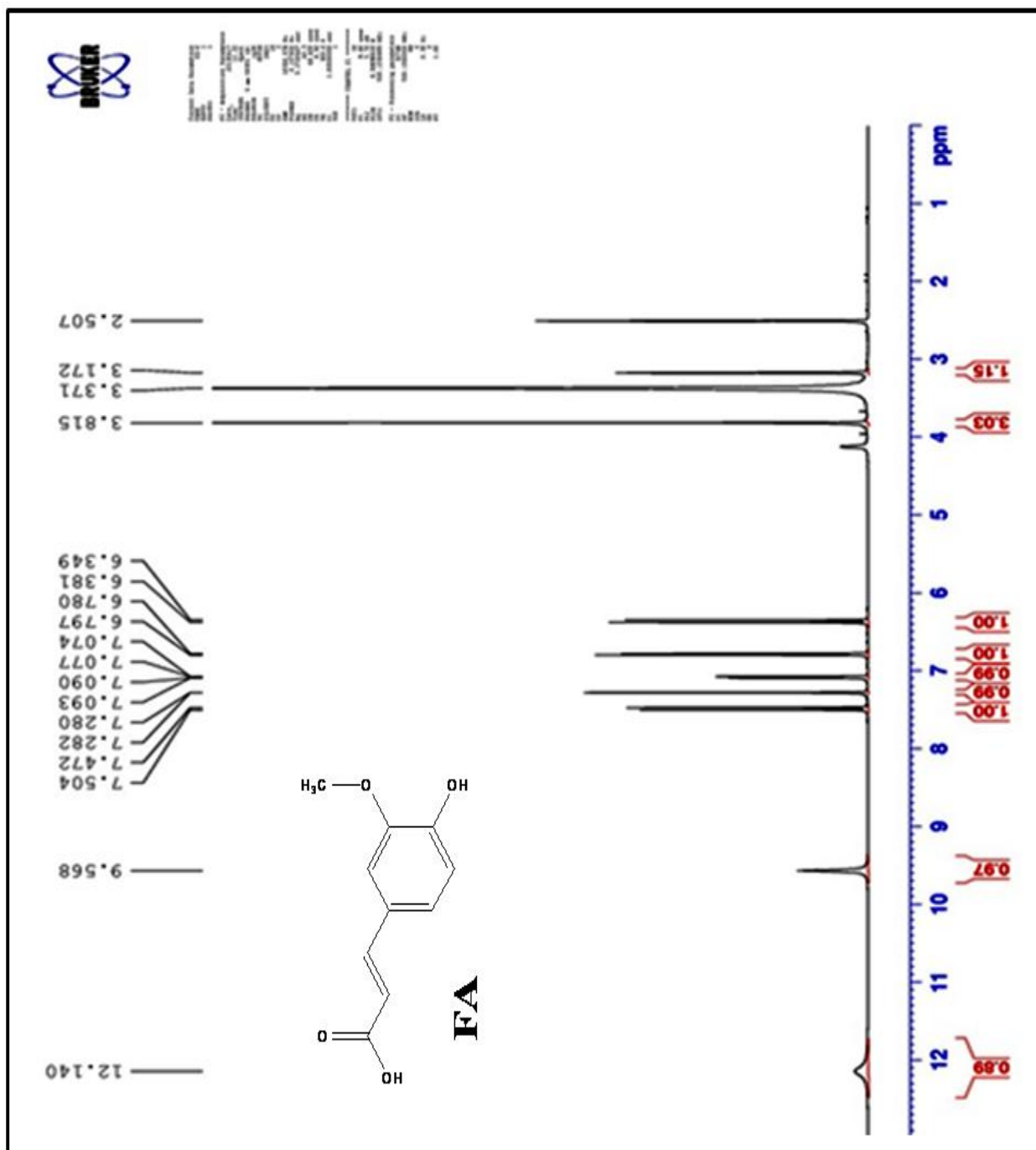


Figure 2.7: ¹H-NMR spectrum of ferulic acid isolated from *Parthenium hysterophorus* L.

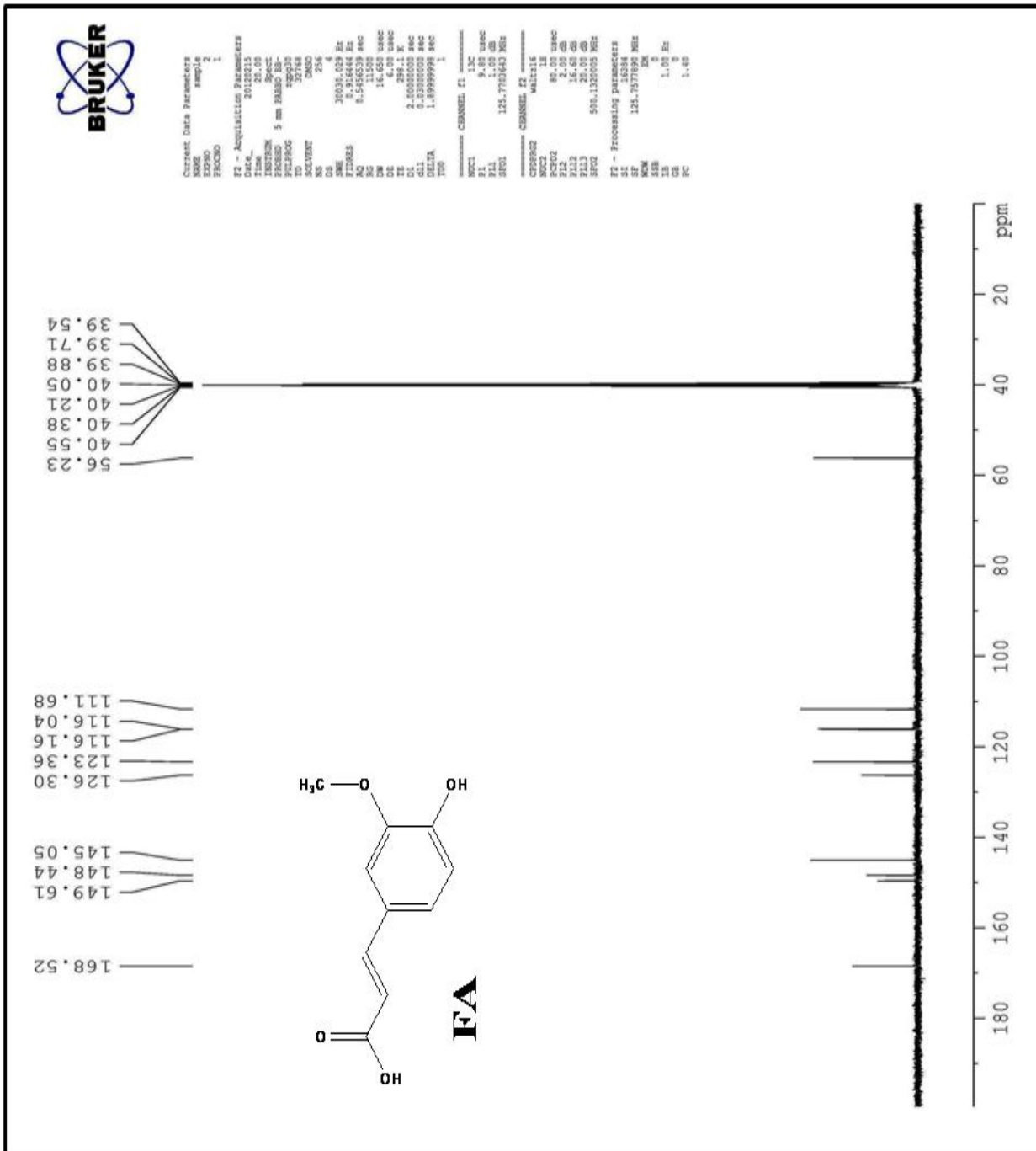


Figure 2.8: ¹³C-NMR spectrum of ferulic acid isolated from *Parthenium hysterophorus* L.

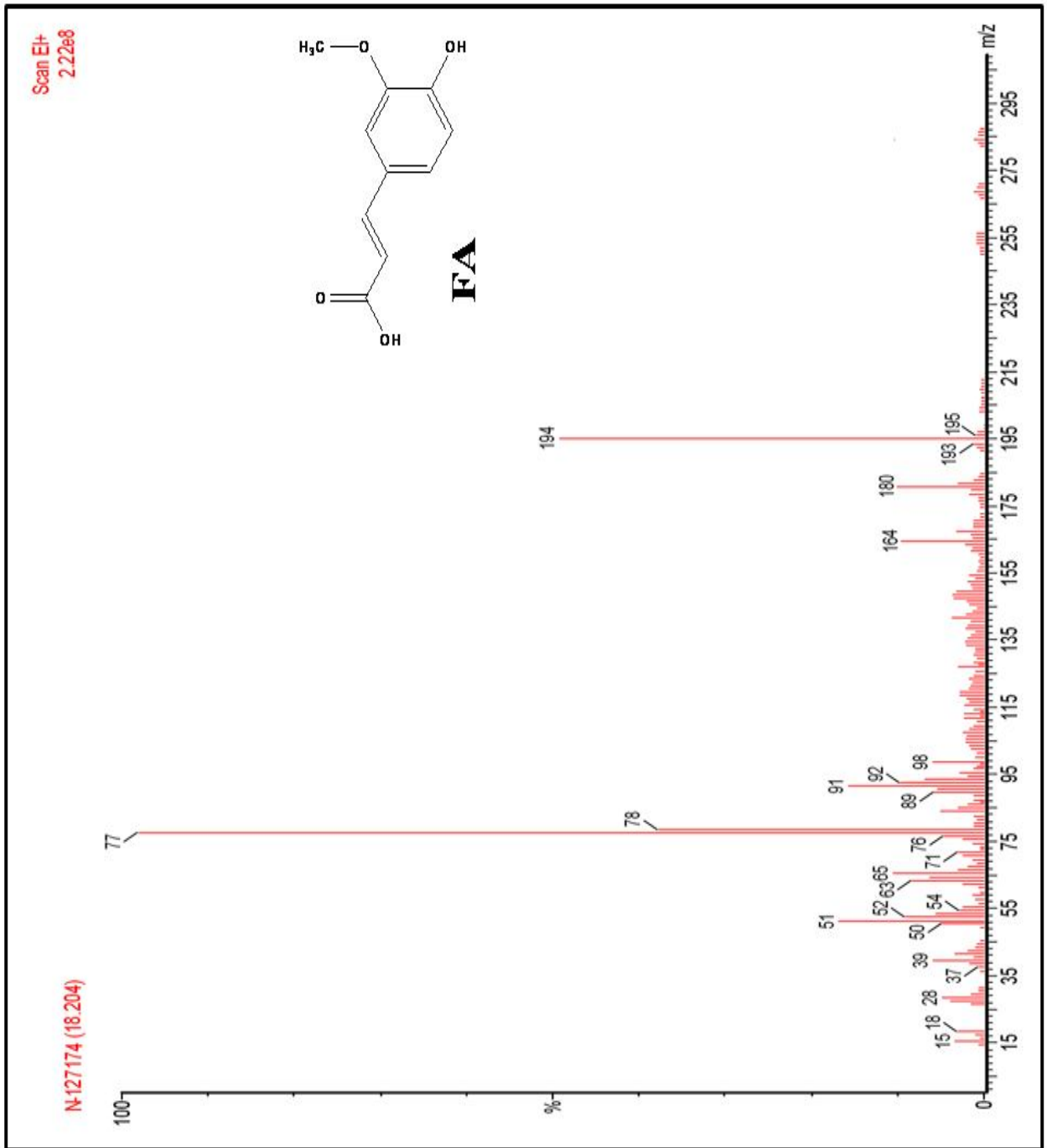


Figure 2.9: GC-Mass spectrum of ferulic acid isolated from *Parthenium hysterophorus* L.

2.3.3. Crystal structure description

Molecular structures of the above acids were confirmed by single crystal X-ray diffractometer, which showed that *p*-coumaric acid crystallizes in the monoclinic crystal system with space group *P 21/c*, and rest of the two hydroxycinnamic acids (caffeic and ferulic) were crystallized in the monoclinic crystal system with space group *P 21/n* (Figure 2.10). Refinement parameters and the crystallographic data for these compounds are given in Table 2.1.

Compounds	<i>p</i> -Coumaric acid	Caffeic acid	Ferulic acid
Formula	C ₉ H ₈ O ₃	C ₉ H ₈ O ₄	C ₁₀ H ₁₀ O ₄
Formula weight	164.15	180.15	194.18
Crystal System	Monoclinic	Monoclinic	Monoclinic
Space Group	<i>P 21/c</i>	<i>P 21/n</i>	<i>P 21/n</i>
<i>a</i> (Å)	8.7126(4)	6.7041(10)	4.6452(2)
<i>b</i> (Å)	5.2604(2)	5.7865(10)	16.8406(6)
<i>c</i> (Å)	17.2083(8)	21.1768(5)	12.0347(4)
α (°)	90.00	90.00	90.00
β (°)	99.68(2)	93.91(10)	90.139(2)
γ (°)	90.00	90.00	90.00
<i>V</i> (Å ³)	777.44(6)	819.60(3)	941.45(6)
<i>Z</i>	4	4	4
<i>D</i> _{Calc} (g/cm ³)	1.403	1.460	1.370
μ (Mo K α) (cm ⁻¹)	0.106	0.116	0.107
<i>F</i> (000)	344.0	376.0	408.0
Crystal size	0.27x0.23x0.18	0.29x0.24x0.17	0.31x0.27x0.23
Theta range for data collection (°)	2.37-30.27	3.13-28.25	2.08-26.44
No. of measured reflections	2295	2018	1930
No. of observed reflections	1749	1656	1581
Data/restraints/parameters	2295/0/111	2018/0/121	1930/0/130
Goodness-of-fit	0.712	0.659	1.230
Final R indices [<i>I</i> > 2(<i>I</i>) ^a R ₁	0.0437	0.0398	0.0413
^b wR ₂	0.1206	0.1066	0.1469
CCDC	945006	945005	909271
^a R ₁ = $\sum \ F_o\ - \ F_c\ / \sum \ F_o\ $, ^b wR ₂ = $\{\sum [w(F_o^2 - F_c^2)^2] / \sum w(F_o^2)^2\}^{1/2}$			

Table 2.1: Crystallographic data collection and refinement parameters for *p*-coumaric, caffeic and ferulic acids.

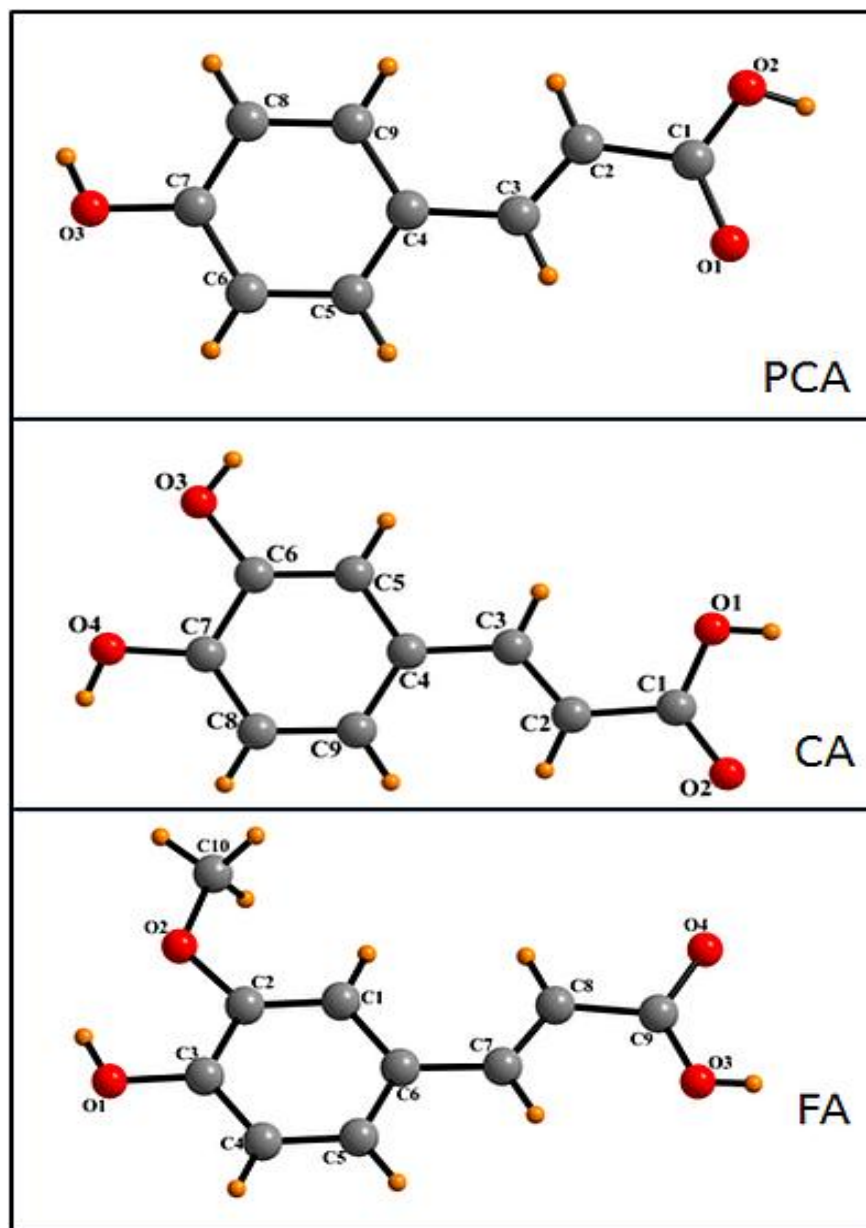


Figure 2.10: Ball & stick models of the solid state single crystal structure of PCA, CA and FA. Color code: C, grey; H, orange; O, red.

In ferulic acid, the crystal packing shows that the dominant O-H...O hydrogen bond is formed via the interaction of OH of -COOH group of one molecule with the oxygen atom of the C=O group of adjacent molecule and vice-versa forming a dimer which is responsible for the formation of $R_2^2(8)$ motif (Figure 2.11) via strong [O3-H3...O4, 1.882(1) Å] non-covalent intramolecular interactions (Table 2.2).

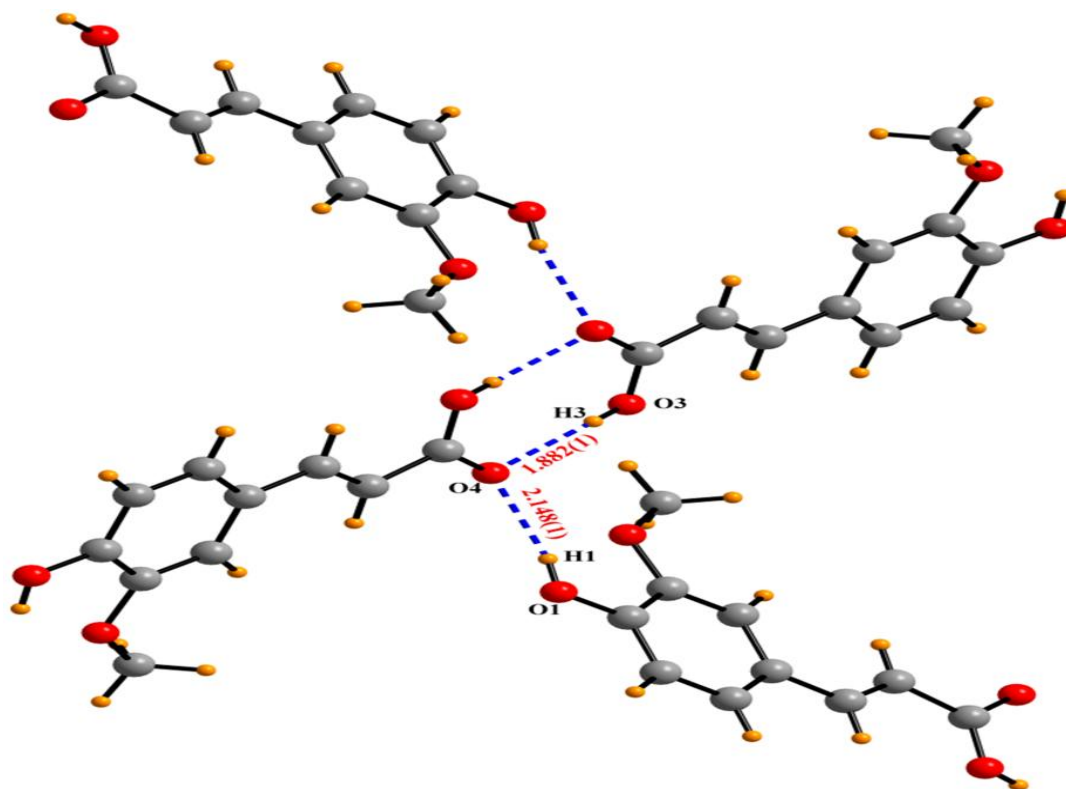


Figure 2.11: Various O-H...O non-covalent interactions in ferulic acid.

D-H...A	d(D-H)	d(H-A)	d(D-A)	<(DHA)>
O1-H1...O4	0.821	2.148 (1)	2.898	152.0
O3-H3...O4	0.820	1.882(1)	2.637	152.6

Table 2.2: Non-covalent interactions for ferulic acid [Distances (Å) Angles (°)].

On the other side, the phenolic group (-OH) of ferulic acid also exhibits a strong O-H...O [O1-H1...O4, 2.148 (1) Å] non-covalent interaction with the C=O group of adjacent acid molecule (Figure 2.11). All the interactions are involved in the formation of three dimensional (3-D) zig-zag views of ferulic acid obtained from crystallographic data, are depicted in Figure 2.12.

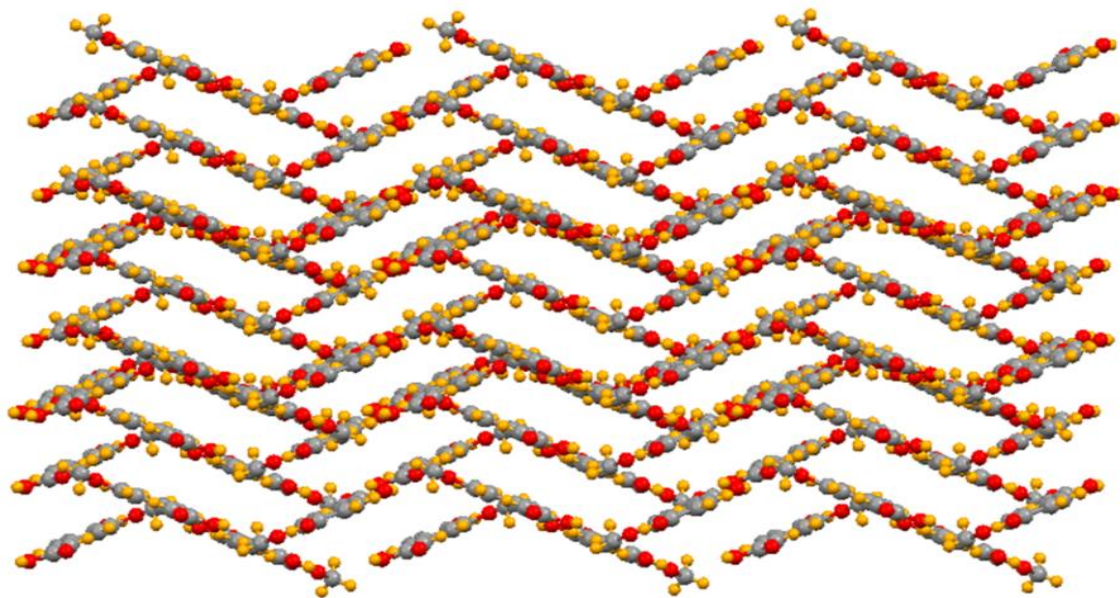


Figure 2.12: Three dimensional zig-zag views representing the arrangement of atom present in ferulic acid.

2.3.4. Thermal analysis

The thermal stability of the PCA, CA and FA is demonstrated by TG-DTA-DTG study. The TGA-DTG curves are shown in Figure 2.13, and thermo-analytical data for these acids are listed in Table 2.3. The thermograms clearly indicate that these acids are stable up to 100°C but at higher temperatures, curves shows irregular pattern. All three acids have undergone in one stage thermal decomposition during thermal analysis. The *p*-coumaric acid consists of 98.3% mass loss in one step, which corresponds to DTG peak at 224°C. In this step *p*-coumaric acid (198-407 °C) releases endothermically at 221°C. The thermal decomposition of caffeic acid at temperature range 201-427°C predicts the weight loss of 97.6 % with the DTG peak at 232°C due to its endothermic decomposition at 231°C, while the decomposition of ferulic acid occurs in one step and leaves out with 99.1% weight loss (DTG peak at 260°C) in between 200-432°C, corresponds to endotherm at 173°C in DTA thermogram.

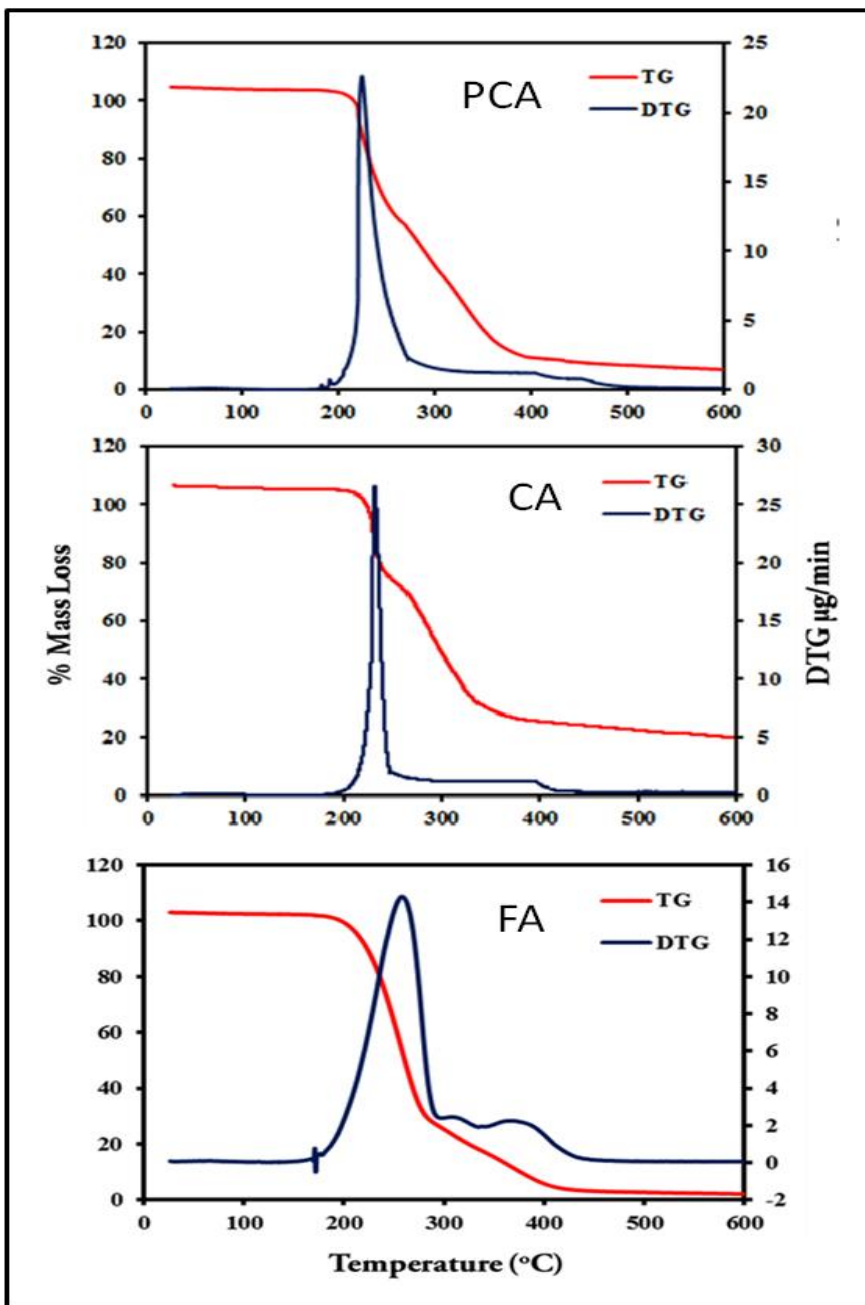


Figure 2.13: Simultaneous TG-DTG analysis curves of *p*-coumaric, caffeic and ferulic acids.

Compounds name	Stage	TG		DTA		DTG
		T range /°C	Observed mass loss (%)	Peak temp/ °C	nature	Peak temp/ °C
<i>p</i> -coumaric acid	I	198-407	98.3	221	Endo	224
Caffeic acid	I	201-427	97.6	231	Endo	232
Ferulic acid	I	200-432	99.1	173	Endo	260

Table 2.3: TG-DTA-DTG data of *p*-coumaric, caffeic and ferulic acids.

2.3.5. Geometry optimization and statistical analysis

The optimized geometries of PCA, CA and FA showed positive harmonic vibrational frequencies, which indicate that, it attains a global minimum on the potential energy surface. The optimized geometries (Figure 2.14) found to possess degree of freedom (54, 57 and 66), total energy (-573.605, -648.842 and -688.012 Hartree), dipole moment (3.21, 2.49 and 3.22 Debye) in PCA, CA and FA, respectively and this agrees with the structure, obtained from single crystal X-ray diffraction. The comparison between experimental and simulated structural parameters such as bond lengths and bond angles is provided in Table 2.4 and 2.5. From the statistical analysis of both the data, it was found that the value of correlation coefficient (R) for structural parameters is 0.985, 0.992, 0.984, 0.975, and 0.913, 0.933 in PCA, CA and FA, respectively. The statistical analysis has been performed to validate the theoretical data with the experimental one [Sharma et al. 2009; Kumar and Bhalla 2011; Kanwar et al. 2012; Devi et al. 2013] and the plots for curve-fitting analysis are displayed in Figure 2.15 and 2.16, respectively. The results of spectroscopic analysis and structural parameters clearly show that the data obtained from theoretical simulation are in accordance with those obtained experimentally.

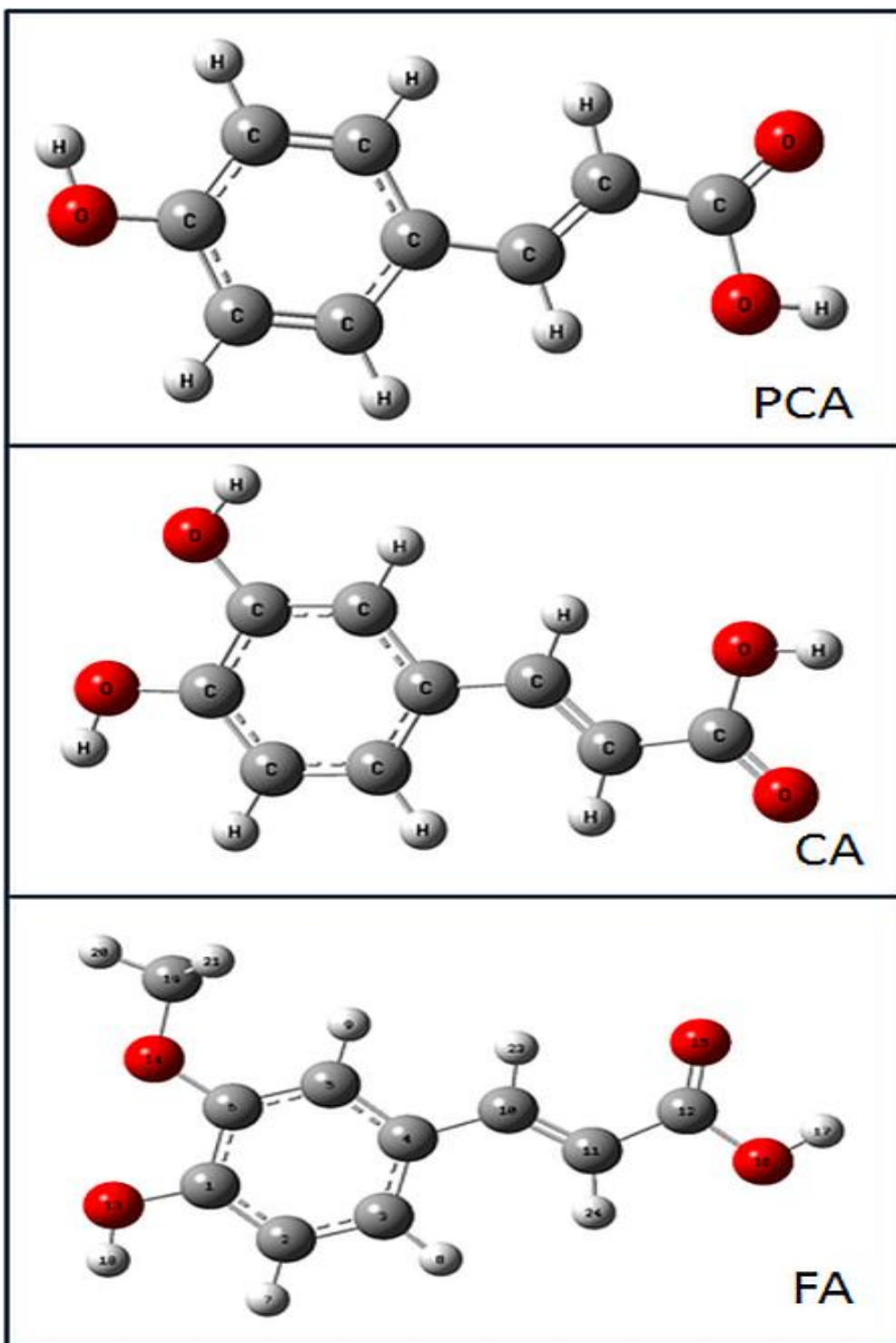


Figure 2.14: Optimized geometries of PCA, CA and FA at DFT/B3LYP/6-311G** basis set.

Bond Length (Å)	X-ray	B3LYP/ 6-311G**	Bond Length (Å)	X-ray	B3LYP/ 6-311G**
<i>p</i>-Coumaric acid					
O1—C1	1.271(2)	1.210	C4—C5	1.397(2)	1.406
O2—C1	1.263(2)	1.363	C5—H5	0.930(1)	1.085
O2—H2	0.820(1)	0.967	C5—C6	1.387(2)	1.386
O3—H3	0.821(1)	0.963	C6—H6	0.930(1)	1.083
O3—C7	1.376(2)	1.360	C6—C7	1.381(2)	1.396
C1—C2	1.470(2)	1.468	C7—C8	1.386(2)	1.400
C2—H2A	0.930(2)	1.083	C8—H8	0.930(1)	1.086
C2—C3	1.328(2)	1.345	C8—C9	1.384(2)	1.385
C3—H3A	0.930(1)	1.086	C9—C4	1.398(2)	1.405
C3—C4	1.463(2)	1.459	C9—H9	0.930(1)	1.083
Caffeic acid					
O1—C1	1.304(2)	1.363	C3—H3A	0.929(2)	1.086
O1—H1	0.819(1)	0.968	C4—C9	1.395(2)	1.401
O2—C1	1.234(2)	1.210	C4—C5	1.396(2)	1.408
O3—C6	1.359(2)	1.363	C5—C6	1.386(2)	1.387
O3—H3	0.820(1)	0.963	C5—H5	0.930(1)	1.087
O4—C7	1.363(2)	1.359	C6—C7	1.395(2)	1.408
O4—H4	0.820(1)	0.963	C7—C8	1.384(2)	1.395
C1—C2	1.462(2)	1.468	C8—C9	1.385(2)	1.389
C2—C3	1.321(2)	1.345	C8—H8	0.929(2)	1.086
C2—H2	0.930(2)	1.083	C9—H9	0.929(2)	1.082
C3—C4	1.464(2)	1.459			
Ferulic acid					
O1—C3	1.360(2)	1.358	C4—C5	1.378(3)	1.389
O1—H1	0.821(1)	0.963	C4—H4	0.930(2)	1.086
O2—C2	1.368(2)	1.358	C5—C6	1.389(2)	1.399
O2—C10	1.411(2)	1.421	C5—H5	0.930(2)	1.083
O3—C9	1.252(2)	1.361	C6—C7	1.458(2)	1.457
O3—H3	0.820(1)	0.968	C7—C8	1.328(2)	1.344
O4—C9	1.288(2)	1.211	C7—H7	0.930(2)	1.088
C1—C2	1.375(2)	1.389	C8—C9	1.465(2)	1.471
C1—C6	1.401(2)	1.411	C8—H8	0.931(2)	1.083
C1—H1A	0.929(1)	1.082	C10—H10A	0.960(2)	1.088
C2—C3	1.401(2)	1.413	C10—H10B	0.960(2)	1.096
C3—C4	1.374(2)	1.393	C10—H10C	0.960(2)	1.096

Table 2.4: Comparison of X-ray structure and calculated bond angles for PCA, CA and FA extracted from *Parthenium hysterophorus* L.

Bond Angle	X-ray	B3LYP/ 6-311G**	Bond Angle	X-ray	B3LYP/ 6-311G**
<i>p</i>-Coumaric acid					
O1—C1—C2	119.16(12)	120.28	C5—C6—H6	120.38(12)	121.48
O2—C1—O1	123.32(13)	121.75	C5—C4—C3	119.37(11)	119.02
O2—C1—C2	117.52(12)	115.97	C6—C7—C8	120.72(10)	119.69
O3—C7—C6	117.43(11)	117.61	C6—C5—C4	121.40(11)	121.84
O3—C7—C8	121.85(10)	122.70	C6—C5—H5	119.27(13)	119.14
C1—O2—H2	109.47(11)	108.70	C7—C8—H8	120.25(11)	119.86
C1—C2—H2A	118.90(13)	117.18	C7—C6—C5	119.31(12)	119.59
C2—C3—C4	127.52(11)	127.60	C7—C6—H6	120.32(11)	119.93
C2—C3—H3A	116.24(12)	117.08	C7—O3—H3	109.49(10)	109.57
C3—C2—C1	122.21(12)	123.97	C8—C9—C4	121.20(11)	121.22
C3—C2—H2A	118.90(14)	118.85	C8—C9—H9	119.38(12)	118.76
C4—C3—H3A	116.24(11)	115.31	C9—C8—C7	119.50(11)	120.14
C4—C5—H5	119.33(11)	119.03	C9—C8—H8	120.25(12)	120.00
C4—C9—H9	119.42(11)	120.01	C9—C4—C3	122.76(11)	123.45
C5—C4—C9	117.87(10)	117.52			
Caffeic acid					
C1—O1—H1	109.46(12)	105.68	C6—C5—C4	120.97(12)	122.09
C6—O3—H3	109.45(12)	109.01	C6—C5—H5	119.50(13)	118.80
C7—O4—H4	109.45(11)	109.11	C4—C5—H5	119.53(12)	119.12
O2—C1—O1	122.45(15)	121.73	O3—C6—C5	124.01(12)	123.77
O2—C1—C2	120.72(13)	124.31	O3—C6—C7	116.35(11)	117.03
O1—C1—C2	116.83(13)	113.96	C5—C6—C7	119.64(12)	119.20
C3—C2—C1	124.21(13)	123.91	O4—C7—C6	115.95(11)	117.25
C3—C2—H2	117.90(16)	122.82	O4—C7—C8	124.06(12)	123.63
C1—C2—H2	117.89(14)	113.27	C8—C7—C6	119.98(12)	119.12
C2—C3—C4	125.97(13)	127.52	C9—C8—C7	120.04(13)	121.28
C2—C3—H3A	117.03(16)	117.02	C9—C8—H8	119.98(14)	119.86
C4—C3—H3A	117.00(13)	115.46	C7—C8—H8	119.98(15)	118.87
C9—C4—C5	118.43(12)	117.90	C8—C9—C4	120.92(13)	120.41
C9—C4—C3	122.57(12)	123.56	C8—C9—H9	119.58(14)	119.12
C5—C4—C3	119.00(12)	118.53	C4—C9—H9	119.50(15)	120.47
Ferulic acid					
C3—O1—H1	109.47(12)	108.91	C5—C6—C1	118.08(13)	118.29
C2—O2—C10	117.75(12)	118.24	C5—C6—C7	119.55(13)	123.45
C9—O3—H3	109.44(12)	106.06	C1—C6—C7	122.36(13)	118.26
C2—C1—C6	120.30(13)	121.84	C8—C7—C6	128.59(13)	128.19
C2—C1—H1A	119.89(13)	119.77	C8—C7—H7	115.70(15)	115.81
C6—C1—H1A	119.81(13)	118.39	C6—C7—H7	115.71(14)	116.00
O2—C2—C1	125.89(13)	125.51	C7—C8—C9	121.05(13)	119.96
O2—C2—C3	113.48(12)	115.56	C7—C8—H8	119.48(15)	123.34
C1—C2—C3	120.62(12)	118.93	C9—C8—H8	119.46(14)	116.70
O1—C3—C4	119.46(14)	123.36	O3—C9—O4	122.66(13)	122.00

O1—C3—C2	121.28(12)	117.18	O3—C9—C8	119.80(13)	111.28
C4—C3—C2	119.25(13)	119.46	O4—C9—C8	117.54(12)	126.72
C3—C4—C5	120.03(15)	121.18	O2—C10—H10A	109.50(18)	105.69
C3—C4—H4	119.98(16)	118.87	O2—C10—H10B	109.46(16)	111.51
C5—C4—H4	119.99(16)	119.95	O2—C10—H10C	109.49(16)	111.51
C4—C5—C6	121.71(15)	120.30	H10A—C10—H10B	109.51(21)	109.40
C4—C5—H5	119.13(16)	119.19	H10A—C10—H10C	109.44(20)	109.31
C6—C5—H5	119.16(15)	120.51	H10B—C10—H10C	109.42(18)	109.31

Table 2.5: Comparison of X-ray structure and calculated bond angles for PCA, CA and FA extracted from *Parthenium hysterophorus* L.

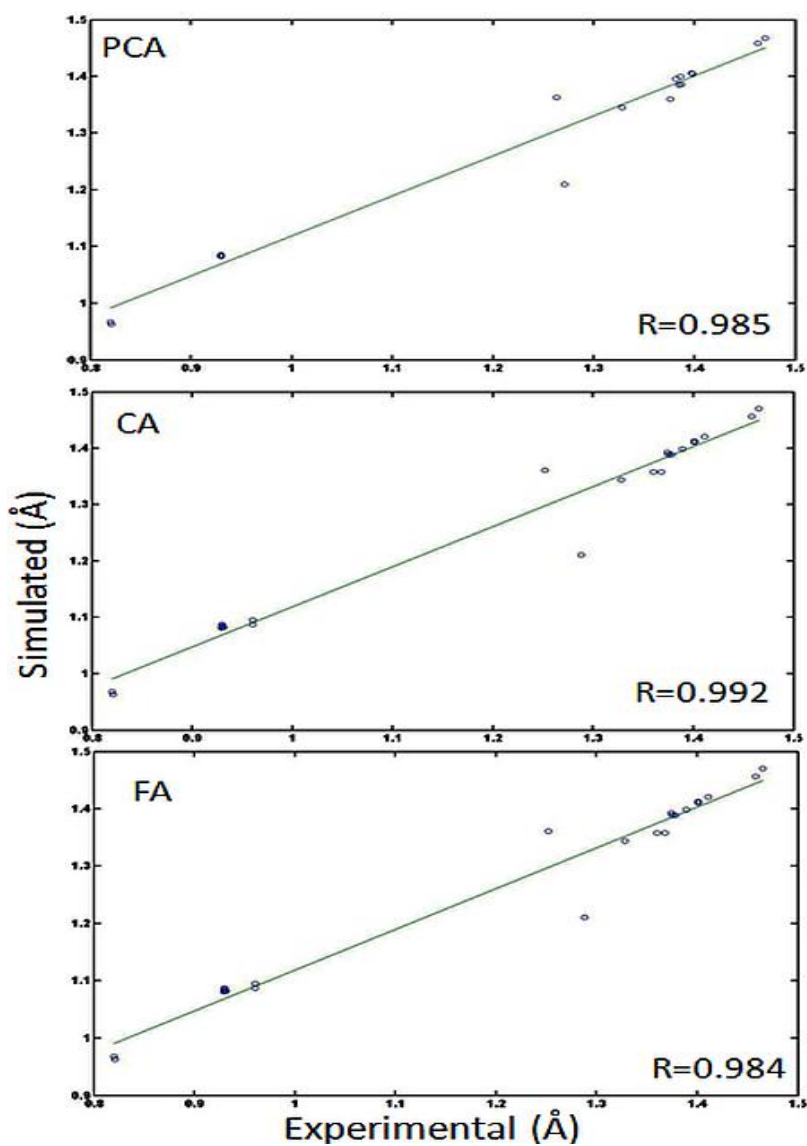


Figure 2.15: Pictorial presentation of linear correlation plots between experimental and simulated values of bond lengths for PCA, CA and FA.

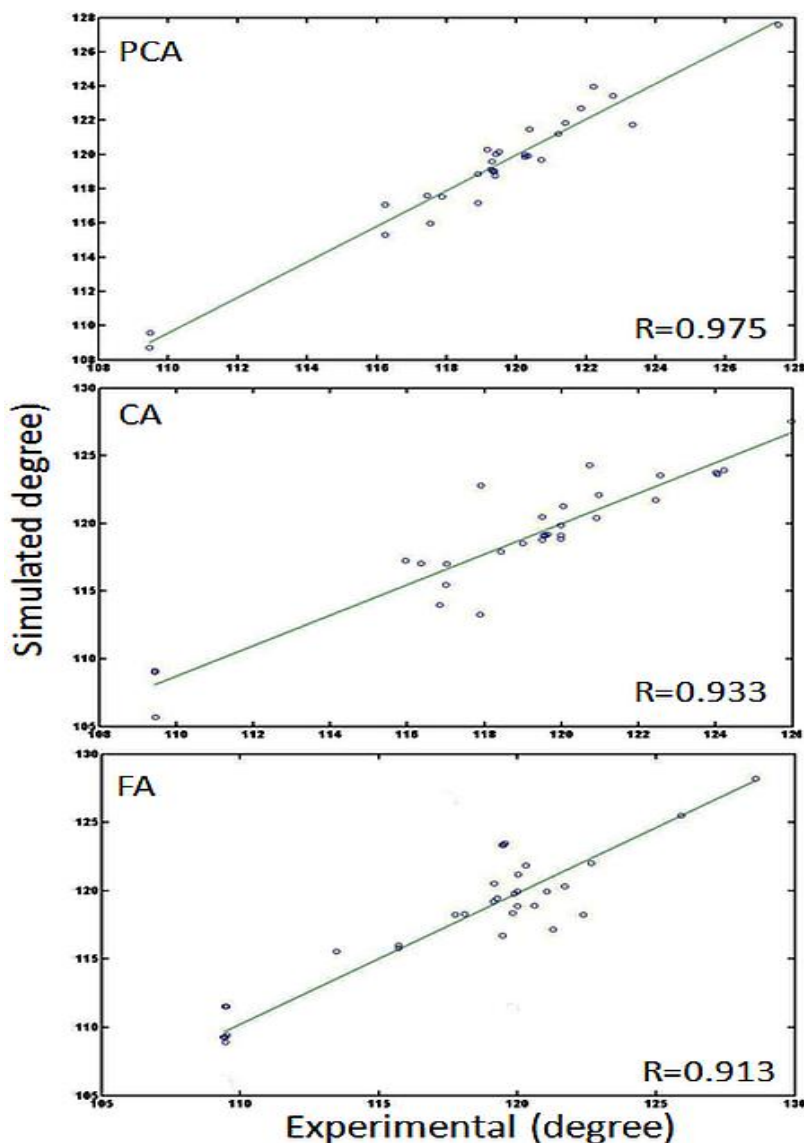


Figure 2.16: Pictorial presentation of linear correlation plots between experimental and simulated values of bond angles for PCA, CA and FA.

2.3.6. Frontier molecular orbital (FMOs) analysis

There are several ways for the calculation of excitation energies and the simplest one, involves the difference between the highest occupied molecular orbital (HOMO; ability to donate the electron) and the lowest unoccupied molecular orbital (LUMO; ability of a molecule to obtain the electron) of neutral system. They are called as frontier molecular orbitals and play a major role in the computation of electronic and optical properties of a molecule. Analysis of the wave

function indicates that the electron absorption corresponds to the transition from the ground to the first excited state and is mainly described by one electron excitation from HOMO to LUMO. To evaluate the energetic behavior of PCA, CA and FA, calculations were performed in the gas phase. The energy gap between HOMO-LUMO also helps in the computation of chemical hardness, chemical softness, kinetic stability, optical polarizability of a molecule, and the calculated values for the above parameters are summarized in Table 2.6.

Parameters	PCA	CA	FA
Total energy (a.u)	-573.605	-648.842	-688.153
Dipole moment (Debye)	3.218	2.498	2.497
E_{HOMO} (eV)	-6.248	-6.004	-5.882
E_{LUMO} (eV)	-1.907	-1.916	-1.838
$E_{\text{HOMO}}-E_{\text{LUMO}}$	-4.342	-4.088	-4.044
Chemical potential (eV)	4.077	3.960	3.860
Electronegativity (eV)	-2.171	-2.044	-2.022
Chemical hardness (eV)	4.077	3.960	3.860
Chemical softness (eV^{-1})	0.123	0.126	0.129
Electrophilic index (eV)	0.577	0.527	0.529

Table 2.6: Calculated values of total energy, dipole moment, energy for HOMO-LUMO, electronegativity, electrophilic index, chemical potential, chemical hardness and chemical softness for PCA, CA and FA in gas phase at DFT/B3LYP/6-311G** basis set.

The molecular orbital diagram for PCA, CA and FA has been computed at DFT/B3LYP/6-311G** basis set and is depicted in Figure 2.17 with their respective energy values, which clearly defines that in PCA, the charge density in HOMO is shifting from benzene ring to the ester and carboxylic side chain groups in the LUMO position. These are also a shifting of electron density in phenolic -OH group has been occurred from HOMO to LUMO. In CA, the charge is transferred from -COOH to -OCH₃ group from HOMO to LUMO. While in case of FA, charge is shifting

from $-\text{OCH}_3$ group towards the $-\text{COOH}$ group from HOMO to LUMO and the phenolic $-\text{OH}$ group has electron density on it in both cases (HOMO and LUMO). The calculated values of energy for HOMO are -6.248, -6.004, and -5.882eV, and for LUMO they are -1.907, -1.916, and -1.838eV while the values for HOMO-LUMO energy gap are found to be -4.342, -4.088, and -4.044eV in case of PCA, CA and FA, respectively. This explains the eventual charge transfer interaction within the molecule.

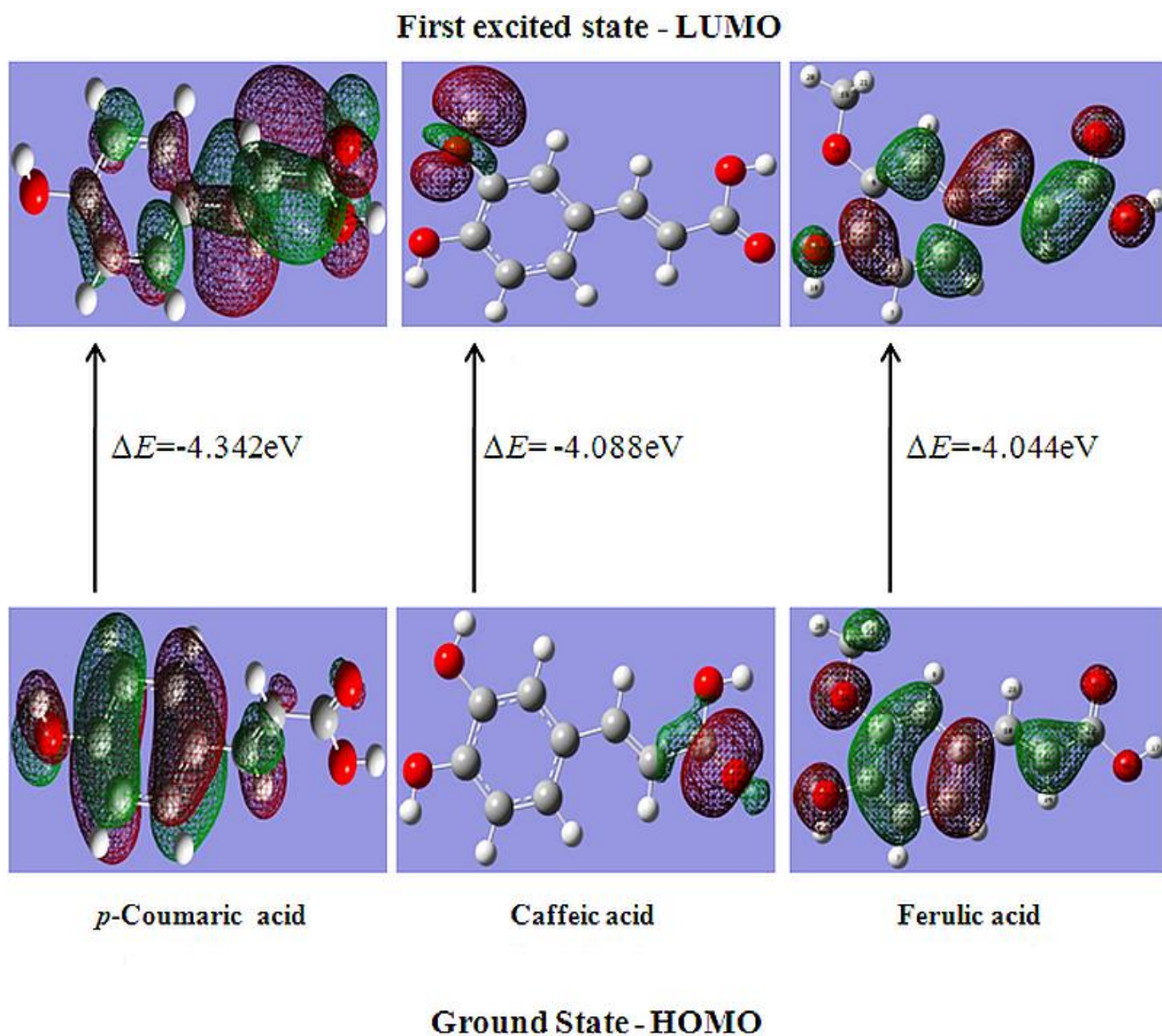


Figure 2.17: Molecular orbital surfaces and energy (eV) of PCA, CA, and FA for HOMO and LUMO in gas phase.

2.4. Concluding remarks

In summary, three hydroxycinnamic acids have been extracted and purified from *Parthenium hysterophorus* by alkali treatment and subsequently characterized experimental as well as theoretical methods. The intermolecular hydrogen bonding between donor and acceptor exists only in ferulic acid. The model developed here comprises of geometry optimization at DFT/B3LYP/6-311G** basis set. The structural parameters like bond lengths and bond angles have been calculated at the same level of basis set and compared with the experimentally obtained X-ray crystallographic results, and they showed satisfying correlations. The electronic properties and HOMO–LUMO energies were also performed. Theoretical studies suggest that structures of PCA, CA and FA are same in both the gas and solid phases. The results of thermal study indicate that the PCA, CA and FA are stable at room temperature, and they decompose mainly in a single step at high temperature.

CHAPTER-3

Synthesis, structural and thermal characterization of mono and bis-amide derivatives of ferulic acid

Naresh Kumar, Sandeep Kumar, Sheenu Abbat, Kumar Nikhil, Sham M. Sondhi, P.V. Bharatam, Partha Roy and Vikas Pruthi (2014). 3D-QSAR modeling of ferulic acid and its amide derivatives: Synthesis, structural characterization, anticancer and antioxidant activities. European Journal of Medicinal Chemistry (Under review)

Synthesis, structural and thermal characterization of mono and bis-amide derivatives of ferulic acid

3.1. Introduction

Synthesis of heterocyclic molecules have received much attention of scientific community because of their potential applications in biological activities is an interesting area of research [Basoglu et al. 2013]. The limitations of existing anticancer/antimicrobial drugs caused by various reasons including drug resistance, serious side effects, and lack of efficiency made infectious disease a vicious cycle. In organic and medicinal chemistry, several N-containing heterocyclic compounds have been used as exclusive building blocks. Triazoles show a number of potential activities in the medicinal chemistry. Ribavirin (antiviral), rizatriptan (antimigraine), alprazolam (psychotropic), fluconazole, and itraconazole (antifungal) possess triazole nucleus, and have been used for potent drugs [Holla et al., 2006; Walczak et al., 2004; Ashok et al., 2007]. A β -lactamase inhibitor, Tazobactam is another example of triazole containing structure, which has been used as antibiotic piperacillin [Kategaonkar et al., 2010].

Amide derivatives were associated with broad spectrum of biological activities including antituberculosis, antidiabetic, antitumor, anticonvulsant, analgesic, anti-inflammatory, insecticidal, antifungal, and antitumor properties [Graybill et al. 1992; Tamm et al. 2003; Hegab et al. 2007; Warnecke et al. 2007; Siddiqui et al. 2008; kumar et al. 2011; Parkesh et al. 2012]. Ferulic acid is a naturally occurring phenolic acid known for its wide range of biological activities [Kumar et al. 2015] and structural modifications of it have high impact into their biological activity [Hosoda et al. 2002; Murakami et al. 2002; Nomura et al. 2003; Ergün et al. 2011]. Our work is primarily motivated by the broad spectrum of biological activities exhibited by ferulic acid, its derivatives

and the compounds possessing amide moiety. We had developed a strategy towards the synthesis of a number of novel amide derivatives by structural modifications of ferulic acid with different kinds of primary amines.

3.2. Experimental section

3.2.1. Materials

All manipulations were carried out under air atmosphere. Ethanol, Acetonitrile, Chloroform and methanol were used as received. All the amines and other chemical reagents were of analytical grade and purchased from Sigma-Aldrich, Chemical company, USA.

3.2.2. Instrumentation

Microwave reactor Anton Paar (monowave 300) and microwave oven model M197DL (Samsung) were used for microwave irradiation. Melting points (mp) were determined on a JSGW apparatus and are uncorrected. Compounds were carefully dried under vacuum for several hours prior to elemental analysis on the CHNS analyzer by using Elementar Vario EL III. The FT-IR spectra were obtained on a Thermo Nicolet Nexus FT-IR spectrometer in KBr. The NMR spectra were obtained on Avance 500 Bruker Biospin Intl 500MHz with Fourier transform technique using TMS as internal standard. Perkin Elmer Clarus 500 gas chromatograph built-in with MS detector was applied for recording the ESI-MS spectrum. Thin layer chromatography (TLC) was performed on silica gel G for TLC (Merck), and spots were visualized by iodine vapors or by irradiation with ultraviolet light (254nm). Compounds **IIIa-IIIo**, **Va-Vg**, **VIIa-VIIg** and **IXa-IXe** were purified by crystallization from methanol. Thermogravimetry (TG), differential thermal analysis (DTA) and derivative thermogravimetry (DTG) were carried out by using a mass of 0.045g at 10°C/min under the nitrogen at 200 ml/min flow rate on a thermogravimetric analyzer (PerkinElmer's, California, USA).

3.2.3. Syntheses of amide derivatives ferulic acid

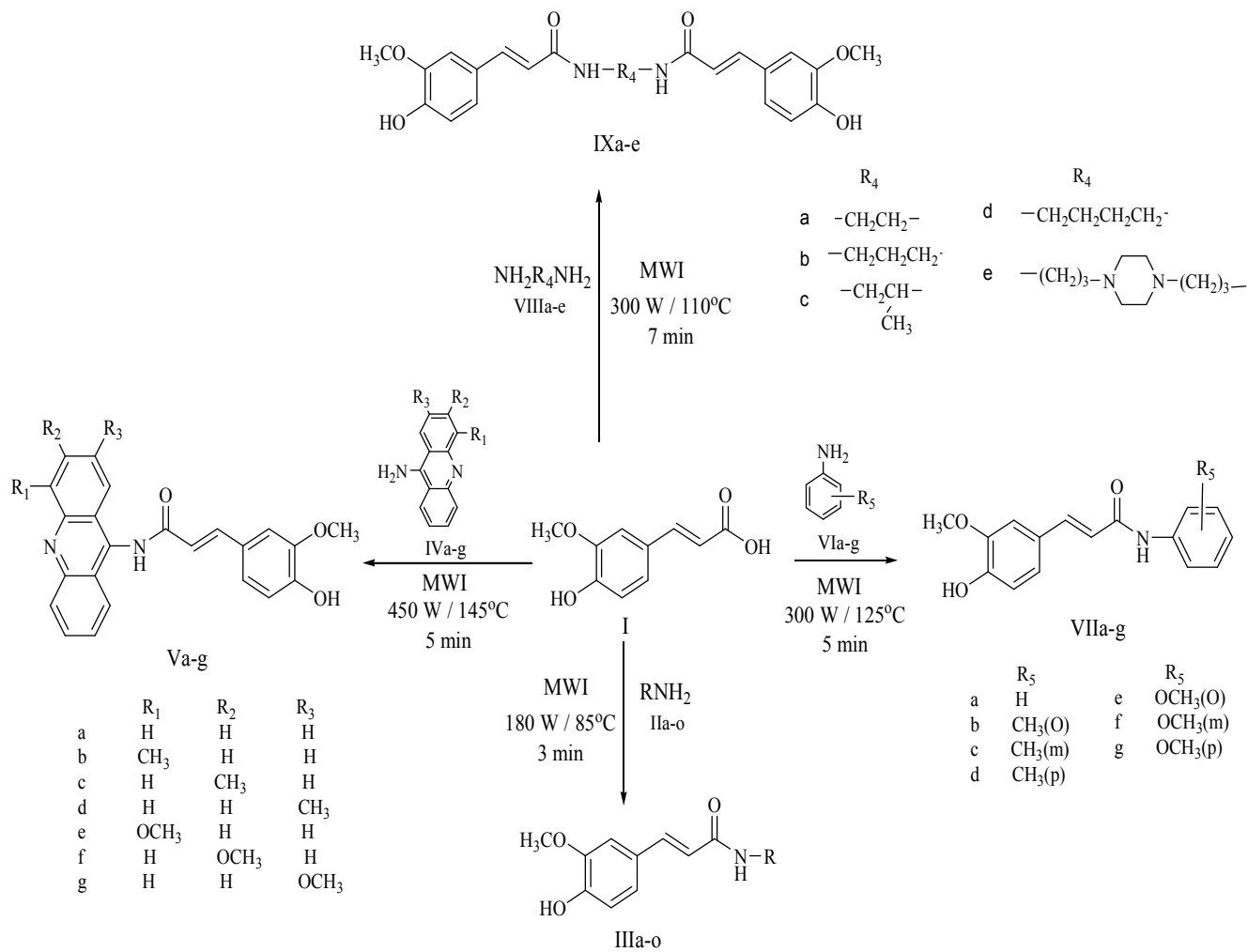
Four series (**IIIa-IIIo**, **Va-Vg**, **VIIa-VIIg** and **IXa-IXe**) of mono and bis-amide derivatives of ferulic acid have been synthesized in this chapter. The schematic representation of the synthesized molecules has been given in scheme 1.

3.2.3.1. General procedure for synthesis of mono-amide derivatives of ferulic acid

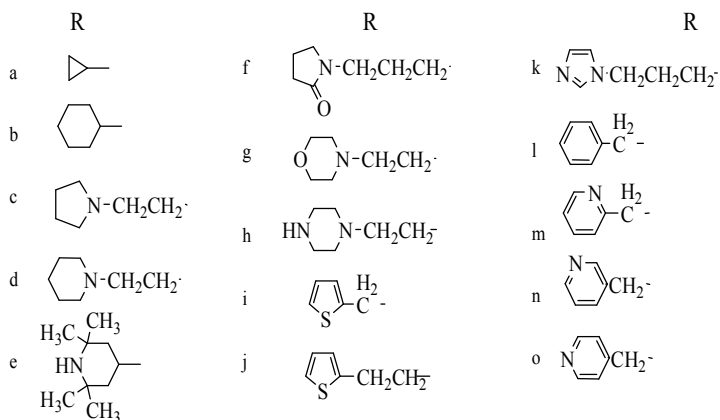
(*E*)-3-(4-hydroxy-3-methoxyphenyl)acrylic acid (Ferulic acid) and the corresponding amines (**IIa-IIo**, **IVa-IVg**, **Via-VIg** and **VIIIa-VIIIe**) were mixed together thoroughly in an equimolar molar ratio in a petri disc. The reaction mixture was subjected to microwave irradiation at 180-450 Watt for 3-10 min and then progress of the reactions was monitored by TLC on silica gel using ethyl acetate: methanol (4:1, 3:2 and 7:3) as solvent of elution. TLC indicated absence of starting materials and hence reaction was complete. The crude products thus so obtained were purified by crystallization from methanol to give a pure products (**IIIa-IIIo**, **Va-Vg**, **VIIa-VIIg** and **IXa-IXe**) in high yield.

3.2.3.1.1. Synthesis of (*E*)-*N*-cyclopropyl-3-(4-hydroxy-3-methoxyphenyl)acrylamide (**IIIa**)

Yield: 87%. mp: 110-112°C. FT-IR (KBr, cm^{-1}) ν_{max} : 3435, 2929, 1666, 1606, 1597, 1571. $^1\text{H-NMR}$ (500 MHz, $\text{DMSO-}d_6$, ppm) δ : 0.371-0.405 (m, 2H, CH_2), 0.566-0.580 (d, 2H, $J = 7$ Hz, CH_2), 2.217-2.245 (m, 1H, CH), 3.805 (s, 3H, OCH_3), 5.444 (s, 1H, NH), 6.340-6.372 (d, 1H, $J = 16$ Hz, Ar), 6.773-6.789 (d, 1H, $J = 8$ Hz, Ar), 7.052-7.068 (d, 1H, $J = 8$ Hz, Ar), 7.258 (s, 1H, Ar), 7.430-7.462 (d, 1H, $J = 16$ Hz, Ar), 10.273 (s, 1H, OH). $^{13}\text{C-NMR}$ (125 MHz, $\text{DMSO-}d_6$, ppm) δ : 13.552, 24.102, 56.097, 112.274, 116.442, 117.277, 120.941, 128.775, 144.608, 145.442, 151.175, 166.091. GC-MS, m/z : 234 (M^+_{+1} , 1 %), 233 (M^+ , 32 %), 232 (M^+_{-1} , 1 %), 192 ($\text{H}_3\text{CO-C}_6\text{H}_3(\text{OH})-\text{CH}=\text{CH}-\text{C}(=\text{O})\text{NH}^+$, 22 %), 93 ($\text{HO-C}_6\text{H}_4^+$, 13 %), 92 ($\text{C}_6\text{H}_4(\text{OH})^+$, 22 %), 78 (C_6H_5^+ , 100 %), 77 (C_6H_6^+ , 21 %). Anal. Calcd. (%) for $\text{C}_{13}\text{H}_{15}\text{NO}_3$ (233.26): C, 66.94; H, 6.48; N, 6.00; Found: C, 66.13; H, 6.29; N, 5.57.

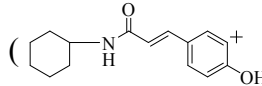
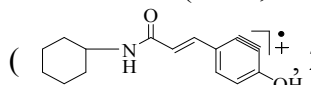
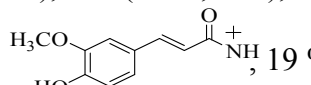
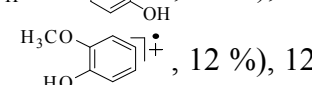
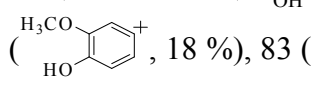
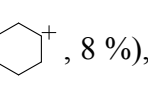
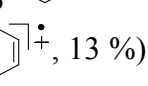


where R is same for IIa-o and IIIa-o

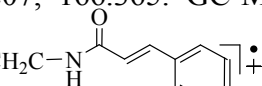
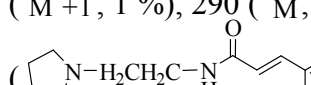
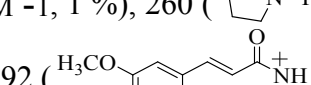
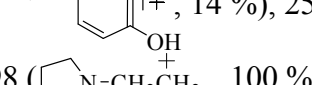


Scheme 1: Synthesis of amide derivatives of ferulic acid i.e. IIIa-o, Va-g, VIIa-g and IXa-e.

3.2.3.1.2. (E)-N-cyclohexyl-3-(4-hydroxy-3-methoxyphenyl)acrylamide (IIIb)

Yield: 98%. mp: 180-182°C. FT-IR (KBr, cm^{-1}) ν_{max} : 3435, 2934, 2857, 1689, 1634, 1594. $^1\text{H-NMR}$ (500 MHz, $\text{DMSO-}d_6$, ppm) δ : 1.133-1.193 (q, 1H, $J = 30$ Hz, $J = 13$ Hz, CH_2), 1.208-1.258 (t, 4H, $J = 25$ Hz, $J = 13$ Hz, $2 \times \text{CH}_2$), 1.542-1.568 (d, 1H, $J = 8$ Hz, CH_2), 1.667-1.692 (d, 2H, $J = 12.5$ Hz, CH_2), 1.829-1.851 (d, 2H, $J = 11$ Hz, CH_2), 2.756-2.805 (m, 1H, CH), 3.791 (s, 3H, OCH_3), 5.444 (s, 1H, NH), 6.284-6.315 (d, 1H, $J = 15.5$ Hz, Ar), 6.758-6.774 (d, 1H, $J = 8$ Hz, Ar), 6.958-6.975 (d, 1H, $J = 8.5$ Hz, Ar), 7.159 (s, 1H, Ar), 7.238-7.270 (d, 1H, $J = 16$ Hz, Ar), 10.215 (s, 1H, OH). $^{13}\text{C-NMR}$ (125 MHz, $\text{DMSO-}d_6$, ppm) δ : 21.001, 28.538, 33.388, 46.784, 57.320, 112.070, 116.272, 117.585, 120.302, 128.412, 144.328, 145.780, 151.117, 166.670. GC-MS m/z : 276 (M^+ , 1 %), 275 (M^+ , 25 %), 274 (M^+ , 1 %), 244 (, 16 %), 243 (, 20 %), 192 (, 19 %), 124 (, 12 %), 123 (, 18 %), 83 (, 8 %), 82 (, 13 %). Anal. Calcd. (%) for $\text{C}_{16}\text{H}_{21}\text{NO}_3$ (275.34): C, 69.79; H, 7.69; N, 5.09; Found: C, 67.63; H, 7.56; N, 4.89.

3.2.3.1.3. (E)-3-(4-hydroxy-3-methoxyphenyl)-N-(2-(pyrrolidin-1-yl)ethyl)acrylamide (IIIc)

Yield: 83%. mp: 98-100°C. FT-IR (KBr, cm^{-1}) ν_{max} : 3407, 2961, 1638, 1597, 1578, 1557. $^1\text{H-NMR}$ (500 MHz, $\text{DMSO-}d_6$, ppm) δ : 1.676 (s, 4H, $2 \times \text{CH}_2$), 2.366-2.535 (m, 6H, $3 \times \text{CH}_2$), 2.753-2.778 (t, 2H, $J = 12.5$ Hz, $J = 6.5$ Hz, CH_2), 3.792 (s, 3H, OCH_3), 5.463 (s, 1H, NH), 6.301-6.332 (d, 1H, $J = 15.5$ Hz, Ar), 6.764-6.780 (d, 1H, $J = 8$ Hz, Ar), 6.974-6.990 (d, 1H, $J = 8$ Hz, Ar), 7.176 (s, 1H, Ar), 7.277-7.308 (d, 1H, $J = 15.5$ Hz, Ar), 10.229 (s, 1H, OH). $^{13}\text{C-NMR}$ (125 MHz, $\text{DMSO-}d_6$, ppm) δ : 27.103, 37.937, 50.007, 59.050, 112.167, 116.016, 117.175, 120.114, 121.944, 128.234, 129.114, 136.664, 144.205, 145.445, 151.207, 166.365. GC-MS, m/z : 291 (M^+ , 1 %), 290 (M^+ , 27 %), 289 (M^+ , 1 %), 260 (, 14 %), 259 (, 23 %), 192 (, 30 %), 98 (, 100 %).

71 ($\text{HC}^{\oplus}=\text{CH}-\text{COOH}$, 27 %). Anal. Calcd. (%) for $\text{C}_{16}\text{H}_{22}\text{N}_2\text{O}_3$ (290.36): C, 66.18; H, 7.64; N, 9.65; Found: C, 65.49; H, 7.54; N, 9.17.

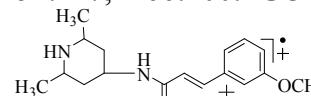
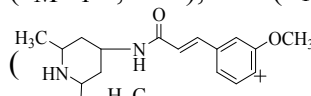
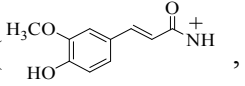
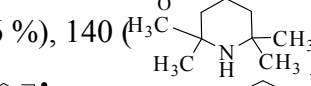
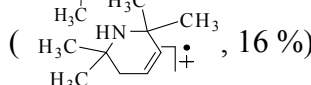
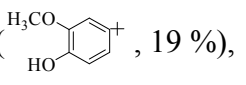
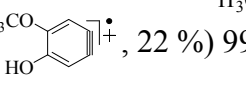
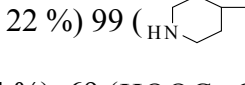
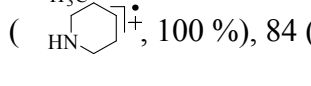
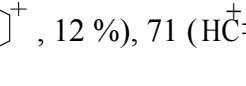
3.2.3.1.4. (E)-3-(4-hydroxy-3-methoxyphenyl)-N-(2-(piperidin-1-yl)ethyl)acrylamide (III d)

Yield: 87%. mp: 98-100°C. FT-IR (KBr, cm^{-1}) ν_{max} : 3394, 3273, 2935, 2838, 1638, 1593, 1565. $^1\text{H-NMR}$ (500 MHz, $\text{DMSO-}d_6$, ppm) δ : 1.359 (s, 2H, CH_2), 1.462-1.494 (q, 4H, $J = 5.5$ Hz, $J = 5$ Hz, $2 \times \text{CH}_2$), 2.266-2.499 (m, 6H, $3 \times \text{CH}_2$), 2.785-2.796 (d, 2H, $J = 5.5$ Hz, CH_2), 3.788 (s, 3H, OCH_3), 5.498 (s, 1H, NH), 6.298-6.330 (d, 1H, $J = 16$ Hz, Ar), 6.763-6.779 (d, 1H, $J = 8$ Hz, Ar), 6.969-6.981 (d, 1H, $J = 6$ Hz, Ar), 7.165 (s, 1H, Ar), 7.270-7.301 (d, 1H, $J = 15.5$ Hz, Ar), 10.227 (s, 1H, OH). $^{13}\text{C-NMR}$ (125 MHz, $\text{DMSO-}d_6$, ppm) δ : 25.049, 26.529, 36.989, 53.039, 54.727, 57.090, 112.081, 116.151, 117.165, 120.080, 128.208, 144.146, 145.178, 151.165, 166.800. GC-MS m/z : 305 ($\text{M}^{\oplus}+1$, 2 %), 304 (M^{\oplus} , 33 %), 303 ($\text{M}^{\oplus}-1$, 2 %), 274 ($\text{C}_{17}\text{H}_{24}\text{N}_2\text{O}_3$, 30 %), 273 ($\text{C}_{17}\text{H}_{24}\text{N}_2\text{O}_3$, 22 %), 192 ($\text{C}_{17}\text{H}_{24}\text{N}_2\text{O}_3$, 33 %), 112 ($\text{C}_{17}\text{H}_{24}\text{N}_2\text{O}_3$, 34 %), 99 ($\text{C}_{17}\text{H}_{24}\text{N}_2\text{O}_3$, 19 %), 85 ($\text{C}_{17}\text{H}_{24}\text{N}_2\text{O}_3$, 100 %), 84 ($\text{C}_{17}\text{H}_{24}\text{N}_2\text{O}_3$, 17 %), 71 ($\text{HC}^{\oplus}=\text{CH}-\text{COOH}$, 24 %), 70 ($\text{HOOC}-\text{C}\equiv\text{CH}^{\oplus}$, 28 %), 69 ($\text{HOOC}-\text{C}\equiv\text{C}^{\oplus}$, 43 %). Anal. Calcd. (%) for $\text{C}_{17}\text{H}_{24}\text{N}_2\text{O}_3$ (304.38): C, 67.08; H, 7.95; N, 9.20; Found: C, 66.56; H, 7.89; N, 9.01.

3.2.3.1.5. (E)-3-(4-hydroxy-3-methoxyphenyl)-N-(2,2,6,6-tetramethylpiperidin-4-yl)acrylamide (III e)

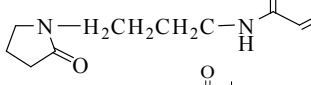
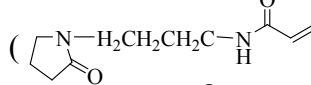
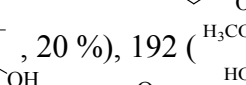
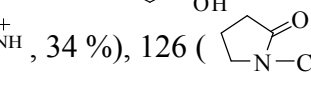
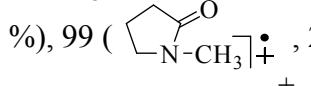
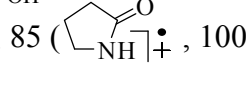
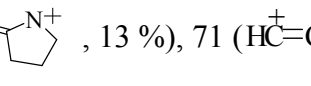
(III e)

Yield: 84%. mp: 118-120°C. FT-IR (KBr, cm^{-1}) ν_{max} : 3433, 2961, 1629, 1516. $^1\text{H-NMR}$ (500 MHz, $\text{DMSO-}d_6$, ppm) δ : 0.988 (s, 2H, CH_2), 1.061 (s, 6H, $2 \times \text{CH}_3$), 1.126 (s, 6H, $2 \times \text{CH}_3$), 1.706-1.727 (d, 2H, $J = 8.5$ Hz, CH_2), 3.170-3.184 (d, 1H, $J = 7$ Hz, CH), 3.792 (s, 3H, OCH_3), 5.446 (s, 1H, NH), 6.277-6.309 (d, 1H, $J = 16$ Hz, Ar), 6.759-6.775 (d, 1H, $J = 4$ Hz, Ar), 6.946-6.962 (d, 1H, $J = 4$ Hz, Ar), 7.147 (s, 1H, Ar), 7.209-7.241 (d, 1H, $J = 16$ Hz, Ar), 10.241 (s, 1H, OH). $^{13}\text{C-NMR}$ (125 MHz, $\text{DMSO-}d_6$, ppm) δ : 29.109, 33.128, 46.004, 47.770, 57.090, 112.117,

116.128, 117.085, 120.172, 128.151, 144.518, 145.660, 151.117, 166.200. GC-MS m/z : 333 (\dot{M}^+ , 2 %), 332 (\dot{M} , 35 %), 331 ($\dot{M}-1$, 1 %), 288 (, 30 %), 287 (, 20 %), 192 (, 26 %), 140 (, 13 %), 139 (, 16 %), 123 (, 19 %), 122 (, 22 %), 99 (, 25 %), 85 (, 100 %), 84 (, 12 %), 71 ($\text{HC}^+=\text{CH}-\text{COOH}$, 24 %), 69 ($\text{HOOC}-\text{C}\equiv\text{C}^+$, 40 %).

Anal. Calcd. (%) for $\text{C}_{19}\text{H}_{28}\text{N}_2\text{O}_3$ (332.44): C, 68.65; H, 8.49; N, 8.43; Found: C, 67.82; H, 8.36; N, 8.12.

3.2.3.1.6. (E)-3-(4-hydroxy-3-methoxyphenyl)-N-(3-(2-oxopyrrolidin-1-yl)propyl)acrylamide (III f)

Yield: 95%. mp: 105-107°C. FT-IR (KBr, cm^{-1}) ν_{max} : 3415, 3150, 2932, 1678, 1609, 1597, 1555. $^1\text{H-NMR}$ (500 MHz, $\text{DMSO-}d_6$, ppm) δ : 1.523-1.609 (m, 2H, CH_2), 1.875-1.936 (m, 2H, CH_2), 2.190-2.222 (t, 2H, $J = 16$ Hz, $J = 8$ Hz, CH_2), 2.540-2.568 (t, 2H, $J = 14$ Hz, $J = 7$ Hz, CH_2), 3.149-3.195 (t, 2H, $J = 15$ Hz, $J = 8$ Hz, CH_2), 3.209-3.249 (t, 2H, $J = 13$ Hz, $J = 7$ Hz, CH_2), 3.843 (s, 3H, OCH_3), 5.841 (s, 1H, NH), 6.300-6.332 (d, 1H, $J = 16$ Hz, Ar), 6.759-6.775 (d, 1H, $J = 8$ Hz, Ar), 6.987-7.003 (t, 1H, $J = 8$, $J = 7$ Hz, Ar), 7.190-7.192 (d, 1H, $J = 1$ Hz, Ar), 7.296-7.327 (d, 1H, $J = 15.5$ Hz, Ar), 10.275 (s, 1H, OH). $^{13}\text{C-NMR}$ (125 MHz, $\text{DMSO-}d_6$, ppm) δ : 17.103, 27.937, 32.103, 37.937, 41.397, 43.027, 56.410, 112.167, 116.366, 117.645, 120.054, 129.344, 144.645, 145.121, 151.147, 166.161, 173.315. GC-MS, m/z : 319 (\dot{M}^+ , 2 %), 318 (\dot{M} , 48 %), 317 ($\dot{M}-1$, 1 %), 288 (, 30 %), 287 (, 20 %), 192 (, 34 %), 126 (, 22 %), 99 (, 25 %), 85 (, 100 %), 84 (, 13 %), 71 ($\text{HC}^+=\text{CH}-\text{COOH}$, 25 %), 69 ($\text{HOOC}-\text{C}\equiv\text{C}^+$, 40 %). Anal. Calcd. (%) for $\text{C}_{17}\text{H}_{22}\text{N}_2\text{O}_4$ (318.37): C, 64.13; H, 6.97; N, 8.80; Found: C, 63.74; H, 6.89; N, 8.51.

3.2.3.1.7. (E)-3-(4-hydroxy-3-methoxyphenyl)-N-(2-morpholinoethyl)acrylamide (IIIg)

Yield: 92%. mp: 121-123°C. FT-IR (KBr, cm^{-1}) ν_{max} : 3431, 3219, 2936, 2820, 1638, 1597.

$^1\text{H-NMR}$ (500 MHz, $\text{DMSO-}d_6$, ppm) δ : 2.355-2.423 (q, 4H, $J = 22$ Hz, $J = 12$ Hz, $2 \times \text{CH}_2$), 2.779-2.803 (t, 2H, $J = 12$ Hz, $J = 6$ Hz, CH_2), 3.556-3.573 (t, 6H, $J = 8.5$ Hz, $J = 4.5$ Hz, $3 \times \text{CH}_2$), 3.793 (s, 3H, OCH_3), 5.557 (s, 1H, NH), 6.304-6.335 (d, 1H, $J = 15.5$ Hz, Ar), 6.764-6.780 (d, 1H, $J = 8$ Hz, Ar), 6.982-6.995 (d, 1H, $J = 6.5$ Hz, Ar), 7.179 (s, 1H, Ar), 7.286-7.332 (dd, 1H, $J = 7.5$ Hz, $J = 7$ Hz, Ar), 10.286 (s, 1H, OH). $^{13}\text{C-NMR}$ (125 MHz, $\text{DMSO-}d_6$, ppm) δ : 37.189, 39.442, 52.040,

54.727, 67.090, 112.211, 116.448, 117.085, 120.882, 128.848, 144.145, 145.678, 151.207, 166.040. GC-MS m/z : 307 ($\dot{\text{M}}^+_{+1}$, 2%), 306 ($\dot{\text{M}}^+$, 47%), 305 ($\dot{\text{M}}^+_{-1}$, 2%), 276 ($\text{O} \begin{array}{c} \diagup \\ \diagdown \end{array} \text{N-H}_2\text{CH}_2\text{C-NH-C(=O)-CH=CH-C}_6\text{H}_3\text{(OH)}^+$, 28%), 275 ($\text{O} \begin{array}{c} \diagup \\ \diagdown \end{array} \text{N-H}_2\text{CH}_2\text{C-NH-C(=O)-CH=CH-C}_6\text{H}_3\text{(OH)}^+$, 20%), 192 ($\text{H}_3\text{CO-C}_6\text{H}_3\text{(OH)-CH=CH-C(=O)-NH}^+$, 22%), 114 ($\text{O} \begin{array}{c} \diagup \\ \diagdown \end{array} \text{N-CH}_2\text{CH}_2^+$, 14%), 101 ($\text{O} \begin{array}{c} \diagup \\ \diagdown \end{array} \text{N-CH}_3^+$, 18%), 100 ($\text{O} \begin{array}{c} \diagup \\ \diagdown \end{array} \text{N-CH}_2^+$, 25%), 87 ($\text{O} \begin{array}{c} \diagup \\ \diagdown \end{array} \text{NH}^+$, 100%), 71 ($\text{HC}^+=\text{CH-COOH}$, 24%), 69 ($\text{HOOC-C}\equiv\text{C}^+$, 38%).

Anal. Calcd. (%) for $\text{C}_{16}\text{H}_{22}\text{N}_2\text{O}_4$ (306.36): C, 62.73; H, 7.24; N, 9.14; Found: C, 61.84; H, 7.17; N, 8.97.

3.2.3.1.8. (E)-3-(4-hydroxy-3-methoxyphenyl)-N-(2-(piperazin-1-yl)ethyl)acrylamide (IIIh)

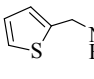
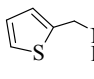
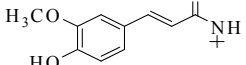
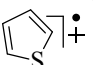
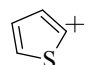
Yield: 86%. mp: 170-172°C. FT-IR (KBr, cm^{-1}) ν_{max} : 3401, 2995, 2826, 1632, 1585, 1507.

$^1\text{H-NMR}$ (500 MHz, $\text{DMSO-}d_6$, ppm) δ : 2.305-2.336 (d, 6H, $J = 15.5$ Hz, $3 \times \text{CH}_2$), 2.703 (s, 6H, $3 \times \text{CH}_2$), 3.782-3.793 (d, 3H, $J = 5.5$ Hz, OCH_3), 5.422 (s, 1H, NH), 6.282-6.314 (d, 1H, $J = 16$ Hz, Ar), 6.739-6.770 (t, 1H, $J = 15.5$ Hz, $J = 7.5$ Hz, Ar), 6.966-7.035 (d, 1H, $J = 8.5$ Hz, Ar), 7.168 (s, 1H, Ar), 7.259-7.290 (d, 2H, $J = 15.5$ Hz, Ar), 10.237 (s, 1H, OH). $^{13}\text{C-NMR}$ (125 MHz, $\text{DMSO-}d_6$, ppm) δ : 37.109, 46.004, 52.390, 54.744, 57.090, 112.287, 116.448, 117.055, 120.882,

128.141, 144.146, 145.570, 151.047, 166.740. GC-MS m/z : 306 ($\dot{\text{M}}^+_{+1}$, 2%), 305 ($\dot{\text{M}}^+$, 51%), 304 ($\dot{\text{M}}^+_{-1}$, 2%), 275 ($\text{HN} \begin{array}{c} \diagup \\ \diagdown \end{array} \text{N-CH}_2\text{CH}_2\text{-NH-C(=O)-CH=CH-C}_6\text{H}_3\text{(OH)}^+$, 24%), 274 ($\text{HN} \begin{array}{c} \diagup \\ \diagdown \end{array} \text{N-CH}_2\text{CH}_2\text{-NH-C(=O)-CH=CH-C}_6\text{H}_3\text{(OH)}^+$, 17%), 192 ($\text{H}_3\text{CO-C}_6\text{H}_3\text{(OH)-CH=CH-C(=O)-NH}^+$, 33%), 113 ($\text{HN} \begin{array}{c} \diagup \\ \diagdown \end{array} \text{N-CH}_2\text{CH}_2^+$, 28%), 86 ($\text{HN} \begin{array}{c} \diagup \\ \diagdown \end{array} \text{N}^+$, 23%), 85

(HN $\text{C}_4\text{H}_8\text{N}^+$, 100 %), 84 (HN $\text{C}_4\text{H}_7\text{N}^+$, 17 %), 71 (HC \equiv CH-COOH, 25 %), 70 (HOOC-C \equiv CH $\dot{+}$, 30 %), 69 (HOOC-C \equiv C $\dot{+}$, 40 %). Anal. Calcd. (%) for C₁₆H₂₃N₃O₃ (305.37): C, 62.93; H, 7.59; N, 13.76; Found: C, 61.97; H, 7.52; N, 13.31.

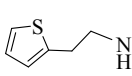
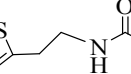
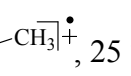
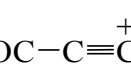

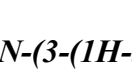
3.2.3.1.9. (E)-3-(4-hydroxy-3-methoxyphenyl)-N-(thiophen-2-ylmethyl)acrylamide (IIIi)

Yield: 90%. mp: 111-113°C. FT-IR (KBr, cm⁻¹) ν_{max} : 3434, 2926, 1685, 1616, 1591, 1564. ¹H-NMR (500 MHz, DMSO-*d*₆, ppm) δ : 2.933 (s, 2H, CH₂), 3.808 (s, 3H, OCH₃), 5.463 (s, 3H, NH), 6.329-6.360 (d, 1H, *J* = 15.5 Hz, Ar), 6.768-6.784 (d, 1H, *J* = 8 Hz, Ar), 6.886-6.890 (d, 1H, *J* = 2 Hz, Ar), 6.944-6.963 (q, 1H, *J* = 9.5 Hz, *J* = 5.5 Hz, Ar), 7.022-7.043 (q, 1H, *J* = 10.5 Hz, *J* = 8.5 Hz, Ar), 7.229-7.233 (d, 1H, *J* = 2 Hz, Ar), 7.329-7.338 (d, 1H, *J* = 4.5 Hz, Ar), 7.378-7.399 (d, 1H, *J* = 10.5 Hz, Ar), 10.253 (s, 1H, OH). ¹³C-NMR (125 MHz, DMSO-*d*₆, ppm) δ : 39.442, 50.407, 56.090, 112.941, 116.116, 117.175, 120.442, 121.608, 128.775, 129.175, 136.109, 144.274, 145.442, 151.277, 166.421. GC-MS, *m/z*: 290 (M⁺₊₁, 1.5 %), 289 (M⁺, 27 %), 288 (M⁺₋₁, 1 %), 259 (, 12 %), 258 (, 21 %), 192 (, 29 %), 84 (, 100 %), 83 (, 16 %). Anal. Calcd. (%) for C₁₅H₁₅NSO₃ (289.35): C, 62.26; H, 5.23; N, 4.84; S, 11.08; Found: C, 61.87; H, 5.12; N, 4.59; S, 10.63.

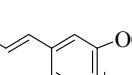
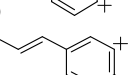
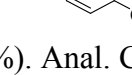
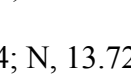

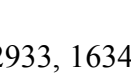
3.2.3.1.10. (E)-3-(4-hydroxy-3-methoxyphenyl)-N-(2-(thiophen-2-yl)ethyl)acrylamide (IIIj)

Yield: 95%. mp: 140-142°C. FT-IR (KBr, cm⁻¹) ν_{max} : 3431, 2930, 2838, 1634, 1593, 1568. ¹H-NMR (500 MHz, DMSO-*d*₆, ppm) δ : 2.848-2.874 (t, 2H, *J* = 13 Hz, *J* = 6.5 Hz, CH₂), 2.913-2.951 (q, 2H, *J* = 12.5 Hz, *J* = 6.5 Hz, CH₂), 3.801 (s, 3H, OCH₃), 5.501 (s, 1H, NH), 6.330-6.361 (d, 1H, *J* = 15.5 Hz, Ar), 6.769-6.785 (d, 1H, *J* = 8 Hz, Ar), 6.885-6.891 (d, 1H, *J* = 3 Hz, Ar), 6.945-6.962 (m, 1H, Ar), 7.023-7.042 (dd, 1H, *J* = 8 Hz, *J* = 1.5 Hz, Ar), 7.229-7.232 (s, 1H, Ar), 7.329-7.338 (d, 1H, *J* = 4.5 Hz, Ar), 7.389-7.410 (d, 1H, *J* = 15.5 Hz, Ar), 10.242 (s, 1H, OH).

^{13}C -NMR (125 MHz, DMSO- d_6 , ppm) δ : 28.393, 38.222, 39.442, 50.407, 112.167, 116.050, 117.175, 120.555, 121.944, 128.204, 129.114, 136.364, 144.205, 145.445, 151.147, 166.511.

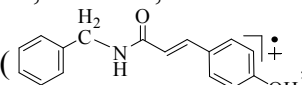
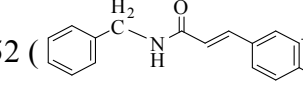
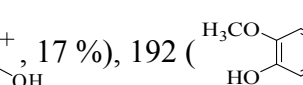
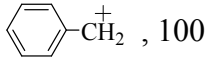
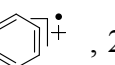
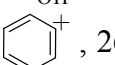
GC-MS, m/z : 304 ($\dot{\text{M}}^+$, 2 %), 303 ($\dot{\text{M}}^+$, 34 %), 302 ($\dot{\text{M}}^-$, 1.8 %), 273 (, 38 %), 272 (, 23 %), 192 (, 45 %), 111 (, 40 %), 98 (, 25 %), 83 (, 100 %), 71 ($\text{HC}^+=\text{CH}-\text{COOH}$, 22 %), 70 ($\text{HOOC}-\text{C}\equiv\text{CH}^+$, 28%), 69 ($\text{HOOC}-\text{C}\equiv\text{C}^+$, 33 %). Anal. Calcd. (%) for $\text{C}_{16}\text{H}_{17}\text{NSO}_3$ (303.38): C, 63.34; H, 5.65; N, 4.62; S, 10.57; Found: C, 62.97; H, 5.53; N, 4.29; S, 10.17.

3.2.3.1.11. (E)-N-(3-(1H-imidazol-1-yl)propyl)-3-(4-hydroxy-3-methoxyphenyl)acrylamide (IIIk)

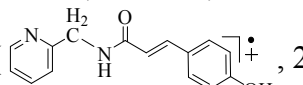
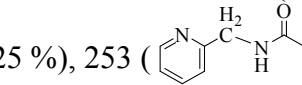
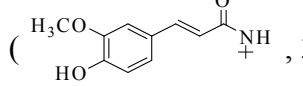
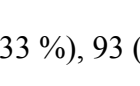
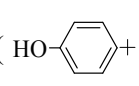
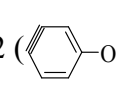
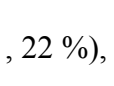
Yield: 86%. mp: 148-150°C. FT-IR (KBr, cm^{-1}) ν_{max} : 3413, 3254, 2930, 1636, 1590. ^1H -NMR (500 MHz, DMSO- d_6 , ppm) δ : 1.856-1.894 (q, 2H, $J = 6.5$ Hz, $J = 6$ Hz, CH_2), 2.569-2.595 (t, 2H, $J = 13$ Hz, $J = 6.5$ Hz, CH_2), 3.797 (s, 3H, OCH_3), 4.029-4.053 (q, 2H, $J = 5$ Hz, $J = 4.5$ Hz, CH_2), 5.530 (s, 1H, NH), 6.302-6.337 (d, 1H, $J = 17.5$ Hz, Ar), 6.765-6.781 (d, 1H, $J = 8$ Hz, Ar), 6.886 (s, 1H, Ar), 6.978-7.016 (t, 1H, $J = 19$ Hz, $J = 5.5$ Hz, Ar), 7.172 (s, 2H, Ar), 7.279-7.339 (t, 1H, $J = 30$ Hz, $J = 14.5$ Hz, Ar), 7.633 (s, 1H, Ar), 10.233 (s, 1H, OH). ^{13}C -NMR (125 MHz, DMSO- d_6 , ppm) δ : 31.003, 38.009, 50.287, 56.570, 112.787, 116.088, 117.085, 120.202, 121.899, 128.004, 128.994, 136.143, 144.205, 145.940, 151.167, 166.151. GC-MS m/z : 302 ($\dot{\text{M}}^+$, 2 %), 301 ($\dot{\text{M}}^+$, 34 %), 300 ($\dot{\text{M}}^-$, 2 %), 284 (, 8 %), 271 (, 38 %), 270 (, 22 %), 192 (, 28 %), 81 (, 100 %), 67 (, 33 %). Anal. Calcd. (%) for $\text{C}_{16}\text{H}_{19}\text{N}_3\text{O}_3$ (301.34): C, 63.77; H, 6.36; N, 13.94; Found: C, 62.48; H, 6.24; N, 13.72.

3.2.3.1.12. (E)-N-benzyl-3-(4-hydroxy-3-methoxyphenyl)acrylamide (IIIl)

Yield: 81%. mp: 135-137°C. FT-IR (KBr, cm^{-1}) ν_{max} : 3431, 3007, 2933, 1634, 1598, 1504. ^1H -NMR (500 MHz, DMSO- d_6 , ppm) δ : 3.789 (s, 2H, CH_2), 3.885 (s, 3H, OCH_3), 5.558 (s, 1H, NH), 6.319-6.350 (d, 1H, $J = 15.5$ Hz, Ar), 6.770-6.786 (d, 1H, $J = 8$ Hz, Ar), 7.014-7.030 (d, 1H,

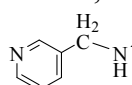
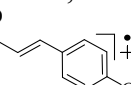
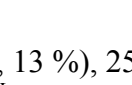
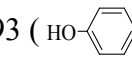
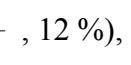
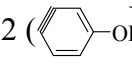
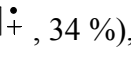
$J = 8$ Hz, Ar), 7.212-7.247 (t, 2H, $J = 17.5$ Hz, $J = 10.5$ Hz, Ar), 7.304-7.391 (m, 5H, Ar), 10.267 (s, 1H, OH). $^{13}\text{C-NMR}$ (125 MHz, DMSO- d_6 , ppm) δ : 45.333, 55.162, 112.139, 116.403, 118.775, 120.141, 126.242, 127.441, 128.167, 129.454, 141.358, 143.587, 145.557, 151.112, 167.241. GC-MS m/z : 284 ($\dot{\text{M}}^+$, 1%), 283 ($\dot{\text{M}}^+$, 30%), 282 ($\dot{\text{M}}^-1$, 1%), 253 (, 14%), 252 (, 17%), 192 (, 20%), 91 (, 100%), 78 (, 28%), 77 (, 26%). Anal. Calcd. (%) for $\text{C}_{17}\text{H}_{17}\text{NO}_3$ (283.32): C, 72.07, H, 6.05, N, 4.94; Found: C, 71.26; H, 5.94; N, 4.08.

3.2.3.1.13. (E)-3-(4-hydroxy-3-methoxyphenyl)-N-(pyridin-2-ylmethyl)acrylamide (III_m)

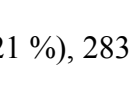
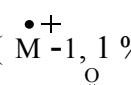
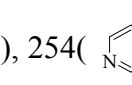
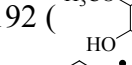
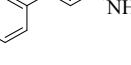
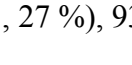
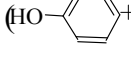
Yield: 98%. mp: 120-122°C. FT-IR (KBr, cm^{-1}) ν_{max} : 3425, 2895, 1635, 1594, 1557, 1479. $^1\text{H-NMR}$ (500 MHz, DMSO- d_6 , ppm) δ : 3.796 (s, 2H, CH_2), 3.894 (s, 3H, OCH_3), 5.262 (s, 1H, NH), 6.328-6.360 (d, 1H, $J = 16$ Hz, Ar), 6.774-6.791 (d, 1H, $J = 8.5$ Hz, Ar), 7.006-7.024 (d, 1H, $J = 9$ Hz, Ar), 7.027 (s, 1H, Ar), 7.243-7.267 (t, 1H, $J = 8.5$ Hz, $J = 6.5$ Hz, Ar), 7.345-7.377 (d, 1H, $J = 14$ Hz, Ar), 7.437-7.453 (d, 1H, $J = 8$ Hz, Ar), 7.750-7.780 (t, 1H, $J = 15$ Hz, $J = 7.5$ Hz, Ar), 8.500-8.508 (d, 1H, $J = 4$ Hz, Ar), 10.254 (s, 1H, OH). $^{13}\text{C-NMR}$ (125 MHz, DMSO- d_6 , ppm) δ : 48.209, 55.607, 112.782, 116.328, 118.182, 120.028, 121.212, 124.118, 128.282, 137.116, 144.328, 145.137, 147.144, 151.567, 156.151, 167.371. GC-MS m/z : 285 ($\dot{\text{M}}^+$, 1%), 284 ($\dot{\text{M}}^+$, 34%), 283 ($\dot{\text{M}}^-1$, 1%), 254 (, 25%), 253 (, 28%), 192 (, 33%), 93 (, 13%), 92 (, 22%), 78 (, 100%), 77 (, 26%). Anal. Calcd. (%) for $\text{C}_{16}\text{H}_{16}\text{N}_2\text{O}_3$ (285.32): C, 67.59; H, 5.67; N, 9.85; Found: C, 66.11; H, 5.63; N, 9.18.

3.2.3.1.14. (E)-3-(4-hydroxy-3-methoxyphenyl)-N-(pyridin-3-ylmethyl)acrylamide (III_n)

Yield: 96%. mp: 128-130°C. FT-IR (KBr, cm^{-1}) ν_{max} : 3425, 2907, 1636, 1586, 1511. $^1\text{H-NMR}$ (500 MHz, DMSO- d_6 , ppm) δ : 3.762 (s, 2H, CH_2), 3.806 (s, 3H, OCH_3), 5.241 (s, 1H, NH), 6.330-6.362 (d, 1H, $J = 16$ Hz, Ar), 6.773-6.789 (d, 1H, $J = 8$ Hz, Ar), 7.039-7.055 (d, 1H, $J = 8$

Hz, Ar), 7.242 (s, 1H, Ar), 7.316-7.341 (q, 1H, $J = 12.5$ Hz, $J = 5$ Hz, Ar), 7.405-7.437 (d, 1H, $J = 16$ Hz, Ar), 7.443-7.458 (d, 1H, $J = 7.5$ Hz, Ar), 8.417-8.426 (d, 1H, $J = 4.5$ Hz, Ar), 8.529 (s, 1H, Ar), 10.278 (s, 1H, 1×OH). $^{13}\text{C-NMR}$ (125 MHz, DMSO- d_6 , ppm) δ : 45.009, 55.627, 112.162, 116.333, 118.022, 120.028, 121.242, 124.288, 128.167, 137.555, 144.358, 145.137, 147.747, 151.377, 156.282, 167.451. GC-MS m/z : 285 ($\dot{\text{M}}^+$, 1 %), 284 ($\dot{\text{M}}^+$, 41 %), 283 ($\dot{\text{M}}^-$, 1 %), 254 (, 13 %), 253 (, 22 %), 192 (, 31 %), 93 (, 12 %), 92 (, 34 %), 78 (, 100 %), 77 (, 19 %). Anal. Calcd. (%) for $\text{C}_{16}\text{H}_{16}\text{N}_2\text{O}_3$ (285.32): C, 67.59; H, 5.67; N, 9.85; Found: C, 66.23; H, 5.62; N, 9.12.

3.2.3.1.15. (E)-3-(4-hydroxy-3-methoxyphenyl)-N-(pyridin-4-ylmethyl)acrylamide (IIIo)

Yield: 98%. mp: 160-162°C. FT-IR (KBr, cm^{-1}) ν_{max} : 3431, 3002, 1636, 1595, 1520, 1459. $^1\text{H-NMR}$ (500 MHz, DMSO- d_6 , ppm) δ : 3.771 (s, 2H, CH_2), 3.804 (s, 3H, OCH_3), 5.438 (s, 1H, NH), 6.338-6.369 (d, 1H, $J = 14.5$ Hz, Ar), 6.772-6.789 (d, 1H, $J = 8.5$ Hz, Ar), 7.047-7.063 (d, 1H, $J = 8$ Hz, Ar), 7.252 (s, 1H, Ar), 7.350-7.359 (d, 2H, $J = 4.5$ Hz, Ar), 7.423-7.454 (d, 1H, $J = 14.5$ Hz, Ar), 8.473-8.483 (d, 2H, $J = 5$ Hz, Ar), 10.233 (s, 1H, OH). $^{13}\text{C-NMR}$ (125 MHz, DMSO- d_6 , ppm) δ : 44.274, 55.327, 112.070, 116.016, 118.585, 120.442, 124.412, 128.782, 144.328, 145.780, 147.810, 149.147, 151.817, 167.181. GC-MS m/z : 285 ($\dot{\text{M}}^+$, 1 %), 284 ($\dot{\text{M}}^+$, 21 %), 283 ($\dot{\text{M}}^-$, 1 %), 254 (, 18 %), 253 (, 22 %), 192 (, 27 %), 93 (, 12 %), 92 (, 29 %), 78 (, 100 %), 77 (, 16 %). Anal. Calcd. (%) for $\text{C}_{16}\text{H}_{16}\text{N}_2\text{O}_3$ (285.32): C, 67.59; H, 5.67; N, 9.85; Found: C, 66.03; H, 5.59; N, 9.09.

3.2.3.1.16. (E)-N-(acridin-9-yl)-3-(4-hydroxy-3-methoxyphenyl)acrylamide (Va)

Yield: 85%. mp: 262-264°C. FT-IR (cm^{-1}): 3331, 3172, 1649, 1616, 1589, 1558. $^1\text{H-NMR}$ (500 MHz, DMSO- d_6 , ppm) δ : 3.791 (s, 3H, 1× OCH_3), 5.444 (s, 1H, 1×NH), 6.284-6.315 (d, 1H, $J = 15.5$ Hz, Ar), 6.758-6.774 (d, 1H, $J = 8$ Hz, Ar), 6.958-6.975 (d, 1H, $J = 8.5$ Hz, Ar), 7.159 (s,

1H, Ar), 7.238-7.270 (d, 1H, $J = 11$ Hz, Ar), 7.381-7.411 (d, 2H, $J = 15$ Hz, $J = 7.5$ Hz, Ar), 7.474-7.491 (d, 2H, $J = 8.5$ Hz, Ar), 7.775-7.806 (q, 2H, $J = 15.5$ Hz, $J = 7.5$ Hz, Ar), 8.077-8.095 (d, 2H, $J = 9$ Hz, Ar), 10.215 (s, 1H, OH). ^{13}C -NMR (125 MHz, DMSO- d_6 , ppm) δ : 56.139, 112.978, 114.222, 116.169, 118.129, 120.108, 124.221, 126.136, 128.551, 129.109, 129.988, 144.155, 144.998, 148.143, 151.363, 164.555, 167.747. APCI-MS, m/z : 371.19 ($\dot{\text{M}}^+$, 100 %). Anal. Calcd. (%) for $\text{C}_{23}\text{H}_{18}\text{N}_2\text{O}_3$ (370.40): C, 74.58; H, 4.90; N, 7.56; Found: C, 73.17; H, 4.79; N, 7.09.

3.2.3.1.17. (*E*)-3-(4-hydroxy-3-methoxyphenyl)-*N*-(4-methylacridin-9-yl)acrylamide (Vb)

Yield: 88%. mp: 271-273°C. FT-IR (cm^{-1}): 3378, 3121, 1646, 1618, 1593, 1562. ^1H -NMR (500 MHz, DMSO- d_6 , ppm) δ : 2.283 (s, 3H, CH_3), 3.781 (s, 3H, OCH_3), 5.497 (s, 1H, NH), 6.284-6.314 (d, 1H, $J = 15$ Hz, Ar), 6.758-6.785 (m, 2H, Ar), 6.961-6.979 (d, 1H, $J = 9$ Hz, Ar), 7.159-7.181 (q, 2H, $J = 10.5$ Hz, $J = 4.5$ Hz, Ar), 7.270-7.296 (t, 2H, $J = 13$ Hz, $J = 7.5$ Hz, Ar), 7.381-7.411 (t, 1H, $J = 15$ Hz, $J = 7.5$ Hz, Ar), 7.474-7.491 (d, 1H, $J = 8.5$ Hz, Ar), 7.778-7.797 (d, 1H, $J = 9.5$ Hz, Ar), 8.077-8.095 (d, 1H, $J = 9$ Hz, Ar), 10.238 (s, 1H, OH). ^{13}C -NMR (125 MHz, DMSO- d_6 , ppm) δ : 22.394, 56.101, 108.551, 112.449, 116.169, 118.383, 119.338, 120.812, 122.222, 126.228, 127.127, 128.225, 128.787, 129.127, 129.978, 130.998, 136.109, 144.129, 145.119, 148.143, 151.363, 155.441, 164.145, 167.148. APCI-MS, m/z : 385.11 ($\dot{\text{M}}^+$, 100 %). Anal. Calcd. (%) for $\text{C}_{24}\text{H}_{20}\text{N}_2\text{O}_3$ (384.43): C, 74.98; H, 5.24; N, 7.29; Found: C, 74.21; H, 5.13; N, 6.91.

3.2.3.1.18. (*E*)-3-(4-hydroxy-3-methoxyphenyl)-*N*-(3-methylacridin-9-yl)acrylamide (Vc)

Yield: 89%. mp: 259-261°C. FT-IR (cm^{-1}): 3391, 3211 1641, 1607, 1591, 1555. ^1H -NMR (500 MHz, DMSO- d_6 , ppm) δ : 2.275 (s, 3H, CH_3), 3.789 (s, 3H, OCH_3), 5.497 (s, 1H, NH), 6.284-6.314 (d, 1H, $J = 15$ Hz, Ar), 6.758-6.784 (d, 2H, $J = 13$ Hz, Ar), 6.951-6.988 (m, 2H, Ar), 7.158-7.187 (q, 2H, $J = 14.5$ Hz, $J = 9.5$ Hz, Ar), 7.272-7.303 (q, 2H, $J = 15.5$ Hz, $J = 10.5$ Hz, Ar),

7.381-7.412 (t, 1H, $J = 15.5$ Hz, $J = 7.5$ Hz, Ar), 7.474-7.493 (d, 1H, $J = 9.5$ Hz, Ar), 7.779-7.797 (d, 1H, $J = 9$ Hz, Ar), 8.077-8.098 (d, 1H, $J = 10.5$ Hz, Ar), 10.222 (s, 1H, OH). ^{13}C -NMR (125 MHz, DMSO- d_6 , ppm) δ : 26.084, 56.003, 107.109, 112.129, 116.119, 118.383, 119.337, 120.812, 122.112, 127.228, 127.786, 128.225, 128.888, 129.127, 129.988, 131.838, 139.443, 144.116, 145.993, 147.443, 148.333, 151.141, 164.313, 167.313. APCI-MS, m/z : 385.18 ($\dot{\text{M}}^+$, 100 %). Anal. Calcd. (%) for $\text{C}_{24}\text{H}_{20}\text{N}_2\text{O}_3$ (384.43): C, 74.98; H, 5.24; N, 7.29; Found: C, 73.67; H, 5.15; N, 6.69.

3.2.3.1.19. (E)-3-(4-hydroxy-3-methoxyphenyl)-N-(2-methylacridin-9-yl)acrylamide (Vd)

Yield: 88%. mp: 262-264°C. FT-IR (cm^{-1}): 3331, 3201, 1638, 1603, 1586, 1553. ^1H -NMR (500 MHz, DMSO- d_6 , ppm) δ : 2.278 (s, 3H, CH_3), 3.666 (s, 3H, OCH_3), 5.517 (s, 1H, NH), 6.288-6.317 (d, 1H, $J = 14.5$ Hz, Ar), 6.752-6.781 (d, 1H, $J = 14.5$ Hz, Ar), 6.953-6.985 (m, 2H, Ar), 7.155-7.185 (q, 2H, $J = 15$ Hz, $J = 9.5$ Hz, Ar), 7.274-7.301 (q, 2H, $J = 12.5$ Hz, $J = 7$ Hz, Ar), 7.382-7.414 (t, 1H, $J = 16$ Hz, $J = 7.5$ Hz, Ar), 7.474-7.494 (d, 1H, $J = 10$ Hz, Ar), 7.778-7.798 (d, 1H, $J = 10$ Hz, Ar), 8.070-8.091 (d, 1H, $J = 10.5$ Hz, Ar), 10.092 (s, 1H, OH). ^{13}C -NMR (125 MHz, DMSO- d_6 , ppm) δ : 27.274, 55.333, 107.239, 112.129, 116.264, 118.387, 119.399, 120.274, 121.025, 127.128, 128.028, 128.325, 128.888, 129.240, 130.838, 133.194, 135.423, 144.196, 145.923, 146.433, 148.334, 151.148, 164.311, 167.510. APCI-MS, m/z : 385.17 ($\dot{\text{M}}^+$, 100 %). Anal. Calcd. (%) for $\text{C}_{24}\text{H}_{20}\text{N}_2\text{O}_3$ (384.43): C, 74.98; H, 5.24; N, 7.29; Found: C, 73.53; H, 5.13; N, 6.51.

3.2.3.1.20. (E)-3-(4-hydroxy-3-methoxyphenyl)-N-(4-methoxyacridin-9-yl)acrylamide (Ve)

Yield: 91%. mp: 281-283°C. FT-IR (cm^{-1}): 3403, 3151, 1642, 1609, 1591, 1558. ^1H -NMR (500 MHz, DMSO- d_6 , ppm) δ : 3.777 (s, 3H, OCH_3), 3.881 (s, 3H, OCH_3), 5.465 (s, 1H, NH), 6.285-6.315 (d, 1H, $J = 15$ Hz, Ar), 6.753-6.781 (m, 2H, Ar), 6.963-6.978 (d, 1H, $J = 7.5$ Hz, Ar), 7.157-7.182 (q, 2H, $J = 12.5$ Hz, $J = 6.5$ Hz, Ar), 7.268-7.305 (q, 2H, $J = 18.5$ Hz, $J = 11.5$ Hz,

Ar), 7.383-7.413 (t, 1H, $J = 15$ Hz, $J = 8.5$ Hz, Ar), 7.473-7.493 (d, 1H, $J = 10$ Hz, Ar), 7.755-7.777 (d, 1H, $J = 11$ Hz, Ar), 8.083-8.103 (d, 1H, $J = 10$ Hz, Ar), 10.317 (s, 1H, OH). $^{13}\text{C-NMR}$ (125 MHz, $\text{DMSO-}d_6$, ppm) δ : 55.209, 56.099, 106.239, 108.109, 112.274, 113.333, 116.339, 118.274, 120.035, 122.128, 125.088, 127.125, 128.088, 128.130, 129.838, 130.144, 139.433, 144.196, 144.923, 148.433, 151.144, 156.148, 164.111, 167.192. APCI-MS, m/z : 401.48 ($\dot{\text{M}}^+$, 100 %). Anal. Calcd. (%) for $\text{C}_{24}\text{H}_{20}\text{N}_2\text{O}_4$ (400.43): C, 71.99; H, 5.03; N, 7.00; Found: C, 71.16; H, 4.93; N, 6.43.

3.2.3.1.21. (E)-3-(4-hydroxy-3-methoxyphenyl)-N-(3-methoxyacridin-9-yl)acrylamide (Vf)

Yield: 93%. mp: 278-280°C. FT-IR (cm^{-1}): $^1\text{H-NMR}$ (500 MHz, $\text{DMSO-}d_6$, ppm) δ : 3.695 (s, 3H, OCH_3), 3.789 (s, 3H, OCH_3), 5.506 (s, 1H, NH), 6.286-6.315 (d, 1H, $J = 14.5$ Hz, Ar), 6.754-6.784 (d, 1H, $J = 15$ Hz, Ar), 6.944-6.983 (m, 2H, Ar), 7.152-7.183 (q, 2H, $J = 15.5$ Hz, $J = 11$ Hz, Ar), 7.272-7.309 (q, 2H, $J = 18.5$ Hz, $J = 10.5$ Hz, Ar), 7.380-7.411 (t, 1H, $J = 15.5$ Hz, $J = 7.5$ Hz, Ar), 7.474-7.493 (d, 1H, $J = 9.5$ Hz, Ar), 7.778-7.798 (d, 1H, $J = 10$ Hz, Ar), 8.077-8.099 (d, 1H, $J = 11$ Hz, Ar), 10.335 (s, 1H, OH). $^{13}\text{C-NMR}$ (125 MHz, $\text{DMSO-}d_6$, ppm) δ : 55.739, 56.359, 105.444, 107.298, 112.528, 116.835, 117.298, 118.238, 118.535, 120.158, 122.998, 127.125, 128.078, 128.908, 129.128, 129.825, 144.833, 145.116, 148.923, 150.133, 151.796, 159.516, 164.235, 167.199. APCI-MS, m/z : 401.49 ($\dot{\text{M}}^+$, 100 %). Anal. Calcd. (%) for $\text{C}_{24}\text{H}_{20}\text{N}_2\text{O}_4$ (400.43): C, 71.99; H, 5.03; N, 7.00; Found: C, 70.33; H, 4.97; N, 6.55.

3.2.3.1.22. (E)-3-(4-hydroxy-3-methoxyphenyl)-N-(2-methoxyacridin-9-yl)acrylamide (Vg)

Yield: 90%. mp: 275-277°C. FT-IR (cm^{-1}): 3407, 3161, 1642, 1611, 1581, 1567. $^1\text{H-NMR}$ (500 MHz, $\text{DMSO-}d_6$, ppm) δ : 3.669 (s, 3H, OCH_3), 3.785 (s, 3H, OCH_3), 5.458 (s, 1H, NH), 6.292-6.322 (d, 1H, $J = 15$ Hz, Ar), 6.777-6.807 (d, 1H, $J = 15$ Hz, Ar), 6.944-6.983 (m, 2H, Ar), 7.161-7.189 (q, 2H, $J = 14$ Hz, $J = 9$ Hz, Ar), 7.271-7.304 (q, 2H, $J = 16.5$ Hz, $J = 11.5$ Hz, Ar), 7.377-7.413 (t, 1H, $J = 18$ Hz, $J = 10.5$ Hz, Ar), 7.477-7.494 (d, 1H, $J = 8.5$ Hz, Ar), 7.778-7.798

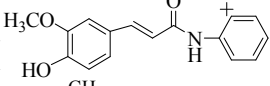
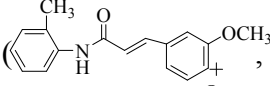
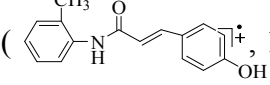
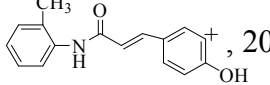
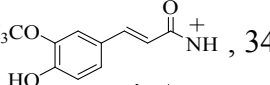
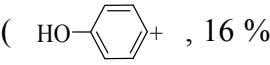
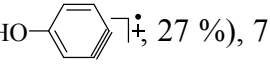
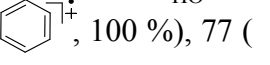
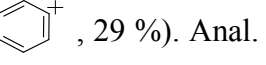
(d, 1H, $J = 10$ Hz, Ar), 8.077-8.097 (d, 1H, $J = 10$ Hz, Ar), 10.458 (s, 1H, OH). $^{13}\text{C-NMR}$ (125 MHz, DMSO- d_6 , ppm) δ : 55.509, 56.451, 105.209, 108.099, 112.329, 116.333, 118.299, 120.232, 121.535, 123.858, 127.088, 128.125, 128.778, 129.088, 129.708, 130.127, 143.833, 144.816, 144.923, 147.433, 151.196, 156.516, 163.105, 167.119. APCI-MS, m/z : 401.47 ($\dot{\text{M}}^+$, 100 %). Anal. Calcd. (%) for $\text{C}_{24}\text{H}_{20}\text{N}_2\text{O}_4$ (400.43): C, 71.99; H, 5.03; N, 7.00; Found: C, 70.21; H, 4.94; N, 6.18.

3.2.3.1.23. Synthesis of (*E*)-3-(4-hydroxy-3-methoxyphenyl)-*N*-phenylacrylamide (VIIa)

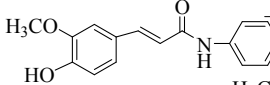
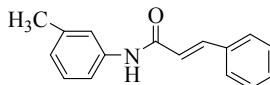
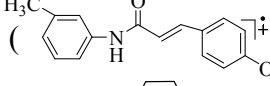
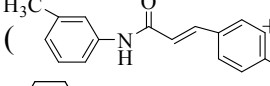
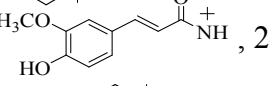
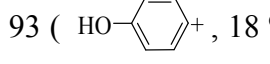
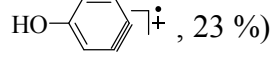
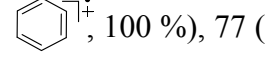
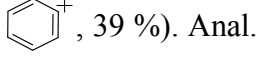
yield: 97%. mp: 138-140°C. FT-IR (cm^{-1}): 3434, 3292, 1664, 1614, 1513, 1429, 1322, 1274, 1203, 1173, 1108, 1032. $^1\text{H-NMR}$ (500 MHz, DMSO- d_6 , ppm) δ : 3.787 (s, 3H, OCH₃), 6.318-6.350 (d, 1H, $J = 16$ Hz, Ar), 6.770-6.786 (d, 1H, $J = 8$ Hz, Ar), 7.014-7.030 (d, 1H, $J = 8$ Hz, Ar), 7.213-7.255 (t, 2H, $J = 21$ Hz, $J = 21$ Hz, Ar), 7.303-7.339 (m, 5H, Ar), 8.391 (s, 1H, NH), 10.367 (s, 1H, OH). $^{13}\text{C-NMR}$ (125 MHz, DMSO- d_6 , ppm) δ : 56.320, 112.085, 116.070, 118.444, 120.585, 121.302, 124.412, 128.328, 129.338, 135.780, 144.117, 149.167, 151.447, 166.118. GC-MS, m/z : 270 ($\dot{\text{M}}^+$, 1.3 %), 269 ($\dot{\text{M}}^+$, 31.2 %), 252 (, 23 %), 239 (, 12 %), 238 (, 25 %), 192 (, 28 %), 93 (, 10 %), 92 (, 7 %), 91 (, 100 %), 77 (, 25 %). Anal. Calcd. (%) for $\text{C}_{16}\text{H}_{15}\text{NO}_3$ (269.29): C, 71.36, H, 5.61, N, 5.20; Found: C, 70.11, H, 5.57, N, 4.93.

3.2.3.1.24. (*E*)-3-(4-hydroxy-3-methoxyphenyl)-*N*-*o*-tolylacrylamide (VIIb)

Yield: 87%. mp: 162-164°C. FT-IR (cm^{-1}): 3436, 3015, 2968, 1691, 1665, 1619, 1597. $^1\text{H-NMR}$ (500 MHz, DMSO- d_6 , ppm) δ : 2.738 (s, 3H, CH₃), 3.799 (s, 3H, OCH₃), 6.326-6.364 (d, 1H, $J = 19$ Hz, Ar), 6.774-6.790 (d, 1H, $J = 8$ Hz, Ar), 7.007-7.022 (d, 1H, $J = 7.5$ Hz, Ar), 7.207 (s, 1H, Ar), 7.240-7.267 (t, 1H, $J = 13.5$ Hz, $J = 8$ Hz, Ar), 7.345-7.376 (d, 1H, $J = 15.5$ Hz, Ar), 7.437-7.453 (d, 1H, $J = 8$ Hz, Ar), 7.765-7.783 (d, 1H, $J = 9$ Hz, Ar), 8.500-8.505 (d, 1H, $J = 2.5$ Hz, Ar), 8.953 (s, 1H, NH), 10.242 (s, 1H, OH). $^{13}\text{C-NMR}$ (125 MHz, DMSO- d_6 , ppm) δ : 16.333,

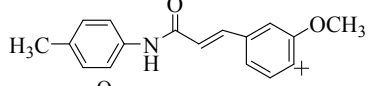
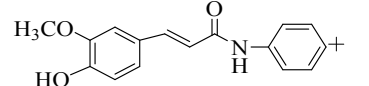
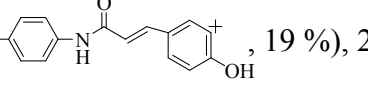
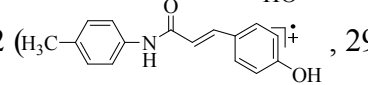
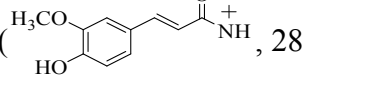
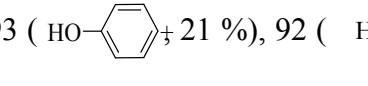
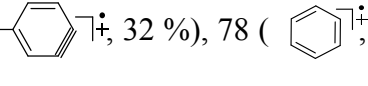
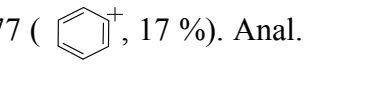
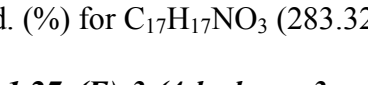
56.087, 112.114, 116.016, 118.044, 120.828, 121.512, 124.492, 126.493, 128.545, 129.328, 134.801, 135.780, 144.145, 145.497, 151.457, 166.048. GC-MS, m/z : 284 (\dot{M}^+ , 1.1 %), 283 (\dot{M}^+ , 26.3 %), 282 (\dot{M}^- , 1.0%), 268 (, 8 %), 266 (, 15 %), 253 (, 18 %), 252 (, 20 %), 192 (, 34 %), 93 (, 16 %), 92 (, 27 %), 78 (, 100 %), 77 (, 29 %). Anal. Calcd. (%) for $C_{17}H_{17}NO_3$ (283.32): C, 72.07, H, 6.05, N, 4.94; Found: C, 71.43, H, 5.97, N, 4.01.

3.2.3.1.25. (E)-3-(4-hydroxy-3-methoxyphenyl)-N-m-tolylacrylamide (VIIc)

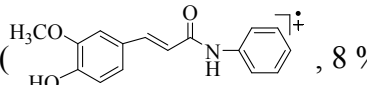
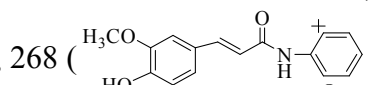
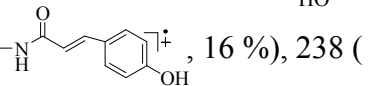
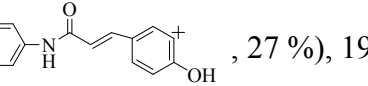
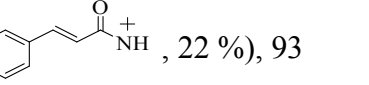
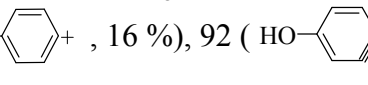
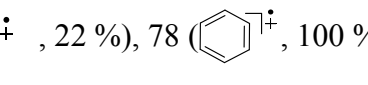
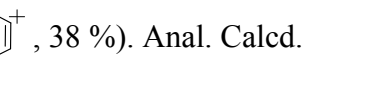
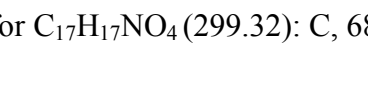
Yield: 80%. mp: 164-166°C. FT-IR (cm^{-1}): 3435, 3189, 3014, 1690, 1665, 1618, 1584, 1564. 1H -NMR (500 MHz, DMSO- d_6 , ppm) δ : 2.857 (s, 3H, CH₃), 3.842 (s, 3H, OCH₃), 6.329-6.363 (d, 1H, $J = 17$ Hz, Ar), 6.773-6.787 (d, 1H, $J = 7$ Hz, Ar), 7.039-7.057 (d, 1H, $J = 9$ Hz, Ar), 7.240 (s, 1H, Ar), 7.315-7.341 (m, 1H, Ar), 7.409-7.437 (d, 1H, $J = 14$ Hz, Ar), 7.743-7.759 (d, 1H, $J = 8$ Hz, Ar), 8.418-8.425 (d, 1H, $J = 3.5$ Hz, Ar), 8.528 (s, 1H, Ar), 8.879 (s, 1H, NH), 10.241 (s, 1H, OH). ^{13}C -NMR (125 MHz, DMSO- d_6 , ppm) δ : 26.444, 56.007, 112.114, 116.016, 118.044, 119.205, 120.828, 121.512, 124.492, 128.545, 129.328, 135.801, 138.780, 144.145, 145.497, 151.457, 167.048. GC-MS, m/z : 284 (\dot{M}^+ , 0.97 %), 283 (\dot{M}^+ , 33.6 %), 282 (\dot{M}^- , 0.9 %), 268 (, 8 %), 266 (, 19 %), 253 (, 21 %), 252 (, 26 %), 192 (, 24 %), 93 (, 18 %), 92 (, 23 %), 78 (, 100 %), 77 (, 39 %). Anal. Calcd. (%) for $C_{17}H_{17}NO_3$ (283.32): C, 72.07, H, 6.05, N, 4.94; Found: C, 71.21, H, 5.92, N, 4.17.

3.2.3.1.26. (E)-3-(4-hydroxy-3-methoxyphenyl)-N-p-tolylacrylamide (VIIId)

Yield: 83%. mp: 158-160°C. FT-IR (cm^{-1}): 3436, 3015, 2978, 1691, 1665, 1619, 1597, 1515, 1464, 1431, 1379, 1273, 1206, 1177, 1113, 1034. 1H -NMR (500 MHz, DMSO- d_6 , ppm) δ : 2.851 (s, 3H, CH₃), 3.832 (s, 3H, OCH₃), 6.337-6.365 (d, 1H, $J = 14$ Hz, Ar), 6.772-6.789 (d, 1H, $J = 8.5$ Hz, Ar), 7.046-7.062 (d, 1H, $J = 8$ Hz, Ar), 7.256 (s, 1H, Ar), 7.350-7.359 (d, 2H, $J = 4.5$

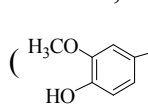
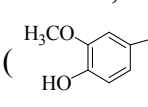
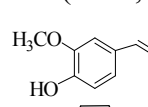
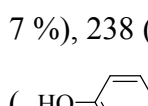
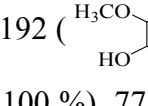
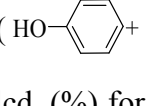
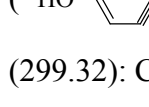
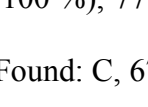
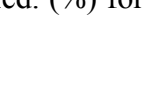
Hz, Ar), 7.420-7.451 (d, 1H, $J = 15.5$ Hz, Ar), 8.475-8.485 (d, 2H, $J = 5$ Hz, Ar), 8.885 (s, 1H, NH), 10.247 (s, 1H, OH). $^{13}\text{C-NMR}$ (125 MHz, DMSO- d_6 , ppm) δ : 26.828, 56.507, 112.545, 116.016, 118.145, 120.828, 121.452, 127.545, 129.518, 132.800, 134.970, 144.145, 145.497, 151.457, 167.278. GC-MS, m/z : 284 ($\dot{\text{M}}^+$, 0.97 %), 283 ($\dot{\text{M}}$, 41 %), 282 ($\dot{\text{M}}^-1$, 0.9 %), 268 (, 12 %), 266 (, 20 %), 253 (, 19 %), 252 (, 29 %), 192 (, 28 %), 93 (, 21 %), 92 (, 32 %), 78 (, 100 %), 77 (, 17 %). Anal. Calcd. (%) for $\text{C}_{17}\text{H}_{17}\text{NO}_3$ (283.32): C, 72.07, H, 6.05, N, 4.94; Found: C, 71.09, H, 5.94, N, 4.05.

3.2.3.1.27. (E)-3-(4-hydroxy-3-methoxyphenyl)-N-(2-methoxyphenyl)acrylamide (VIIe)

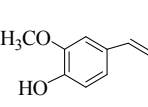
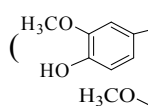
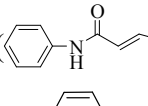
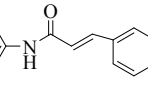
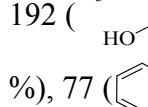
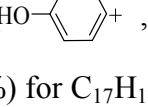
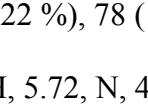
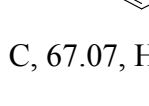

Yield: 79%. mp: 174-176°C. FT-IR (cm^{-1}): 3437, 3377, 1691, 1645, 1620, 1588, 1563. $^1\text{H-NMR}$ (500 MHz, DMSO- d_6 , ppm) δ : 3.702 (s, 3H, OCH₃), 3.799 (s, 3H, OCH₃), 6.329-6.367 (d, 1H, $J = 19$ Hz, Ar), 6.774-6.790 (d, 1H, $J = 8$ Hz, Ar), 7.006-7.022 (d, 1H, $J = 8$ Hz, Ar), 7.207 (s, 1H, Ar), 7.241-7.267 (t, 1H, $J = 13$ Hz, $J = 6.5$ Hz, Ar), 7.344-7.374 (d, 1H, $J = 15$ Hz, Ar), 7.437-7.453 (d, 1H, $J = 8$ Hz, Ar), 7.758-7.784 (t, 1H, $J = 13$ Hz, $J = 4$ Hz, Ar), 8.501-8.508 (d, 1H, $J = 3.5$ Hz, Ar), 8.988 (s, 1H, NH), 10.372 (s, 1H, OH). $^{13}\text{C-NMR}$ (125 MHz, DMSO- d_6 , ppm) δ : 56.004, 56.997, 112.112, 116.016, 118.048, 120.828, 121.342, 124.772, 126.498, 128.577, 129.328, 134.805, 135.784, 144.145, 145.497, 151.428, 167.005. GC-MS, m/z : 300 ($\dot{\text{M}}^+$, 0.93 %), 299 ($\dot{\text{M}}^+$, 26 %), 269 (, 8 %), 268 (, 18 %), 239 (, 16 %), 238 (, 27 %), 192 (, 22 %), 93 (, 16 %), 92 (, 22 %), 78 (, 100 %), 77 (, 38 %). Anal. Calcd. (%) for $\text{C}_{17}\text{H}_{17}\text{NO}_4$ (299.32): C, 68.22, H, 5.72, N, 4.68; Found: C, 67.37, H, 5.67, N, 4.02.

3.2.3.1.28. (E)-3-(4-hydroxy-3-methoxyphenyl)-N-(3-methoxyphenyl)acrylamide (VIIIf)

Yield: 84%. mp: 128-130°C. FT-IR (cm^{-1}): 3433, 3347, 1689, 1663, 1623, 1596, 1560. $^1\text{H-NMR}$ (500 MHz, DMSO- d_6 , ppm) δ : 3.709 (s, 3H, OCH₃), 3.802 (s, 3H, OCH₃), 6.327-6.361 (d,

1H, $J = 17$ Hz, Ar), 6.777-6.791 (d, 1H, $J = 7$ Hz, Ar), 7.039-7.059 (d, 1H, $J = 10$ Hz, Ar), 7.240 (s, 1H, Ar), 7.314-7.343 (q, 1H, $J = 10$ Hz, $J = 9$ Hz, Ar), 7.409-7.437 (d, 1H, $J = 14$ Hz, Ar), 7.740-7.756 (d, 1H, $J = 8$ Hz, Ar), 8.419-8.426 (d, 1H, $J = 3.5$ Hz, Ar), 8.552 (s, 1H, Ar), 8.844 (s, 1H, NH), 10.241 (s, 1H, OH). ^{13}C -NMR (125 MHz, DMSO- d_6 , ppm) δ : 56.024, 56.797, 112.204, 116.088, 118.074, 119.275, 120.525, 121.512, 124.444, 128.545, 129.928, 135.800, 138.788, 144.244, 145.397, 151.357, 167.119. GC-MS, m/z : 300 ($\dot{\text{M}}^+_{+1}$, 1.2 %), 299 ($\dot{\text{M}}^+$, 17 %), 269 (, 10 %), 268 (, 17 %), 239 (, 7 %), 238 (, 23 %), 192 (, 25 %), 93 (, 17 %), 92 (, 21 %), 78 (, 100 %), 77 (, 38 %). Anal. Calcd. (%) for $\text{C}_{17}\text{H}_{17}\text{NO}_4$ (299.32): C, 68.22, H, 5.72, N, 4.68; Found: C, 67.41, H, 5.63, N, 4.11.

3.2.3.1.29. (*E*)-3-(4-hydroxy-3-methoxyphenyl)-*N*-(4-methoxyphenyl)acrylamide (VIIg)

Yield: 83%. mp: 136-138°C. FT-IR (cm^{-1}): 3436, 3359, 1686, 1661, 1620, 1526, 1471, 1429, 1381, 1334, 1271, 1215, 1147, 1034. ^1H -NMR (500 MHz, DMSO- d_6 , ppm) δ : 3.711 (s, 3H, OCH₃), 3.803 (s, 3H, OCH₃), 6.338-6.368 (d, 1H, $J = 15$ Hz, Ar), 6.772-6.788 (d, 1H, $J = 8$ Hz, Ar), 7.050-7.066 (d, 1H, $J = 8$ Hz, Ar), 7.253 (s, 1H, Ar), 7.356-7.366 (d, 2H, $J = 5$ Hz, Ar), 7.425-7.455 (d, 1H, $J = 15$ Hz, Ar), 8.475-8.485 (d, 2H, $J = 5$ Hz, Ar), 8.888 (s, 1H, NH), 10.236 (s, 1H, OH). ^{13}C -NMR (125 MHz, DMSO- d_6 , ppm) δ : 56.084, 56.587, 112.445, 116.022, 118.255, 120.808, 121.402, 127.745, 129.517, 132.800, 134.878, 144.455, 145.497, 151.667, 167.378. GC-MS, m/z : 300 ($\dot{\text{M}}^+_{+1}$, 1.2 %), 299 ($\dot{\text{M}}^+$, 29 %), 269 (, 18 %), 268 (, 37 %), 239 (, 15 %), 238 (, 22 %), 192 (, 32 %), 93 (, 16 %), 92 (, 22 %), 78 (, 100 %), 77 (, 37 %). Anal. Calcd. (%) for $\text{C}_{17}\text{H}_{17}\text{NO}_4$ (299.32): C, 68.22, H, 5.72, N, 4.68; Found: C, 67.07, H, 5.61, N, 3.99.

3.2.3.2. General procedure for synthesis of bis-amide derivatives of ferulic acid

(*E*)-3-(4-hydroxy-3-methoxyphenyl)acrylic acid (0.388 g, 2 mmol) together with the variety of bis-amine derivatives were mixed together thoroughly in a 2:1 molar ratio of respectively. This reaction mixture was subjected to microwave irradiation at 300 Watt for 7 min and then progress of reaction was monitored by TLC on silica gel using ethyl acetate: methanol (4:1) as solvent of elution. TLC indicated absence of starting materials and hence reaction was complete. The crude product so obtained was purified by crystallization from methanol to give pure products.

3.2.3.2.1. Synthesis of *N,N'*-ethylen-Bis[(*E*)-3-(4-hydroxy-3-methoxyphenyl)-acrylamide] (IXa)

Yield: 93%. mp: 146-148°C. FT-IR (cm⁻¹): 3431, 3146, 2904, 1641, 1599, 1556. ¹H-NMR (500 MHz, DMSO-*d*₆, ppm) δ: 3.469-3.499 (t, 4H, *J* = 15 Hz, *J* = 7.5 Hz, 2×CH₂), 3.797 (s, 6H, 2×OCH₃), 5.485 (s, 2H, 2×NH), 6.285-6.315 (d, 2H, *J* = 15 Hz, Ar), 6.758-6.778 (d, 2H, *J* = 10 Hz, Ar), 6.959-6.975 (d, 2H, *J* = 8 Hz, Ar), 7.185 (s, 2H, Ar), 7.252-7.278 (d, 2H, *J* = 13 Hz, Ar), 10.222 (s, 2H, 2×OH). ¹³C-NMR (125 MHz, DMSO-*d*₆, ppm) δ: 39.002, 56.320, 112.070, 116.302, 118.444, 120.585, 128.445, 143.135, 144.412, 151.447, 166.298. APCI-MS, *m/z*: 413.40 (M^+ , 100 %). Anal. Calcd. (%) for C₂₂H₂₄N₂O₆ (412.44): C, 64.07; H, 5.87; N, 6.79; Found: C, 63.48; H, 5.79; N, 6.37.

3.2.3.2.2. *N,N'*-(trimethylene)-Bis[(*E*)-3-(4-hydroxy-3-methoxyphenyl)-acrylamide] (IXb)

Yield: 97%. mp: 114-116°C. FT-IR (cm⁻¹): 3534, 3436, 3013, 2916, 1639, 1592, 1566, 1551. ¹H-NMR (500 MHz, DMSO-*d*₆, ppm) δ: 1.949-1.979 (m, 2H, CH₂), 2.922-2.952 (m, 4H, 2×CH₂), 3.797 (s, 6H, 2×OCH₃), 5.478 (s, 2H, 2×NH), 6.289-6.319 (d, 2H, *J* = 15 Hz, Ar), 6.752-6.772 (d, 2H, *J* = 10 Hz, Ar), 6.958-6.976 (d, 2H, *J* = 9 Hz, Ar), 7.193 (s, 2H, Ar), 7.250-7.276 (d, 2H, *J* = 13 Hz, Ar), 10.219 (s, 2H, 2×OH). ¹³C-NMR (125 MHz, DMSO-*d*₆, ppm) δ: 28.412, 39.007, 56.740, 112.075, 116.304, 118.418, 120.665, 128.044, 143.105, 144.902, 151.457,

166.898. APCI-MS, m/z : 427.32 (\dot{M}^+ , 100 %). Anal. Calcd. (%) for $C_{23}H_{26}N_2O_6$ (426.46): C, 64.78; H, 6.15; N, 6.57; Found: C, 64.01; H, 6.08; N, 6.29.

3.2.3.2.3. *N,N'*-propylen-Bis[(*E*)-3-(4-hydroxy-3-methoxyphenyl)-acrylamide] (IXc)

Yield: 93%. mp: 94-96°C. FT-IR (cm^{-1}): 3436, 3197, 2935, 1596, 1591, 1582, 1566. 1H -NMR (500 MHz, DMSO- d_6 , ppm) δ : 1.402-1.430 (d, 3H, $J = 14$ Hz, CH₃), 2.761-2.783 (q, 1H, $J = 7$ Hz, $J = 4$ Hz, CH), 3.703 (s, 3H, OCH₃), 3.787 (s, 3H, OCH₃), 4.769-4.799 (d, 2H, $J = 15$ Hz, CH₂), 6.329-6.367 (d, 1H, $J = 19$ Hz, Ar), 6.774-6.790 (d, 1H, $J = 8$ Hz, Ar), 7.005-7.026 (d, 1H, $J = 10.5$ Hz, Ar), 7.207 (s, 1H, Ar), 7.241-7.266 (t, 1H, $J = 12.5$ Hz, $J = 7$ Hz, Ar), 7.347-7.379 (d, 1H, $J = 16$ Hz, Ar), 7.440-7.456 (d, 1H, $J = 8$ Hz, Ar), 7.557-7.883 (t, 2H, $J = 13$ Hz, $J = 7.5$ Hz, Ar), 8.498-8.508 (d, 1H, $J = 5$ Hz, Ar), 8.978 (s, 2H, 2×NH), 10.308 (s, 2H, 2×OH). ^{13}C -NMR (125 MHz, DMSO- d_6 , ppm) δ : 17.997, 46.099, 47.949, 56.311, 112.089, 116.833, 118.588, 120.685, 127.894, 143.111, 144.232, 151.252, 166.448. APCI-MS, m/z : 427.34 (\dot{M}^+ , 100 %). Anal. Calcd. (%) for $C_{23}H_{26}N_2O_6$ (426.46): C, 64.78; H, 6.15; N, 6.57; Found: C, 64.14; H, 6.11; N, 6.01.

3.2.3.2.4. *N,N'*-butylen-Bis[(*E*)-3-(4-hydroxy-3-methoxyphenyl)-acrylamide] (IXd)

Yield: 95%. mp: 136-138°C. FT-IR (cm^{-1}): 3401, 3188, 2935, 1642, 1617, 1589, 1561. 1H -NMR (500 MHz, DMSO- d_6 , ppm) δ : 1.940-1.970 (t, 4H, $J = 15$ Hz, $J = 12.5$ Hz, 2×CH₂), 2.925-2.955 (t, 4H, $J = 15$ Hz, $J = 7.5$ Hz, 2×CH₂), 3.751 (s, 6H, 2×OCH₃), 5.431 (s, 2H, 2×NH), 6.286-6.316 (d, 2H, $J = 15$ Hz, Ar), 6.757-6.777 (d, 2H, $J = 10$ Hz, Ar), 6.953-6.971 (d, 2H, $J = 9$ Hz, Ar), 7.188 (s, 2H, Ar), 7.248-7.274 (d, 2H, $J = 13$ Hz, Ar), 10.275 (s, 2H, 2×OH). ^{13}C -NMR (125 MHz, DMSO- d_6 , ppm) δ : 27.417, 41.949, 56.340, 112.099, 116.333, 118.208, 120.185, 127.994, 143.515, 144.432, 151.457, 166.168. APCI-MS, m/z : 441.15 (\dot{M}^+ , 100 %). Anal. Calcd. (%) for $C_{24}H_{28}N_2O_6$ (440.49): C, 65.44; H, 6.41; N, 6.36; Found: C, 64.89; H, 6.33; N, 5.97.

3.2.3.2.5. *N,N'*-3-(4-(3-aminopropyl)piperazin-1-yl)propylen)-Bis[(*E*)-3-(4-hydroxy-3-methoxyphenyl)-acrylamide] (IXe)

Yield: 89%. mp: 130-132°C. FT-IR (cm⁻¹): 3371, 3163, 1647, 1612, 1589, 1572. ¹H-NMR (500 MHz, DMSO-*d*₆, ppm) δ: 1.892-1.922 (t, 4H, *J* = 15 Hz, *J* = 7.5 Hz, 2×CH₂), 2.825-2.855 (t, 12H, *J* = 15 Hz, *J* = 7.5 Hz, 6×CH₂), 3.881 (s, 6H, 2×OCH₃), 3.947-3.977 (m, 4H, 2×CH₂), 5.416 (s, 2H, 2×NH), 6.306-6.336 (d, 2H, *J* = 15 Hz, Ar), 6.753-6.773 (d, 2H, *J* = 10 Hz, Ar), 6.970-6.988 (d, 2H, *J* = 9 Hz, Ar), 7.106 (s, 2H, Ar), 7.244-7.274 (d, 2H, *J* = 15 Hz, Ar), 10.236 (s, 2H, 2×OH). ¹³C-NMR (125 MHz, DMSO-*d*₆, ppm) δ: 27.107, 38.009, 51.509, 53.522, 56.451, 112.329, 116.833, 118.208, 120.235, 127.858, 143.127, 144.833, 151.116, 166.115. APCI-MS, *m/z*: 553.29 (\dot{M}^+ , 100 %). Anal. Calcd. (%) for C₃₀H₄₀N₄O₆ (552.66): C, 65.20; H, 7.30; N, 10.14; Found: C, 64.89; H, 7.21; N, 9.93.

3.3. Results and discussion

3.3.1. Chemistry

We have successfully synthesized the four series of mono and bis-amide derivatives of ferulic acid (**IIIa-IIIo**, **Va-Vg**, **VIIa-VIIg** and **IXa-IXe**) by simple grinding the mixture of ferulic acid and corresponding amines (**IIa-IIo**, **IVa-IVg**; **VIa-VIg** and **VIIIa-VIIIe**) in 1:1 mole ratio within 3-10 minutes at room temperature. The crude products so obtained were purified by crystallization with methanol to give the pure products in good yields. The structural studies had been carried out by FT-IR, NMR and mass spectroscopy as well as elemental analysis for C, H, and N. The NMR (¹H and ¹³C-NMR, DMSO-*d*₆) and mass (GC and APCI-MS) spectra of all the synthesized derivatives are provided in the Figure 3.1 to 3.34. The spectral and elemental analysis of above mentioned compounds reported in the experimental section have fully support the chemical structures assigned to them. The ¹H-NMR spectra for all the compounds taken after

keeping the compounds for ten days at room temperature did not show any change, similarly the spectra were also collected after six months from the previous data collection and found no change in it with respect to the starting spectroscopic data. These studies confirmed that these amide derivatives are stable in solid as well liquid phase after a long period of time and the results was also supported by their thermal studies. The biophysical techniques such as IR, NMR, mass spectroscopy and crystallography are most advanced and reliable tools used for the confirmation of structures of newly synthesized molecules both in solution and solid phase [Arora and Tamm 2001; Yadav et al. 2007; Kumar et al. 2011].

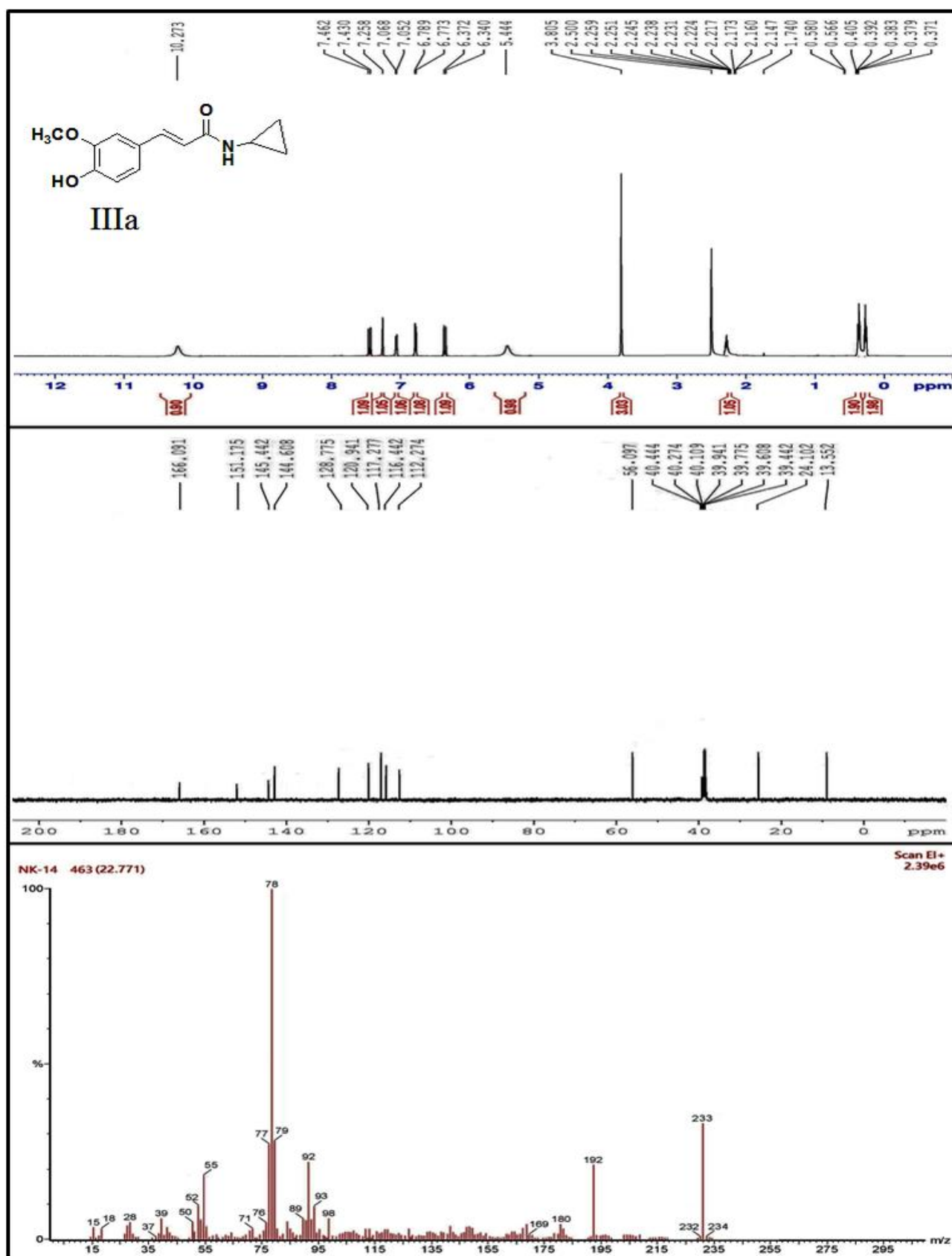


Figure 3.1: ¹H, ¹³C-NMR and GC-MS spectra of IIIa.

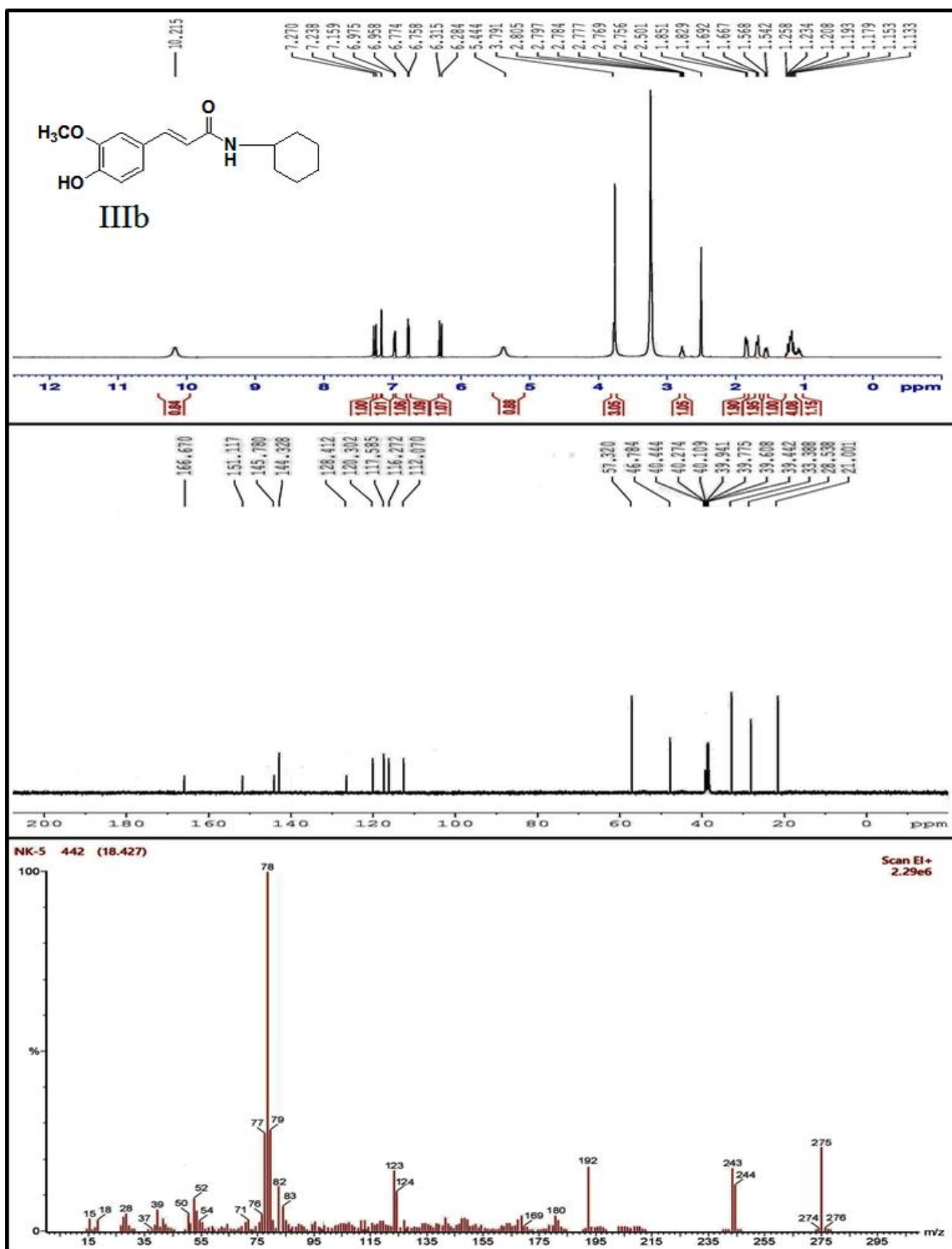


Figure 3.2: ^1H , ^{13}C -NMR and GC-MS spectra of IIIb.

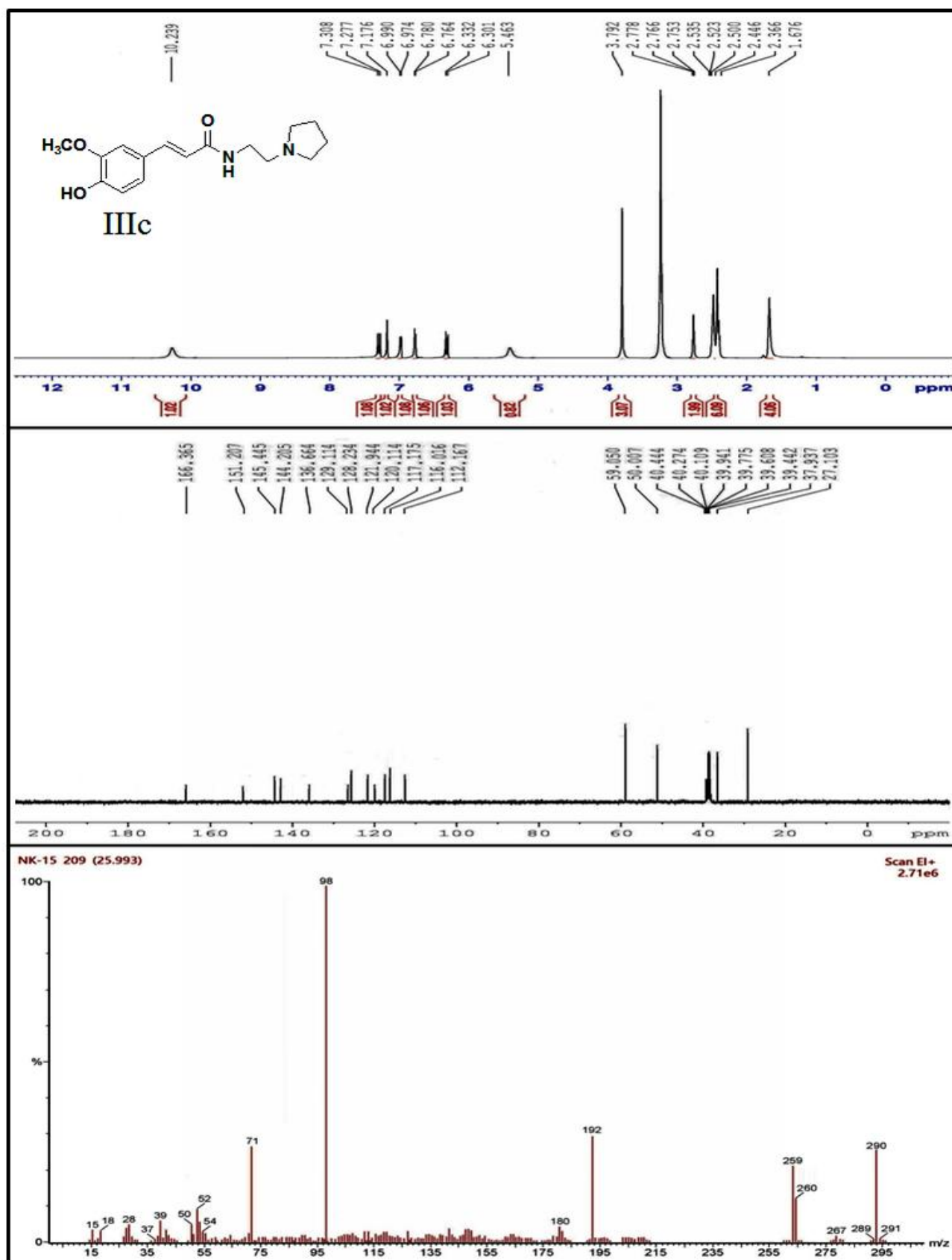


Figure 3.3: ¹H, ¹³C-NMR and GC-MS spectra of IIIc.

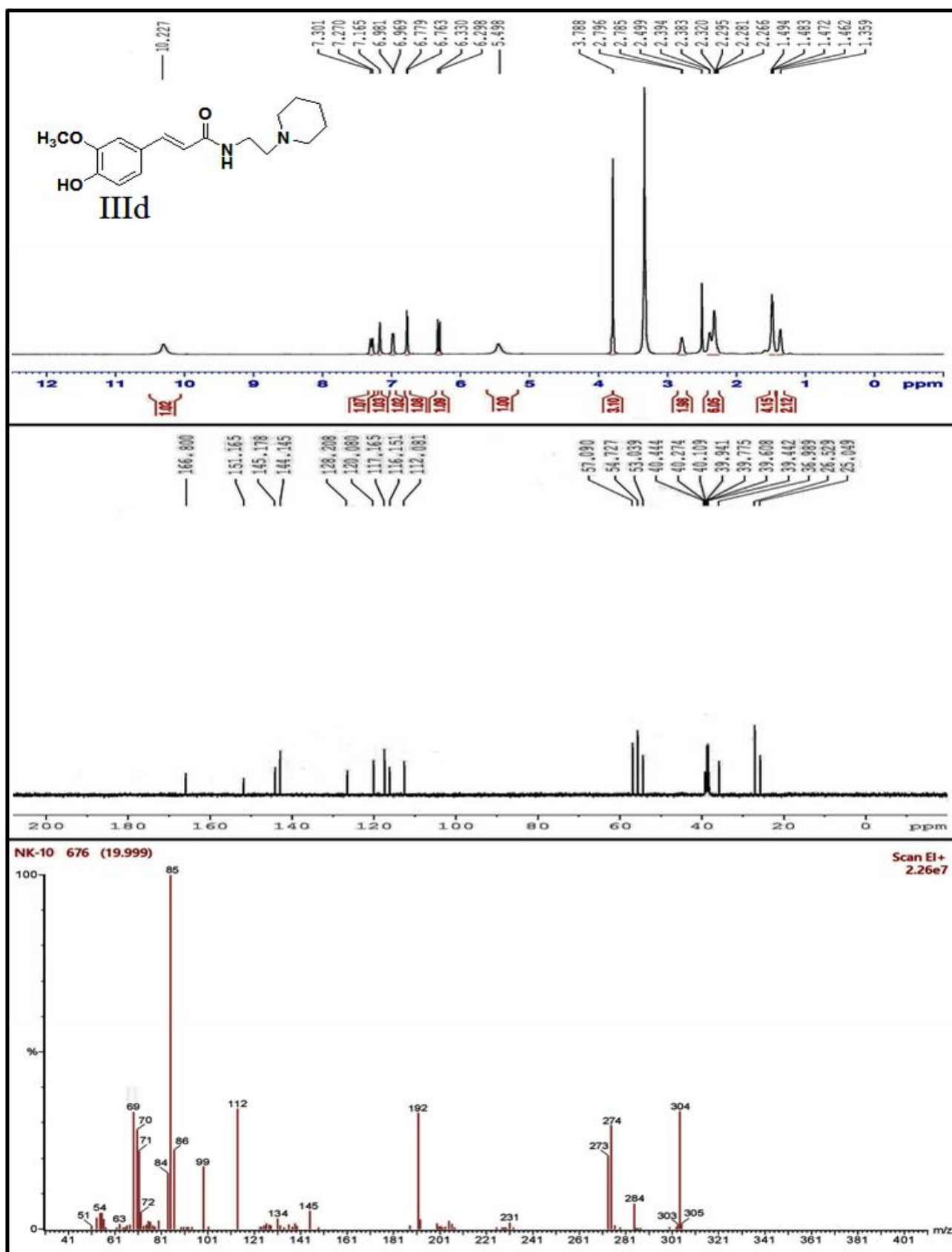


Figure 3.4: ¹H, ¹³C-NMR and GC-MS spectra of IIIc.

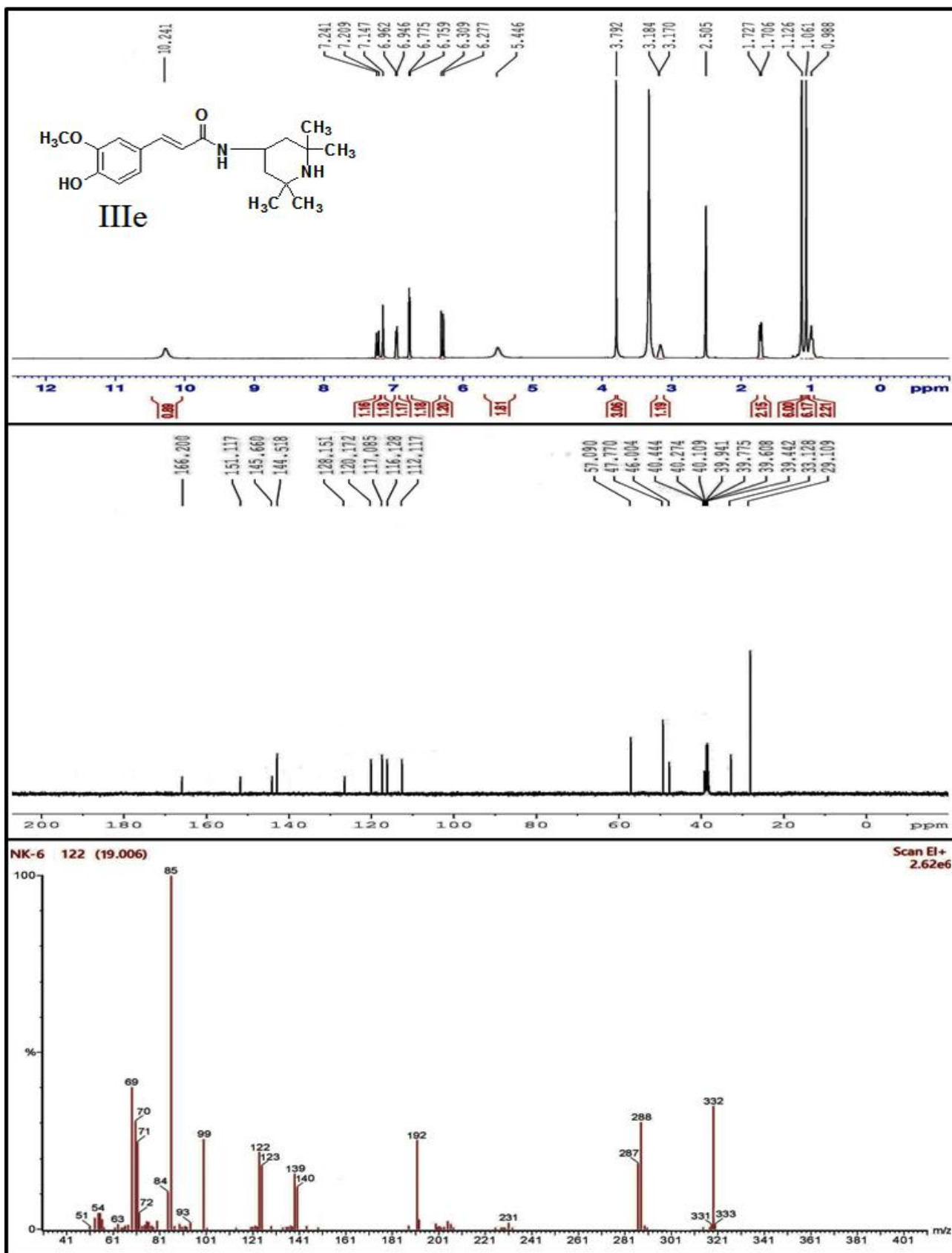


Figure 3.5: ^1H , ^{13}C -NMR and GC-MS spectra of IIIe.

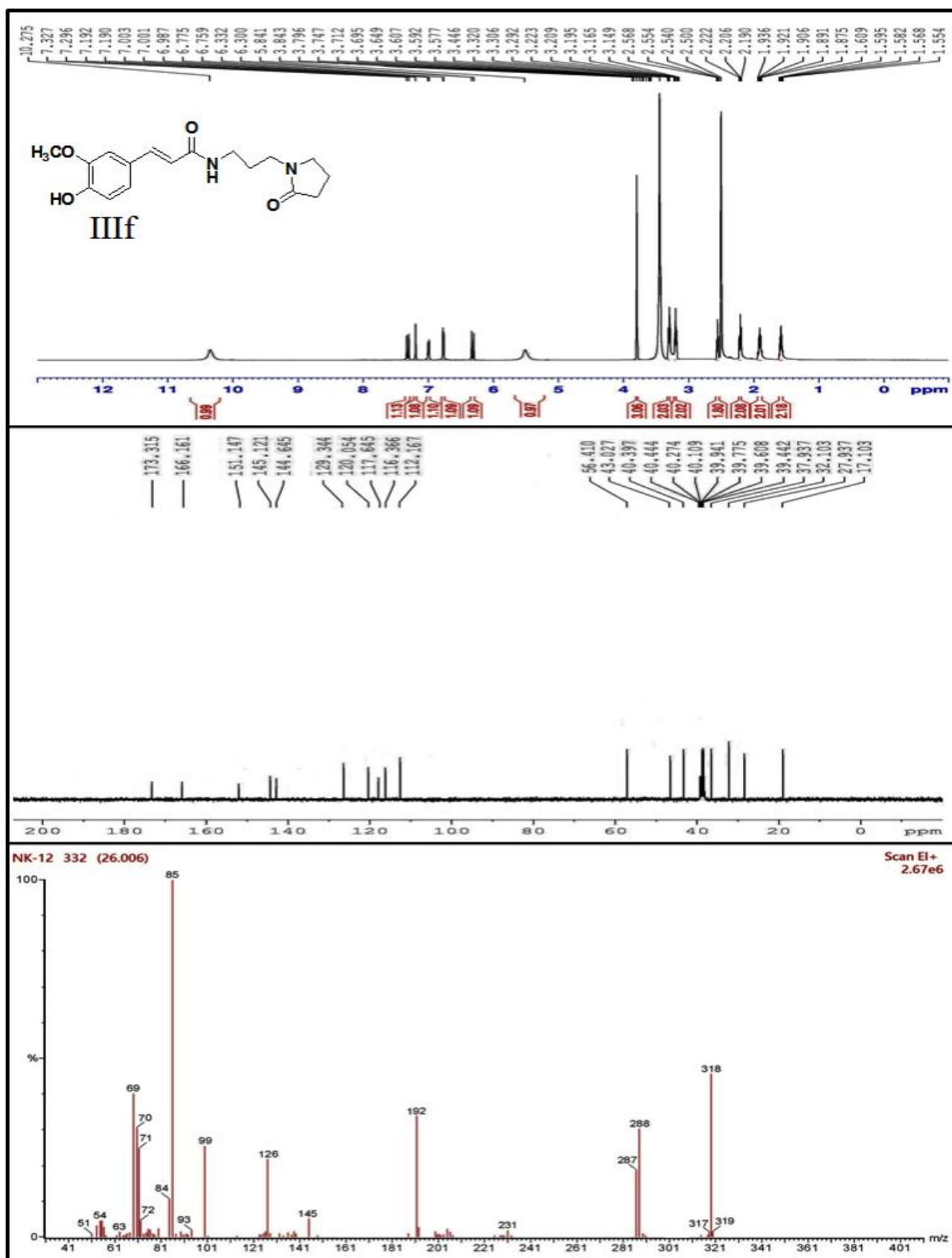


Figure 3.6: ^1H , ^{13}C -NMR and GC-MS spectra of IIIf.

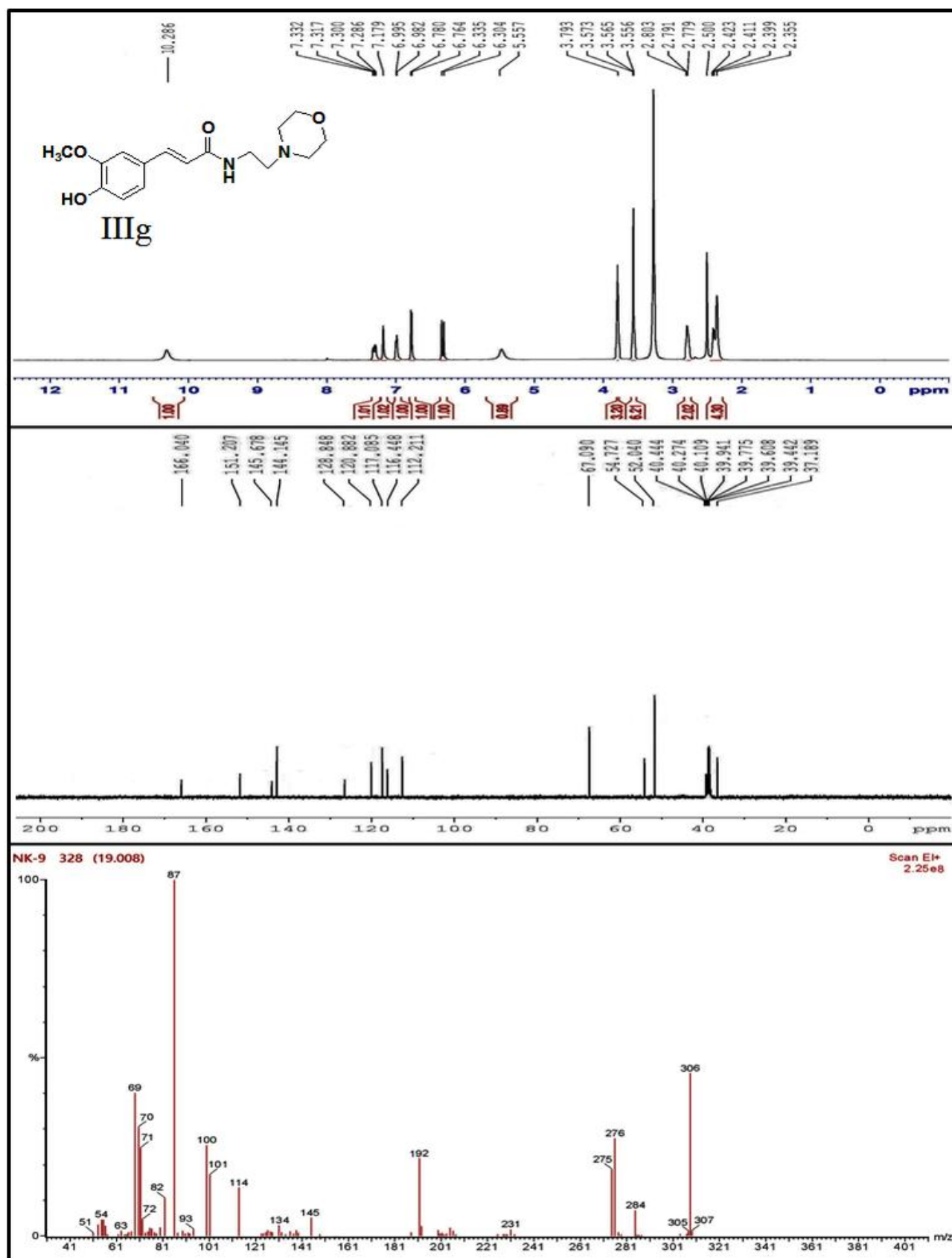


Figure 3.7: ¹H, ¹³C-NMR and GC-MS spectra of IIIg.

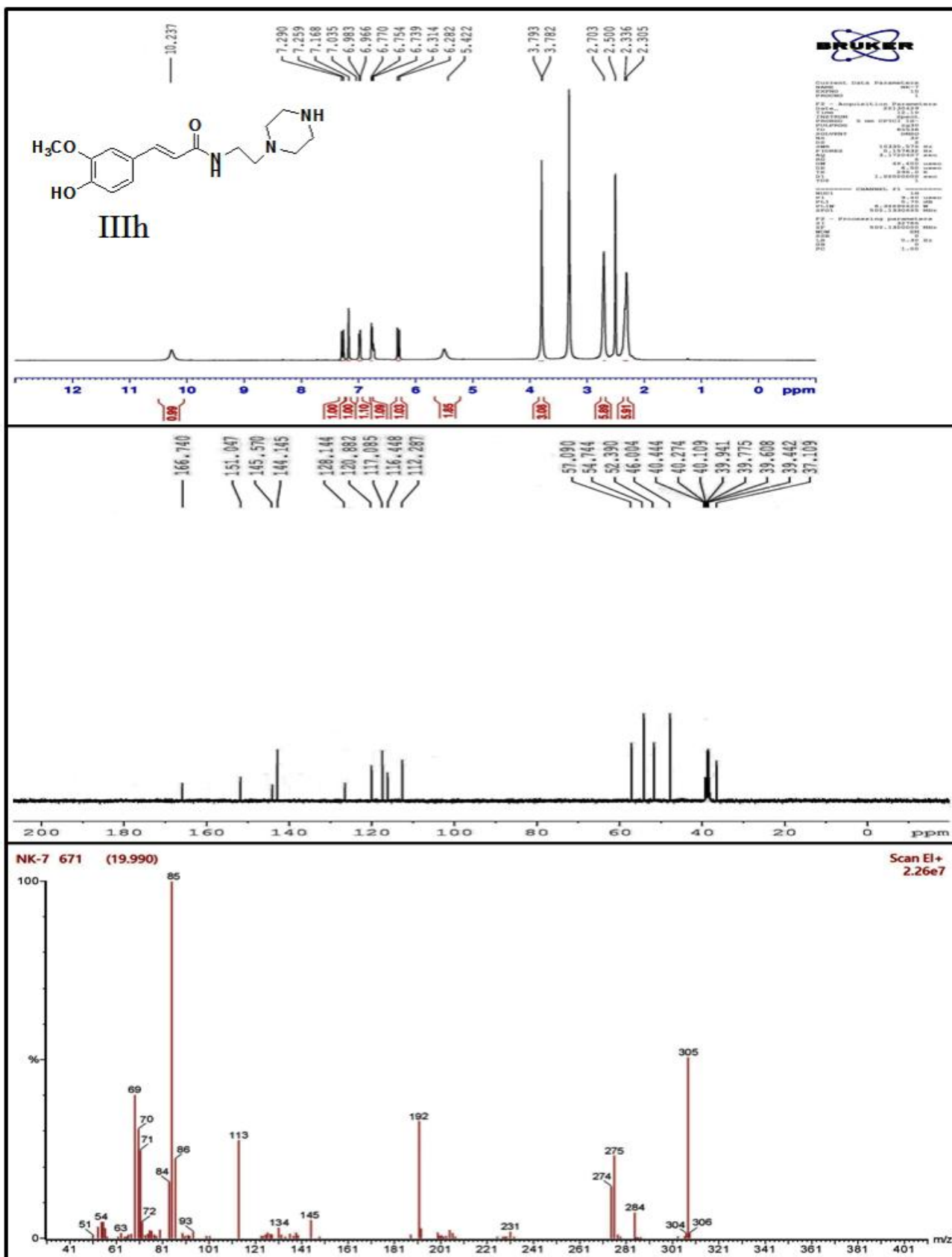


Figure 3.8: ¹H, ¹³C-NMR and GC-MS spectra of IIIh.

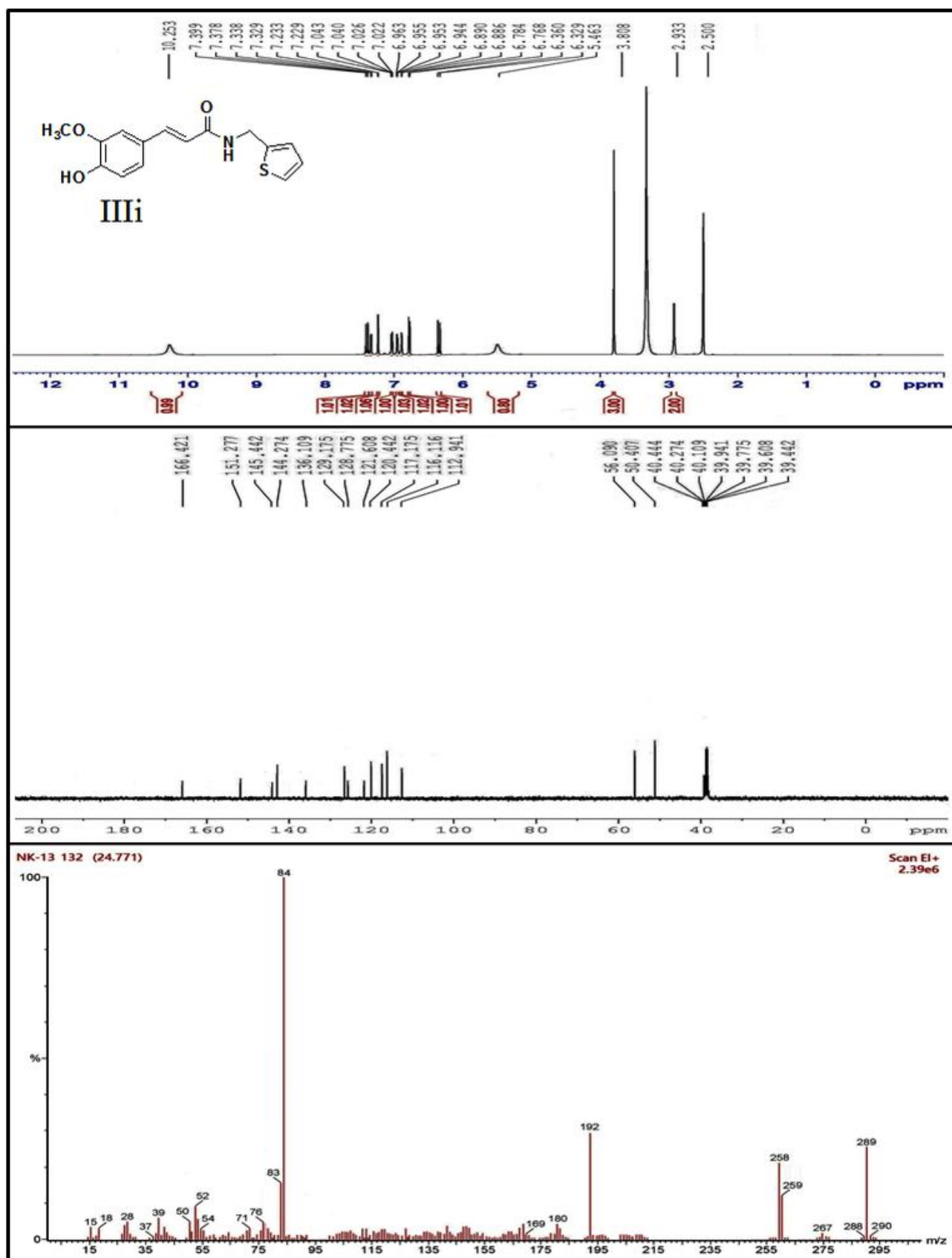


Figure 3.9: ^1H , ^{13}C -NMR and GC-MS spectra of IIIi.

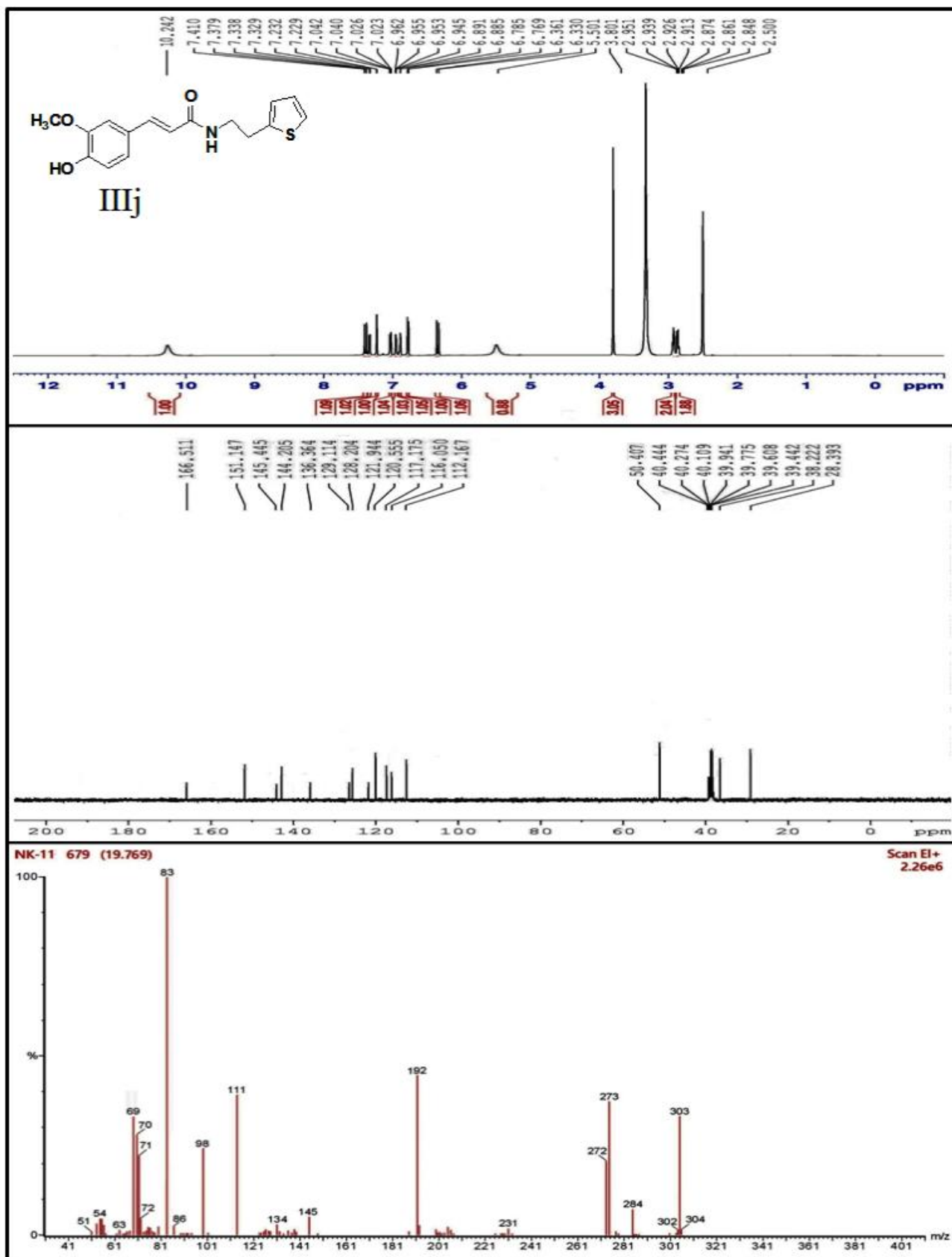


Figure 3.10: ¹H, ¹³C-NMR and GC-MS spectra of IIIj.

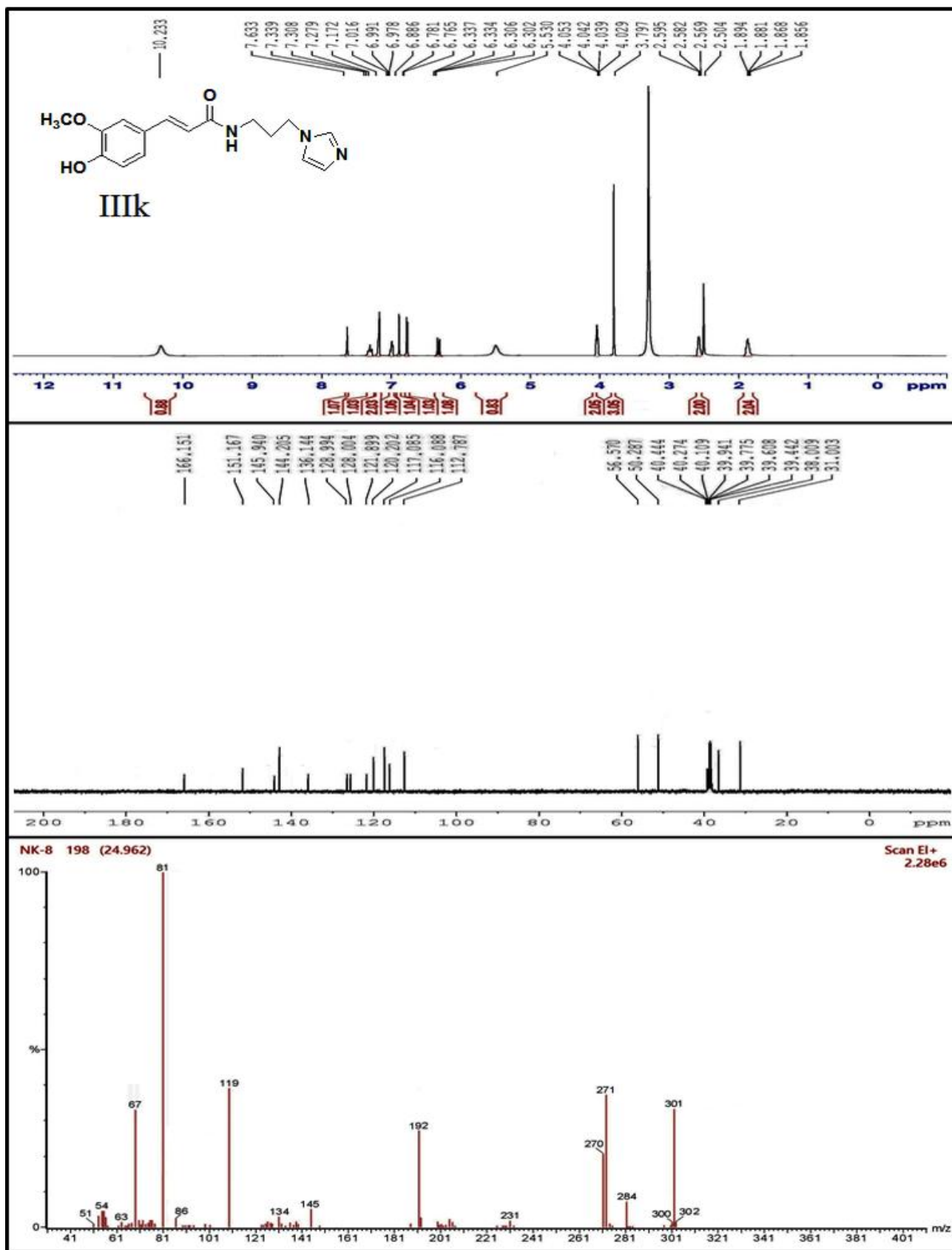


Figure 3.11: ¹H, ¹³C-NMR and GC-MS spectra of IIIk.

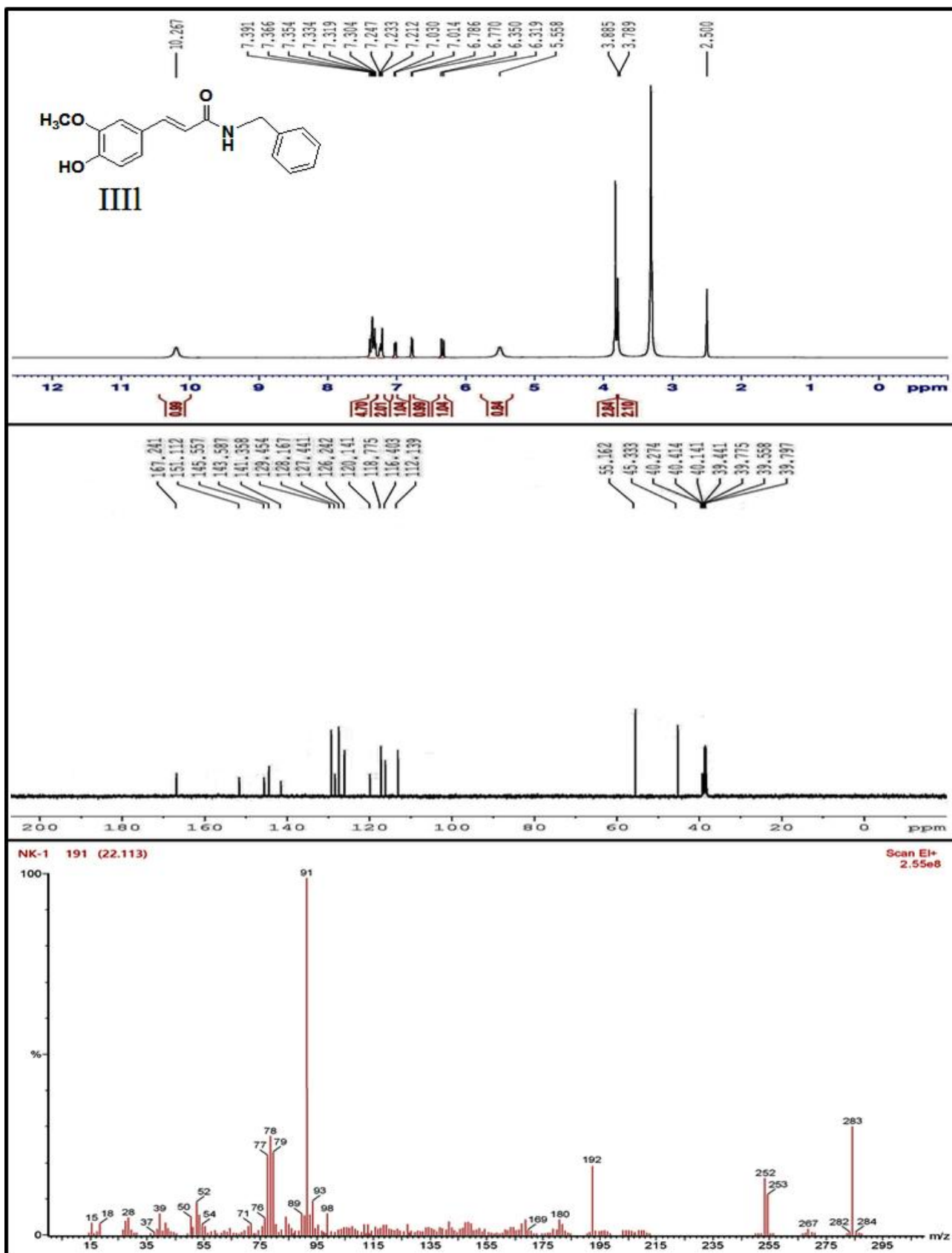


Figure 3.12: ^1H , ^{13}C -NMR and GC-MS spectra of III.

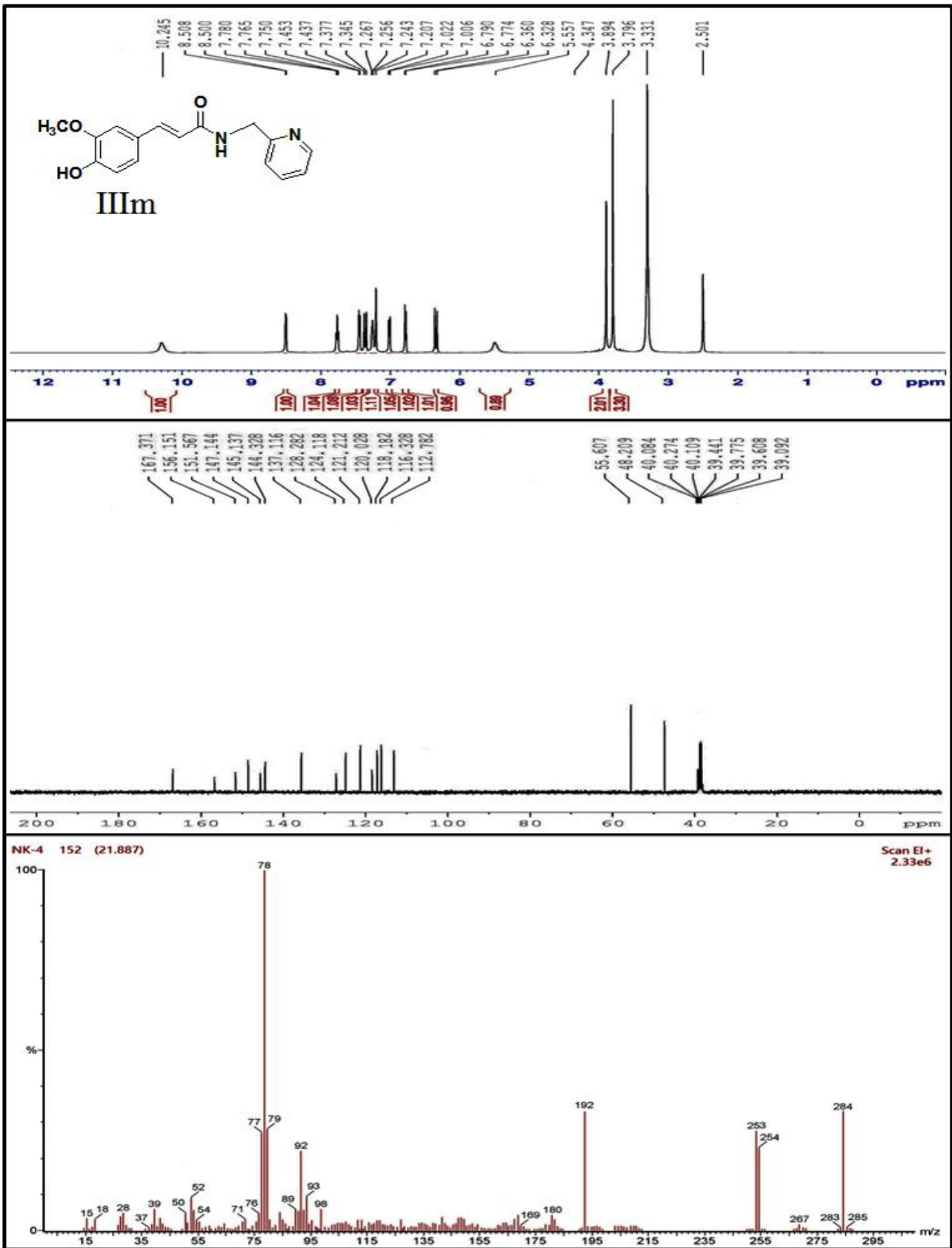


Figure 3.13: ¹H, ¹³C-NMR and GC-MS spectra of IIIm.

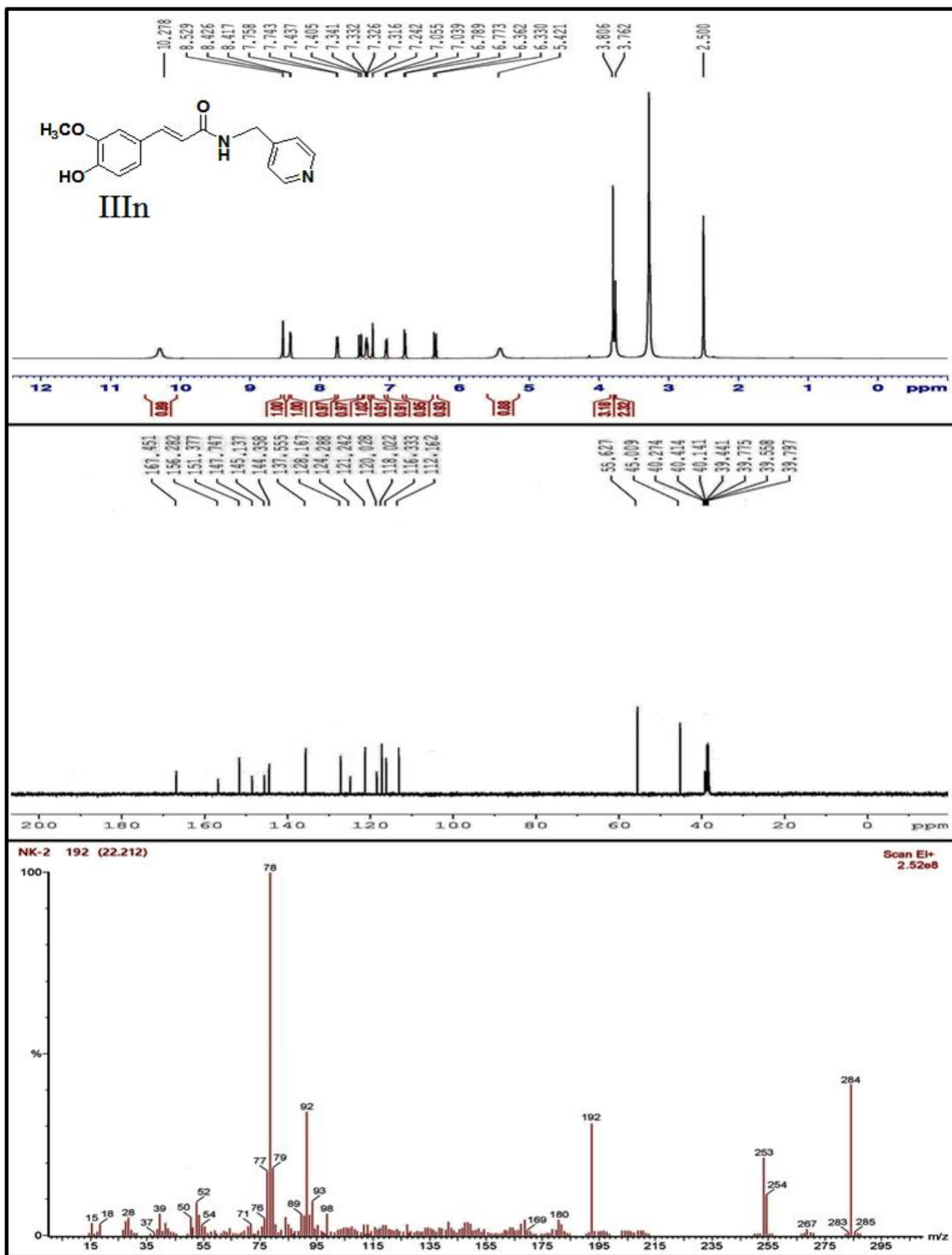


Figure 3.14: ¹H, ¹³C-NMR and GC-MS spectra of IIIIn.

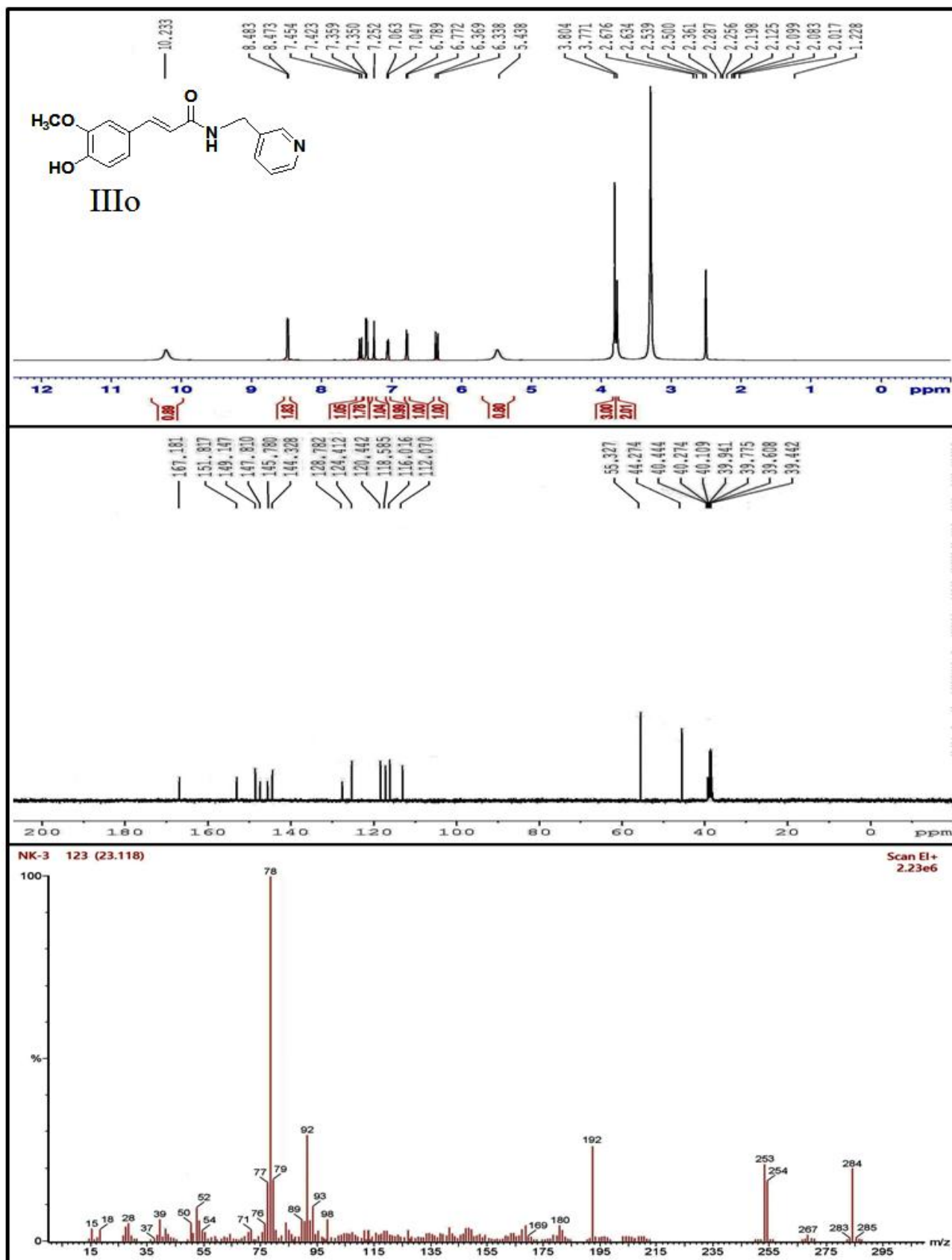


Figure 3.15: ¹H, ¹³C-NMR and GC-MS spectra of IIIo.

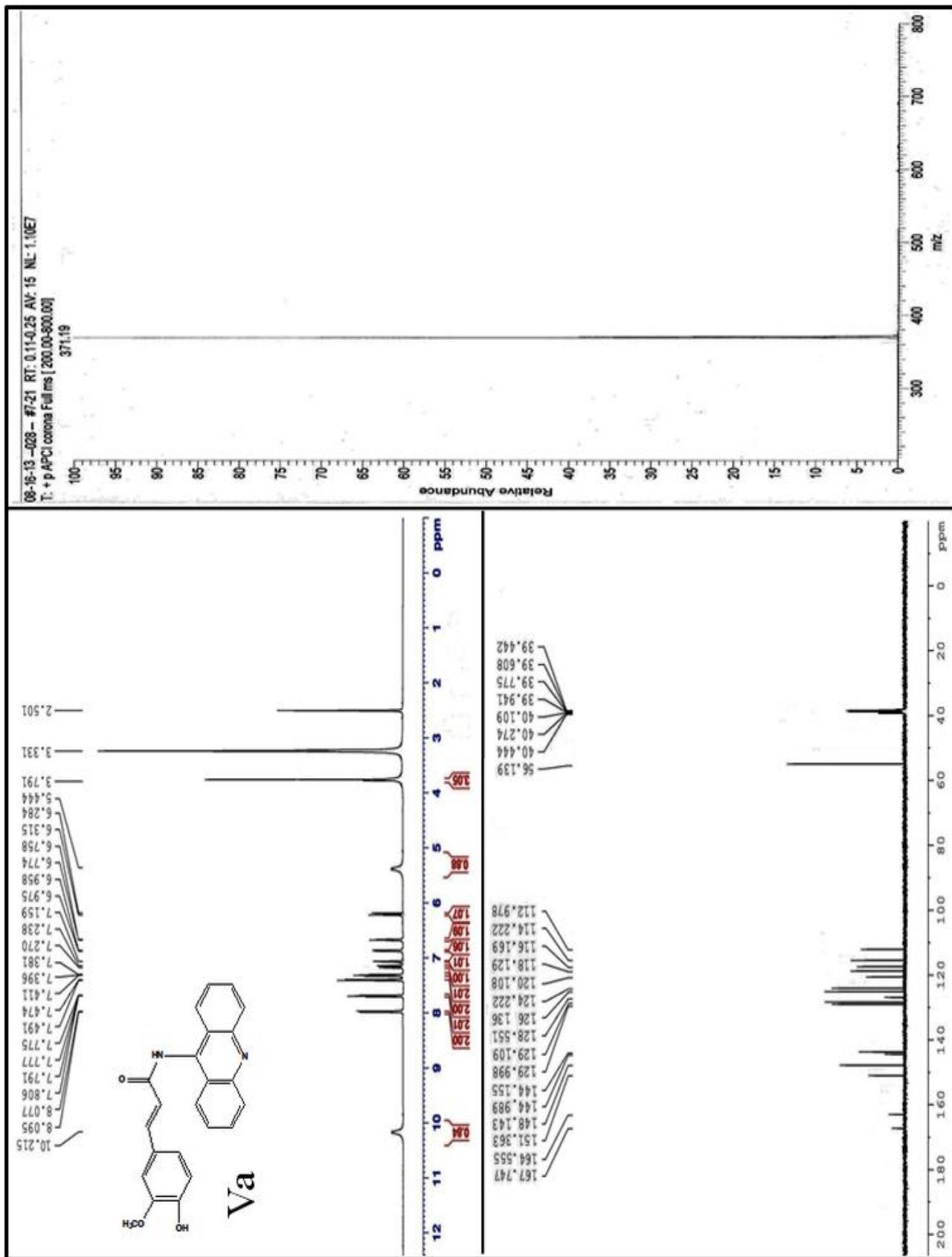


Figure 3.16: ¹H, ¹³C-NMR and APCI-MS spectra of Va.

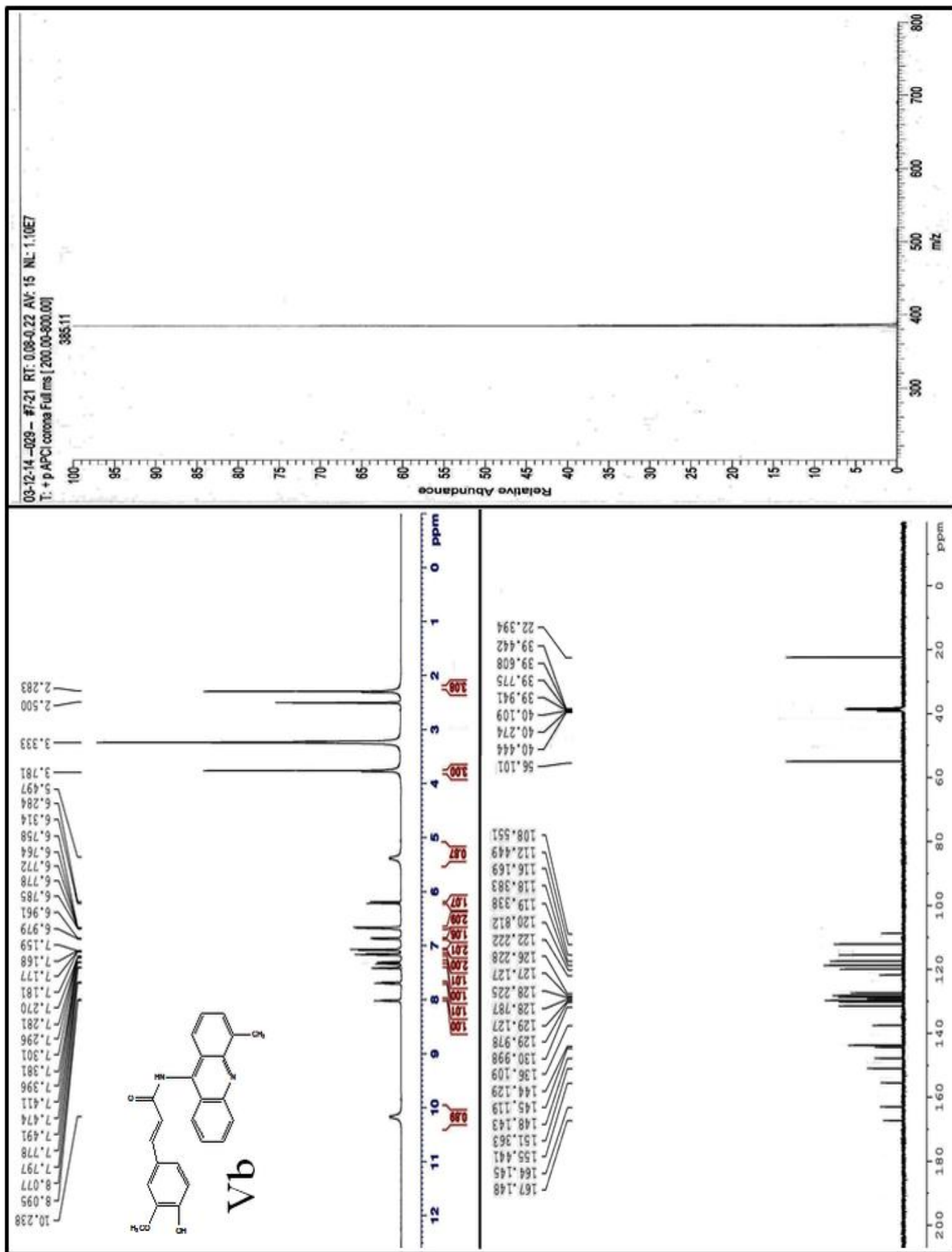


Figure 3.17: ^1H , ^{13}C -NMR and APCI-MS spectra of Vb.

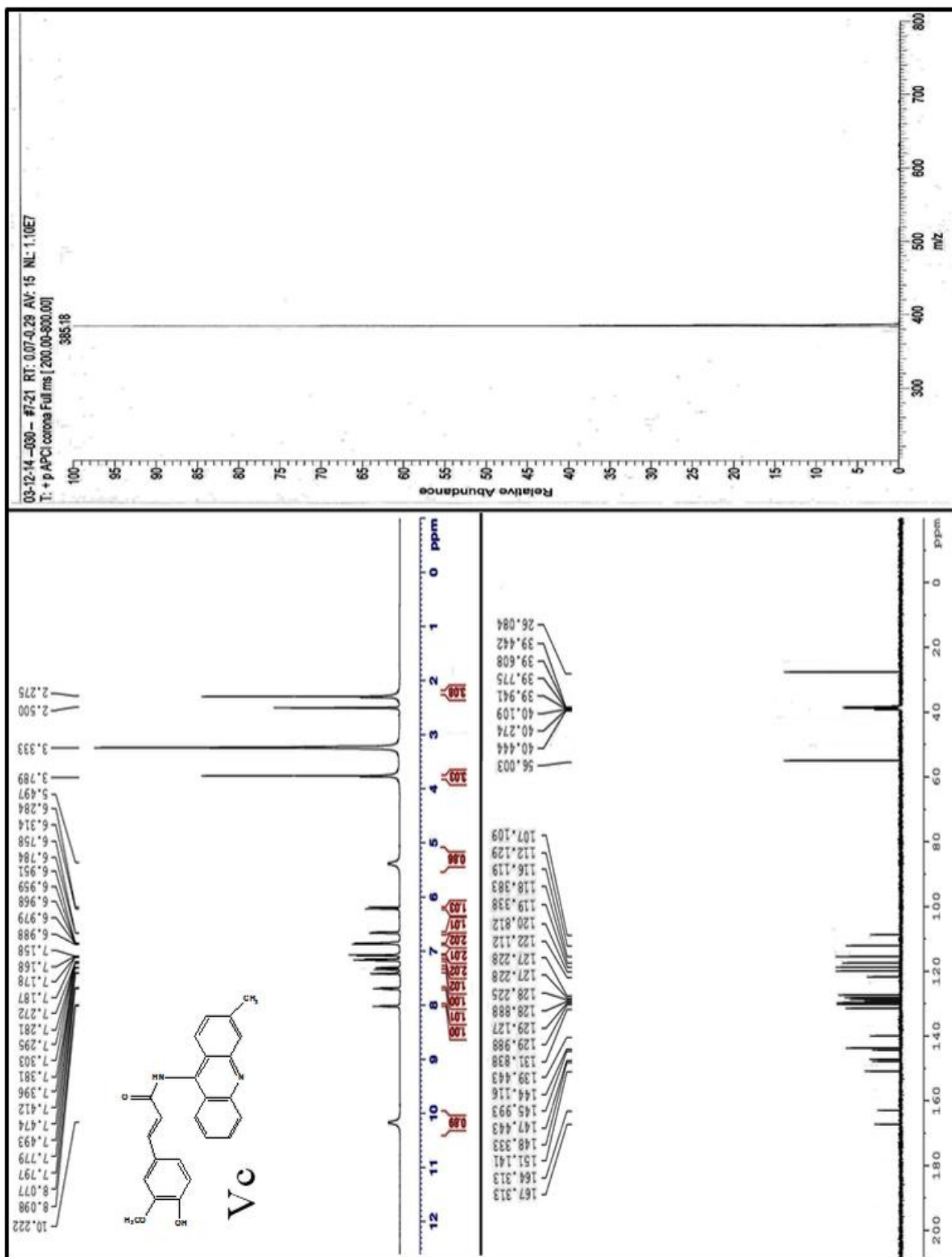


Figure 3.18: ^1H , ^{13}C -NMR and APCI-MS spectra of Vc.

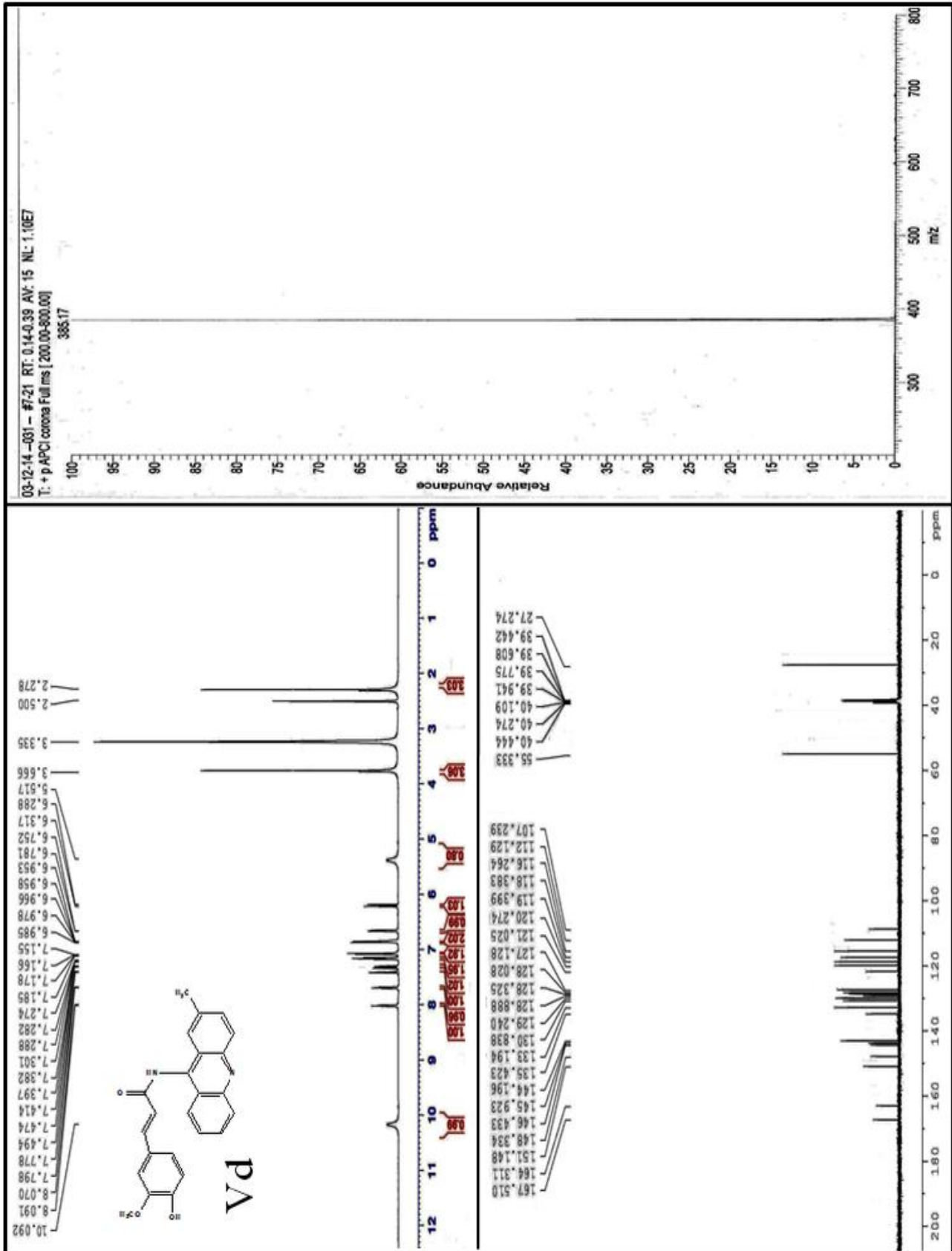


Figure 3.19: ¹H, ¹³C-NMR and APCI-MS spectra of Vd.

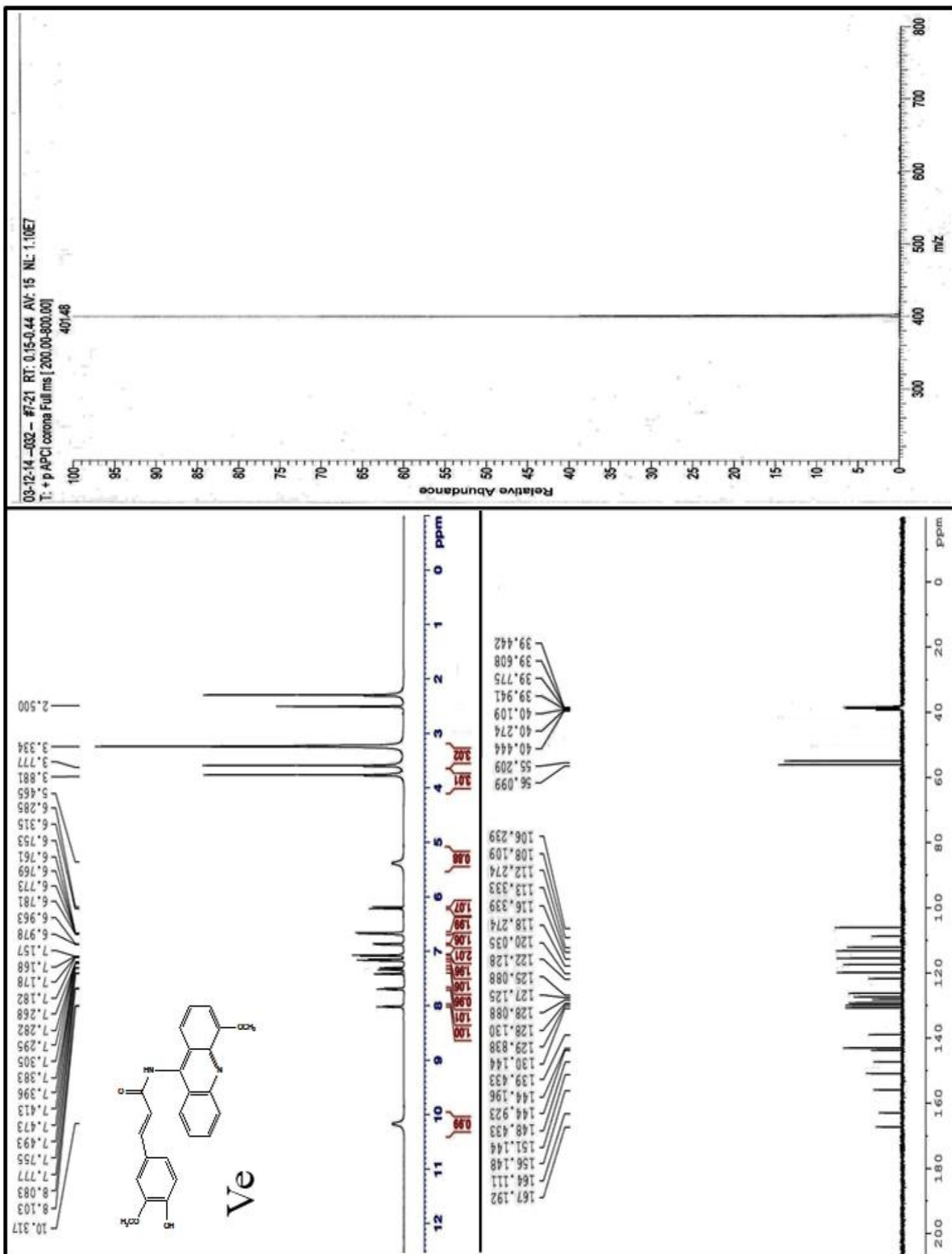


Figure 3.20: ¹H, ¹³C-NMR and APCI-MS spectra of Ve.

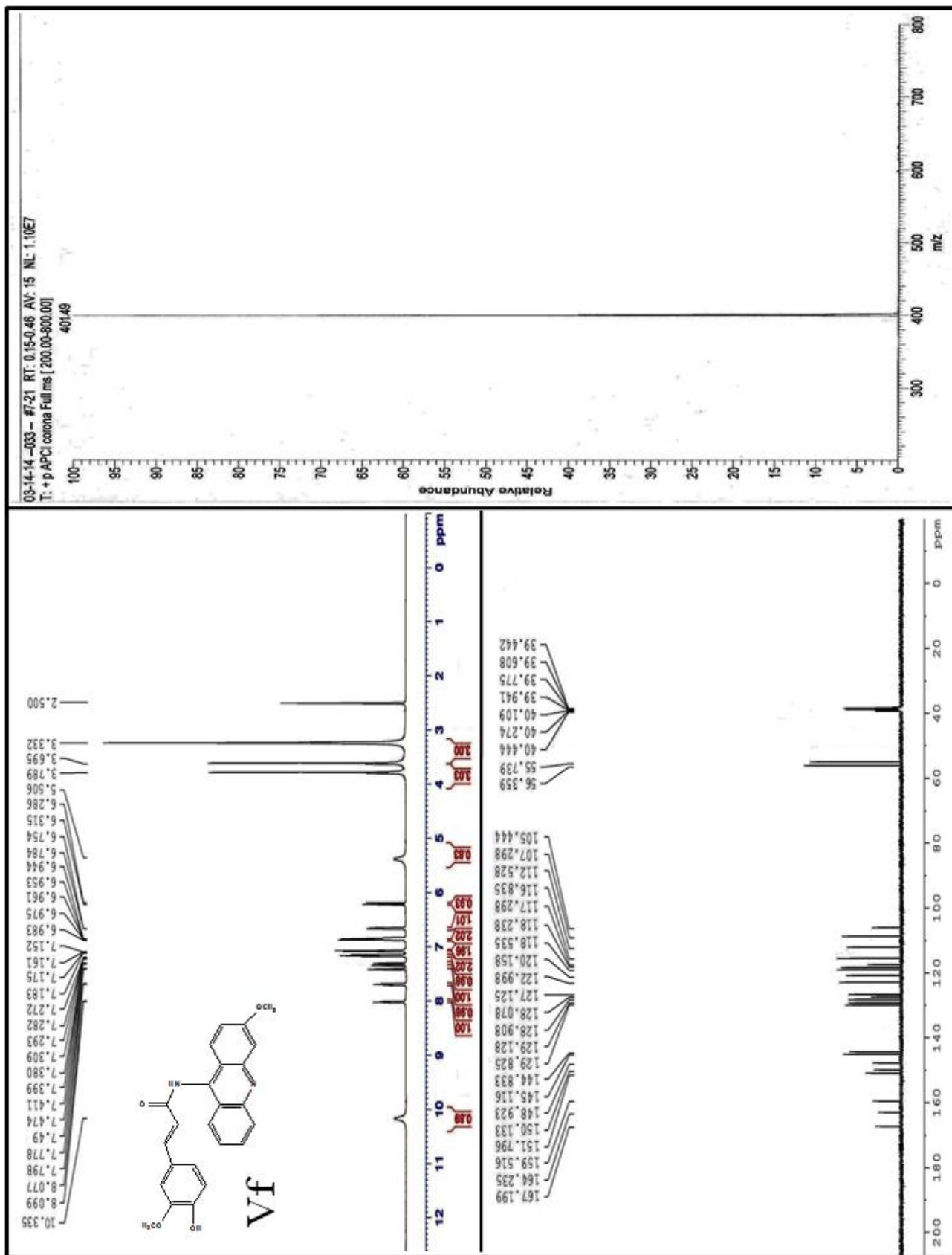


Figure 3.21: ^1H , ^{13}C -NMR and APCI-MS spectra of Vf.

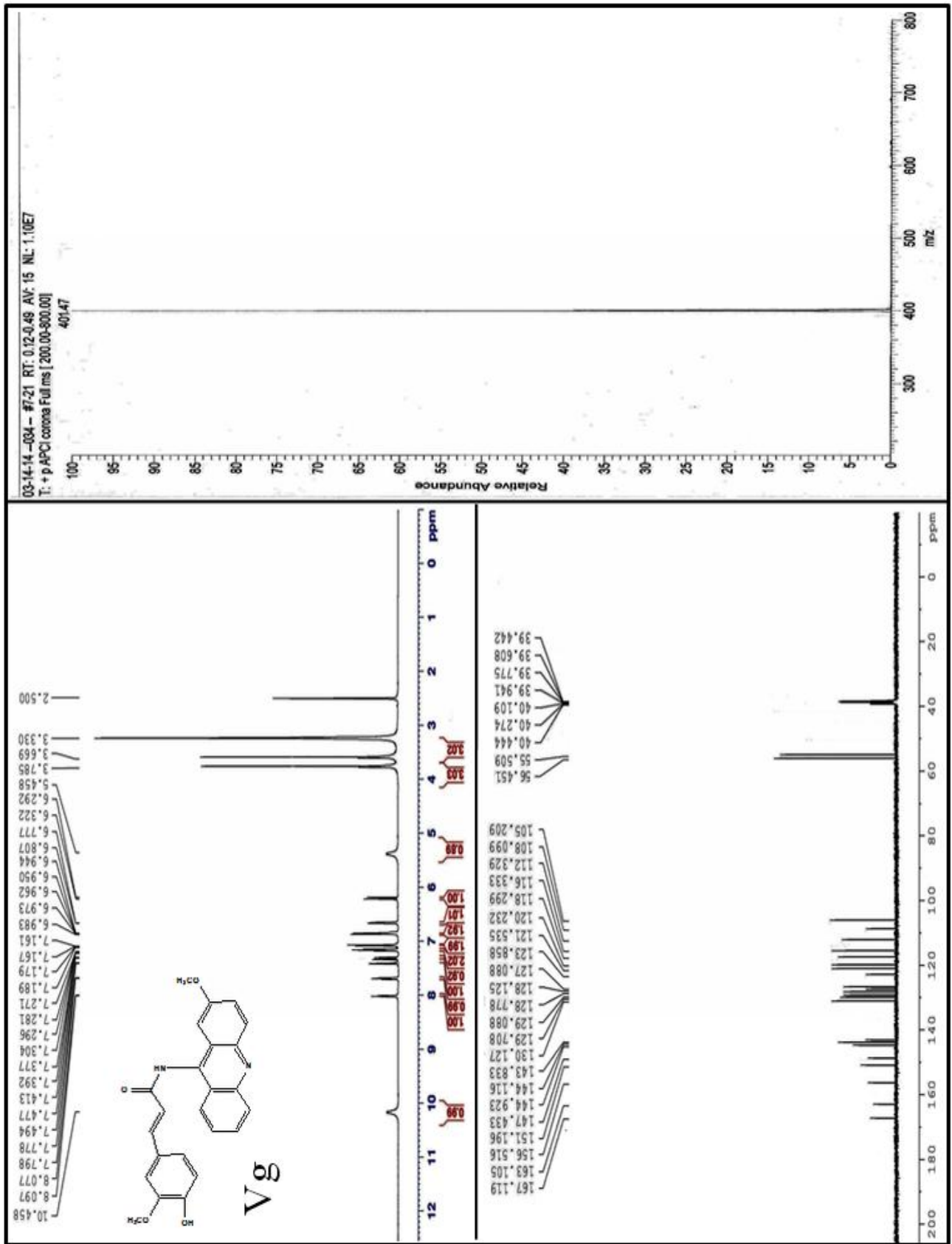


Figure 3.22: ^1H , ^{13}C -NMR and APCI-MS spectra of Vg.

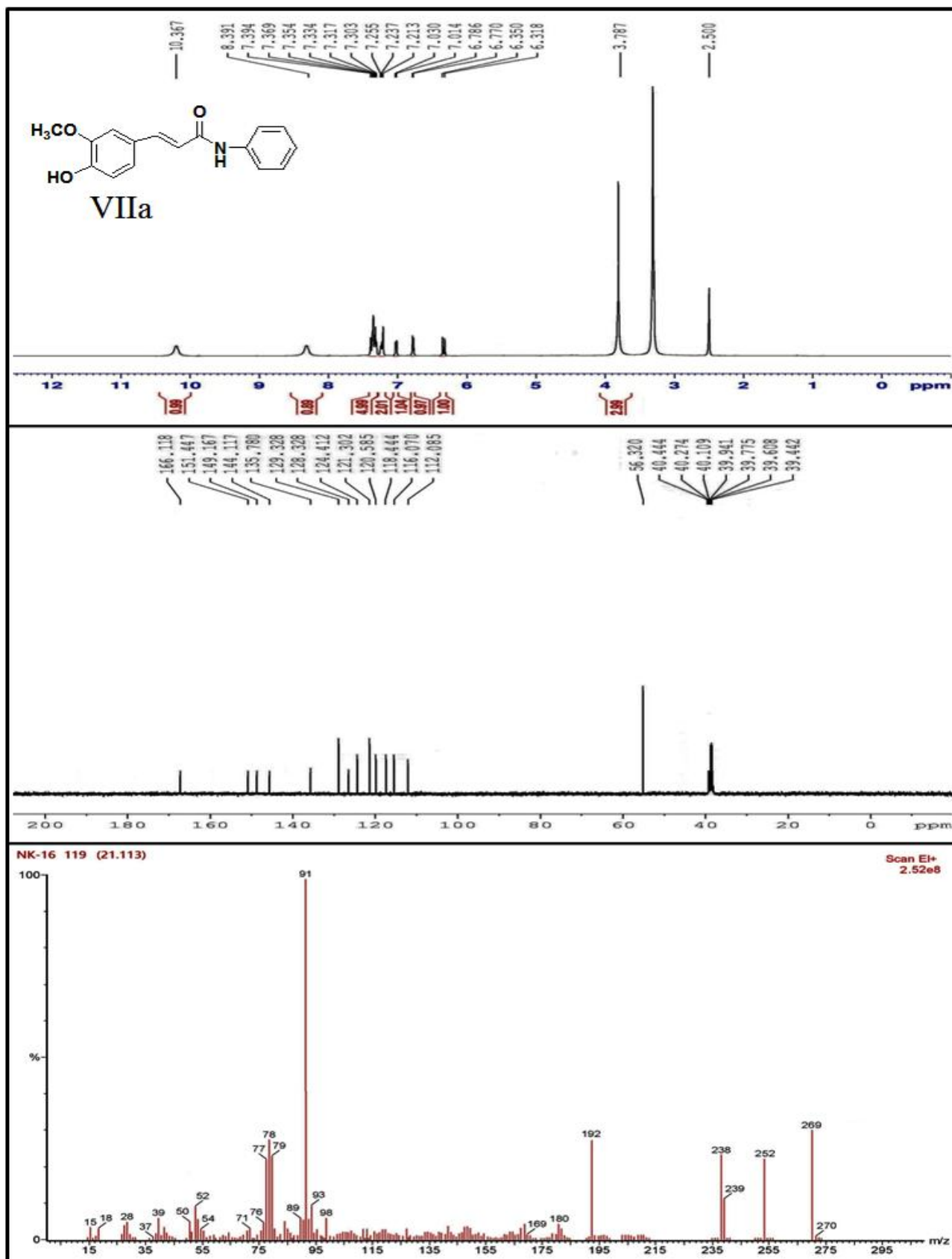


Figure 3.23: ^1H , ^{13}C -NMR and GC-MS spectra of VIIa.

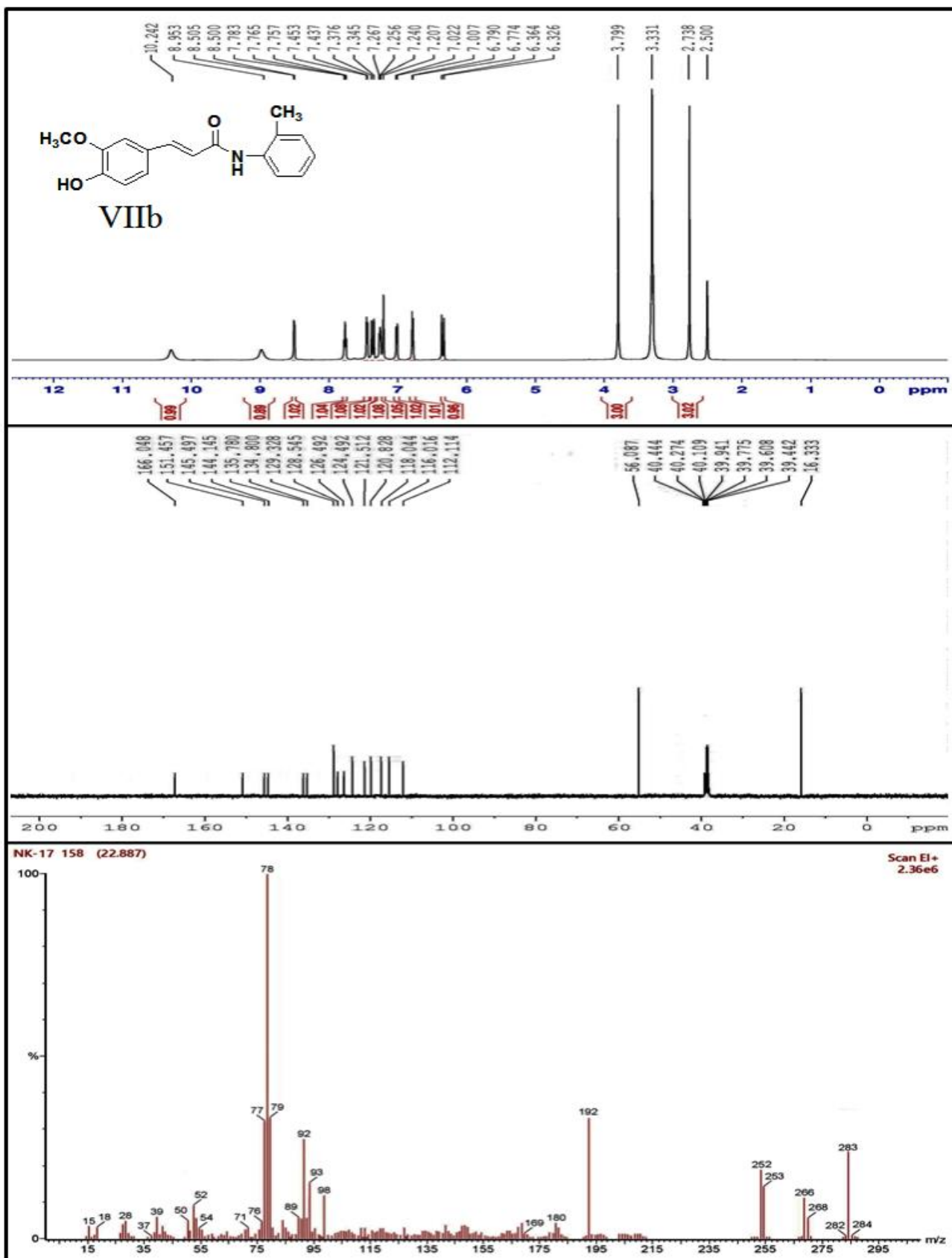


Figure 3.24: ¹H, ¹³C-NMR and GC-MS spectra of VIIb.

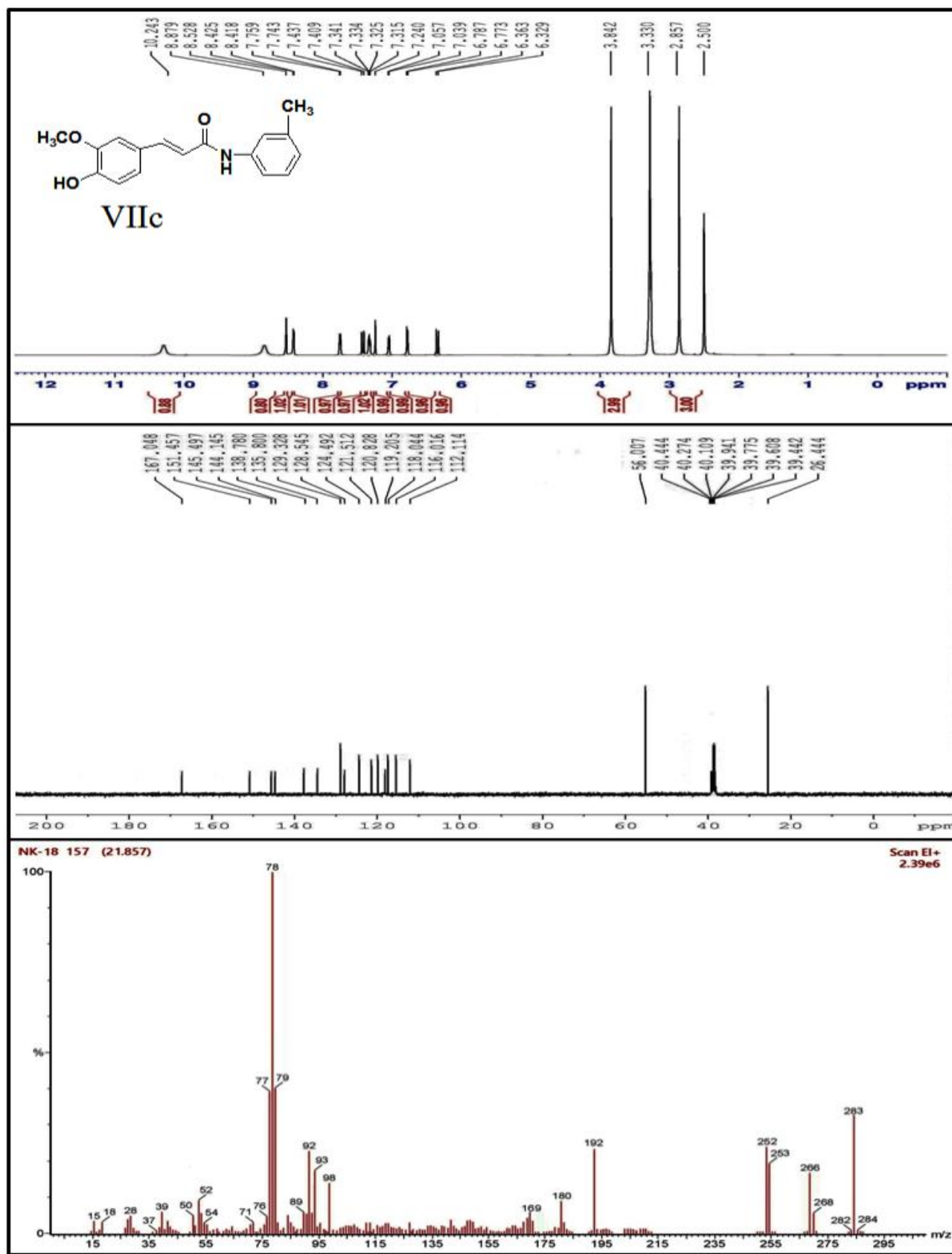


Figure 3.25: ¹H, ¹³C-NMR and GC-MS spectra of VIIc.

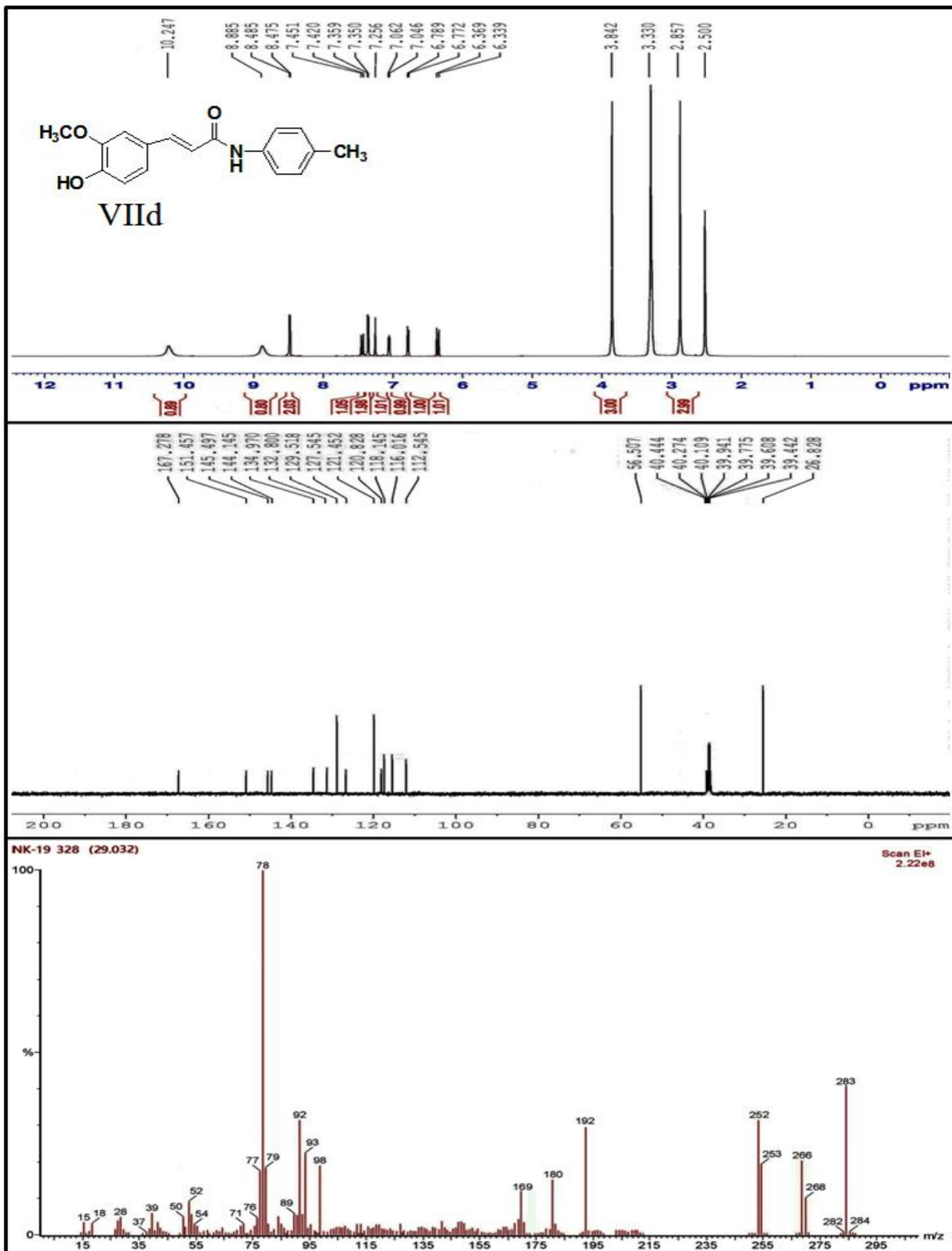


Figure 3.26: ¹H, ¹³C-NMR and GC-MS spectra of VIIId.

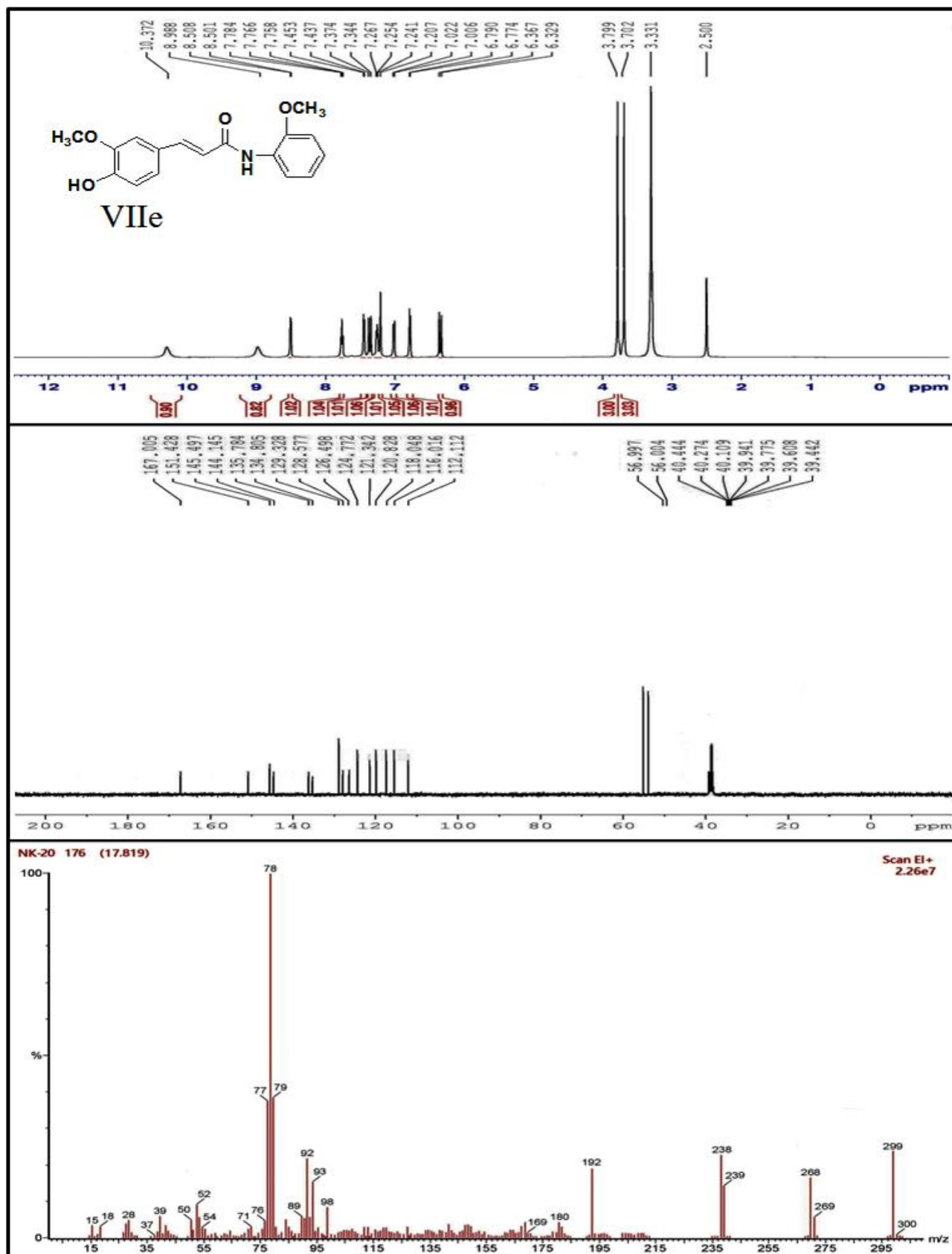


Figure 3.27: ¹H, ¹³C-NMR and GC-MS spectra of VIIe.

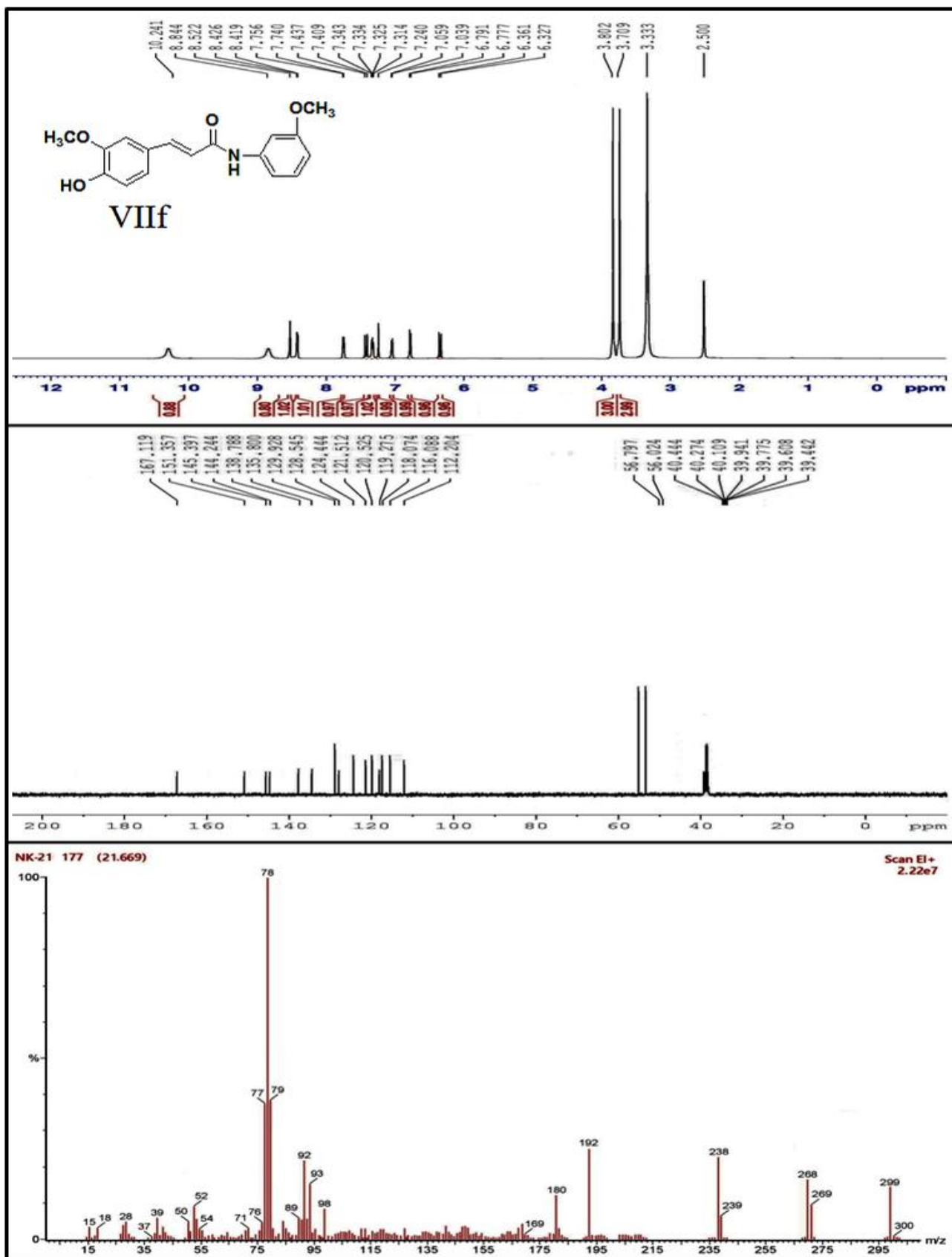


Figure 3.28: ¹H, ¹³C-NMR and GC-MS spectra of VIII f.

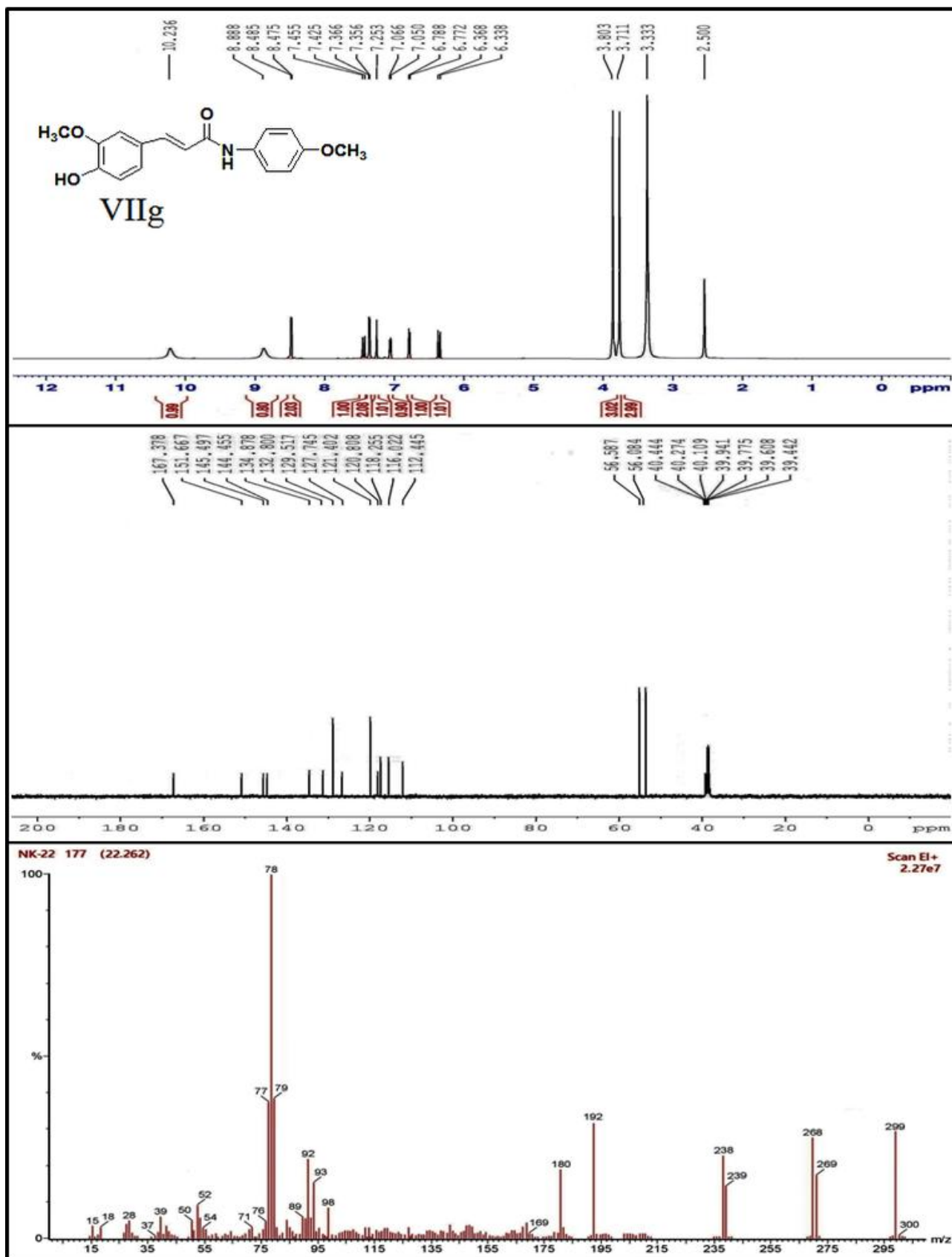


Figure 3.29: ¹H, ¹³C-NMR and GC-MS spectra of VIIg.

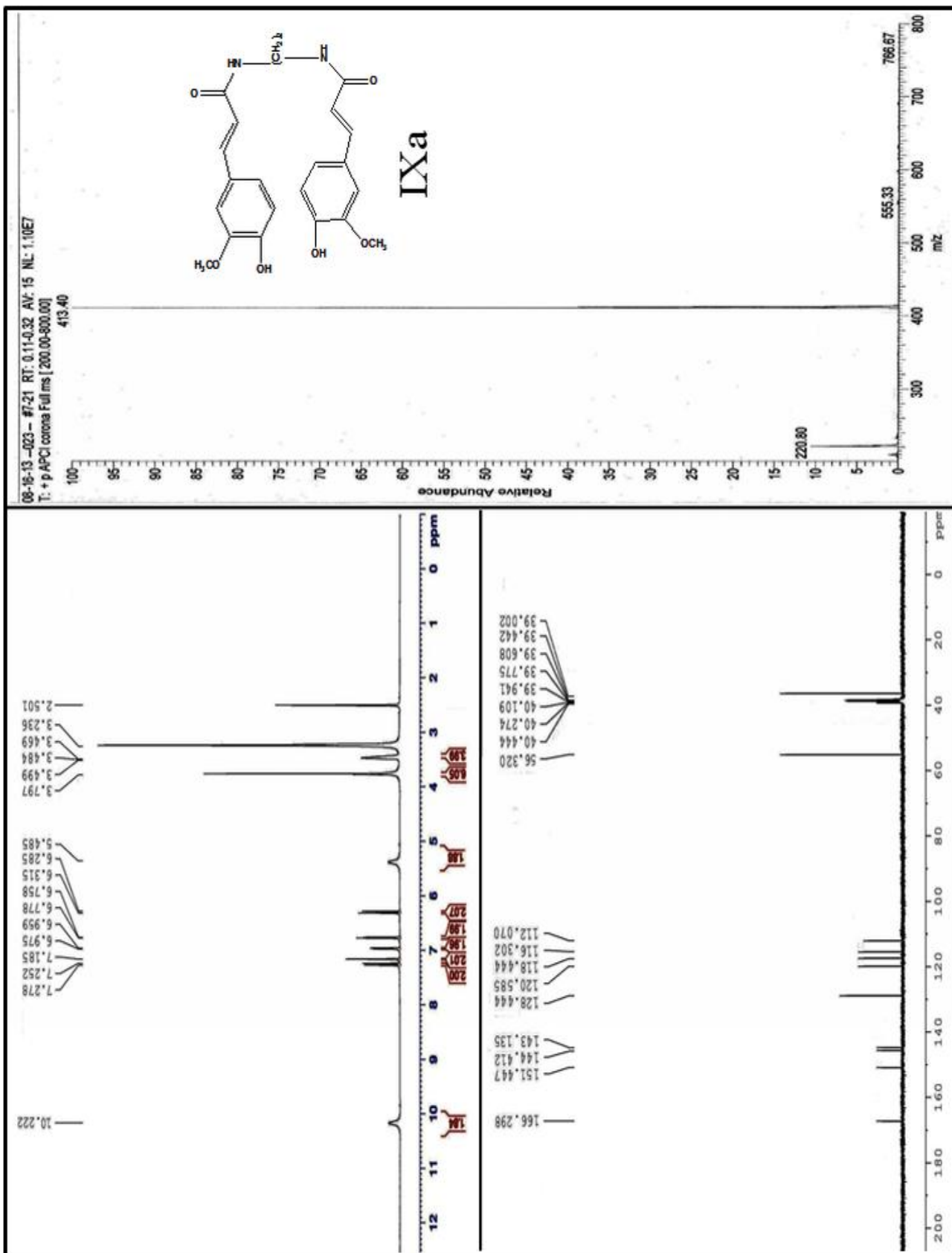


Figure 3.30: ^1H , ^{13}C -NMR and APCI-MS spectra of IXa.

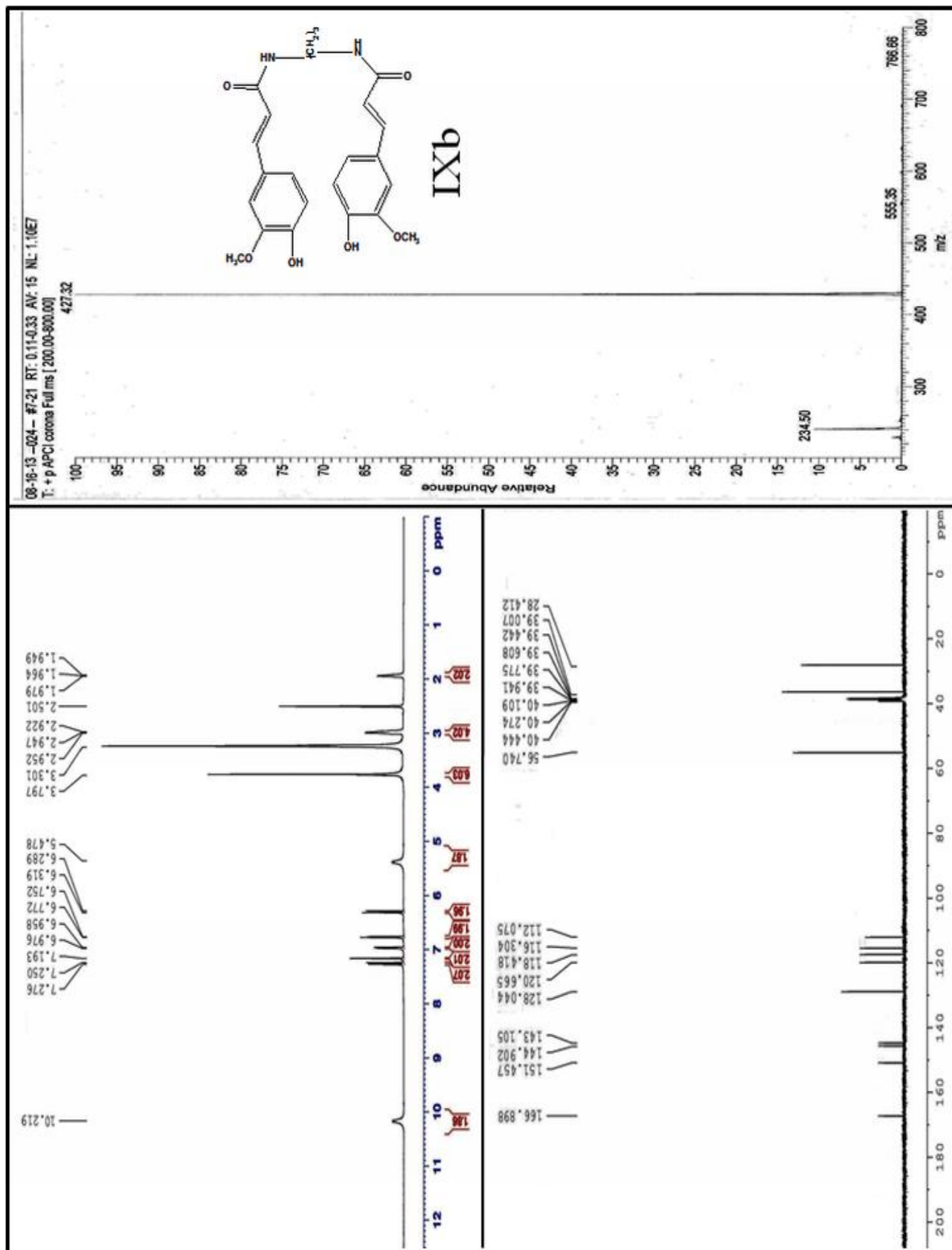


Figure 3.31: ^1H , ^{13}C -NMR and APCI-MS spectra of IXb.

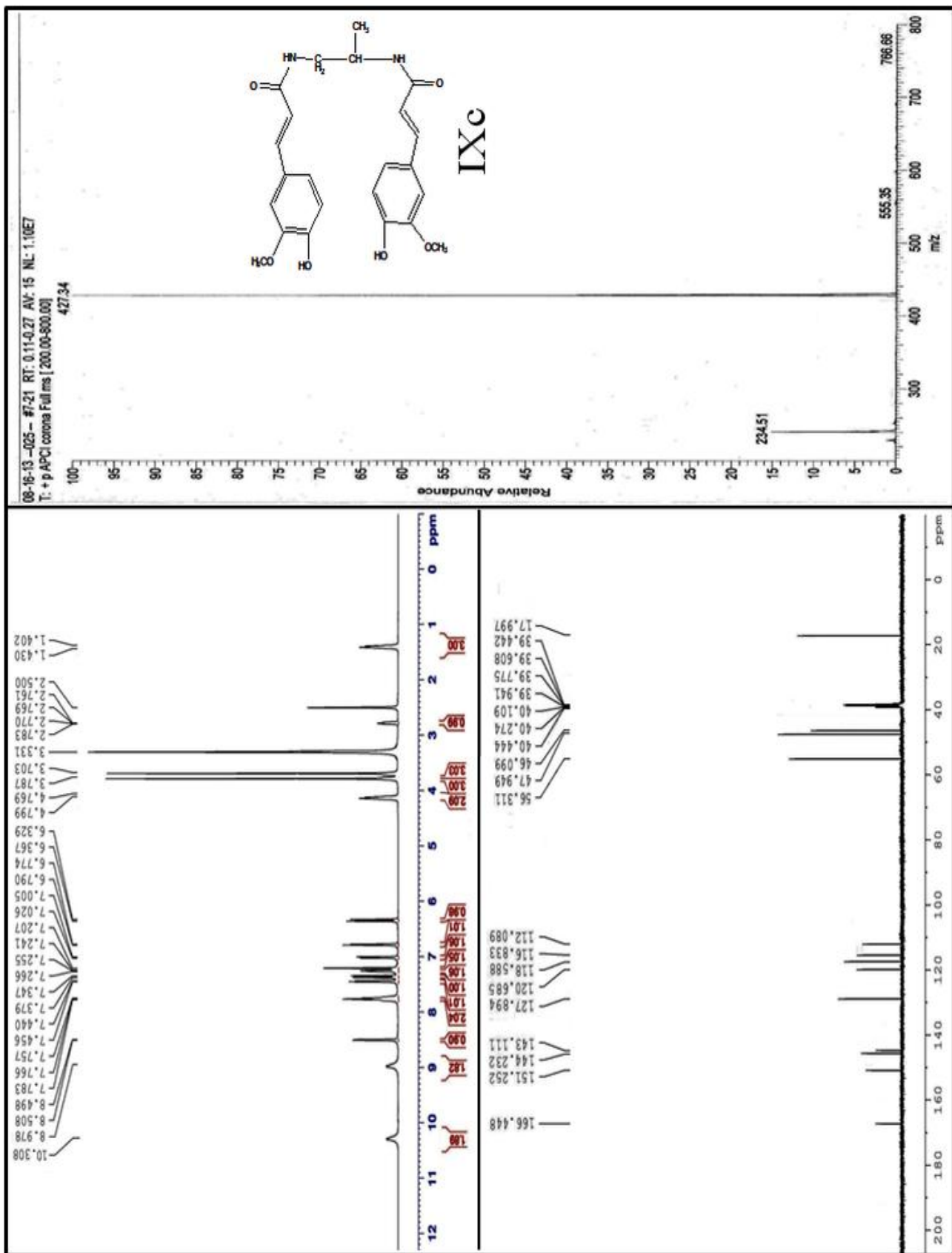


Figure 3.32: ^1H , ^{13}C -NMR and APCI-MS spectra of IXc.

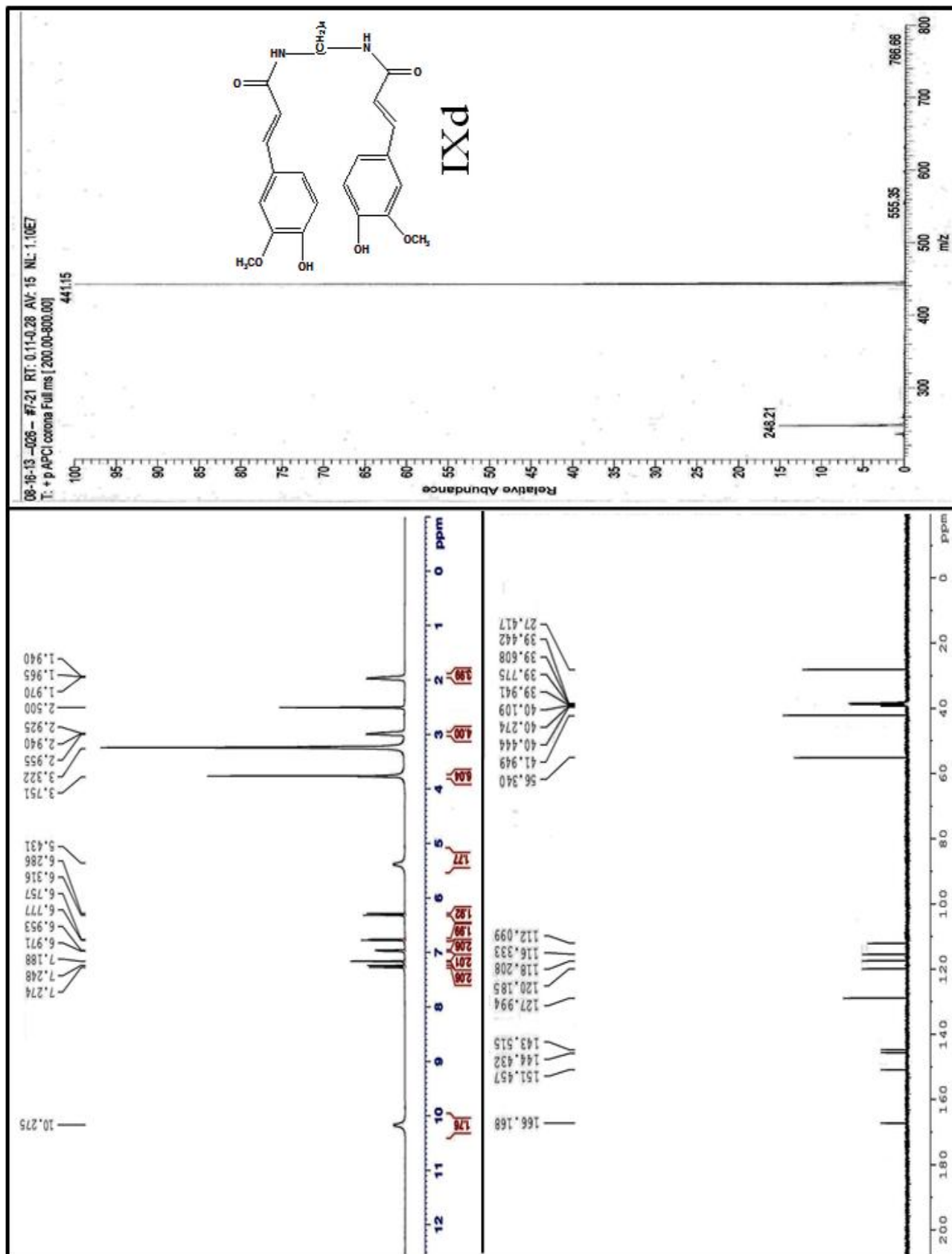


Figure 3.33: ¹H, ¹³C-NMR and APCI-MS spectra of IXd.

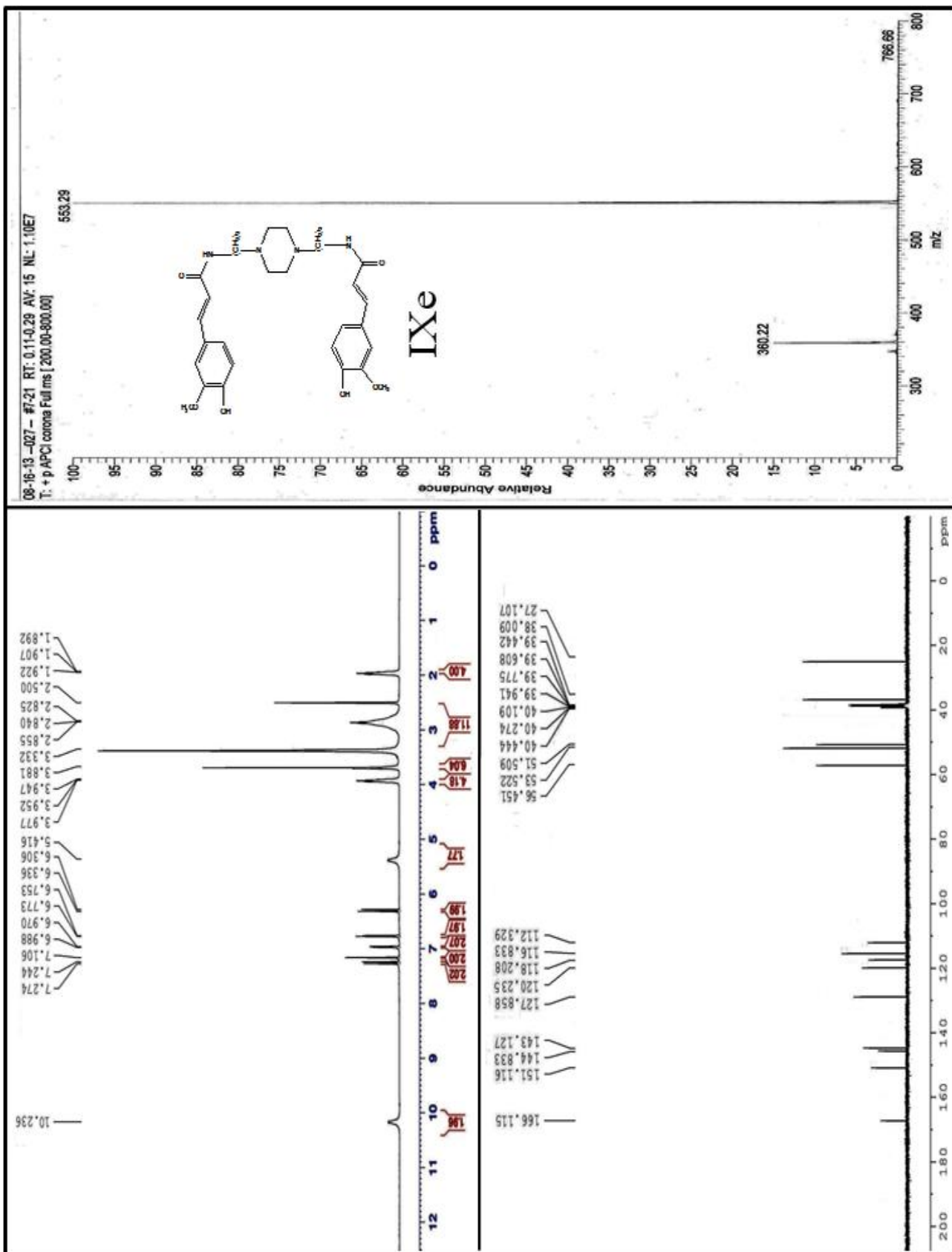


Figure 3.34: ¹H, ¹³C-NMR and APCI-MS spectra of IXe.

3.3.2. Thermal analysis

The analysis for the thermal stability of four series of ferulic acid derivatives has been examined by TG, DTA and DTG technique from 20-600°C at a heating rate of 10°C min⁻¹ (mass 0.045 g) under nitrogen atmosphere (Table 3.1). The graphical representation of TG-DTG analysis of the first compound from each series has been shown in the Figure 3.35. The results of thermal analysis showed that all the derivatives are stable up to 100°C and decomposed through one step, but at higher temperatures the TG-DTG curves show irregular pattern. The compound **IIIa** was decomposed immediately after melting, and the decomposition continues up to 364°C with 98.1% weight loss due to decomposition of *(E)-N-cyclopropyl-3-(4-hydroxy-3-methoxyphenyl)acrylamide*, corresponds to endotherm at 292°C in DTA. The DTG peak is perceived at 205°C. The same behavior is also observed for **IIIb-IIIo**. In **Va**, the weight loss (97.6%) in the temperature range of 264°C and 378°C (DTG peak at 341°C) corresponds to complete removal of *(E)-N-(acridin-9-yl)-3-(4-hydroxy-3-methoxyphenyl)acrylamide* due to its endothermic nature of decomposition at 295°C. All other compounds **Vb-Vg** also follow the same thermal decomposition pattern. The thermal decomposition of **VIIa** occurs in the temperature range 174-402°C, which shows the weight loss of 97.9% with the DTG peak at 257°C. In this step, *(E)-3-(4-hydroxy-3-methoxyphenyl)-N-phenylacrylamide* leaves out endothermically at 239°C. The compounds **VIIb-VIIg** also follow the same way of decomposition pattern as **VIIa**. Like other derivatives the compound **IXa** also undergoes one step decomposition with the mass loss of 98.9%, which corresponds to the DTG peak at 198°C. In this step *N,N'-ethylen-bis[(E)-3-(4-hydroxy-3-methoxyphenyl)-acrylamide]* (148-367°C) releases endothermically at 173°C. Other compounds of bis-amide series, **IXb-IXe** also showed the same stability behavior (Table 3.1).

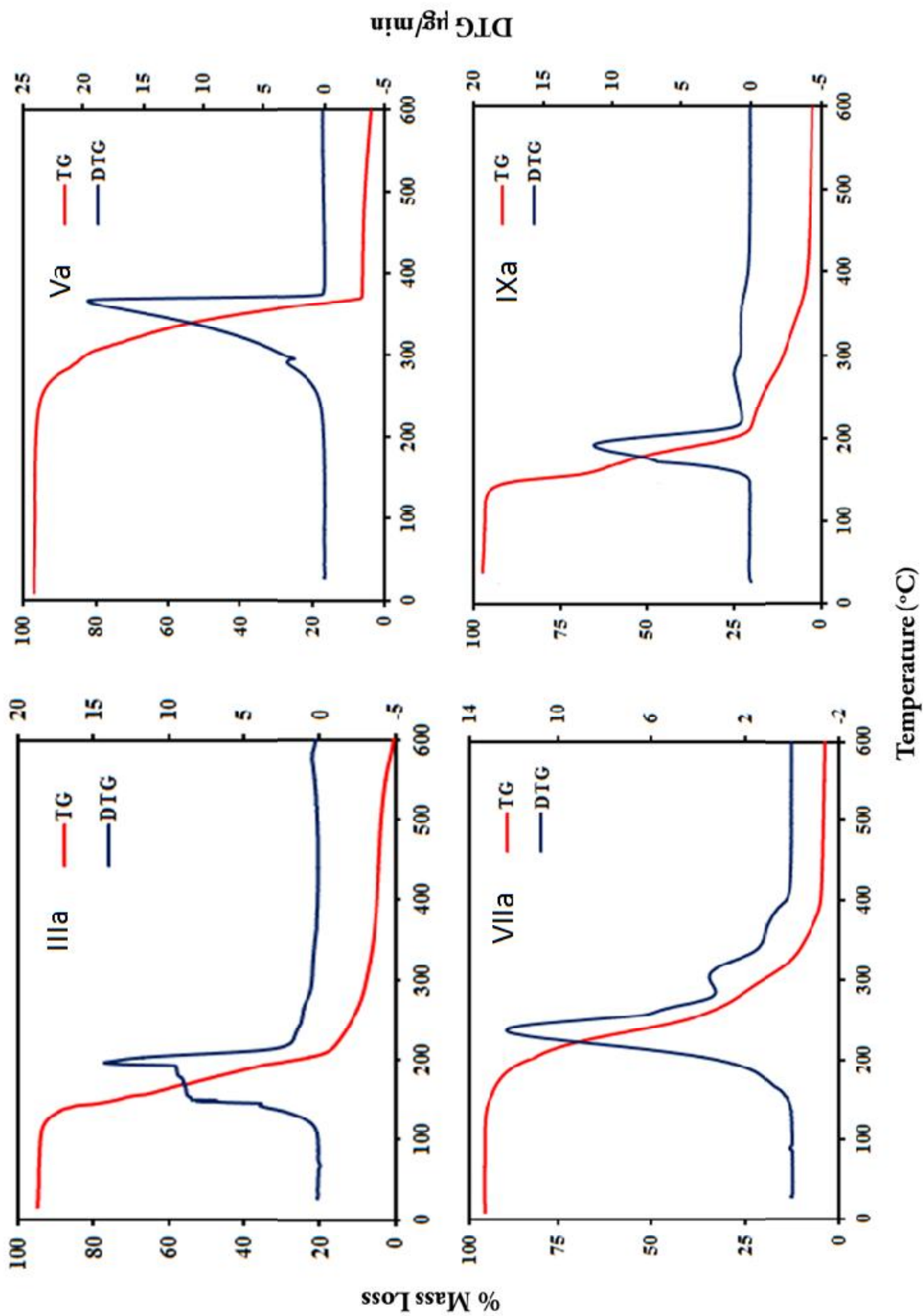


Figure 3.35: Simultaneous TG-DTG analysis curves of IIIa, Va, VIIa, and IXa under nitrogen.

Compound name	Stage	TG		DTA		DTG
		Temp. range /°C	Observed mass loss (%)	Peak temp/ °C	nature	Peak temp./°C
IIIa	I	123-364	98.1	292	Endo	205
IIIb	I	121-367	98.7	271	Endo	201
IIIc	I	127-359	97.9	279	Endo	209
III d	I	119-361	99.3	291	Endo	213
IIIe	I	117-359	98.6	263	Endo	207
III f	I	111-371	97.2	289	Endo	199
III g	I	123-345	97.5	259	Endo	211
III h	I	115-373	99.1	261	Endo	217
III i	I	116-358	96.9	278	Endo	187
III j	I	131-377	98.3	247	Endo	214
III k	I	138-363	97.6	291	Endo	224
III l	I	113-368	97.4	274	Endo	219
III m	I	115-374	98.1	267	Endo	223
III n	I	112-365	98.5	293	Endo	231
III o	I	110-357	96.9	281	Endo	229
Va	I	264-378	97.6	295	Endo	341
Vb	I	259-381	99.2	289	Endo	347
Vc	I	257-379	98.1	293	Endo	338
Vd	I	261-371	98.5	297	Endo	343
Ve	I	267-387	97.9	278	Endo	349

Vf	I	255-383	98.4	266	Endo	337
Vg	I	249-389	97.2	278	Endo	321
VIIa	I	174-402	97.9	239	Endo	257
VIIb	I	169-389	98.3	241	Endo	261
VIIc	I	177-393	97.1	233	Endo	259
VIIId	I	161-381	98.7	239	Endo	267
VIIe	I	173-398	99.1	242	Endo	269
VIIIf	I	179-407	98.4	237	Endo	271
VIIg	I	165-413	97.8	229	Endo	249
IXa	I	148-367	98.9	173	Endo	198
IXb	I	152-369	99.1	189	Endo	201
IXc	I	157-371	97.6	177	Endo	191
IXd	I	144-361	98.2	201	Endo	207
IXe	I	140-359	99.4	183	Endo	194

Table 3.1: TG-DTA-DTG data of compounds IIIa-IIIo, Va-g, VIIa-g and IXa-e.

3.4. Concluding remarks

Thirty four mono and bis-amide derivatives of ferulic acid have been synthesized by microwave assisted condensation under solvent free condition. All the compounds were found to produced in the good yield with 80-98% within 3-10 min. The compounds were purified and fully characterized by experimental techniques such as elemental analysis, FT-IR, NMR and mass spectroscopy. Thermal study shows that all synthesized derivatives are stable at room temperature, and decompose at high temperature.

CHAPTER-4

Biological applications of ferulic acid amide derivatives

Naresh Kumar, Sandeep Kumar, Sheenu Abbat, Kumar Nikhil, Sham M. Sondhi, P.V. Bharatam, Partha Roy and Vikas Pruthi (2014). 3D-QSAR modeling of ferulic acid and its amide derivatives: Synthesis, structural characterization, anticancer and antioxidant activities. European Journal of Medicinal Chemistry (Under review)

Biological applications of ferulic acid amide derivatives

4.1. Introduction

The dietary antioxidants play the shielding role against the growth and evolution in the pathological conditions produced due to the oxidative stress, which is the main cause in many diseases like atherosclerosis, neurodegenerative, diabetes, cancer, and aging and in human beings. Due to the high concentrations in food and beverages, polyphenols are the main source of antioxidants, and is easily absorbed by intestine. Caffeic and ferulic acid are present in the higher amount in the human diet as compared to other phenolic acids. That why they have drawn the attention of scientific community towards their potential properties particularly antioxidant activity and other biological effects [Clifford 1999; Herrmann 1989; Scalbert et al. 2000; Pulido et al. 2003; Sajjadi et al. 2004; Wiegand et al. 2009; Piazzon et al. 2012; Ferhat et al. 2014]. Cancer is one of the major health problems around the world, and according to the report of world health organization (WHO) approximately more than twice people died every year from cancer than AIDS, malaria, and tuberculosis together, it is expected that the number of deaths due to cancer will be increase up to 80% by 2030. There are a limited number of good anticancer drugs present in the market, and still there is an imperative requirement to discover the new compounds, which can act as anticancer agents [Dougherty et al. 1991; Settimo et al. 1998; Skalkos et al. 1998; Sondhi et al. 2010]. Cinnamic acid and its natural analogues are unique anticancer agents [De et al. 2011]. There are many research groups around the globe, who are working on development of new drugs and softwares for designing and calculations of novel molecules of biological interest to reduce the number of deaths due to the diseases like cancer, AIDS, diabetes and many more life

reducing conditions [Steindl et al. 2006; Langer and Wolber 2007; Wolber et al. 2008; Ashish et al. 2010; Kumar and Sharma 2010; Kaundal and Sharma 2010; Singh et al. 2010; Schuster et al. 2010; Monga et al. 2011; Rathore et al. 2011 and 2012;].

Ferulic acid is an ubiquitous phenolic derivative of cinnamic acid [Rosazza et al. 1995], exhibits a wide range of biomedical effects viz., anticancer, antioxidant, antimicrobial, anti-inflammatory, antiallergic, antithrombotic, antiviral and hepatoprotective properties [Kumar et al. 2014]. The wide variety of biological applications exhibited by ferulic acid has also been discussed in details in the first chapter of this thesis [Mori et al. 1999; Middleton et al. 2000; Toshihiro et al. 2000; Ou and Kwok, 2004; Dorn et al. 2010; Chung et al. 2011; Mori et al. 2013; Kumar et al. 2014]. Different kinds of ferulic acid derivatives have been made by various research groups, which also showed the anticancer, antioxidant, histone deacetylase inhibitor, antimicrobial, anti-inflammatory activities and other biological functions [Murakami et al. 2002; Hosoda et al. 2002; Zarth et al. 2011; Li et al. 2012; Sultana 2012; Paiva et al. 2013; Wang et al. 2013; Lu et al. 2014; Huang et al. 2013; Piazzon et al. 2012]. The amide derivatives are associated with a wide range of biological activities as many anti-diabetic agents such as sulfonylurea compounds are also found to contain the bond-structure of amide [Haring et al. 2013].

4.2. Experimental section

4.2.1. Materials

Ferulic acid has been isolated and purified from *Parthenium hysteroporous*. Chemicals like Penicillin, MTT (3-(4,5-dimethyl-2-thiazolyl)-2,5-diphenyl-2H tetrazolium bromide), streptomycin, cell culture grade DMSO, cyclophosphamide, 5-fluorouracil (5-FU), and actidione (cycloheximide) have been purchased from Himedia and all other cell culture reagents were from GIBCO (Invitrogen, USA).

4.2.2. *In vitro* cytotoxicity assay

The different types of human cancer cell lines (Breast: MCF-7 and MDA-MB-231, Lung: A549, Cervical: HeLa and Liver: HepG2) and normal stem cell line (BM-MSC) taken in this research work have been acquired from NCCS, Pune. The cells were grown in the tissue culture flasks at 37°C within the carbon dioxide incubator (5% CO₂, 90% RH) by using growth medium which containing the RPMI-1640 medium (with 2 mM glutamine), supplemented with 10% fetal bovine serum, 100 µg/mL streptomycin and 100 units/mL penicillin at pH 7.4. In brief, 5×10³ cells in 200 ml of medium were seeded in 96-well Elisa plates. Serial dilutions of tested synthesized derivatives ranging from 0 to 100 mM in DMSO were putted to the monolayer and 0.1% DMSO was used as vehicle control during MTT assay. After 24 hrs of cell culture, 50 ml (5 mg/ml) of MTT was added in the culture plates and incubated at 37°C for 4 hrs in CO₂ incubator under dark. MTT mixed culture plates was aspirated; 25 ml of Sorensen glycine buffer (0.1 M glycine and 0.1 M NaCl, pH 10.5) with 200 ml of DMSO have been added into the plates to lyse the cells and solubilization of the water insoluble formazones. Finally, the absorbance of all the lysates were taken at 570 nm with the help of Fluostar optima microplate reader (BMG Labtech, Germany). The IC₅₀ values were calculated by using the software graph pad prism 5.02 and the percentage inhibition was calculated with the help of mathematical formula which is given below:

$$\frac{\text{Mean OD of vehicle treated cells(negative control)} - \text{Mean OD of treated cells} \times 100}{\text{Mean OD of vehicle treated cells(negative control)}}$$

4.2.3. *In vitro* antioxidant activity assay

The assay used for the determination of spectral values of tested compounds having modifications in the earlier reported method [Blois 1958]. The present used microplate assay has

benefits being environment friendly as well as time and sample saving compared to commonly used methods (labor, time, sample and reagent consuming) for the testing of antioxidant activity of compounds. Briefly, methanolic DPPH solutions (50 μ L, 100 μ g/mL) were added into each sample of different concentration (200 μ L, 12.5–100 μ g/mL). The solutions (sample with DPPH) were mixed gently and incubated for 30 min in the dark at room temperature and absorbance was recorded at 517 nm. Different concentrations of methanolic DPPH (5–50 μ g/mL) has been taken in the formation of standard curve. The concentration of DPPH in the reaction mixture was calculated according to the method reported earlier [Li et al. 2012].

The scavenging capability of test compounds was calculated using the following equation:

$$\text{DPPH}\cdot \text{ scavenging activity (\%)} = \left(1 - \frac{\lambda_{517-S}}{\lambda_{517-C}}\right) \times 100$$

Where, λ_{517-C} is absorbance of a control with no radical scavenger and λ_{517-S} is absorbance of the remaining DPPH in the presence of scavenger.

4.3. Results and discussion

Fully characterized and purified mono and bis-amide derivatives of ferulic acid have been screened for their *in vitro* anticancer and antioxidant activity by MTT and DPPH assay, respectively.

4.3.1. In vitro anticancer activity

The evaluation of *in vitro* cytotoxicity of all the four series (**IIIa-IIIo**, **Va-Vg**, **VIIa-VIIg** and **IXa-IXe**) of compounds had been carried out by MTT assay against the five different human cancer cell lines, i.e., breast (MDA-MB-231 and MCF-7), cervical (HeLa), lung (A549), and liver (HepG2) along with a normal stem cell line at the concentration of 10 μ M. The results obtained from MTT assay are summarized in Table 4.1, showed that 21 compounds (**IIIi-IIIo**, **Va-Vg**, and

VIIa-VIIg) out of all 34 exhibited noticeable activity against all the cancer cell lines and very less or negligible effect on the normal stem cells. The anticancer activity exhibited by these derivatives was comparatively high as compared to isolated ferulic acid (Table 4.1). These results infer that the amide derivatives are good compounds for anticancer activity. Further, these 21 compounds were studied for their IC₅₀ value (Table 4.2), and found that it lied between 07.11 to 18.28 μ M in different kind of cancer cells. The compounds **Va-Vg** (containing acridine moiety) showed the best activity against all the cell lines as they have a very good range of IC₅₀ (07.11-11.08 μ M).

Compound name	Breast (MCF-7)	Breast (MDA-MB-231)	Lung (A549)	Liver (HepG2)	Cervical (HeLa)	Normal (stem)
IIIa	29.19	16.98	26.17	27.69	22.73	NA
IIIb	27.95	30.18	19.07	34.94	31.88	NA
IIIc	23.51	21.77	27.28	20.65	25.68	NA
IIId	32.30	24.22	33.89	25.14	29.22	NA
IIIe	27.72	21.87	35.52	29.69	32.17	NA
IIIf	26.85	27.22	31.13	29.92	30.24	NA
IIIg	20.28	29.29	17.81	24.93	23.74	06.63
IIIh	25.35	30.55	31.12	29.75	27.93	NA
IIIi	59.09	51.48	54.04	53.55	65.62	11.36
IIIj	62.55	56.83	56.81	50.63	61.91	13.63
IIIk	43.36	47.77	52.27	51.39	55.71	07.68
IIIl	51.92	56.55	56.12	47.68	58.42	18.37
IIIm	58.22	55.09	58.34	44.72	55.43	14.21
IIIn	55.88	57.68	53.42	51.09	53.14	15.34
IIIo	50.81	58.33	56.49	41.62	54.11	08.44
Va	57.24	60.82	69.95	59.36	78.11	17.24
Vb	75.53	77.25	72.64	61.95	71.39	16.47
Vc	66.64	74.10	75.10	63.35	69.19	12.49
Vd	68.97	78.11	79.17	66.46	82.95	06.63

Ve	66.26	62.84	78.56	63.51	81.01	09.76
Vf	79.11	61.12	80.63	66.37	70.97	17.05
Vg	78.04	69.51	83.71	68.32	73.82	19.13
VIIa	51.67	51.91	60.26	45.35	63.41	08.44
VIIb	48.62	43.88	61.03	48.35	59.42	12.69
VIIc	49.68	47.82	53.34	52.33	55.84	08.96
VIIId	51.63	55.14	65.88	55.91	60.69	10.27
VIIe	39.07	40.78	58.42	46.58	54.48	08.01
VIIIf	42.68	49.83	55.49	50.46	57.28	06.25
VIIg	48.63	55.66	60.65	56.68	63.98	03.68
IXa	24.01	19.09	27.18	25.77	29.09	NA
IXb	33.63	25.02	31.76	20.96	32.95	NA
IXc	27.57	22.24	31.64	23.76	38.01	NA
IXd	28.96	19.95	27.51	22.67	23.59	05.59
IXe	26.91	19.37	27.19	22.59	16.92	08.61
Ferulic acid	23.56	20.18	20.66	21.09	21.91	NA
5-Fluorouracil	15.54	20.22	30.17	32.72	23.84	25.21
Cyclophosphamide	13.17	15.84	11.18	19.50	20.16	19.27
Cycloheximide	15.22	17.96	14.11	22.13	22.37	23.98

Table 4.1: *In vitro* anticancer activity (% growth inhibition) of ferulic acid amide derivatives at 10 μ M concentration.

Compound name	Breast (MCF-7)	Breast (MDA-MB-231)	Lung (A549)	Liver (HepG2)	Cervical (HeLa)
IIIi	12.88±3.96	14.08±2.59	13.45±3.35	15.91±3.98	10.97±3.79
IIIj	09.87±2.97	12.97±3.41	13.44±4.02	16.14±3.88	12.07±4.01
IIIk	17.29±1.96	16.91±2.76	12.09±3.72	14.61±3.19	12.26±3.81
IIIl	11.98±3.12	12.28±3.88	12.18±4.12	15.17±3.21	12.05±4.04
IIIm	11.42±3.77	13.06±4.22	12.22±5.03	16.82±4.05	13.71±3.51
III n	13.09±4.38	14.32±3.72	12.55±3.09	15.49±3.13	12.83±2.92
IIIo	13.44±2.76	14.91±3.23	13.77±3.54	18.28±3.34	15.82±4.43
Va	09.17±3.47	08.99±3.52	07.84±2.89	10.59±4.27	07.51±3.84
Vb	07.49±3.22	07.29±2.72	08.13±3.11	09.88±4.67	08.75±3.72
Vc	09.23±3.69	07.66±3.36	07.21±3.53	10.21±4.37	08.06±4.19
Vd	08.38±3.64	07.48±3.01	07.11±3.48	09.31±4.05	07.29±3.55
Ve	09.74±3.09	09.89±3.71	07.48±4.52	10.41±3.86	07.14±2.68
Vf	08.06±3.09	10.34±3.19	08.11±3.72	11.08±4.12	08.98±3.18
Vg	08.12±3.88	08.99±3.13	08.04±3.92	10.37±3.79	09.65±4.27
VIIa	13.05±3.72	12.67±3.72	09.77±3.72	15.92±4.29	09.89±3.72
VIIb	15.81±3.65	17.64±3.81	09.19±3.53	13.54±4.78	10.89±3.72
VIIc	15.28±3.37	16.01±3.22	09.16±3.21	12.13±4.09	09.74±3.98
VII d	12.78±3.88	12.49±2.82	08.98±3.56	11.05±3.82	09.53±3.09
VIIe	15.27±3.33	17.04±2.98	11.67±4.01	14.36±2.98	10.62±3.76
VII f	16.55±3.19	13.14±3.64	10.84±3.09	13.02±3.44	09.87±2.97
VII g	16.17±3.22	12.74±3.86	09.54±2.64	13.11±3.73	09.17±4.12

Table 4.2: IC₅₀ (μM) values of *in vitro* anti-proliferative activity of active ferulic acid amide derivatives.

4.3.2. *In vitro* antioxidant activity

The compound, 1,1-diphenyl-2-picrylhydrazyl radical (DPPH) is a well-known reagent for the evaluation of free radical scavenging activity, possesses an unpaired electron, and exhibits a stable violet color in methanol solution at 517 nm. In the methanol solution, DPPH is reduced into

DPPH-H due to the presence of hydrogen donating molecule or compound [Sharma et al. 2009]. The Table 4.3 summarizes the EC₅₀ values of free radical scavenging activities of all newly synthesized compounds by using DPPH assay. Data revealed that nine compounds (**III**f, **III**l, **III**o, **VII**e and **IX**a-**IX**e) showed good DPPH radical scavenging activity with EC₅₀ ranges from 18.37 to 25.44 μM compared to ascorbic acid (EC₅₀; 20.14 μM). Thirteen compounds from all showed poor antioxidant activity having EC₅₀ values more than 35 μM, while twelve compounds exhibits moderate activity with EC₅₀, 26.89-34.81 μM.

Comp. Name	EC ₅₀	Comp. Name	EC ₅₀
IIIa	46.83±3.48	Vd	49.95±4.34
IIIb	31.54±2.74	Ve	35.24±3.72
IIIc	38.85±3.49	Vf	41.17±3.82
III d	36.28±2.94	Vg	37.96±3.68
IIIe	47.29±3.27	VIIa	27.14±3.57
III f	23.39±3.84	VIIb	37.73±2.97
IIIg	28.11±2.72	VIIc	33.12±2.83
IIIh	34.28±2.46	VII d	34.81±2.79
IIIi	28.65±2.79	VII e	23.64±3.73
IIIj	26.94±3.26	VII f	32.78±2.96
IIIk	42.83±3.62	VIIg	27.43±3.37
III l	19.87±3.32	IX a	18.37±2.74
III m	29.78±3.71	IXb	20.09±2.77
III n	28.19±3.63	IXc	21.81±2.56
III o	25.44±3.67	IXd	20.89±3.52
Va	36.55±3.62	IXe	24.68±2.69
Vb	45.58±4.28	Ferulic acid	34.16±2.52
Vc	48.41±3.54	Ascorbic acid	16.64±1.51

Table 4.3: EC₅₀ (μg/ml) values of *in vitro* free radical scavenging activity of active ferulic acid amide derivatives.

4.4. Concluding remarks

Ferulic acid is an important lead compound for the design of anticancer and antioxidant compounds. Microwave assisted synthesized mono and bis-amide derivatives of ferulic acid have been screened for their *in vitro* anticancer activity at 10 μ M concentrations by MTT assay and 21 compounds from this series was found to exhibits noticeable cytotoxicity effect against all the tested cancer cell lines (MCF-7, MDA-MB-231, A549, HepG2 and HeLa). Subsequently, the IC₅₀ values of 21 promising compounds have been calculated. The anticancer activity exhibited by these derivatives was comparatively high as compared to isolated ferulic acid. The most promising compound against Breast cancer cell lines (MCF-7 and MDA-MB-231) was **Vb** with IC₅₀ values 7.49 \pm 3.22 and 7.29 \pm 2.72 μ M; Lungs (A549) and Liver (HepG2) cancer cell line was **Vd** with IC₅₀ values 7.11 \pm 3.48 and 8.31 \pm 4.05 μ M and Cervical (HeLa) cancer cell line was **Ve** with IC₅₀ values 7.14 \pm 2.68 μ M, respectively. Further, considering that ferulic acid showed good antioxidant activity due to the presence of phenolic hydroxyl group, all the 34 derivatives were tested for their antioxidant activity by DPPH assay. Most of the derivatives were found to possess improved free radical scavenging activity compared to ferulic acid. Out of all 34 compounds, **III_f**, **III_l**, **III_o**, **VII_e** and **IX_a-IX_e** were found to have EC₅₀ values between 18.37-24.68 μ M. The most promising compound in the DPPH assay was **IX_a** with 18.37 \pm 2.74 μ M IC₅₀. It may be envisaged that there is a probable relation between the observed anticancer and antioxidant property of ferulic acid derivatives.

CHAPTER-5

Quantum chemical calculations and 3D-quantitative structure activity relationship (QSAR) modeling of ferulic acid amide derivatives

1. **Naresh Kumar**, Sandeep Kumar, Sheenu Abbat, Kumar Nikhil, Sham M. Sondhi, P.V. Bharatam, Partha Roy and Vikas Pruthi (2014). 3D-QSAR modeling of ferulic acid and its amide derivatives: Synthesis, structural characterization, anticancer and antioxidant activities. European Journal of Medicinal Chemistry (Under review)
2. **Naresh Kumar** and Vikas Pruthi (2015) Theoretical studies on Electronic Structure and Properties of Some Ferulic Acid Amide Derivatives. (to be communicated)

Quantum chemical calculations and 3D-quantitative structure activity relationship (QSAR) modeling of ferulic acid amide derivatives

5a.1. Quantum chemical calculations

The calculations of electronic excited state of a molecule are one of the key concerns in current quantum chemistry. The complete understanding about the potential energy surface, excitation energies and excited state properties are a crucial component in the theoretical explanation of electron transfer processes during the absorption and emission of light by an atom/molecule. Such procedures have their importance in many areas of science viz., Physics, Chemistry and Biology. Over the last five decades, computational chemists have developed many tools/software's for the invaluable calculations/interpretation of experimental measurements of a wide range of molecular properties of atoms, molecules and compounds viz. chemical reactivity, catalytic activity, bioactivity, structural parameters (total energy, dipole moment, bond lengths and angles), electronic (absorption and emission spectra), NMR spectral analysis and many more. The DFT has developed to a stage that can provide precious help in the interpretation of the above mentioned properties. Nowadays, DFT has become a common tool for the recognition and estimation about the behavior of a multi atom system by the prediction of chemical, physical and biological phenomena of importance. We had also applied the DFT approach for the structure optimization and computation of structural parameters viz. Total energy, dipole moment, the energies of HOMO-LUMO, electronegativity, chemical hardness, chemical softness, electrophilic index and many more for the newly synthesized ferulic acid derivatives by Gaussian 09 suite.

A typical molecular system consists of many nuclei and numerous electrons interacting via coulomb interactions with each other. The Born-Oppenheimer approximation is invariably used in

dealing with the molecules to separate electronic and nuclear motions. As electrons are much lighter in comparison of nuclei, can respond instantaneously to any change in the nuclear positions. Hence, for a precise approximation, one can consider the electrons in a molecule to be moving in the field of fixed nuclei. DFT has its historical origins in the Thomas-Fermi statistical model of the atom and its logical foundations were laid by the theorems of Hohenberg and Kohn [Hohenberg et al. 1964]. For the system which contains many electrons in its ground state (time independent), the above researchers established a correspondence between the electron density and external potential. Further, they expressed the energy of a system as a functional of the density and demonstrated that the correct density minimizes this functional in the vibrational sense. The expression for the energy functional is defined as:

$$E[\rho] = T[\rho] + V_{\text{ext}}[\rho] + U[\rho]$$

Where, $T[\rho]$ is the kinetic energy functional, $V_{\text{ext}}[\rho]$ is the potential energy functional and $U[\rho]$ gives the energy of the electron-electron interactions.

5a.2. Theoretical methods

The geometry optimization for all the newly synthesized ferulic acid derivatives was done by means of DFT with a hybrid function B3LYP and because of its excellent compromise between computational time and description of electronic correlation [Becke, 1993; Frisch et al., 2009; Peng et al., 1996; Stephens et al., 1994]. All the calculations were performed by Gaussian 09 suite at DFT methods with 6-311G** basis sets. The GaussView 5.0 generated Z-matrix has been taken as input files for geometry optimization during the simulation process for each compound. The GaussView 5.0 has also been used in the visualization of output files for the same. The energy calculations for frontier molecular orbitals, electronegativity (χ), chemical hardness

(η), softness (S) and electrophilic index (ω) were also calculated by using the Koopmans theorem for closed shell molecule [Koopmans, 1934] and described as:

In a molecule, chemical hardness determines the resistance to change in the electron distribution. It is related with the reactivity and stability of a chemical system and can be calculated by using the equation 1.

$$\eta = -(E_{\text{HOMO}} + E_{\text{LUMO}})/2 \quad (1)$$

The softness is the property of a molecule which helps in the calculation of chemical reactivity. It is the reciprocal of hardness and calculated by using the equation 2.

$$S = \frac{1}{2\eta} \quad (2)$$

The negative of electronegativity of a molecule is called as electronic chemical potential and calculated with the help of equation 3.

$$\mu = (E_{\text{HOMO}} + E_{\text{LUMO}})/2 \quad (3)$$

The capacity of attraction of electrons by an atom/functional group is known as electronegativity which is determined according to the equation 4.

$$\chi = (E_{\text{HOMO}} - E_{\text{LUMO}})/2 \quad (4)$$

Electrophilic index, capacity of a species to accept electrons, is calculated with the help of electronic chemical potential and chemical hardness as described in equation 5. It is used for the evaluation of energy stabilization when a system accepts the extra amount of electronic charge from its environment [Lee et al., 1988].

$$\omega = \frac{\chi^2}{2\eta} \quad (5)$$

5a.3. Results and discussion

5a.3.1. Geometry optimization

The optimized geometries of all the 34 compounds (**IIIa-IIIo**, **Va-Vg**, **VIIa-VIIg** and **IXa-IXe**) showed the positive harmonic vibrational frequencies which indicated that the optimized structure attained the global minimum on the potential energy surface. The simulations were also performed for the calculations of single-point energy, and zero-point corrected total energies. The optimized structure of all these molecules at DFT/B3LYP/6-311G** basis set has been shown in Figure 5.1a-d.

5a.3.2. Frontier Molecular Orbital (FMOs) analysis

To evaluate the energetic behavior of synthesized amide derivatives, calculations were carried out both in solvent and gaseous phase. As discussed in the section 2.3.6 of this thesis, the energy gap between HOMO and LUMO helps in the computation of physio-chemical, electronic and optical properties of a molecule/compound. The energies of HOMO and LUMO orbitals and physio-chemical properties have been calculated at DFT/B3LYP/6-311G** basis set and given in Table 5.1. The total energy calculated for all the derivatives is less as compared to the ferulic acid. The value of dipole moment in the molecules **IIIa-IIIo** and **VIIa-VIIg** is almost near the ferulic acid, which is drastically increased in the **Va-Vg** and bis amides (**IXa-IXe**). This is probably due to the bulky side chains present in these derivatives. The molecular orbital diagram for all ferulic acid amide derivatives are illustrated in Figure 5.2 to 5.5. In the molecules **IIIa to IIIo**, the -OCH₃ group is taking part in HOMO but not in LUMO and the charge is transferring from the -OCH₃ group of ferulic acid to the attached amide group containing N-H and N-C bond. The -OCH₃ group is taking part in HOMO but not in LUMO (Figure 5.2a-c).

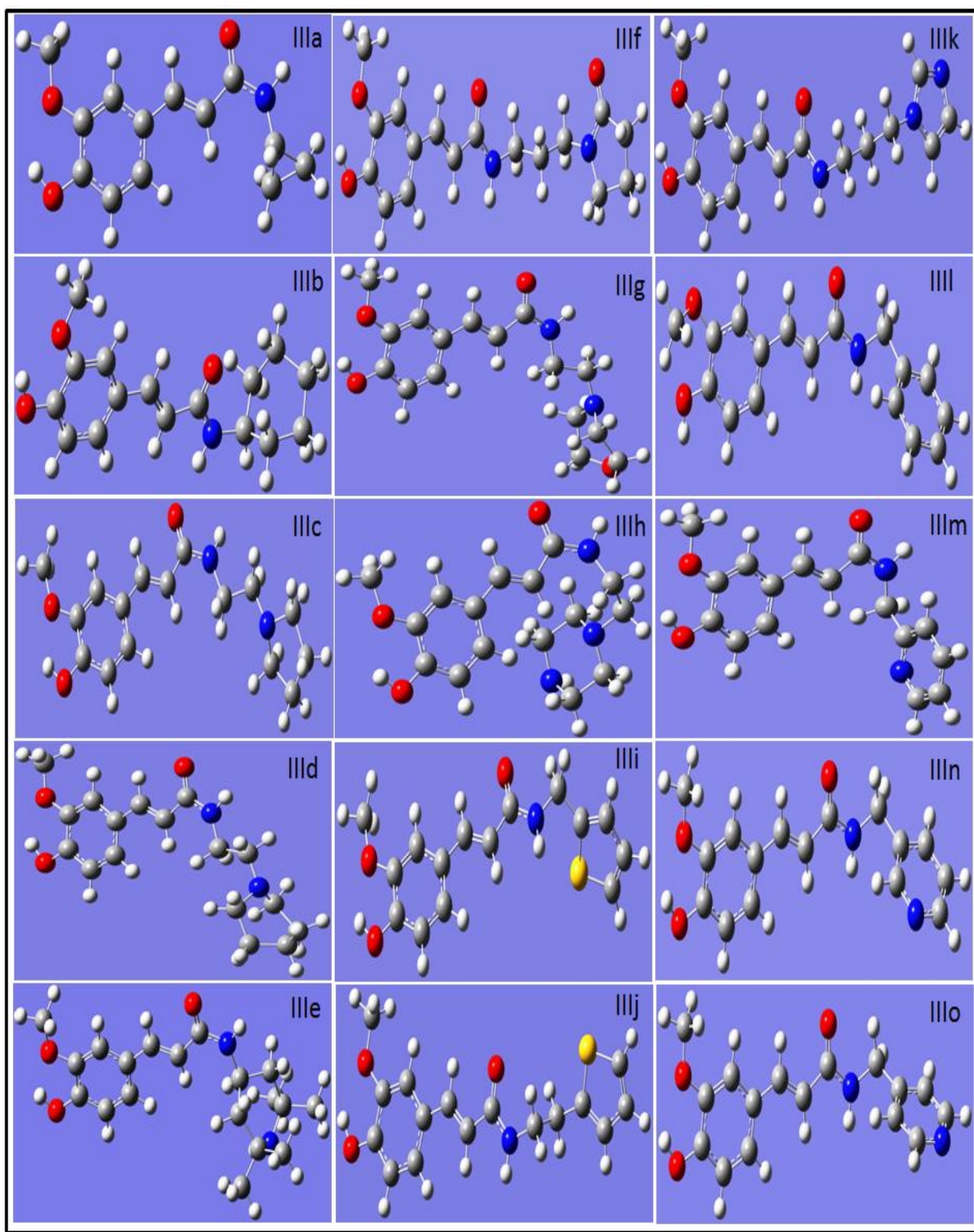


Figure 5.1a

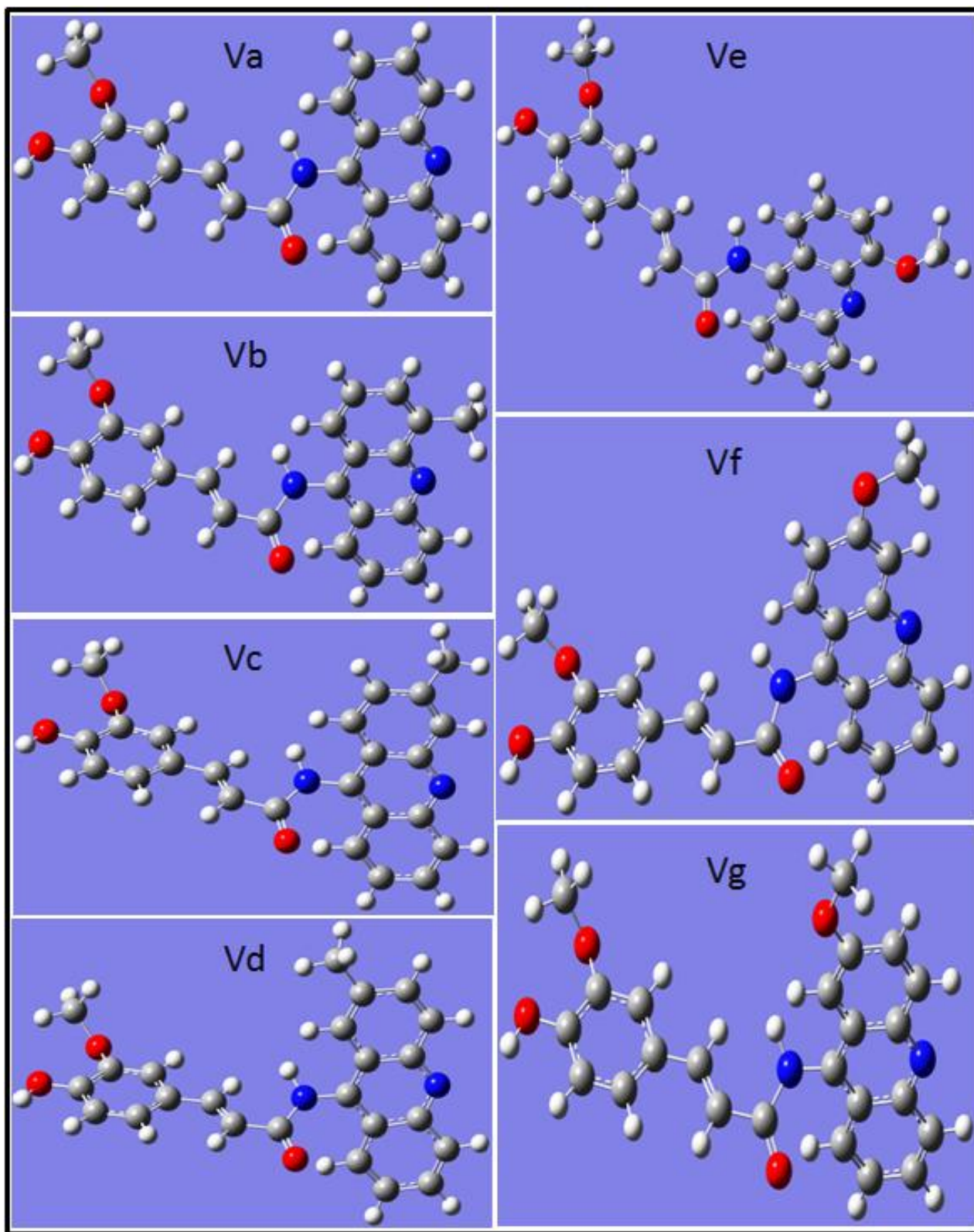


Figure 5.1b

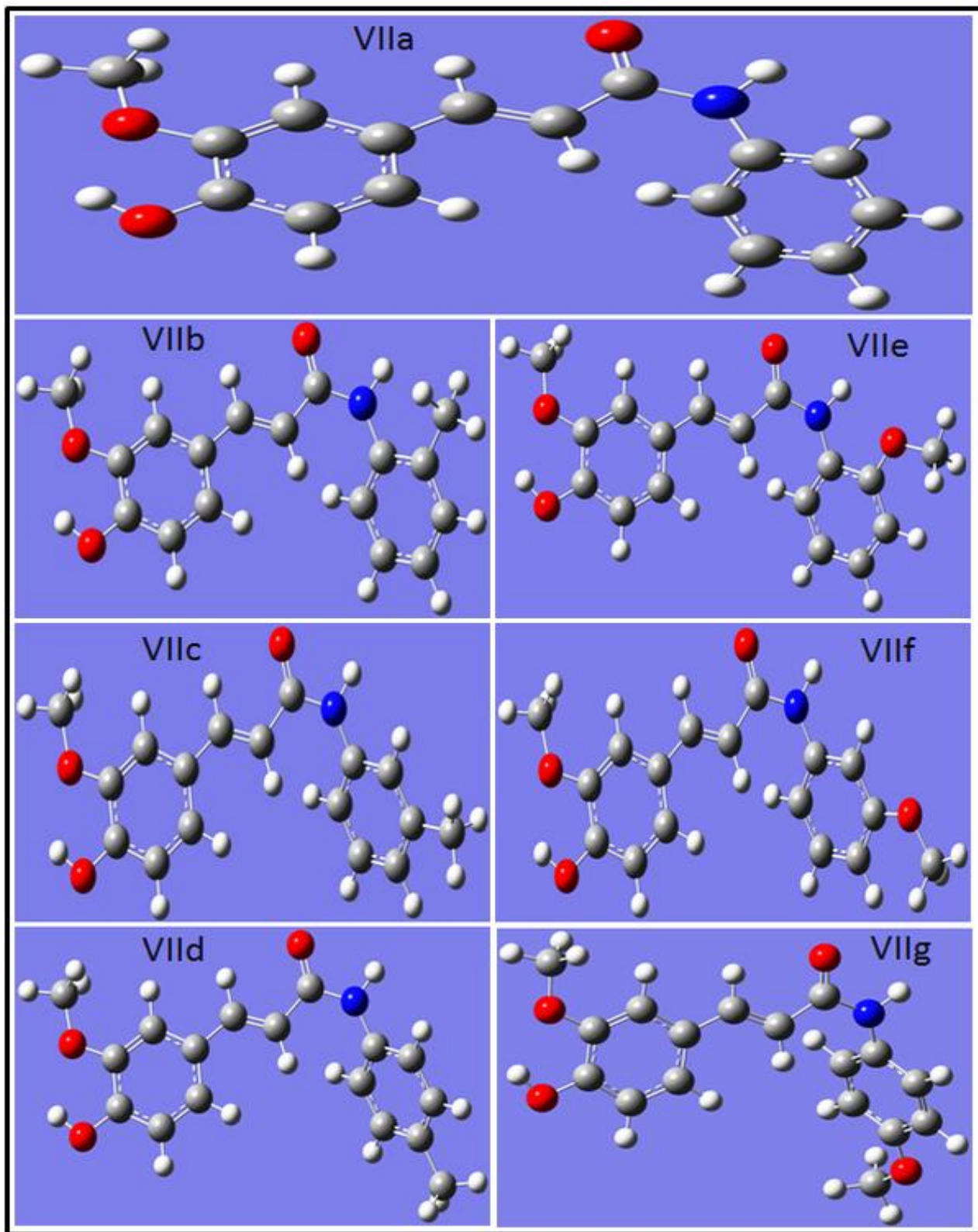


Figure 5.1c

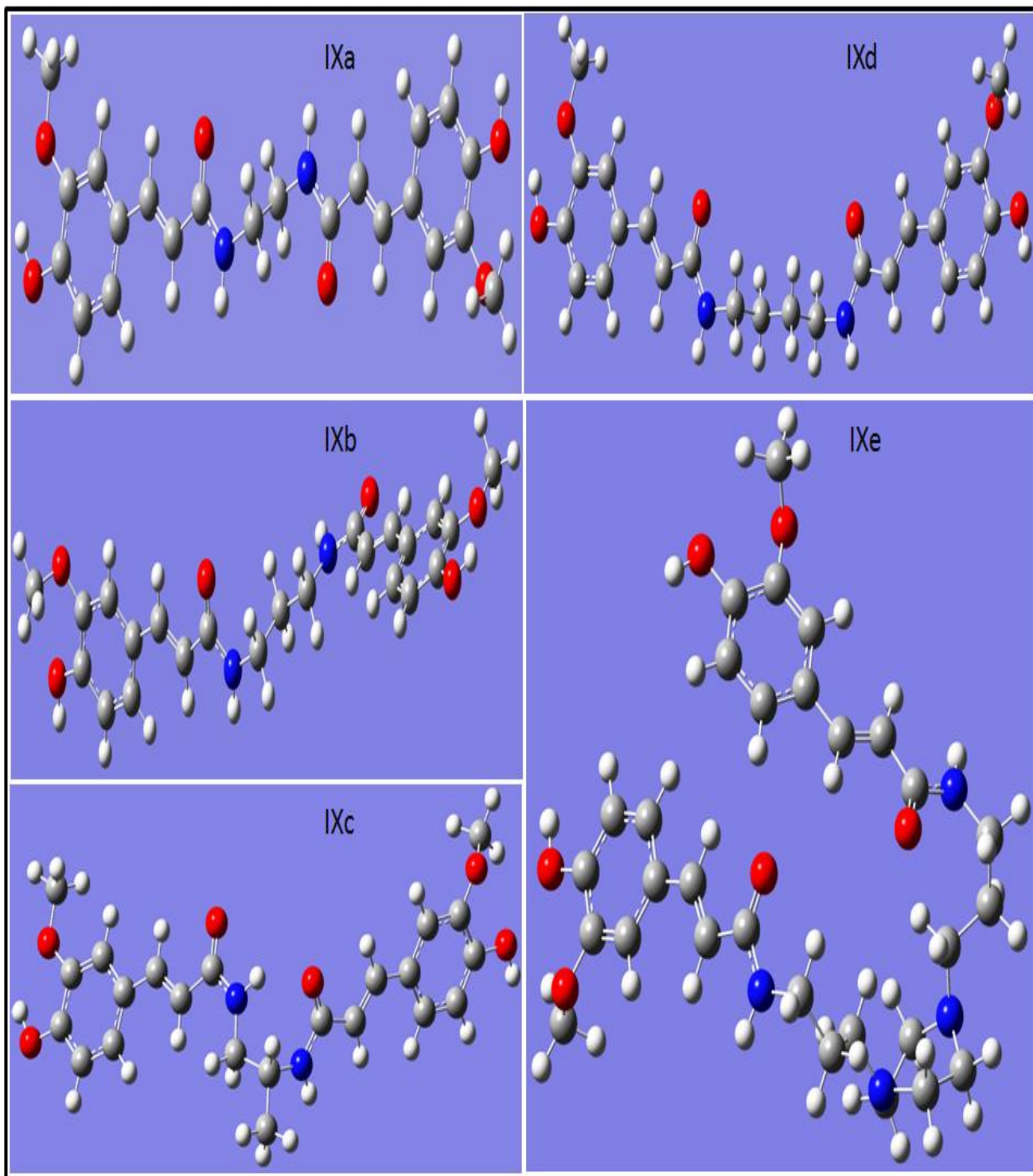


Figure 5.1d

Figure 5.1: Optimized structure of (a) IIIa-IIIo (b) Va-Vg (c) VIIa-VIIg and (d) IXa-IXe at DFT/B3LYP/6-311G** basis set.

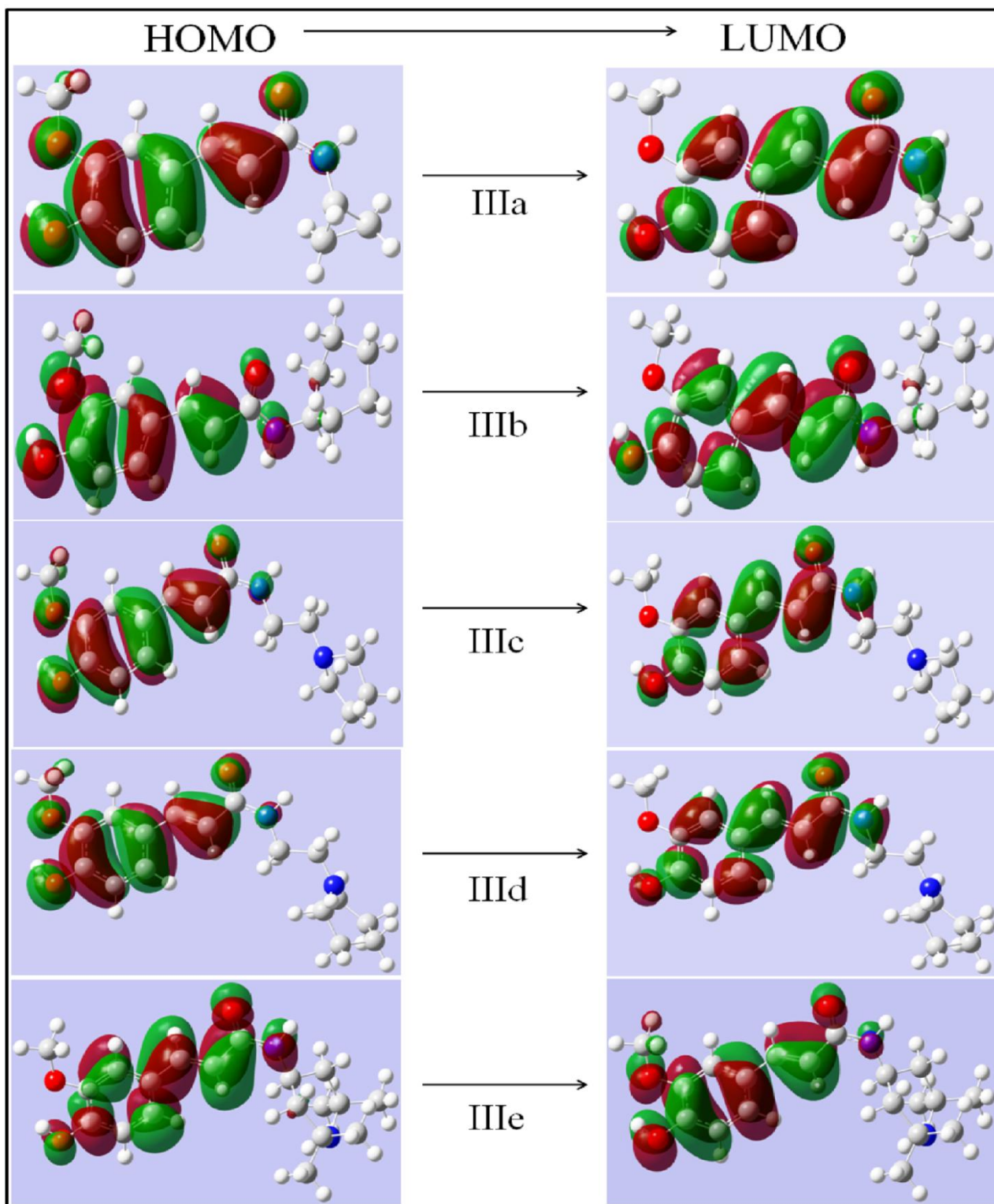


Figure 5.2a

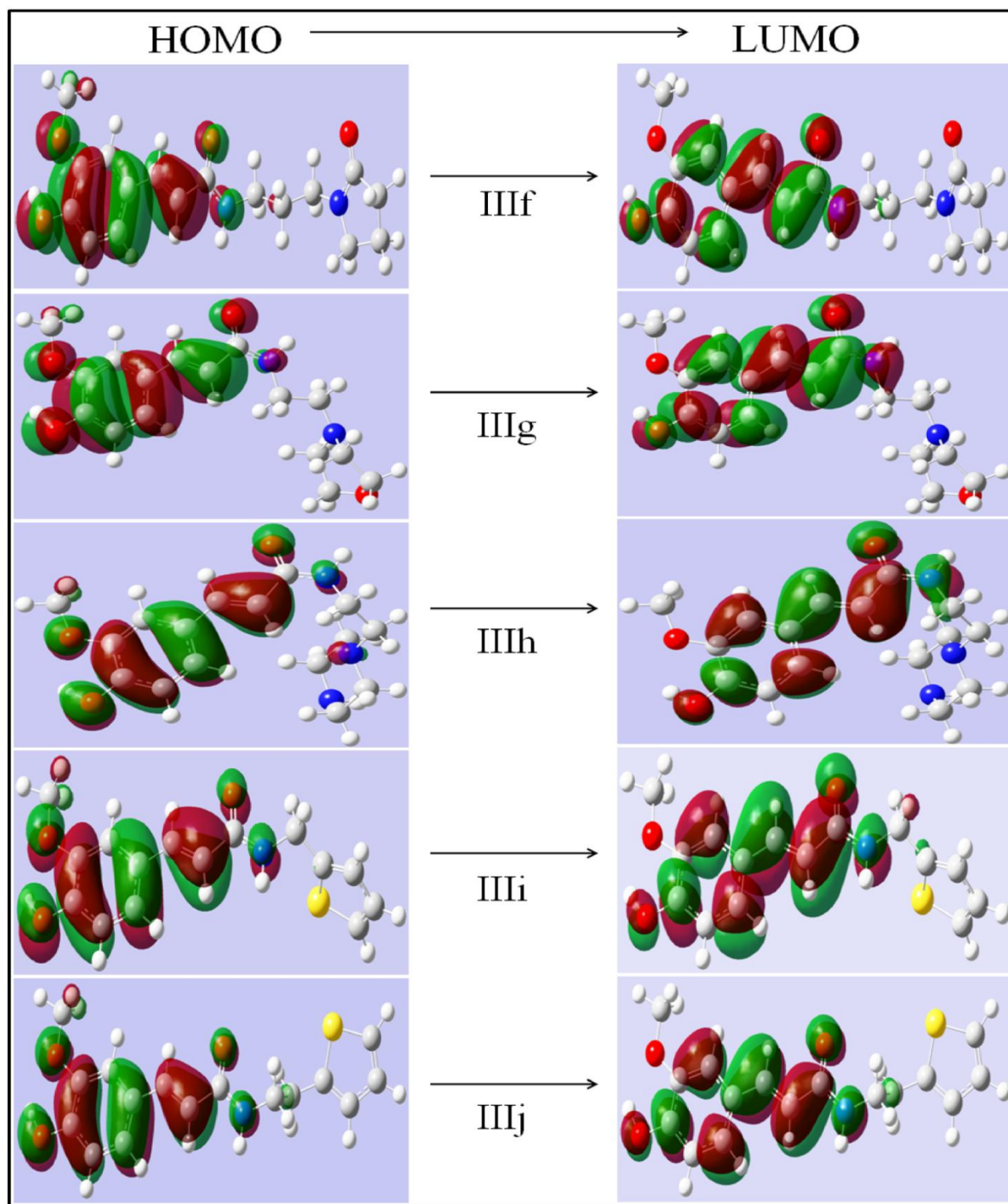


Figure 5.2b

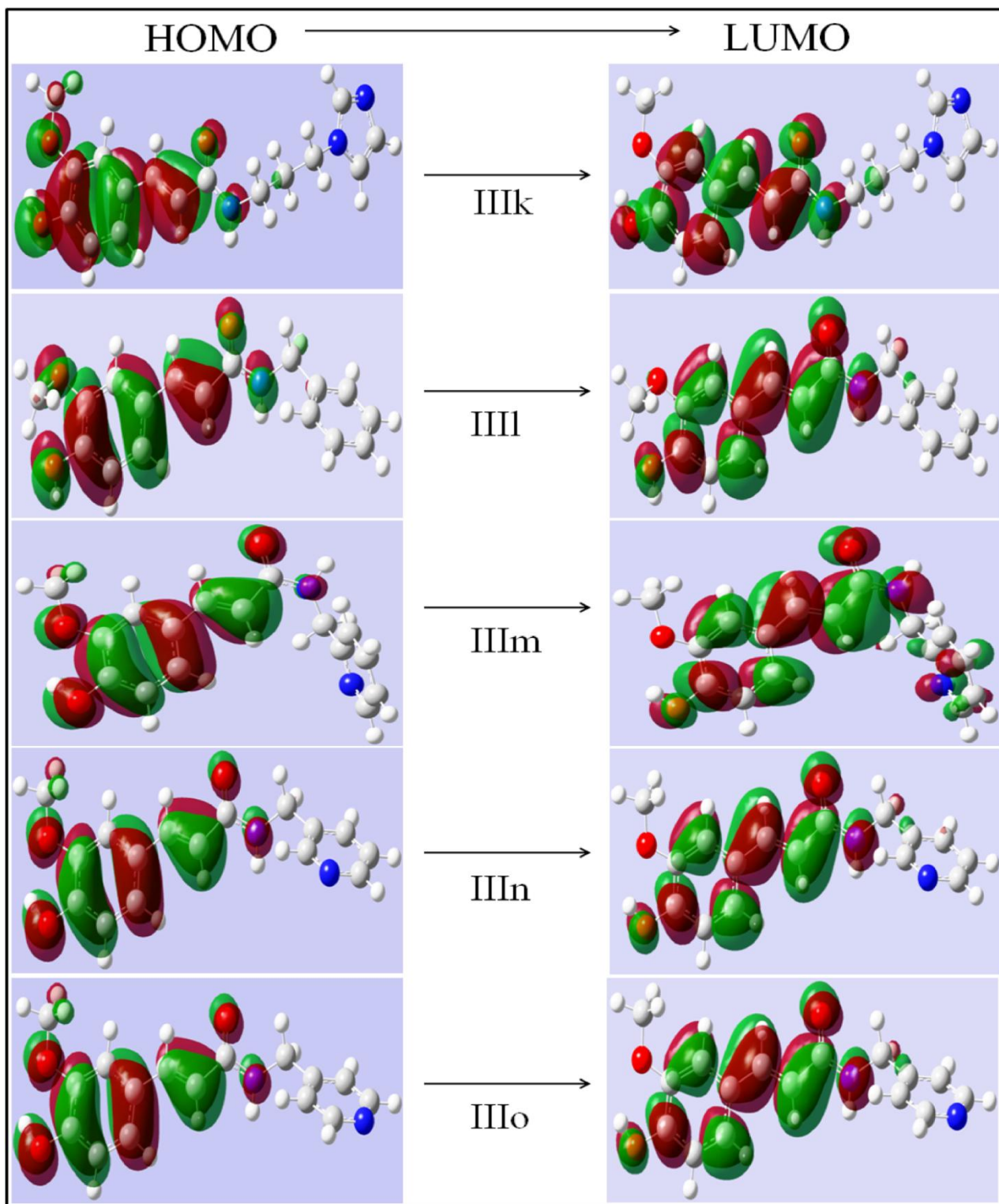


Figure 5.2c

Figure 5.2: Frontier molecular orbitals for optimized geometries of (a) IIIa-IIIe (b) IIIf-IIIk and (c) IIIk-IIIo at DFT/B3LYP/6-311G** basis set.

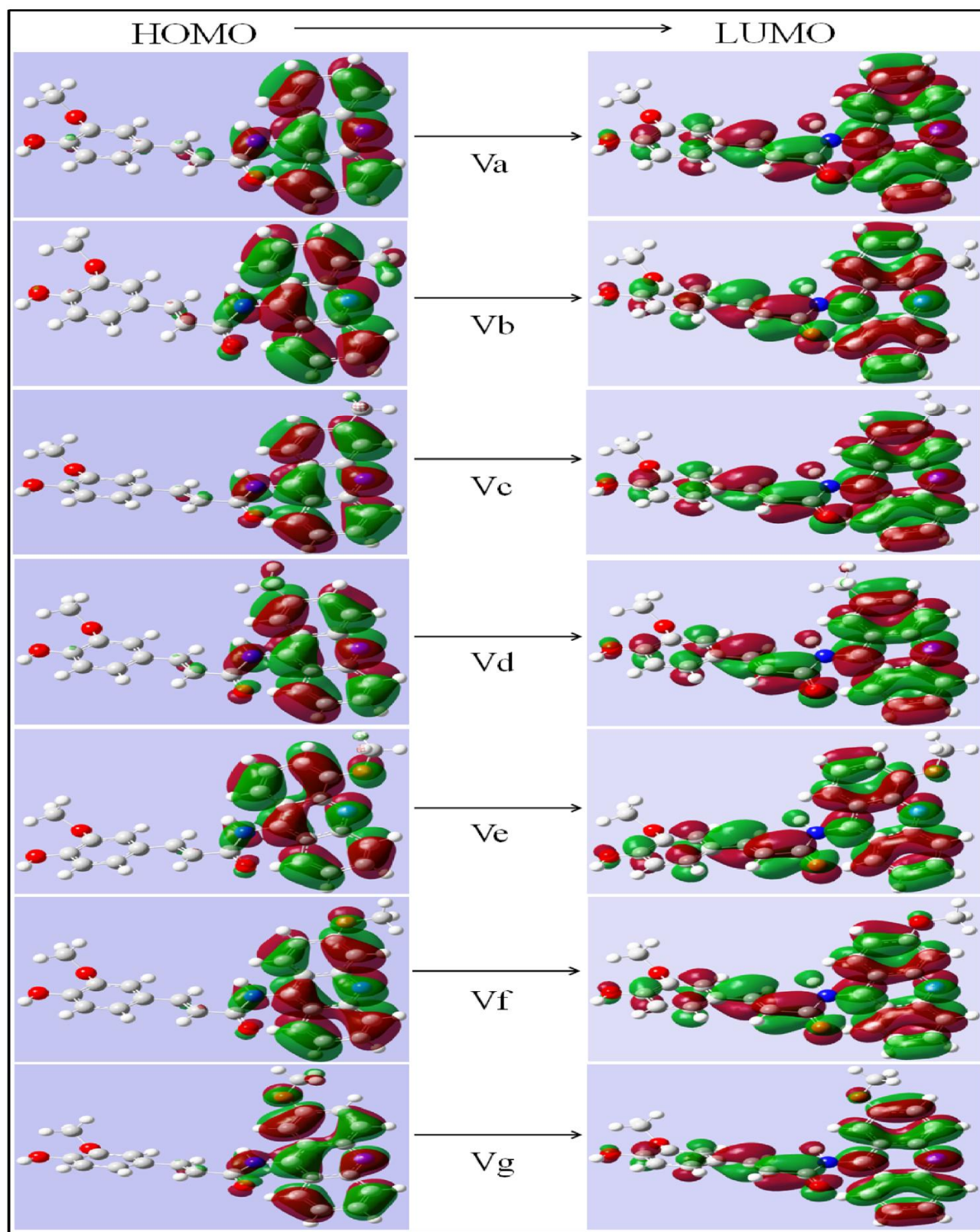


Figure 5.3: Frontier molecular orbitals for optimized geometries of Va-Vg at DFT/B3LYP/6-311G** basis set.

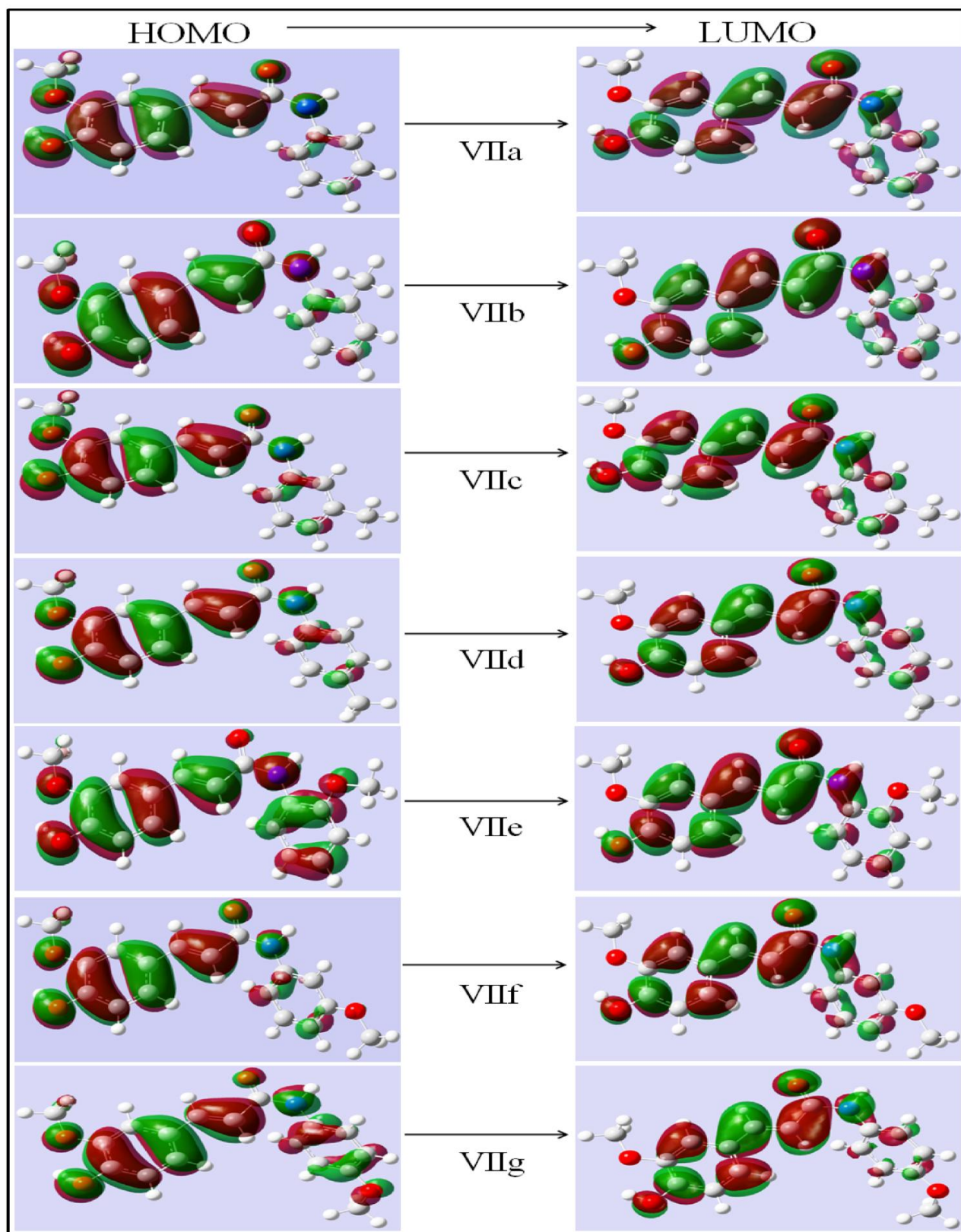


Figure 5.4: Frontier molecular orbitals for optimized geometries of VIIa-VIIg at DFT/B3LYP/6-311G** basis set.

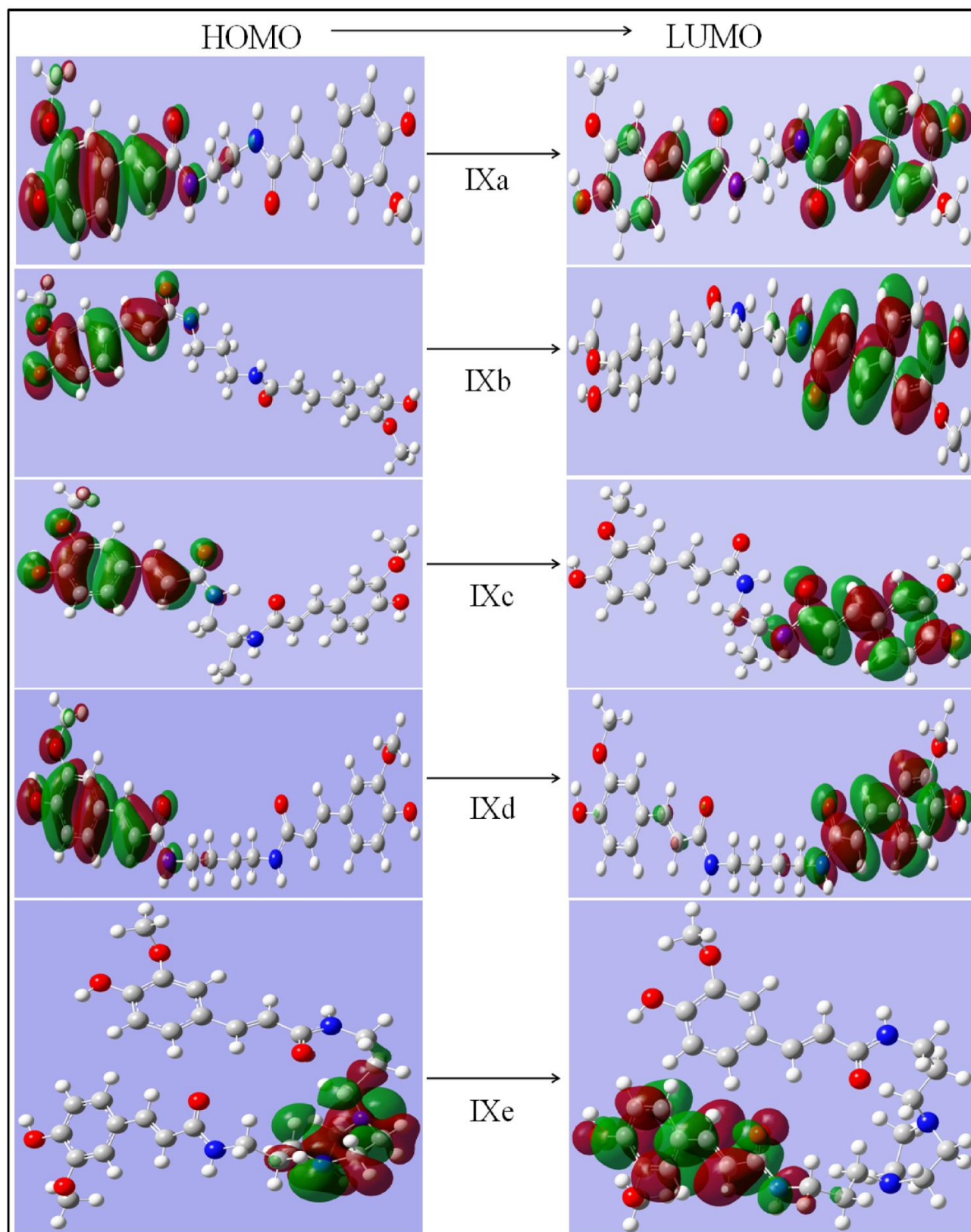


Figure 5.5: Frontier molecular orbitals for optimized geometries of IXa-IXe at DFT/B3LYP/6-311G** basis set.

Compound Name	Total Energy (HF)	Dipole moment (Debye)	E_{HOMO} (eV)	E_{LUMO} (eV)	$E_{\text{HOMO}} - E_{\text{LUMO}}$ (eV)	Chemical potential (eV)	Chemical hardness (eV)	Chemical softness (eV) ⁻¹	Electro-negativity (eV)	Electrophilic index (eV)
IIIa	-785.003	1.459	-5.725	-1.561	-4.163	-3.643	3.643	0.13725	-2.082	0.595
IIIb	-903.008	1.406	-5.722	-1.495	-4.226	-3.609	3.609	0.138562	-2.113	0.619
IIIc	-958.356	1.351	-5.700	-1.515	-4.185	-3.608	3.608	0.1386	-2.093	0.607
III d	-997.675	1.785	-5.717	-1.530	-4.187	-3.624	3.624	0.137988	-2.094	0.605
IIIe	-1076.337	1.614	-5.743	-1.548	-4.195	-3.646	3.646	0.137155	-2.098	0.604
III f	-1071.756	4.365	-5.745	-1.523	-4.221	-3.634	3.634	0.137589	-2.110	0.613
III g	-1033.572	2.437	-5.767	-1.591	-4.176	-3.679	3.679	0.135906	-2.088	0.593
III h	-1013.716	1.382	-5.657	-1.488	-4.168	-3.574	3.573	0.139958	-2.084	0.608
III i	-1259.471	1.462	-5.762	-1.560	-4.201	-3.661	3.661	0.136575	-2.101	0.603
III j	-1298.796	1.942	-5.769	-1.567	-4.202	-3.668	3.668	0.136314	-2.101	0.602
III k	-1011.321	4.937	-5.844	-1.661	-4.182	-3.753	3.752	0.133245	-2.091	0.583
III l	-938.699	5.434	-5.974	-1.594	-4.381	-3.784	3.784	0.132135	-2.191	0.634
III m	-954.746	1.905	-5.745	-1.617	-4.127	-3.681	3.681	0.135833	-2.064	0.578
III n	-954.747	2.492	-5.801	-1.615	-4.185	-3.708	3.708	0.134844	-2.093	0.591
III o	-954.748	3.786	-5.862	-1.687	-4.175	-3.775	3.774	0.132468	-2.088	0.577
Va	-1222.757	6.746	-5.732	-2.313	-3.418	-4.023	4.023	0.124301	-1.709	0.363
Vb	-1262.086	6.305	-5.665	-2.270	-3.395	-3.968	3.968	0.126024	-1.698	0.363
Vc	-1262.085	6.839	-5.671	-2.245	-3.425	-3.958	3.958	0.126326	-1.713	0.371

Vd	-1262.085	6.949	-5.665	-2.243	-3.422	-3.954	3.954	0.126454	-1.711	0.370
Ve	-1337.307	6.327	-5.461	-2.158	-3.302	-3.809	3.809	0.131251	-1.651	0.358
Vf	-1337.313	5.876	-5.606	-2.197	-3.408	-3.902	3.902	0.128156	-1.704	0.372
Vg	-1337.309	6.662	-5.463	-2.219	-3.244	-3.841	3.841	0.130174	-1.622	0.343
VIIa	-899.383	1.634	-5.763	-1.675	-4.088	-3.719	3.719	0.134445	-2.044	0.562
VIIb	-938.710	1.327	-5.743	-1.651	-4.092	-3.697	3.697	0.135245	-2.046	0.566
VIIc	-938.711	1.364	-5.738	-1.649	-4.088	-3.694	3.694	0.135373	-2.044	0.566
VIIId	-938.710	1.650	-5.728	-1.634	-4.094	-3.681	3.681	0.135833	-2.047	0.569
VIIe	-963.542	1.729	-5.267	-1.323	-3.944	-3.295	3.295	0.151745	-1.972	0.590
VIIIf	-963.581	1.431	-5.189	-1.288	-3.901	-3.239	3.239	0.154392	-1.951	0.587
VIIg	-963.523	1.855	-5.295	-1.344	-3.951	-3.319	3.319	0.150625	-1.976	0.588
IXa	-1413.996	4.647	-5.734	-1.581	-4.153	-3.658	3.658	0.136705	-2.077	0.589
IXb	-1453.312	5.607	-5.698	-1.666	-4.031	-3.682	3.682	0.135796	-2.016	0.552
IXc	-1453.317	6.284	-5.606	-1.725	-3.880	-3.665	3.665	0.136407	-1.941	0.513
IXd	-1492.642	4.922	-5.701	-1.523	-4.177	-3.612	3.612	0.138427	-2.089	0.604
IXe	-1838.054	4.215	-4.946	-1.604	-3.341	-3.275	3.275	0.152672	-1.670	0.426
Ferulic acid	-688.153	2.497	-5.882	-1.838	-4.044	-3.860	3.860	0.129534	-2.022	0.529

Table 5.1: Calculated values of total energy, dipole moment, frontier molecular orbitals, electronegativity, chemical potential, chemical hardness, chemical softness, and electrophilic index for ferulic acid amides derivatives at DFT/B3LYP/6-311G** basis set.

In case of compounds **Va-Vg** (Figure 5.3), the charge density in HOMO is moving towards LUMO from the acridine moiety to the ferulic acid unit. This may be the main cause of the higher anticancer activities shown by these compounds compared to other derivatives and ferulic acid. As in all other compounds, the ferulic acid moiety is involved in the formation of HOMO. The same pattern of charge distribution and transfer are seen in **VIIa-VIIg** (Figure 5.4) as noticed in **IIIa-IIIo**. The pattern of transfer of charge density in the bis amide derivatives (**IXa-IXd**) are shows that the charge from -OCH₃ group of one unit of ferulic acid in HOMO is transferring to the other unit of ferulic acid except the -OCH₃ group in case of LUMO. This may be due to the more electron acceptance tendency of aromatic ring as compared to the -OCH₃ group. While in case of **IXe**, HOMO is located entirely on the functional group (present in amine, **Scheme 3.1**) attached to the amide and in case of LUMO it is completely transferred to the one unit of ferulic acid moiety (Figure 5.5). It can be clearly seen from the figures that in all the 34 derivatives -OCH₃ group is taking part in the charge distribution in HOMO position except **Va-Vg** and in LUMO position it is transferred.

5a.4. Concluding remarks

The geometries of all the synthesized amide derivatives of ferulic acid have been fully optimized at DFT/B3LYP/6-311G** basis set. The electronic properties like dipole moment, total energy, electronegativity, chemical hardness, chemical potential chemical softness, electrophilic index and analysis of HOMO-LUMO orbitals have been computed at the same level of basis set. Theoretical studies suggest that structures of all the derivatives are found similar in both gas and solid phases.

5b.1. 3D-Quantitative Structure Activity Relationships (3D-QSAR)

Over last three decades, scientists are working on the designing of compounds which can attenuate the toxic effects on the human as well as environment due to the demand of safer chemicals in medical and agricultural fields. For this goal to be achieved one should go for rational molecular design strategies. These methodologies were first implemented in pharmaceutical and drug design, but in the last decade, they have emerged in areas of bioremediation and engineering risk assessment applications. The structure-function relationships include studies of quantitative-structure activity relationships (QSAR), quantitative structure-toxicity relationships (QSTR) and quantitative structure-property relationships (QSPR) and will be referred to as general QSARs. The QSARs have largely been exploited by industries to expeditiously predict the biological or chemical activity of compounds in the environment and engineered systems based on structural-congeneric compounds of known activity and reactivity. These algorithms assist in elucidating the reaction mechanisms and pathways of organic contaminants in the environment and, accordingly, metabolites can be identified. Thus, the purpose of this section is to describe the nature and benefits of QSARs for understanding and predicting the behavior of newly synthesized derivatives of ferulic acid.

5b.2. Theoretical methods

5b.2.1. 3D-QSAR modeling

The ferulic acid amide derivatives used for 3D-QSAR analysis are provided in the previous chapter of this thesis with their estimated values of biological activities. We have generated five comparative molecular field analysis (CoMFA) models based on the anticancer activities of 21 compounds studied on [i] MCF-7 cell line (breast cancer) [ii] MDA-MB231 cell line (breast cancer) [iii] A549 cell line (lung cancer) [iv] HePG2 cell line (liver cancer) [v] HeLa cell line

(cervical cancer) and one CoMFA model based on the antioxidant activity of 34 compounds. The dependent variables during the generation of CoMFA models was the pIC_{50} values of biological activities exhibited by the synthesized derivatives, which have been calculated from growth inhibition constant (IC_{50}) values ($pIC_{50} = -\log IC_{50}$). SYBYL7.1 (Silicon Graphics Octane2 workstation containing IRIX6.5 operating system) was used for all the simulations or calculations performed during the molecular modeling experiments. As, no biological target for these compounds was identified, the most active compound from each cell line with lowest energy conformer has been considered as a template. A preliminary minimization of the most active compound was carried out using 1000 cycle minimization with the standard Tripos force field to do away with close atom or bad van der Waals contacts. The PM3 method was applied for the final energy minimization step with 0.005 kcal/mol energy gradient convergence criterion. The resulting conformer with the lowest potential energy has been selected as a template for the building of 3D-structures of rest of the compounds. The Gasteiger-Huckel charges have also been assigned to all the compounds during their modeling [Gasteiger et al. 1980].

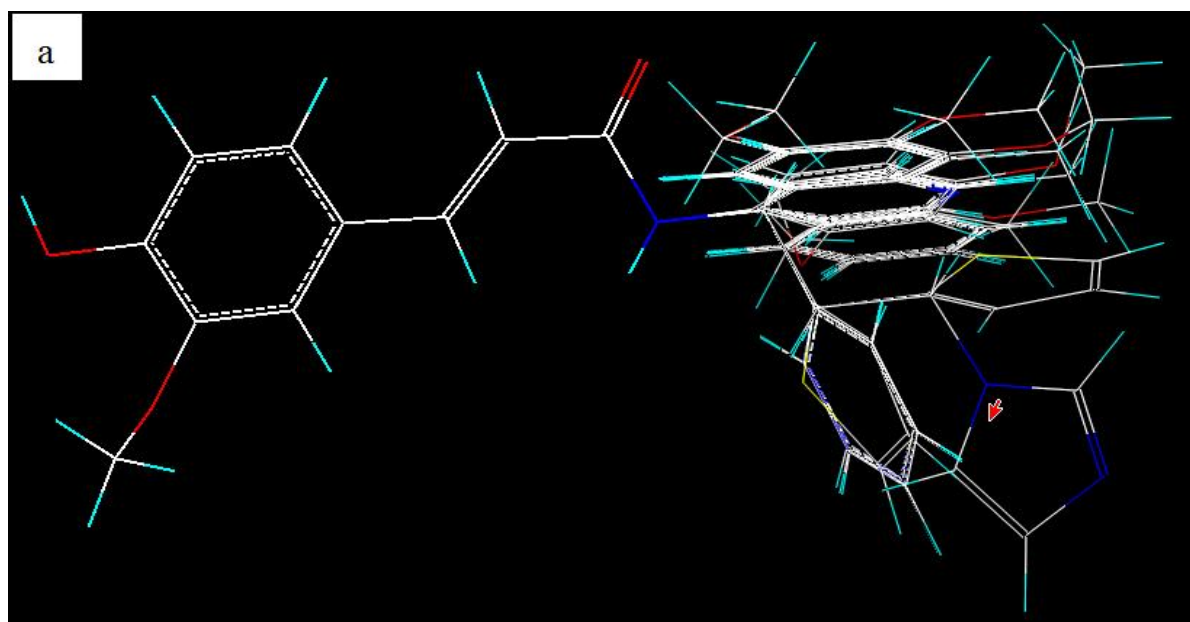


Figure 5.4a

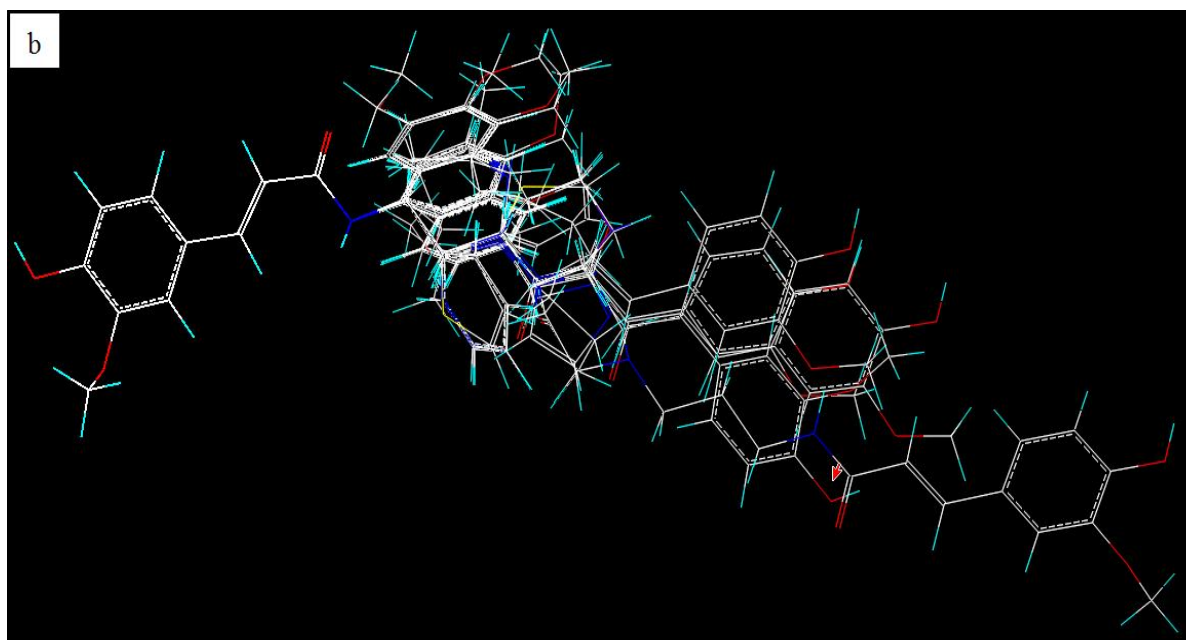


Figure 5.4b

Figure 5.4: Alignment of molecules used for the making of CoMFA model (a) anticancer and (b) antioxidant activities of ferulic acid derivatives.

The training and test set compounds for anticancer models (16 and 5 compounds) and antioxidant model (26 and 8 compounds) was selected randomly. The database alignment method was applied for the alignment of molecules (Figure 5.4a to 5.4b). In the alignment of all molecules, most active compound with lowest energy conformer in each case has been picked as a template. The Comparative Molecular Field Analysis (CoMFA) method was executed for the evaluation of steric and electrostatic fields. All the aligned molecules of training sets have been consigned within a 3-dimensional grid having the spacing of 2.0 Å. The Tripos force field was used for the calculation of van der Waals potential and Coulombic terms for each molecule. The carbon atom with sp^3 hybridization was selected as a probe for the generation of steric (Lennard–Jones potential) and a charge of +1.0 on it to generate electrostatic (Coulomb potential) fields. The energy value of 30.0 kcal/mol was set as default cut-off for the contributions of steric and electrostatic fields. To correlate the CoMFA fields with biological activities of tested compounds,

the Partial Least Square (PLS) analysis was carried out [Cramer et al. 1988; Wold, 1991]. The leave-one-out (LOO) method has been used for the purpose of cross-validation (r^2_{cv}) of data, in order to measure the property of one molecule on the basis of developed model using the data of remaining compounds. A column filter value of 2.0 kcal/mol has been used as a cut-off for all the cross-validation purposes. A 2.0 kcal/mol value for column filter has been used as a cut-off in all the cross-validation purposes. The final CoMFA model has been selected after the non-cross validated (r^2_{ncv}) analysis, due to its high values for (r^2_{cv} , r^2_{ncv}) and small value for standard error of estimation (SEE). In order to evaluate the predictive abilities of the generated models, test set compounds were used which were not included in the training set. The following formula has been used for the predictive correlation (r^2_{pred}):

$$r^2_{pred} = (SD - PRESS)/SD$$

Where; SD is the sum of the squared deviations between the test set biological activities and mean activities of the training set molecules; PRESS is the sum of the squared deviations between the actual and predicted activities of the test compounds [Cramer et al. 1988].

5b.2.2. Statistical analysis

The values of pIC₅₀ for anticancer and antioxidant activities of all the derivatives obtained experimentally and theoretically has been tested statistically for their mathematical significance by using MATLAB R2013a toolbox [Kumar and Bhalla, 2011]. The correlation coefficient (R) value, which measures the potency and direction of a linear association between two variables, was calculated between simulated and experimental data. All the experiments were carried out in triplicate and the mean values were taken for the comparison with the theoretical data.

5b.3. Results and discussion

5b.3.1. Analysis of 3D-QSAR results

A total of six (6) CoMFA models based on the anticancer and antioxidant activities of the compounds on different cell lines were generated. Many models for each cell line were generated and the model having the higher value of external predictive ability has been selected as the best model (Figure 5.5). The summary of statistical analysis for best CoMFA models generated for each case is given in the Table 5.2. The cross-validation coefficient (r^2_{cv}) and the non-cross validation coefficient (r^2_{ncv}) of these models were found to be (i) 0.712 and 0.966 for MCF-7 cell line model (ii) 0.711 and 0.949 for MDA-MB-231 cell line model (iii) 0.858 and 0.991 for A549 cell line model (iv) 0.767 and 0.934 for HepG2 cell line model (v) 0.816 and 0.859 for HeLa cell line model and (vi) 0.583 and 0.903 for anti-oxidant model. The standard error of estimation (SEE) for all the models was found to be significantly low (Table 5.2).

Parameters	Breast (MCF-7)	Breast (MDA-MB-231)	Lung (A549)	Liver (HepG2)	Cervical (HeLa)	Anti-oxidant
r^2_{cv}	0.712	0.711	0.858	0.767	0.816	0.583
r^2_{ncv}	0.966	0.949	0.991	0.934	0.859	0.903
SEE	0.025	0.031	0.011	0.25	0.039	0.044
ONC	4	4	4	3	5	4
r^2_{pred}	0.915	0.822	0.999	0.884	0.0814	0.792
<i>F-value</i>	78.878	51.329	81.318	56.338	85.620	48.960
Field Contributions						
Steric	0.653	0.686	0.524	0.595	0.484	0.592
Electrostatic	0.347	0.314	0.476	0.405	0.516	0.408

Table 5.2: Results of the CoMFA analysis for anticancer and antioxidant activities of ferulic acid derivatives at 2.0 Å grid spacing.

As indicated in the Table 5.3, the predictive correlation coefficient (r^2_{pred}) for all the models was reasonable to suggest that the models are satisfied with good predictive ability. The comparison between experimental and CoMFA generated models values of biological activities of all the compounds from training and test set confirmed their statistical closeness. The linearity of the graphs plotted between the experimental and predicted activities values of the training and test set compounds also indicates that the generated CoMFA models are predictive enough to be used as a guide in the designing of new molecules based on ferulic acid or natural compounds.

The analysis of relative contributions of steric and electrostatic fields for all the models shows that in case of breast cancer, MCF-7 and MDA-MB-231 CoMFA models with significantly high steric contribution were found (~2 times of electrostatic contribution), which indicates that steric interactions are the major contributors towards variation of biological activities of the studied ferulic acid derivatives. This can also be interpreted from contour map analysis, which clearly shows the prominence of steric contribution as compared to the electrostatic one (Figure 5.5a and 5.5b). For the cell lines A549, HePG2 and anti-oxidant models, steric interactions contribute more as compared to electrostatic contribution while, for HeLa model it was found that electrostatic contribution is slightly higher than steric interactions indicating the importance of electrostatic interactions in the variety of biological activities of ferulic acid derivatives. The best selected CoMFA model for MCF-7, green contours were observed near the o-position of the substituted acridine ring and yellow-colored contours were prominent near majority of all other positions of the acridine rings. The green regions indicate that the increasing steric bulk of that position results in enhanced bioactivities of studied compounds and the yellow regions shows that decreasing bulk at those positions results in enhanced bioactivities of studied compounds.

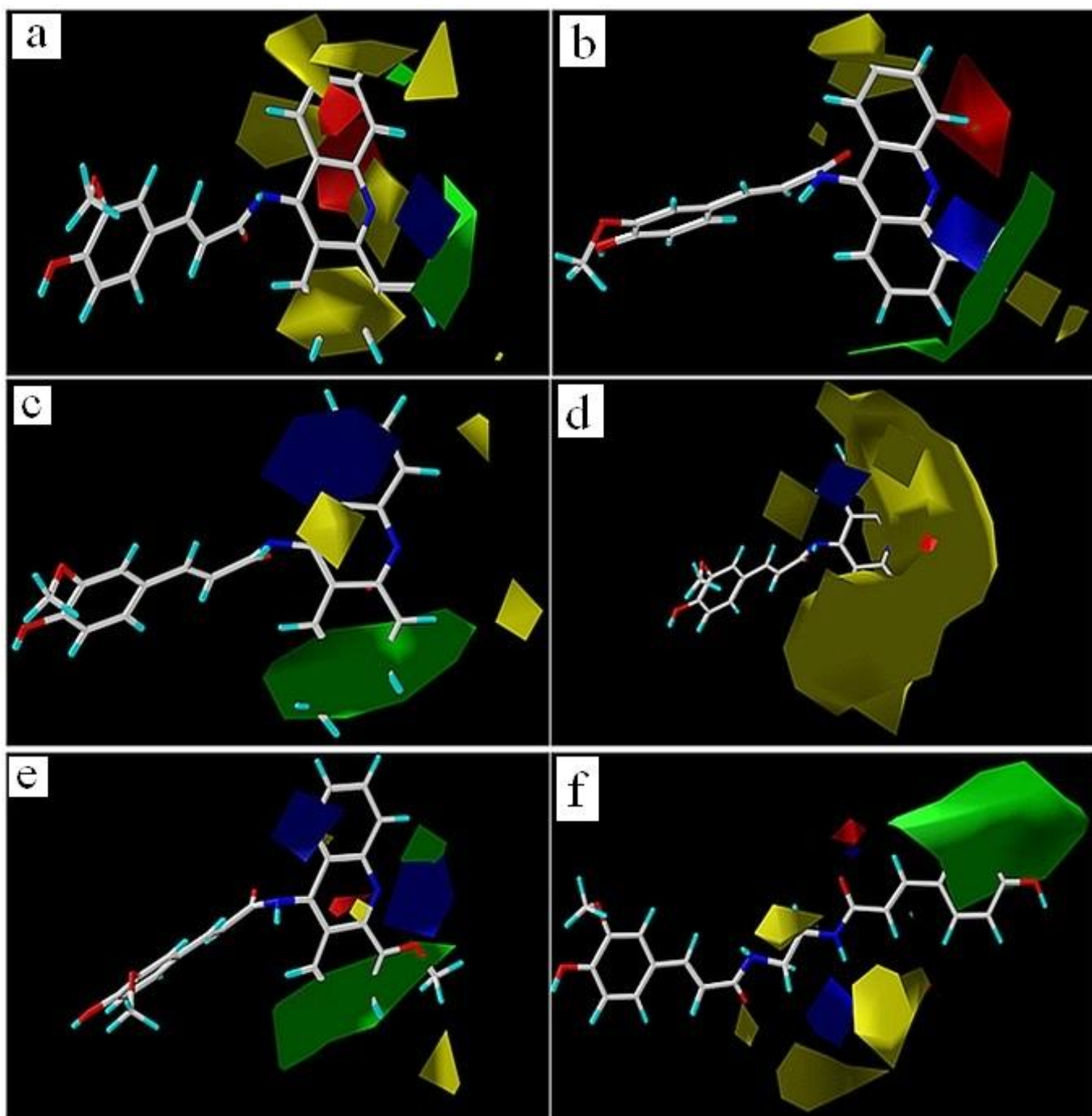


Figure 5.5: STDDEV*COEFF plots of the CoMFA generated steric and electrostatic fields contour maps for (a) MCF-7 (b) MDA-MB-231 (c) A549 (d) HepG2 and (e) HeLa (f) antioxidant models (The most active compound is shown in background). Colour code; Green: sterically favoured, Yellow: sterically disfavoured, Red: negatively charged favoured; and Blue: positively charged favoured regions.

This is an established fact that those compounds with higher pIC50 values have bulky substituents at the o-position of acridine ring and no bulky group was noticed at all other positions of acridine ring. The red and blue regions represent CoMFA electrostatic interaction contour maps. The red contours signify the regions of electron-rich (electronegative) groups presence, resulting in boost up of bioactivity whereas the blue contours corresponds to the regions where an increased positive charge (or decreased negative charge) would results in an improved biological activity. The two small red contours near the central and un-substituted acridine rings were observed while blue contour was observed near the substituted bulky group of acridine ring. On similar lines MDA-MB-231 CoMFA model for breast cancer cell line was analyzed and the green contour was observed near the o-position of acridine ring. A slight disagreement was noticed for the yellow coloured contours, as the number of bulky disfavored regions is less for the MDA-MB-231 model. More importantly in MCF-7 the meta- and para-positions of the substituted acridine ring are demonstrated with yellow contour indicating it as sterically disfavored while the same site is demonstrated with green contours in MDA-MB-231 indicating that at these regions the steric bulk is favored for increasing the biological activity. The similar region in A549 and HeLa models is also demonstrated by green contours indicating that the steric bulk is favored at these regions in these models also (Figure 5.5c and 5.5e). Unlike the breast cancer models, A549 and HeLa models disfavor steric bulk at the ortho position of acridine ring. Moreover, positively charged substituents are favored at the un-substituted acridine ring (indicated by blue contours) of both the models, the effect being more pronounced in case of A549 model. Positively charged substituents are also favored near o-position (towards ferulic acid) of un-substituted acridine ring in A549 and HeLa models (Figure 5.5c and 5.5e). On a comparative scale the negative charge substituents contributes more in the breast cancer cell lines, while in all the other cases very small red contours were noticed. In the HepG2 model steric contribution was found to be relatively higher than

electrostatic contribution (Table 5.3) and the same was also noticed from the contour map analyses (Figure 5.5d). In this model steric bulk is highly disfavored around the acridine ring (as can be seen from the cloud of yellow contour around the acridine ring). Small blue contour around the o-position of the unsubstituted acridine ring, very similar to A549 and HeLa was found, suggesting the importance of the positively charged group at this position. In the anti-oxidant model (Figure 5.5f) green contour around the terminal ring suggests that steric bulk is favored at this position, yellow colour contours around the linker region states that steric bulk is disfavored in this region. Blue contour around the –NH group of linker chain and red contour around the carbonyl group suggests the importance of positively and negatively charged substitutions at these positions.

5b.3.2. Analysis of statistical results

The statistical analysis was done to validate the theoretical and experimental data. The comparison between experimental and simulated values of pIC₅₀ for *in vitro* anticancer and antioxidant activity of all training and test sets molecules used in all the six cases are given in Table 5.3a-d. From the statistical analysis of data, it was found that the value of correlation coefficient (R) for all these cases lies between 0.8699 - 0.9872 in training sets and 0.8554-0.9764 in test sets respectively. The plots for curve fitting analysis are given in Figure 5.6 and Figure 5.7 for training and test set, respectively, which clearly indicates that the theoretical data possesses good correlation with the experimental one. Commenting on the statistical results, we inferred that simulated values of pIC₅₀ lie statistically closed to the values obtained from experimental results and outcome in all the cases to be worthy of respect to their statistical significance for correlation.

Compound Name	Breast (MCF-7)			Compound Name	Breast (MDA-MB-231)		
	pIC ₅₀ (Exp)	pIC ₅₀ (Pred)	Residual		pIC ₅₀ (Exp)	pIC ₅₀ (Pred)	Residual
IIIi	4.907	4.919	-0.012	IIIi	4.955	4.869	0.086
IIIj	5.087	5.090	-0.003	IIIj	4.931	4.946	-0.015
IIIk	4.788	4.804	-0.016	IIIk	4.771	4.799	-0.028
IIIl	4.921	4.928	-0.007	IIIl	4.910	4.881	0.029
IIIm	4.982	4.970	0.012	IIIm	4.884	4.886	-0.002
IIIn	4.917	4.932	-0.015	IIIn	4.875	4.869	0.006
IIIo	4.905	4.902	0.003	IIIo	4.850	4.855	-0.005
Va	5.037	5.038	-0.001	Va	5.052	5.059	-0.007
Vb	5.125	5.109	0.016	Vb	5.137	5.131	0.006
Vc	5.034	5.050	-0.016	Vc	5.116	5.094	0.022
Vd	5.076	5.037	0.039	Vd	5.126	5.070	0.056
Ve	5.011	5.022	-0.011	Ve	5.004	4.999	0.005
Vf	5.093	5.075	0.018	Vf	4.985	5.013	-0.028
Vg	5.090	5.048	0.042	Vg	5.046	5.075	-0.029
VIIa	4.884	4.827	0.057	VIIa	4.897	4.823	0.074
VIIb	4.801	4.814	-0.013	VIIb	4.753	4.775	-0.022
VIIc	4.815	4.851	-0.036	VIIc	4.795	4.825	-0.030
VIIId	4.893	4.917	0.024	VIIId	4.903	4.920	-0.017
VIIe	4.817	4.809	0.008	VIIe	4.768	4.750	0.018
VIIIf	4.781	4.828	-0.047	VIIIf	4.881	4.861	0.020
VIIg	4.791	4.779	0.012	VIIg	4.894	4.894	0.000

Table 5.3a

Compound Name	Lung (A549)			Compound Name	Liver (HepG2)		
	pIC ₅₀ (Exp)	pIC ₅₀ (Pred)	Residual		pIC ₅₀ (Exp)	pIC ₅₀ (Pred)	Residual
IIIi	4.871	4.903	-0.032	IIIi	4.847	4.820	0.027
IIIj	4.872	4.873	-0.001	IIIj	4.894	4.912	-0.018
IIIk	4.917	4.923	-0.006	IIIk	4.838	4.839	-0.001
IIIl	4.914	4.900	0.014	IIIl	4.848	4.817	0.031
IIIm	4.912	4.915	-0.003	IIIm	4.800	4.808	-0.008
IIIn	4.901	4.897	0.004	IIIn	4.832	4.811	0.021
IIIo	4.861	4.860	0.001	IIIo	4.788	4.975	-0.187
Va	5.105	5.115	-0.010	Va	4.975	4.998	-0.023
Vb	5.086	5.101	-0.015	Vb	5.052	4.991	0.061
Vc	5.142	5.130	0.012	Vc	4.990	5.004	-0.014
Vd	5.148	5.147	0.001	Vd	5.081	5.094	-0.013
Ve	5.126	5.120	0.006	Ve	5.017	5.016	0.001
Vf	5.090	5.097	-0.007	Vf	4.996	4.989	0.007
Vg	5.094	5.127	-0.033	Vg	5.028	5.015	0.013
VIIa	5.010	5.029	-0.019	VIIa	4.826	4.877	-0.051
VIIb	5.036	5.030	0.006	VIIb	4.868	4.862	0.006
VIIc	5.038	5.034	0.002	VIIc	4.916	4.906	0.010
VIIId	5.046	5.033	0.013	VIIId	4.956	4.926	0.030
VIIe	4.932	4.934	-0.002	VIIe	4.819	4.797	0.022
VIIIf	4.964	4.992	-0.028	VIIIf	4.885	4.899	-0.014
VIIg	5.020	5.028	-0.008	VIIg	4.876	4.896	-0.020

Table 5.3b

Compound Name	Cervical (HeLa)		
	pIC ₅₀ (Exp)	pIC ₅₀ (Pred)	Residual
IIIi	4.959	4.909	0.050
IIIj	4.918	4.911	0.007
IIIk	4.911	4.921	-0.010
IIIl	4.919	4.901	0.018
IIIm	4.862	4.870	-0.008
IIIn	4.891	4.882	0.009
IIIo	4.801	4.804	-0.003
Va	5.124	5.119	0.005
Vb	5.057	5.091	-0.034
Vc	5.093	5.097	-0.004
Vd	5.137	5.152	-0.015
Ve	5.146	5.136	0.010
Vf	5.046	5.043	0.003
Vg	5.015	5.122	-0.107
VIIa	5.004	4.998	0.006
VIIb	4.962	4.976	-0.014
VIIc	5.011	5.014	-0.003
VII d	5.020	5.015	0.005
VIIe	4.973	4.975	-0.002
VII f	5.005	4.975	0.030
VIIg	5.037	5.033	0.004

Table 5.3c

Compound Name	pIC ₅₀ (Exp)	pIC ₅₀ (Pred)	Residual (Exp-Pred)	Compound Name	pIC ₅₀ (Exp)	pIC ₅₀ (Pred)	Residual (Exp-Pred)
IIIa	4.329	4.404	-0.075	Vc	4.315	4.385	-0.070
IIIb	4.501	4.462	0.039	Vd	4.301	4.342	-0.041
IIIc	4.410	4.403	0.007	Ve	4.452	4.420	0.032
III d	4.440	4.422	0.018	Vf	4.385	4.377	0.008
IIIe	4.325	4.336	-0.011	Vg	4.421	4.370	0.051
III f	4.631	4.634	-0.003	VIIa	4.566	4.528	0.038
III g	4.452	4.428	0.024	VIIb	4.423	4.534	-0.111
III h	4.464	4.438	0.026	VIIc	4.479	4.485	-0.006
III i	4.542	4.541	0.001	VII d	4.458	4.492	-0.034
III j	4.569	4.436	0.133	VII e	4.626	4.644	-0.018
III k	4.368	4.354	0.014	VII f	4.484	4.533	-0.049
III l	4.702	4.587	0.115	VII g	4.561	4.599	-0.038
III m	4.526	4.592	-0.066	IXa	4.735	4.753	-0.018
III n	4.449	4.644	-0.195	IXb	4.697	4.652	0.045
III o	4.594	4.636	-0.042	IXc	4.661	4.656	0.005
Va	4.437	4.391	0.046	IXd	4.680	4.684	-0.004
Vb	4.341	4.370	-0.029	IXe	4.607	4.575	0.032

Table 5.3d

Table 5.3a - 5.3d: pIC₅₀ (experimental and predictive) for all six cases (*In vitro* anticancer and antioxidant activity evaluation).

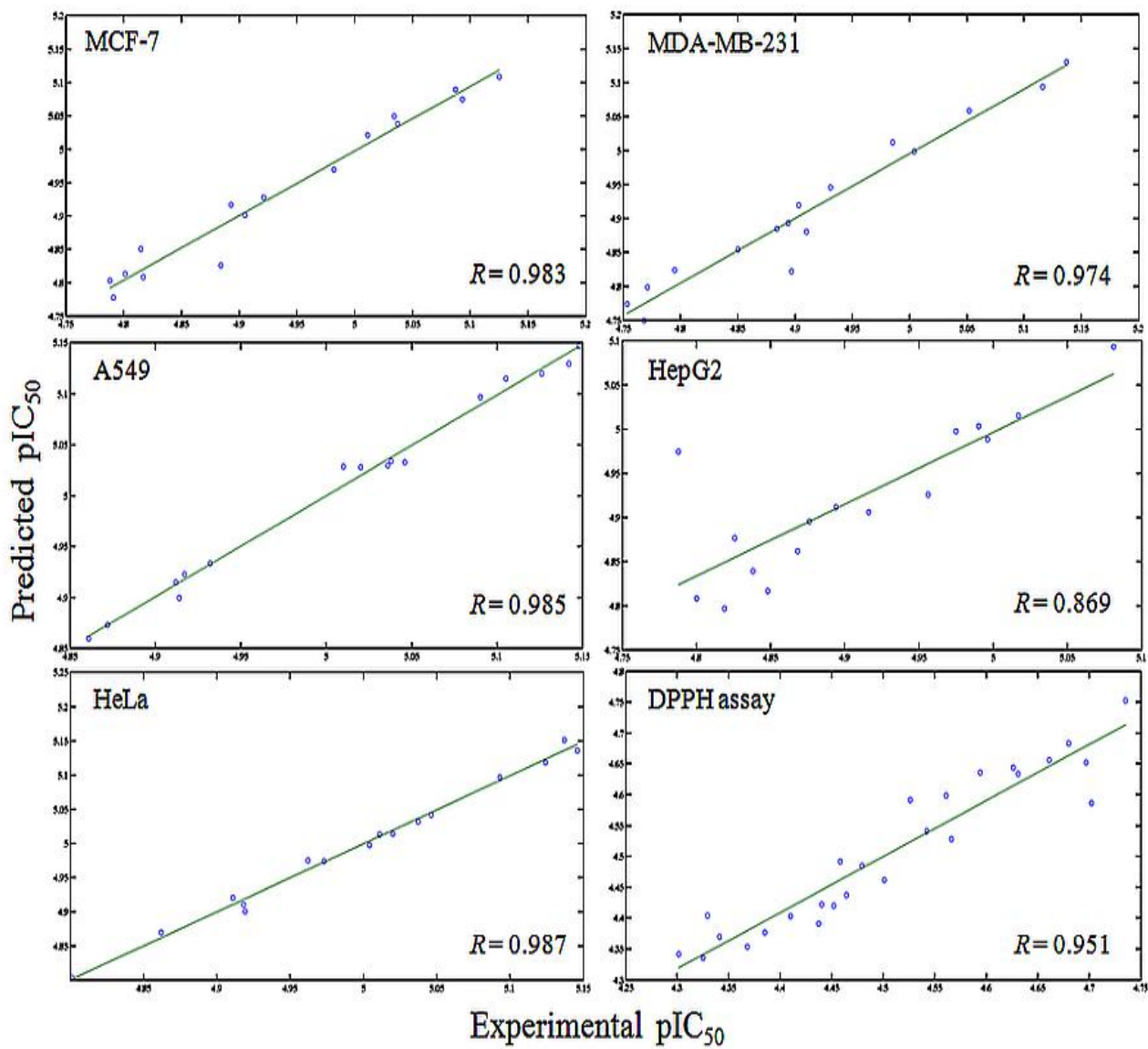


Figure 5.6: Plots of linear correlation between experimental and simulated values of training sets for *in vitro* anticancer and free radical scavenging activity.

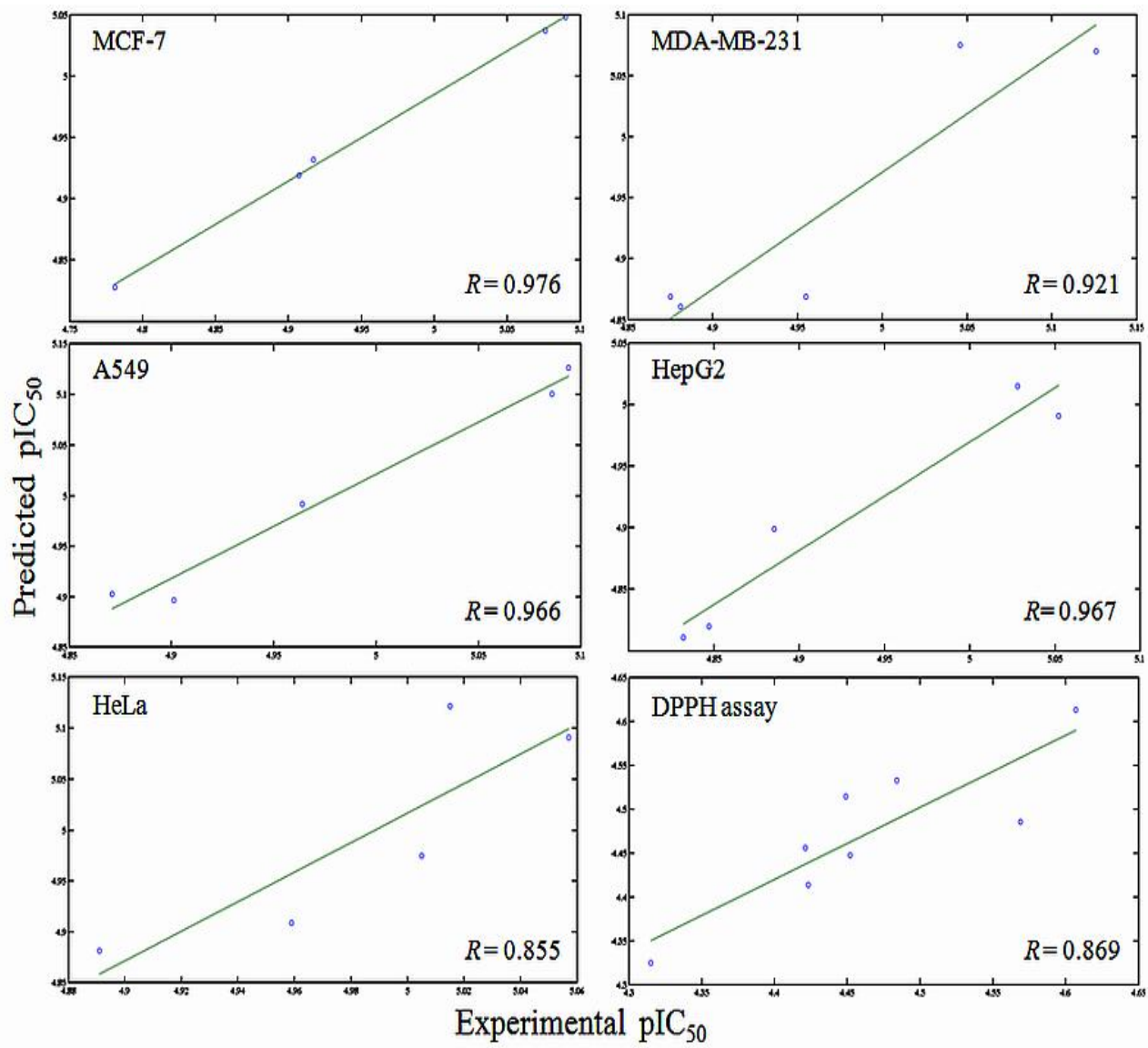


Figure 5.7: Plots of linear correlation between experimental and simulated values of test sets for *in vitro* anticancer and free radical scavenging activity.

5b.4. Concluding remarks

Ferulic acid is an important lead compound for the design of anticancer and antioxidant compounds. It may be envisaged that there is a probable relation between the observed anticancer and antioxidant property of ferulic acid derivatives. To further establish the correlation among the observed IC₅₀ values, QSAR analysis was performed by using the 3D-QSAR-CoMFA method. The six different models were generated (five for anticancer and one for antioxidant) and analyzed. The statistical analysis, contour map analysis, and comparison between steric and electrostatic effects were carried out to understand the structure–activity relationship of ferulic acid derivatives. Analyzing the statistical outcome, we can draw the inference that 3D-QSAR values lie statistically closed to the experimental results for *in vitro* anticancer and antioxidant activity, and data obtained for all the cases found to have significant correlation statistically.

CHAPTER-6

Summary and Future Scope

6.1. Summary

- Starting from an agriculture weed (*Parthenium hysterophorus* L.), three hydroxycinnamic acids (*p*-coumaric, caffeic and ferulic acids) have been extracted and purified.
- Structures of all three acids have been confirmed by elemental analysis, FT-IR, NMR, Mass, and single crystal X-ray crystallography.
- According to thermal study, all acids are stable at room temperature, and decompose at higher temperature.
- Quantum chemical studies have been performed for geometry optimization, computation of structural and electronic properties for *p*-coumaric, caffeic and ferulic acids by means of DFT using Gaussian 09.
- Experimental and theoretical data for structural parameters of *p*-coumaric, caffeic and ferulic acids have been found statistically closed to each other and their structures were found similar both in gas and solvent phase.
- Ferulic acid has selected among the three hydroxycinnamic acids on the basis of its wide variety of biological activities for the synthesis novel of amide derivatives.
- The microwave irradiation synthesis for ferulic acid derivatives has been carried out under solvent free conditions.
- The molecules were synthesized in good yield percentage (80-98%) within 3-10 min of time.

- All the derivatives were fully characterized by elemental analysis, FT-IR, NMR and Mass spectroscopic techniques.
- The derivatives have been screened for the anticancer and antioxidant activity.
- The acridine moiety containing molecules (**Va-Vg**) showed the best activity during MTT assay, and most of the derivatives were found to possess better antioxidant activity as compared to ferulic acid.
- The geometries of all the derivatives were fully optimized, and electronic parameters were computed.
- The 3D-QSAR modeling was carried out for antioxidant and anticancer activity of ferulic acid amide derivatives by CoMFA.
- The biological values were found statistically similar to the computed values.

6.2. Future Scope

With reference to the present work done and targets achieved, some important aspects have been suggested for future. The suggested work for future could not be done due to time constraints and limitation of the work plan for Ph.D studies. The following suggestions are made in this regard:

- As *Parthenium hysterophorus* is an agriculture alien weed, the other phenolic acids and useful compounds present in it can be extracted as natural products, and used for biomedical and industrial applications.
- New derivatives based on *p*-coumaric and caffeic acids can be synthesized and used accordingly.
- The amide derivatives synthesized here can be tested by *in vivo* methods, so that they can be used as an anticancer drug.
- The targets for these compounds can be searched, and virtual screening can also be performed, accordingly.
- Other types of ferulic acid derivatives like esters, halides, amides and many more can also be synthesized based on the given parameters.

Bibliography

- 1) Akihisa, T., Yasukawa, K., Yamaura, M., Ukiya, M., Kimura, Y., Shimizu, N., Arai, K. (2000) Triterpene Alcohol and Sterol Ferulates from Rice Bran and Their Anti-inflammatory Effects. *J Agric Food Chem.*, 48:2313-2322.
- 2) Alam, M.A., Sernia, C., Brown, L. (2013) Ferulic acid improves cardiovascular and kidney structure and function in hypertensive rats. *J Cardiovascular Pharmacol.*, 61:240-248.
- 3) An, S.M., Lee, S.I., Choi, S.W., Moon, S.W., Boo, Y.C. (2008) *p*-coumaric acid not only inhibits human tyrosinase activity in vitro but also melanogenesis in cells exposed to UVB. *Br J dermatol.*, 159:292-299.
- 4) Anvar, U.B., Mazza, G. (2009) Extraction and purification of ferulic acid from flax shives, wheat and corn bran by alkaline hydrolysis and pressurised solvents. *Food Chem.*, 115:1542-1548.
- 5) Aragno, M., Parola, S., Tamagno, E., Brignardello, E., Manti, R., Danni, O., Boccuzzi, G. (2000) Oxidative derangement in rat synaptosomes induced by hyperglycaemia: restorative effect of dehydroepiandrosterone treatment. *Biochem Pharmacol.*, 60:389-395.
- 6) Arora, A., Tamm, L.K. (2001) Biophysical approaches to membrane protein structure determination. *Curr Opin Struct Biol.*, 11:540-547.
- 7) Ashish, Solanki, A.K., Boone, C.D., Krueger, J.K. (2010) Global structure of HIV-1 neutralizing antibody IgG1 b12 is asymmetric. *Biochem Biophys Res Commun.*, 391:947-951.

- 8) Ashok, M., Holla, B.S., Poojary, B. (2007) Convenient one pot synthesis and antimicrobial evaluation of some new Mannich bases carrying 4-methylthiobenzyl moiety. *Eur J Med Chem.*, 42:1095-1101.
- 9) Balasubashini, M.S., Rukkumani, R., Viswanathan, P., Menon, V.P. (2004) Ferulic acid alleviates lipid peroxidation in diabetic rats. *Phytother Res.*, 18:310-314.
- 10) Barone, E., Calabrese, V., Mancuso, C. (2009) Ferulic acid and its therapeutic potential as a hormetin for age-related diseases. *Biogerontology.*, 10:97-108.
- 11) Basoglu, S., Yolal, M., Demirci, S., Demirbas, N., Bektas, H., Karaoglu, S.A. (2013) Design, synthesis and antimicrobial activities of some azole derivatives. *Acta. Pol. Pharm.*, 70:229-236.
- 12) Becke, A.D. (1993) Density functional thermochemistry. III. The role of exact exchange. *J Chem Phys.*, 98:5648-5652.
- 13) Blois, M.S. (1958) Antioxidant Determinations by the Use of a Stable Free Radical. *Nature*, 181:1199-1200.
- 14) Blume, G. (2013) Novel Carrier System for the Transport of Active Substances into the Skin. US Patent: 20,130,011,455.
- 15) Bodini, S.F., Manfredini, S., Epp, M., Valentini, S., Santori, F. (2009) Quorum sensing inhibition activity of garlic extract and *p*-coumaric acid. *Lett Appl Microbiol.*, 49:551-555.
- 16) Bors, W., Michel, C., Schikora, S. (1995) Interaction of flavonoids with ascorbate and determination of their univalent redox potentials: a pulse radiolysis study. *Free Radic Biol Med.*, 19:45-52.
- 17) Bourne, L.C., Rice-Evans, C. (1998) Bioavailability of ferulic acid. *Biochem Biophys Res Comm.*, 253:222-227.

- 18) Boven, M.V., Toppet, S., Cokelaere, M.M., Daenens, P. (1994) Isolation and structural identification of a new simmondsin ferulate from jojoba meal. *J Agric Food Chem.*, 42:1118-1121.
- 19) Brandenburg, K. (1999) DIAMOND: Visual Crystal Structure Information System. Version 2.1c. Crystal Impact GbR, Bonn, Germany.
- 20) Chang, M.X., Xu, L.Y., Tao, J.S., Feng, Y. (1993) Metabolism and pharmacokinetics of ferulic acid in rats. *Zhongguo Zhong Yao Za Zhi* 8:300-302.
- 21) Chesson, A., Provan, G.J., Russell, W.R., Scobbie, L., Richardson, A.J., Stewart, C. (1999) Hydroxycinnamic acids in the digestive tract of livestock and humans. *J Sci Food Agric.*, 79:373-378.
- 22) Cho, J.Y., Kim, H.S., Kim, D.H., Yan, J.J., Suh, H.W., Song, D.K. (2005) Inhibitory effects of long-term administration of ferulic acid on astrocyte activation induced by intracerebroventricular injection of β -amyloid peptide (1-42) in mice. *Prog Neuropsychopharmacol Biol Psychiatry.*, 29:901-907.
- 23) Chung, S.Y., Champagne, E.T. (2011) Ferulic acid enhances IgE binding to peanut allergens in Western blots. *Food Chem.*, 124:1639-1642.
- 24) Clifford, M.N. (1999) Chlorogenic acids and other cinnamates—nature, occurrence and dietary burden. *J Sci Food Agric.*, 79:362-372.
- 25) Cramer, R.D., Patterson, D.E., Bunce, J. D. (1988) Comparative molecular field analysis (CoMFA). 1. Effect of shape on binding of steroids to carrier proteins. *J Am Chem Soc.*, 110:5959-5967.
- 26) Cramer, R.D., Bunce, J.D., Patterson, D.E., Frank, I. E. (1988) Crossvalidation, Bootstrapping, and Partial Least Squares Compared with Multiple Regression in Conventional QSAR Studies. *Quant. Struct. Act. Relat.*, 7:18-25.

- 27) Crozier, A., Jaganath, I.B., Clifford, M.N. (2009) Dietary phenolics: chemistry, bioavailability and effects on health. *Nat Prod Rep.*, 26:1001-1043.
- 28) Devi, S., Sharma, N., Savitri, Bhalla T.C. (2013) Comparative analysis of amino acid sequences from mesophiles and thermophiles in respective of carbon–nitrogen hydrolase family. *3 Biotech.*, 3:491-507.
- 29) Dougherty, T.J., Pandey, R.K. (1991) US 4968715, *Chem. Abstr.* 115:150376.
- 30) Dorn, S., Pfeifer, A., Schlufte, K., Heinze, T. (2010) Synthesis of water-soluble cellulose esters applying carboxylic acid imidazolides. *Polymer Bulletin.*, 64:845-854.
- 31) Dutt, S. (1925) General synthesis of α -unsaturated acids from malonic acid. *Quart J Chem Soc.*, 1: 297-301.
- 32) Ergün, B.C., Çoban, T., Onurdag, F.K., Banoglu, E. (2011) Synthesis, antioxidant and antimicrobial evaluation of simple aromatic esters of ferulic acid. *Arch Pharm Res.*, 34:1251-1261.
- 33) Ferguson, L.R., Shuotun, Z., Harris, P.J. (2005) Antioxidant and antigenotoxic effects of plant cell wall hydroxycinnamic acids in cultured HT-29 cells. *Mol Nutr Food Res.*, 49:585-593.
- 34) Ferhat, M., Ghorab, H., Laggoune, S., Ghannadi, A., Sajjadi, S.E., Touzani, R., Kabouche, A., Kabouche Z. (2014) Composition and Antioxidant Activity of the Essential Oil of *Thymus dreatensis* from Algeria. *Chem. Nat. Comp.*, 50:747-749.
- 35) Frisch, M.J. et al. (2009) Gaussian 09, Revision A.1, Wallingford, CT.
- 36) Gasteiger, J., Marsili, M. (1980) Iterative partial equalization of orbital electronegativity—a rapid access to atomic charges. *Tetrahed.*, 36:3219-3228.
- 37) Gorewit, R.C. (1983) Pituitary and thyroid hormone responses of heifers after ferulic acid administration. *J Dairy Sci.*, 66:624-633.

- 38) Gowri, G., Bugos, R.C., Campbell, W.H., Maxwell, C.A., Dixon, R.A. (1991) Stress responses in alfafa (*Medicago Sativa* L.). X. Molecular cloning and expression of s-adenosyl-L-methionine: caffeic acid 3-O-methyltransferase, a key enzyme of lignin biosynthesis. *Plant Physiol.*, 97:7-14.
- 39) Graf, E. (1992) Antioxidant potential of ferulic acid. *Free Radical Biol Med.*, 3:435-448.
- 40) Graybill, T.L., Ross, M.J., Gauvin, B.R., Gregory, J.S., Harris, A.L., Ator, M.A., Rinker, J.M., Dolle, R.E. (1992) Synthesis and evaluation of azapeptide-derived inhibitors of serine and cysteine proteases. *Bioorg. Med. Chem. Lett.*, 2:1375-1380.
- 41) Gunaseelan, V.N. (1987). Parthenium as an additive with cattle manure in biogas production. *Biol Wastes.*, 21:195-202.
- 42) Guo, T., Sun, Y., Sui, Y., Li, F. (2003) Determination of ferulic acid and adenosine in *Angelicae radix* by micellar electrokinetic chromatography. *Anal Bioanal Chem.*, 375:840-843.
- 43) Hagedorn, S., Kaphammer, B. (1994) Microbial biocatalysis in the generation of flavor and fragrance chemicals. *Annu Rev Microbiol.*, 48:773-780.
- 44) Häring, H.U., Merker, L., Seewaldt-Becker, E., Weimer, M., Meinicke, T., Woerle, H.J., Broedl, U.C. (2013) mpagliflozin as add-on to metformin plus sulfonylurea in patients with type 2 diabetes: a 24-week, randomized, double-blind, placebo-controlled trial. *Diabetes Care.*, 36:3396-3404.
- 45) Harris, P.J., Hartley, R.D. (1980) Phenolic constituents of the cell walls of monocotyledons. *Biochem Syst Ecol.*, 8:153-160.
- 46) Hartley, R.D., Ford, C.W. (1989) Phenolic constituents of plant cell walls and wall degradability, in: Lewis, N. G., Paice, M. G. (Eds.), *Plant Cell Wall Polymers Biogenesis and Biodegradation*, American Chemical Society, Washington DC:137-145.

- 47) Hartley, R.D., Harris, P.J. (1981) Phenolic constituents of the cell walls of dicotyledons. *Biochem Sys Ecol.*, 9:189-203.
- 48) Hegab, M.I., Abdel-Fattah, A.S., Yousef, N.M., Nour, H.F., Mostafa, A.M., Ellithey, M. (2007) Synthesis, X-ray structure, and pharmacological activity of some 6,6-disubstituted chromeno[4,3-b]- and chromeno- [3,4-c]-quinolines. *Arch Pharm.*, 340:396-403.
- 49) Herrmann, K. (1989) Occurrence and content of hydroxycinnamic and hydroxybenzoic acid compounds in foods. *CRC Crit Rev Food Sci Nutr.*, 28:315-347.
- 50) Herrmann, K. (1990) Significance of hydroxycinnamic compounds in food. I. Antioxidant activity-effects on the use, digestibility, and microbial spoilage in food. *Chem Mikrobiol Technol Lebensm.*, 12:137-144.
- 51) Hirose, M., Takahashi, S., Ogawa, K., Futakuchi, M., Shirai, T. (1999) Phenolics: blocking agents for heterocyclic amine-induced carcinogenesis. *Food Chem Toxicol.*, 37:985-992.
- 52) Hlasiwetz, H., Barth, L. (1866) Mittheilungen aus dem chemischen Laboratorium in Innsbruck I, Ueber einige Harze [Zersetzungsproducte derselben durch schmelzendes Kali]. *Liebig's Annalen der Chemie.*, 138:61-76.
- 53) Hohenberg, P., Kohn, W. (1964) Inhomogeneous Electron gas. *Phys. Rev.*, 136:B864-B871.
- 54) Holla, B.S., Rao, B.S., Sarojini, Holla, B.K., Akberali, P.M., Kumari, N.S. (2006) Synthesis and studies on some new fluorine containing triazolothiadiazines as possible antibacterial, antifungal and anticancer agents. *Eur J Med Chem.*, 41:657-663.
- 55) Hosoda, A., Ozaki, Y., Kashiwada, A., Mutoh, M., Wakabayashi, K., Mizuno, K., Nomura, E., Taniguchi, H. (2002) Syntheses of ferulic acid derivatives and their suppressive effects on cyclooxygenase-2 promoter activity. *Bioorg Med Chem.*, 10:1189-1196.
- 56) Hua, D., Ma, C., Song, L., Lin, S., Zhang, Z., Deng, Z., Xu, P. (2007) Enhanced vanillin production from ferulic acid using adsorbent resin. *Appl Microbiol Biotechnol.*, 74:783-790.

- 57) Huang, H.M., Johanning, G.L., O'Dell, B.L. (1986) Phenolic acid content of food plants and possible nutritional implications. *J Agric Food Chem.*, 34:48-51.
- 58) Huang, G.Y., Cui, C., Wang, Z.P., Li, Y.Q., Xiong, L.X., Wang, L.Z., Yu, S.J., Li, Z.M., Zhao, W.G. (2013) Synthesis and characteristics of (Hydrogenated) ferulic acid derivatives as potential antiviral agents with insecticidal activity. *Chem Cent J.*, 7:1-12.
- 59) Hudson, E.A., Dinh, P.A., Kokubun, T., Simmonds, M.S., Gescher, A.C. (2000) Characterization of potentially chemopreventive phenols in extracts of brown rice that inhibit the growth of human breast and colon cancer cells. *Cancer Epidemiol Biomarkers Prev.*, 9:1163-1170.
- 60) Kanski, J., Aksenova, M., Stoyanova, A., Butterfield, D.A. (2002) Ferulic acid antioxidant protection against hydroxyl and peroxy radical oxidation in synaptosomal and neuronal cell culture systems in vitro: structure-activity studies. *J Nutr Biochem.*, 13:273-281.
- 61) Kanwar, R., Sharma N., Bhalla T.C. (2012) Computational Analysis of Amino Acid Sequences in Relation to Thermostability of Interspecific Nitrile Degrading Enzyme (Amidase) from Various Thermophiles/Hyperthermophiles. 1:556 doi:10.4172/scientificreports.556.
- 62) Karakaya, S. (2004) Bioavailability of Phenolic Compounds. *Crit Rev Food Sci Nutr.*, 44:453-464.
- 63) Kategaonkar, A.H., Sonar, S.S., Shelke, K.F., Shingate, B.B., Shingare M.S. (2010) Ionic liquid catalyzed multicomponent synthesis of 3, 4-dihydro-3-substituted-2H-naphtho [2, 1-e][1, 3] oxazine derivatives. *Org. Commun.*, 3:1-7.
- 64) Kaundal, R.K., Sharma, S.S. (2010) Peroxisome proliferator-activated receptor gamma agonists as neuroprotective agents. *Drug News Perspect.*, 23:241-256.

- 65) Kawai, S., Ando, Y., Iyata, Y. (1990) Cosmetics containing anthocyanin-type pigments and the color stabilizer ferulic acid. *Japan Kokai.*, 89:647-692.
- 66) Kern, S.M., Bennett, R.N., Needs, P.W., Mellon, F.A., Kroon, P.A., Garcia-Conesa, M.T. (2003b) Characterization of metabolites of hydroxycinnamates in the in vitro model of human small intestinal epithelium caco-2 cells. *J Agric Food Chem.*, 51:7884-7891.
- 67) Khanduja, K.L., Avti, P.K., Kumar, S., Mittal, N., Sohi, K.K., Pathak, C.M. (2006) Anti-apoptotic activity of caffeic acid, ellagic acid and ferulic acid in normal human peripheral blood mononuclear cells: a Bcl-2 independent mechanism. *Biochim Biophys Acta.*, 1760:283-289.
- 68) Kikugawa, K., Hakamada, T., Hasunuma, M., Kurechi, T. (1983) Reaction of *p*-hydroxycinnamic acid derivatives with nitrite and its relevance to nitrosamine formation. *J Agric Food Chem.*, 1:780-785.
- 69) Kikuzaki, H., Hisamoto, M., Hirose, K., Akiyama, K., Taniguchi, H. (2002) Antioxidant properties of ferulic acid and its related compounds. *J Agric Food Chem.*, 50:2161-2169.
- 70) Kim, K.H., Tsao, R., Yang, R., Gnu, S.W. (2006) Phenolic acid profiles and antioxidant activities of wheat bran extracts and the effect of hydrolysis conditions. *Food Chem.*, 95:466-473.
- 71) King, C., Tang, W., Ngui, J., Tephly, T., Braun, M. (2001) Characterization of rat and human UDP-glucuronosyltransferases responsible for the in vitro glucuronidation of diclofenac. *Toxicol Sci.*, 61:49-53.
- 72) Koopmans, T. (1934) About the allocation of wave functions and eigenvalues of the individual electrons one atom. *Physica.*, 1:104-113.
- 73) Kulik, T.V., Lipkovska, N.A., Barvinchenko, V.N., Palyanytsya, B.B., Kazakova, O.A., Dovbiy, O.A., Pogorelyi, V.K. (2009) Interactions between bioactive ferulic acid and fumed

- silica by UV-Vis spectroscopy, FT-IR, TPD MS investigation and quantum chemical methods. *J Colloid Interface Sci.*, 339:60-68.
- 74) Kumar, N., Pruthi, V. (2014) Potential applications of ferulic acid from natural sources. *Biotechnol Rep.*, 4:86-93.
- 75) Kumar, N., Pruthi, V., Goel, N. (2014) Structural, Thermal and Quantum Chemical Studies of *p*-coumaric and caffeic acids. *J Mol Struct.*, 1085:242-248.
- 76) Kumar N., Bhalla T.C. (2011) *In Silico* Analysis of Amino Acid Sequences in Relation to Specificity and Physiochemical Properties of Some Aliphatic amidases and Kynurenine formamidases. *J Bioinform Seq Anal.*, 3:116-123.
- 77) Kumar, A., Fang, P., Park, H., Guo, M., Nettles, K. and Disney, M.D. (2011) A crystal structure of a model of the repeating r(CGG) transcript found in Fragile X syndrome. *ChemBioChem.*, 12:2140-2142.
- 78) Kumar, A., Park, H., Fang, P., Parkesh, R., Guo, M., Nettles, K.W., Disney, M.D. (2011) Myotonic dystrophy type 1 RNA crystal structures reveal heterogeneous 1×1 nucleotide UU internal loop conformations. *Biochemistry.*, 50:9928-9935.
- 79) Kumar, A., Sharma, S.S. (2010) NF-kappa B inhibitory action of resveratrol: a probable mechanism of neuroprotection in experimental diabetic neuropathy. *Biochem. Biophys. Res. Commun.*, 394:360-365.
- 80) Lafay, S., Gil-izquierdo, A. (2008) Bioavailability of phenolic acids. *Phytochem Rev.*, 7:301-311.
- 81) Lambert, F., Zucca, J., Ness, F., Aigle, M. (2013) Production of ferulic acid and coniferyl alcohol by conversion of eugenol using a recombinant strain of *Saccharomyces cerevisiae*. *Flavour Fragr J.*, 29:14-21.

- 82) Langer, T., Wolber, G. (2007) Pharmacophore definition and 3D searches. *Drug Discovery Today: Technol.*, 1:203-207.
- 83) Lee, C., Yang, W., Parr, R.G. (1988) Development of the Colle-Salvetti correlation-energy formula into a functional of the electron density. *Phys. Rev. B Condens. Matter.* 37:785-789.
- 84) Lin, F.H., Lin, J.Y., Gupta, R.D., Tournas, J.A., Burch, J.A., Selim, M.A., Monteiro-Riviere, N.A., Grichnik, J.M., Zielinski, J., Pinnell, S.R. (2005) Ferulic acid stabilizes a solution of vitamins C and E and doubles its photoprotection of skin. *J Invest Dermatol.*, 125:826-832.
- 85) Lina, C.M., Chiuc, J.H., Wu, I.H., Wang, B.W., Pan, C.M., Cheng, Y.H. (2010) Ferulic acid augments angiogenesis via VEGF, PDGF and HIF-1 α . *J Nutr Biochem.*, 21:627-633.
- 86) Liu, Y. (1987) Pharmaceutical composition for increasing immunity and decreasing side effects of anticancer chemotherapy. US patent: 4687761.
- 87) Li, W.J., Cheng, X.L., Liu, J., Lin, R.C., Wang, G.L., Du, S.S., Liu, Z.L. (2012) Phenolic Compounds and Antioxidant Activities of *Liriope muscari*. *Molecul.*, 17:1797-1808.
- 88) Llorach, R., Espín, J.C., Tomás-Barberán, F.A., Ferreres, F. (2002) Artichoke (*Cynara scolymus L.*) byproducts as a potential source of health-promoting antioxidant phenolics. *J Agric Food Chem.*, 50:3458-3464.
- 89) Lu, W., Wang, F., Zhang, T., Dong, J., Gao, H., Su, P., Shi, Y., Zhang, J. (2014) Search for novel histone deacetylase inhibitors. Part II: Design and synthesis of novel isoferulic acid derivatives. *Bioorg. Med. Chem.*, 22:2707-2713.
- 90) Luceri, C., Giannini, L., Lodovici, M., Antonucci, E., Abbate, R., Masini, E., Dolaro, P. (2007) *p*-Coumaric acid, a common dietary phenol, inhibits platelet activity *in vitro* and *in vivo*. *Br J Nutr.*, 97:458-463.

- 91) Masai, E., Harada, K., Peng, X., Kitayama, H., Katayama, Y., Fukuda, M. (2002) Cloning and characterization of the ferulic acid catabolic genes of *Sphingomonas paucimobilis* SYK-6. *Appl Environ Microbiol.*, 68:4416-4424.
- 92) Masaji, Y. (1999) Preservation Measures for Food Products. Preventive method of coloring agricultural products using ferulic acid. *Tech J Food Chem & Chem.*, 8:76-79.
- 93) Maishi, A.I., Ali, P.K.S., Chaghtai, S.A., Khan, G. (1998) A proving of *Parthenium hysterophorus* L. *Brit Homoeopath J.*, 87:17-21.
- 94) Maoka, T., Tanimoto, F., Sano, M., Tsurukawa, K., Tsuno, T., Tsujiwaki, S., Ishimaru, K., Takii, K. (2008) Effects of dietary supplementation of ferulic acid and gamma-oryzanol on integument color and suppression of oxidative stress in cultured red sea bream, *Pagrus major*. *J Oleo Sci.*, 57:133-140.
- 95) Marinova, E.M., Yanishlieva, N.V., Toneva, A.G. (2006) Antioxidant activity and mechanism of action of ferulic and caffeic acids in different lipid systems. *Italian J Subs Gra.*, 83:6-13.
- 96) Mathew, S., Abraham, T.E. (2005) Studies on the production of feruloyl esterase from cereal brans and sugar cane bagasse by microbial fermentation. *Enzyme Microb Technol.*, 36:565-570.
- 97) Mathew, S., Abraham, T.E. (2006) Bioconversions of ferulic acid, an hydroxycinnamic acid. *Crit Rev Microbiol.*, 32:115-125.
- 98) Mattila, P., Pihlava, J.M., Hellstrom, J. (2005) Contents of phenolic acids, alkyl- and alkenylresorcinols, and avenanthramides in commercial grain products. *J Agric Food Chem.*, 53:8290-8295.
- 99) Mattila, P., Hellstrom, J., Torronen, R. (2006) Phenolic acids in berries, fruits, and beverages. *J Agric Food Chem.*, 54:7193-7199.

- 100) Mattila, P., Hellstrom, J. (2007) Phenolic acids in potatoes, vegetables, and some of their products. *J Food Comp Anal.*, 20:152-160.
- 101) Medina, I., Gallardo, J.M., Gonzalez, M.J., Lois, S., Hedges, N. (2007) Effect of molecular structure of phenolic families as hydroxycinnamic acids and catechins on their antioxidant effectiveness in minced fish muscle. *J Agric Food Chem.*, 55:3889-3895.
- 102) Menendez, J.A., Alejandro, V.M., Cristina, O.F., Rocio, G.V., Alegria, C.P., Alberto, F.G., Antonio, S.C. (2008) Analyzing effects of extra-virgin olive oil polyphenols on breast cancer-associated fatty acid synthase protein expression using reverse-phase protein microarrays. *Int J Mol Med.*, 22:433-439.
- 103) Middleton, E.Jr., Kandaswami, C., Theoharides, T.C. (2000) The effects of plant flavonoids on mammalian cells: implications for inflammation, heart disease, and cancer. *Pharmacol Rev.*, 52:673-751.
- 104) Min, J.Y., Knag, S.M., Park, D.J., Kim, Y.D., Jung, H.N., Yang, J.K., Seo, W.T., Kim, S.W., Karigar, C.S., Choi, M.S. (2006) Enzymatic release of ferulic acid from *Ipomoea batatas* L. (Sweet Potato) stem. *Biotechnol Bioprocess Eng.*, 11:372-376.
- 105) Monga, V., Meena, C.L., Rajput, S., Pawar, C., Sharma, S.S., Lu, X., Gershengorn, M.C., Jain, R. (2011) Synthesis, receptor binding, and CNS pharmacological studies of new thyrotropin-releasing hormone (TRH) analogues. *ChemMedChem.*, 6:531-543.
- 106) Mori, H., Kawabata, K., Yoshimi, N., Tanaka, T., Murakami, T., Okada, T., Murai, H. (1999) Chemopreventive effects of ferulic acid on oral and rice germ on large bowel carcinogenesis. *Anticancer Res.*, 19:3775-3783.
- 107) Mori, T., Koyama, N., Guillot-Sestier, M.V., Tan, J., Town, T. (2013) Ferulic Acid Is a Nutraceutical β -Secretase Modulator That Improves Behavioral Impairment and Alzheimer-like Pathology in Transgenic Mice. *PLoS ONE.*, 8:1-15.

- 108) Muheim, A., Lerch, K. (1999) Towards a high-yield bioconversion of ferulic acid to vanillin. *Appl Microbiol Biotechnol.*, 51:456-461.
- 109) Murakami, A., Nakamura, Y., Koshimizu, K., Takahashi, D., Matsumoto, K., Hagihara, K., Taniguchi, H., Nomura, E., Hosoda, A., Tsuno, T., Maruta, Y., Kim, H.W., Kawabata, K., Ohigashi, H. (2002) FA15, a hydrophobic derivative of ferulic acid, suppresses inflammatory responses and skin tumor promotion: comparison with ferulic acid. *Cancer Lett.*, 180:121-129.
- 110) Nardini, M., Aquino, M.D., Tomassi, G., Gentili, V., Di Felice, M., Scaccini, C. (1995) Inhibition of human low-density lipoprotein oxidation by caffeic acid and other hydroxycinnamic acid derivatives. *Free Radic Biol Med.*, 19:541-552.
- 111) Natalia, N.R., Claire, D., Lullien, P.V., Valerie, M. (2013) Exposure or release of ferulic acid from wheat aleurone: Impact on its antioxidant capacity. *Food Chem.*, 141:2355-2362.
- 112) Nethaji, M., Pattabhi, V., Desiraju, G.R. (1988) Structure of 3-(4-hydroxy-3-methoxyphenyl)-2-propenoic acid (ferulic acid). *Acta Cryst C*44:275-277.
- 113) Nicholas, C.C. (1996) Structure and biogenesis of the cell walls of grasses. *Annu Rev Plant Physiol Plant Mol Biol.*, 47:445-476.
- 114) Nomura, E., Kashiwada, A., Hosoda, A., Nakamura, K., Morishita, H., Tsuno, T., Taniguchi, H. (2003) Synthesis of amide compounds of ferulic acid and their stimulatory effects on insulin secretion in vitro. *Bioorg Med Chem.*, 11:3807-3813.
- 115) Ohsaki, A.Y., Shirakawa, H., Koseki, T., Komai, M. (2008) Novel effects of a single administration of ferulic acid on the regulation of blood pressure and the hepatic lipid metabolic profile in stroke-prone spontaneously hypertensive rats. *J Agric Food Chem.*, 56:2825-2830.

- 116) Okada, T., Nakagawa, K., Yamaguchi, N. (1982) Antioxidative activities of amino compounds on fats and oils. VIII. Antioxidative activity of ferulate and the synergistic effect of amino compounds. *Nippon Shokuhin Kogyo Gakkaishi.*, 29:305-309.
- 117) Oosterveld, A., Pol, I.E., Beldman, G., Voragen, A.G.J. (2001) Isolation of feruloylated arabinans and rhamnogalacturonans from sugar beet pulp and their gel forming ability by oxidative cross-linking. *Carbohydr Polym.*, 44:9-17.
- 118) Ou, S., Kwok, K.C. (2004) Ferulic acid: pharmaceutical functions, preparation and applications in foods. *J Sci Food Agric.*, 84:1261-1269.
- 119) Overhage, J., Priefert, H., Steinbuchel, A. (1999) Biochemical and genetic analyses of ferulic acid catabolism in *Pseudomonas sp.* Strain HR199. *Appl Environ Microbiol.*, 65:4837-4847.
- 120) Overhage, J., Steinbüchel, A., Priefert, H. (2002) Biotransformation of eugenol to ferulic acid by a recombinant strain of *Ralstonia eutropha* H16. *Appl Environ Microbiol.*, 68:4315-4321.
- 121) Ozaki, Y., Ma, J.P. (1990) Inhibitory effects of tetramethylpyrazine and ferulic acid on spontaneous movement of rat uterus *in situ*. *Chem. Pharm. Bull.*, 38:1620-1623.
- 122) Park, S.H., Kim, D.S., Park, S.H., Shin, J.W., Youn, S.W., Park, K.C. (2008) Inhibitory effect of *p*-coumaric acid by *Rhodiola sachalinensis* on melanin synthesis in B16F10 cells. *Pharmazie.*, 63:290-295.
- 123) Patel, S. (2011) Harmful and beneficial aspects of *Parthenium hysterophorus*: an update. *3 Biotech.*, 1:1-9.
- 124) Paiva, L.B.D., Goldbeck, R., Santos, W.D.D., Squina, F.M. (2013) Ferulic acid and derivatives: molecules with potential application in the pharmaceutical field. *Brazilian J Pharm Scien.*, 49:395-411.

- 125) Parkesh, R., Childs-Disney, J.L., Nakamori, M., Kumar, A., Wang, E., Wang, T., Hoskins, J., Tran, T., Housman, D., Thornton, C.A., Disney, M.D. (2012) Design of a Bioactive Small Molecule That Targets the Myotonic Dystrophy Type 1 RNA via an RNA Motif-Ligand Database and Chemical Similarity Searching. *J. Am. Chem. Soc.*, 134:4731-4742.
- 126) Peng, C., Ayala, P.Y., Schlegel, H.B., Frisch, M.J. (1996) Using redundant internal coordinates to optimize equilibrium geometries and transition states. *J Comput Chem.*, 17:49-56.
- 127) Piazzon A., Vrhovsek, U., Masuero, D., Mattivi, F., Mandoj, F., Nardini, M. (2012). Antioxidant activity of phenolic acids and their metabolites: Synthesis and antioxidant properties of the sulphate derivatives of ferulic and caffeic acids and of the acyl glucuronide of ferulic acid. *J Agric Food Chem.*, 60:12312-12323.
- 128) Pietta, P.G. (2000) Flavonoids as antioxidants. *J Nat Prod.*, 63:1035-1042.
- 129) Pulido, R., Hernández-García, M., Saura-Calixto, F. (2003) Contribution of beverages to the intake of lipophilic and hydrophilic antioxidants in the Spanish diet. *Eur J Clin Nutr.*, 57:1275-1282.
- 130) Rajkumar, E.D.M., Kumar, N.V.N., Haran, N.V.H., Ram, N.V.S. (1988). Antagonistic effect of *P. hysterophorus* on succinate dehydrogenase of sheep liver. *J Environ Biol.*, 9:231-237.
- 131) Rathore, Y.S., Solanki, A.K., Dhoke, R.R., Ashish. (2011) SAXS data analysis and modeling of tetravalent neutralizing antibody CD4-IgG2 +/- HIV-1 gp120 revealed that first two gp120 bind to the same Fab arm. *Biochem Biophys Res Commun.*, 415:680-685.
- 132) Rathore, Y.S., Rehan, M., Pandey, K., Sahni G., Ashish. (2012) First structural model of full-length human tissue-plasminogen activator: a SAXS data-based modeling study. *J Phys Chem B.*, 116:496-502.

- 133) Rocha, L.D., Monteiro, M.C., Teodoro, A.J. (2012) Anticancer Properties of Hydroxycinnamic Acids-A Review. *Cancer Clin Oncol.*, 1:109-121.
- 134) Rosazza, J.P.N., Huang, Z., Dostal, L., Volm, T., Rousseau, B. (1995) Review: Biocatalytic transformations of ferulic acid: an abundant aromatic natural product. *J Ind Microbiol.*, 15:457-471.
- 135) Rukkumani, R., Aruna, K., Suresh, V.P., Padmanabhan, M.V. (2004) Hepatoprotective role of ferulic acid: a dose-dependent study. *J Med Food.*, 7:456-461.
- 136) Saija, A., Tomaino, A., Trombetta, D., De Pasquale, A., Uccella, N., Barbuzzi, T., Paolino, D., Bonina, F. (2000) In vitro and in vivo evaluation of caffeic and ferulic acids as topical photoprotective agents. *Int J Pharm.*, 199:39-47.
- 137) Sajjadi, S.E., Naderi, G.H., Ziaii, R., Zolfaghari, B. (2004) The antioxidant activity of polyphenolic fraction of *Thymus daenensis* Celak. *Iranian J Pharm Res.*, 3:80-81.
- 138) Sajjadi, S.E., Shokohinia, Y., Moayedi, N.S. (2012) Isolation and identification of ferulic acid from aerial parts of *Kelussia odoratissima* Mozaff. *Jundishapur J Nat Pharm Prod.*, 7:159-162.
- 139) Sarekha, W., Rangrong, Y. (2013) Preparation, characterization and antioxidant property of water-soluble ferulic acid grafted chitosan. *Carbohydr Polym.*, 96:495-502.
- 140) Scalbert, A., Williamson, G. (2000) Dietary Intake and Bioavailability of Polyphenols. *J. Nutr.*, 130:2073S-2085S.
- 141) Schuster, D., Kern, L., Hristozov, D.P., Terfloth, L., Bienfait, B., Laggner, C., Kirchmair, J., Grienke, U., Wolber, G., Langer, T., Stuppner, H., Gasteiger, J., Rollinger, J.M. (2010) Applications of integrated data mining methods to exploring natural product space for acetylcholinesterase inhibitors. *Comb Chem High Throughput Screen.*, 13:54-66.

- 142) Settimo, A.D., Settimo, F.D., Marini, A.M., Primofiore, G., Salerno, S., Viola, G., Via, L.D., Magno, S.M. (1998) Synthesis, DNA Binding and in vitro activity of purinoquinazoline, pyridopyrimidopurine and pyridopyrimidobenzimidazole derivatives as potential antitumor agent. *Eur. J. Med. Chem.*, 33:685-696.
- 143) Sharma, N., Kushwaha, R., Sodhi, J.S., Bhalla T.C. (2009) *In Silico* Analysis of Amino Acid Sequences in Relation to Specificity and Physiochemical Properties of Some Microbial Nitrilases. *J Proteom Bioinform.*, 2:185-192.
- 144) Sharma, O.P., Bhat, T.K. (2009) DPPH antioxidant assay revisited. *Food Chem.*, 113:1202-1205.
- 145) Sheldrick, G.M. (1990) Phase annealing in SHELX-90: direct methods for larger structures. *Acta Cryst. A*, 46:467-473.
- 146) Sheldrick, G.M. (1996) SADABS: Program for empirical absorption correction of area detector data. University of Gottingen: Gottingen, Germany.
- 147) Sheldrick, G.M. (2000) SHELXTL-NT, Version 6.12, Reference manual, University of Gottingen, Germany.
- 148) Siddiqui, N., Alam, M.S., Ahsan, W. (2008) Synthesis, anticonvulsant and toxicity evaluation of 2-(1H-indol-3-yl)acetyl-N-(substituted phenyl)hydrazine carbothioamides and their related heterocyclic derivatives. *Acta Pharm.*, 58:445-454.
- 149) Singh, I.P., Jain, S.K., Kaur, A., Singh, S., Kumar, R., Garg, P., Sharma, S.S., Arora, S.K. (2010) Synthesis and antileishmanial activity of piperoyl-amino acid conjugates. *Eur J Med Chem.*, 45:3439-3445.
- 150) Skalkos, D., Selman, S.H., Hampton, J.A., Morgan, A.R. (1998) US 5744598, *Chem. Abstr.* 128:330388.

- 151) Sondhi, S.M., Singh, J., Rani, R., Gupta, P.P., Agrawal, S.K., Saxena, A.K. (2010) Synthesis, anti-inflammatory and anticancer activity evaluation of some novel acridine derivatives. *Eur J Med Chem.*, 45:555-563.
- 152) Soto, M.L., Moure, A., Dominguez, H., Parajo, J.C. (2011) Recovery, concentration and purification of phenolic compounds by adsorption: A review. *J Food Eng.*, 105:1-26.
- 153) Spencer, J.P., El Mohsen M.A., Minihane, A.M., Mathers, J.C. (2008) Biomarkers of the intake of dietary polyphenols: strengths, limitations and application in nutrition research. *Br J Nutr.*, 99:12-22.
- 154) Srinivasan, M., Sudheer, A.R., Menon, V.P. (2007) Ferulic Acid: Therapeutic Potential through Its Antioxidant Property. *J Clin Biochem Nutr.*, 40:92-100.
- 155) Steindl, T.M., Schuster, D., Wolber, G., Laggner, C., Langer, T. (2006) High-throughput structure-based pharmacophore modelling as a basis for successful parallel virtual screening. *J Comput Aided Mol Des.*, 20:703-715.
- 156) Stephens, P.J., Devlin, F.J., Chablowski, C.F., Frisch, M.J. (1994) *Ab initio* calculation of vibrational absorption and circular dichroism spectra using density functional force fields. *J Phys Chem.*, 98:11623-11627.
- 157) Strack, D. (1990) Metabolism of hydroxycinnamic acid conjugates. *Bull Liaison-Group Polyphenols.*, 15:55-64.
- 158) Sudheer, A.R., Kalpana, C., Srinivasan, M., Menon, V.P. (2005) Ferulic acid modulates altered lipid profiles and prooxidant/antioxidant status in circulation during nicotine-induced toxicity: A dose dependent study. *Toxicol Mech Methods.*, 15:375-381.
- 159) Sudheer, A.R., Muthukumar, S., Kalpana, C., Srinivasan, M., Menon, V.P. (2007) Protective effect of ferulic acid on nicotine-induced DNA damage and cellular changes in

- cultured rat peripheral blood lymphocytes: a comparison with N-acetylcysteine. *Toxicol In Vitro.*, 21:576-585.
- 160) Sultana, R., Ravagna, A., Mohmmad, A.H., Calabrese, V., Butterfield, D.A. (2005) Ferulic acid ethyl ester protects neurons against amyloid betapeptide(1-42)-induced oxidative stress and neurotoxicity: relationship to antioxidant activity. *J Neurochem.*, 92:749-758.
- 161) Sultana, R. (2012) Ferulic acid ethyl ester as a potential therapy in neurodegenerative disorders. *Biochim. Biophys. Acta.*, 1822:748-752.
- 162) Suzuki, A., Kagawa, D., Fujii, A., Ochiai, R., Tokimitsu, I., Saito, I. (2002) Short- and long-term effects of ferulic acid on blood pressure in spontaneously hypertensive rats. *Am J Hypertens.*, 15:351-358.
- 163) Swisłocka, R., Sadowy, M.K., Kalinowska, M., Lewandowski, W. (2012) Spectroscopic (FT-IR, FT-Raman, ^1H and ^{13}C NMR) and theoretical studies of p-coumaric acid and alkali metal p-coumarates. *Spectroscopy.*, 27:35-48.
- 164) Tamm, L.K., Abildgaard, F., Arora, A., Blad, H., Bushweller, J.H. (2003) Structure, dynamics and function of the outer membrane protein A (OmpA) and influenza hemagglutinin fusion domain in detergent micelles by solution NMR. *FEBS Lett.*, 555:139-143.
- 165) Taubert, D., Breitenbach, T., Lazar, A., Censarek, P., Harlfinger, S., Berkels, R., Klaus, W., Roesen, R. (2003) Reaction rate constants of superoxide scavenging by plant antioxidants. *Free Radic Biol Med.*, 35:1599-1607.
- 166) Tilay, A., Bule, M., Kishenkumar, J., Annapure, U. (2008) Preparation of Ferulic Acid from Agricultural Wastes: Its Improved Extraction and Purification. *J Agric Food Chem.*, 56:7644-7648.

- 167) Toshihiro, A., Ken, Y., Miho, Y., Motohiko, U., Yumiko, K., Naoto, S., Koichi, A. (2000) Triterpene alcohol and sterol ferulates from rice bran and their anti-inflammatory effects. *J Agric Food Chem.*, 48:2313-2319.
- 168) Tsuchiya, T., Takasawa, M. (1975) Oryzanol, ferulic acid, and their derivatives as preservatives. *Japan. Kokai.*, 07:518-521.
- 169) Uraji, M., Kimura, M., Inoue, Y., Kawakami, K., Kumagai, Y., Harazono, K., Hatanaka, T. (2013) Enzymatic production of ferulic acid from defatted rice bran by using a combination of bacterial enzymes. *Appl Biochem Biotechnol.*, 171:1085-1093.
- 170) Van der Logt, E.M., Roelofs, H.M., Nagengast, F.M., Peters, W.H. (2003) Induction of rat hepatic and intestinal UDP-glucuronosyltransferases by naturally occurring dietary anticarcinogens. *Carcinogenesis.*, 24:1651-1657.
- 171) Villa-Caballero, L., Nava-Ocampo, A.A., Frati-Munari, A.C., Ponce-Monter, H. (2000) [Oxidative stress. Should it be measured in the diabetic patient?]. *Gac Med Max* 136:249-256.
- 172) Walczak, K., Gondela, A., Suwinski, J. (2004) Synthesis and anti-tuberculosis activity of N-aryl-C-nitroazoles. *Eur J Med Chem.*, 39:849-853.
- 173) Wang, B., Ouyang, J., Liu, Y., Yang, J., Wei, L., Li, K., Yang, H. (2004) Sodium ferulate inhibits atherosclerogenesis in hyperlipidemia rabbits. *J Cardiovasc Pharmacol.*, 43:549-554.
- 174) Wang, F., Lu, W., Zhang, T., Dong, J., Gao, H., Li, P., Wang, S., Zhang, J. (2013) Development of novel ferulic acid derivatives as potent histone deacetylase inhibitors. *Bioorg. Med. Chem.*, 21:6973-6980.

- 175) Warnecke, A., Fichtner, I., Sass, G., Kratz, F. (2007) Synthesis, cleavage profile, and antitumor efficacy of an albumin-binding prodrug of methotrexate that is cleaved by plasmin and cathepsin B. *Arch Pharm.*, 340:389-395.
- 176) Warren, G.W., Singh, A.K. (2013) Nicotine and lung cancer. *J Carcinog.*, 12:1.
- 177) Wei-Min, W., Liang, L., Yuan, L., Ting, W., Lei, L., Qiang, C., Rui, W. (2007) Free radical scavenging and antioxidative activities of caffeic acid phenethyl ester (CAPE) and its related compounds in solution and membranes: A structure-activity insight. *Food Chem.*, 105:107-115.
- 178) Wiegand, C., Heinze, T., Hipler, U.C. (2009) Comparative in vitro study on cytotoxicity, antimicrobial activity, and binding capacity for pathophysiological factors in chronic wounds of alginate and silver-containing alginate. *Wound Repair Regen.*, 17;511-521.
- 179) Wolber, G., Seidel, T., Bendix, F., Langer, T. (2008) Molecule-pharmacophore superpositioning and pattern matching in computational drug design. *Drug Discov Today.*, 13:23-29.
- 180) Wold, S. (1991) Validation of QSAR's. *Quant. Struct. Act. Relat.*, 10:191-193.
- 181) Wong, D.W., Chan, V.J., Batt, S.B., Sarath, G., Liao, H. (2011) Engineering *Saccharomyces cerevisiae* to produce feruloyl esterase for the release of ferulic acid from switchgrass. *J Ind Microbiol Biotechnol.*, 38:1961-1967.
- 182) Xing, Y., Peng, H.Y., Zhang, M.X., Li, X., Zeng, W.W., Yang, X.E. (2012) Caffeic acid product from the highly copper-tolerant plant *Elsholtzia splendens* post-phytoremediation: its extraction, purification, and identification. *Biomed Biotech Sci B.*, 13:487-493.
- 183) Xu, F., Sun, R.C., Sun, J.X., Liu, C.F., He, B.H., Fan, J.S. (2005) Determination of cell wall ferulic and p-coumaric acids in sugarcane bagasse. *Analytica Chimica Acta.*, 552:207-217.

- 184) Yadav, P.P., Arora, A., Bid, H.K., Konwar, R.R., Kanojiya, S. (2007) New cassane butenolide hemiketal diterpenes from the marine creeper *Caesalpinia bonduc* and their antiproliferative activity. *Tetrahedron Lett.*, 40:7194-7198.
- 185) Yagi, K., Ohishi, N. (1979) Action of ferulic acid and its derivatives as antioxidants. *J Nut Sci Vitam.*, 25:127-130.
- 186) Yang, F., Zhou, B.R., Zhang, P., Zhao, Y.F., Chen, J., Liang, Y. (2007) Binding of ferulic acid to cytochrome c enhances stability of the protein at physiological pH and inhibits cytochrome c-induced apoptosis. *Chem Biol Interact.*, 170:231-243.
- 187) Yang, F., Zhou, B.R., Zhang, P., Zhao, Y.F., Chen, J., Liang, Y. (2007) Binding of ferulic acid to cytochrome c enhances stability of the protein at physiological pH and inhibits cytochrome c-induced apoptosis. *Chem Biol Interact.*, 170:231-243.
- 188) Yildiz, D., Ercal, N., Armstrong, D.W. (1998) Nicotine enantiomers and oxidative stress. *Toxic.*, 130:155-165.
- 189) Zarth, C.S.P., Koschella, A., Pfeifer, A., Dorn, S., Heinze, T. (2011) Synthesis and characterization of novel amino cellulose esters. *Cellulose.*, 18:1315-1325.
- 190) Zhao, Z., Egashira, Y., Sanada, H. (2003a) Digestion and absorption of ferulic acid sugar esters in rat gastrointestinal tract. *J Agric Food Chem.*, 51:5534-5539.
- 191) Zhao, Z., Egashira, Y., Sanada, H. (2003b) Ferulic acid sugar esters are recovered in rat plasma and urine mainly as the sulfoglucuronide of ferulic acid. *J Nutr.*, 133:1355-1361.
- 192) Zhao, Z., Egashira, Y., Sanada, H. (2004) Ferulic acid is quickly absorbed from rat stomach as the free form and then conjugated mainly in liver. *J Nutr.*, 134:3083-3088.
- 193) Zhao, Z., Moghadasian, M.H. (2008) Chemistry, natural sources, dietary intake and pharmacokinetic properties of ferulic acid: A review. *Food Chem.*, 109:691-702.

- 194) Zupfer, J.M., Churchill, K.E., Rasmusson, D.C., Fulcher, R.G. (1998) Variation in ferulic acid concentration among diverse barley cultivars measured by HPLC and microspectrophotometry. *J Agric Food Chem.*, 46:1350-1354.